

SMiRT 20 – Book of abstracts Vol. 1

20th International Conference on
STRUCTURAL MECHANICS
IN REACTOR TECHNOLOGY



SMiRT 20 Secretariat

VTT Technical Research Centre of Finland

P.O. Box 1000, FI-02044 VTT, Finland

Tel +358 20 722 111

Fax +358 20 722 7053

www.vtt.fi/smirt20, www.iasmirt.org



**INTERNATIONAL ASSOCIATION FOR STRUCTURAL MECHANICS in
REACTOR TECHNOLOGY**

VTT SYMPOSIUM 256

Keywords: Nuclear power plants, Nuclear facilities, Nuclear safety, Structural safety, Advanced reactors, Mechanics of materials, Aging, Plant life management, Inspection, Maintenance, Design and qualification, Fracture Mechanics, Structural evaluation, Structural reliability, Probabilistic safety assessment, Extreme loads, Earthquakes, Fuel and core structures, Severe accident management, Computational mechanics, Metal materials, Concrete materials, Containment structures, Seismic loads, Seismic analysis, Design methods

20th International Conference on Structural Mechanics in Reactor Technology

SMiRT 20

Book of abstracts

Vol. 1

Espoo, Finland 2009

Edited by

Seppo Vuori & Rauno Rintamaa

Organised by

VTT



ISBN 978-951-38-6335-7 (soft back ed.)

ISSN 0357-9387 (soft back ed.)

ISBN 978-951-38-6336-4 (URL: <http://www.vtt.fi/publications/index.jsp>)

ISSN 1455-0873 (URL: <http://www.vtt.fi/publications/index.jsp>)

Copyright © VTT 2009

JULKAISIJA – UTGIVARE – PUBLISHER

VTT, Vuorimiehentie 5, PL 1000, 02044 VTT
puh. vaihde 020 722 111, faksi 020 722 7001

VTT, Bergsmansvägen 5, PB 1000, 02044 VTT
tel. växel 020 722 111, fax 020 722 7001

VTT Technical Research Centre of Finland
Vuorimiehentie 5, P.O. Box 1000, FI-02044 VTT, Finland
phone internat. +358 20 722 111, fax + 358 20 722 7001

Preface

The two biggest global challenges facing the energy world today are climate change and the huge increase in energy consumption. Global electricity consumption is expected to double by the year 2030. There will be increasing competition in the world for energy resources. On the other hand there is a need to lower energy intensity of the economy and turn to CO₂-free forms of energy production. Inevitably, the era of cheap energy is over. These are driving forces favourable for increasing nuclear energy production capacity.

In Europe, the EU has put forward a very concrete target. The Heads of State set very ambitious EU mandatory targets for the new Energy and Climate Change policy for 2020. One of those targets requires at least 20% less CO₂ emissions compared to 1990. Targets will not be realistic without considerable investments on new nuclear power plants and their development. Consequently, the European Commission with the support of nuclear industry have launched a Sustainable Nuclear Energy Technology Platform (SNE-TP) in September 2007. In Finland, a decision to build a new (fifth) nuclear power plant (EPR) was already made in 2002, and the licence for the construction was granted in early 2005. Recently new initiatives have been made by the industry for three more nuclear power plants in Finland. The applications for the Decision in Principle for these initiatives are being handled by the Government. Some other countries in Europe have also made initiatives for new builds.

The international conferences on Structural Mechanics in Reactor Technology (SMiRT) have traditionally provided innovative and practical mechanics-based solutions to the planning, design, construction, operation, and regulation of NPPs and related facilities. SMiRT 20 will continue this tradition, bringing together experts and practitioners from around the world to share their knowledge of technology that is most relevant at this time in the nuclear energy industry for both currently operating facilities and future development. Around 400 papers will give

answers to **Challenges Facing Nuclear Renaissance**. Besides technical papers the SMiRT20 Programme consists of Leadership Forum, Technical Plenary Sessions, Panel Workshops and Tutorial Workshops having topics of major interest.

This book of abstracts gives an outline of all technical papers presented in each Technical Divisions. Full papers are published in the DVD Proceedings.

We wish all the SMiRT20 participants and authors a successful conference and pleasant stay in Finland 2009.

Rauno Rintamaa

Chairman

SMiRT 20 Conference

Seppo Vuori

Chairman

Local Organizing Committee

Contents

Preface	3
1. Mechanics of Materials	15
Study of Bree's daigram with nonlinear kinematic hardening model (1-1578)	17
Tensile and toughness properties of materials for the RSE-M Code (1-1654)	19
PACE-1450 – Experimental investigation of the crack behaviour of prestressed concrete containment walls considering the prestressing loss due to aging (1-1671)	20
Acoustic emission monitoring of slow strain rate tensile tests of 304L and 316L stainless steels in supercritical water environments (1-1674)	22
Prediction of fracture toughness for nuclear piping using curved wide-plate test (1-1676)	23
Development of constitutive models for fast reactor design – strategy of the study and results in the first half stage (1-1677)	25
Modeling the pseudoelastic response of shape memory alloy cylindrical shells using a nonlinear finite element formulation (1-1690)	27
A mixed yield surface for modeling the anisotropic creep behavior of Zirconium alloys (1-1695)	29
Local failure criteria for wall-thinning defect in piping components based on simulated specimen and real-scale pipe tests (1-1703)	30
Simulation of roll expansion on Steam Generator tubes (1-1720)	32
Estimation of the Residual Stresses impact on the J parameter calculation in welded joint (1-1735)	35
Development of raman spectroscopy analysis technique for the oxides forming on Hastelloy-XR at elevated temperatures in coolant helium (1-1743)	37
Using spatial statistical analysis of Taylor factors to characterize material susceptibility to intergranular stress corrosion cracking (1-1779)	39
Experimental study of the effect of radiation exposure to concrete (1-1891)	40
Nuclear reactor structure materials study (Survey of relevant ISTC programs) (1-1916)	41

Two scale damage model for HCF uniaxial and biaxial 304L steel tests (1-1917)	45
Concrete shrinkage taken into account as crack width assessment (1-1925)	47
A probabilistic approach for assessing concrete degradation due to leaching (1-1926)	48
Thermal ageing of RPV materials for NPP with VVER (1-1990)	50
Effect of geometrical defects and cracks on the collapse of straight or curved tubes submitted to external pressure (1-1991)	51
Control and exploitation of thermal distortions in welded T-joints (1-1994)	53
Experimental and numerical analysis of cyclic thermal shock at the Paul Scherrer Institut (1-1998)	55
Manifestations of DSA in austenitic stainless steels and inconel alloys (1-2013)	57
Strength and porosity of concrete incorporating polypropylene and steel fibres subjected to high temperature (1-2024)	60
Simulation research of self-healing mechanism for microcapsule composite (1-2054)	61
A simplified ratcheting limit method – uniform modified yield (UMY) approach (1-2058)	63
Application of CFD Code PHOENICS for simulating CYCLONE SEPARATORS (1-2459)	64
Evaluation on the fracture properties of heated concrete by using poly-linear tension softening inverse analysis (1-2531)	65
Study on strength development properties of the internal characteristics of mass concrete (1-2559)	68
Fatigue curve and stress strain response for stainless steel (1-3135)	70
Effect of hardening model on the weld residual stress field in pipe girth welds (1-3142)	73
Theoretical model for the hydrogen-material interaction as a basis for prediction of the material mechanical properties (1-3145)	74
2. Fracture Mechanics and Structural Integrity	77
The demonstration of warm pre-stress effect on RPV steels: experimental results and interpretation by engineering models (2-1579)	79
NESC VII: a European project for application of WPS in RPV assessment including biaxial loading (2-1580)	80
Primary stress index B_2^* for the evaluation of postulated or detected circumferential flaws at the connection straight-pipe / bend (2-1583)	81
Dynamic crack growth and arrest simulation with cohesive zone models, during a pressurized thermal shock in a RPV (2-1596)	83
Numerical study of 3-D constraint effects in ferritic steels (2-1602)	85
A J estimation scheme for surface cracks in piping welds (2-1672)	86

Influence of welding process on fatigue crack propagation properties in structural steel (2-1638)	87
Thermal fatigue analysis of a NPP steam generator injection nozzle model subjected to thermal stratification (2-1710)	88
Structure integrity assessment of pressurizer (2-1723)	90
Bond behavior between reinforcing steel and concrete under multiaxial loading conditions in concrete containments (2-1734)	93
Evaluation of the cleavage fracture toughness of SA508 Gr. 4N low alloy steels in the transition region (2-1788)	96
An analytical thermal fatigue crack growth approach (2-1796)	97
On assessment of initial cracks for RI-ISI analysis purposes (2-1797)	99
On welding residual stresses and their practical inclusion in structural integrity analyses (2-1798)	101
Fracture mechanics evaluation of similar and dissimilar welded fracture specimens under plane-strain (2-1803)	103
Three dimensional damage mechanics analysis of real life reactor piping components under various loading conditions (2-1831)	105
Application of the leak before break concept to CANDU feeder piping with service induced cracking (2-1854)	107
Evaluation of interaction effect for parallel surface cracks in shell-to-nozzle junction with geometrical discontinuity based on limit load analyses (2-1859)	109
Ratcheting-fatigue failure of pressurized elbows made of carbon steel (2-1861)	110
Cyclic tearing of through wall cracked pipes made of carbon steel (2-1863)	113
Fatigue crack initiation and crack growth studies for pipes made of carbon steel (2-1864)	117
Numerical determination of J-integral value and its crack size sensitivity in case Sub-Clad Flaw for WWER Reactor Pressure Vessel Integrity Evaluation (2-1872)	120
Applicability of Leak-Before-Break (LBB) technology for primary coolant piping to CPR1000 nuclear power plants in China (2-1884)	123
Limit load solution for an edge cracked plate under combined independent bi-axial membrane and bending (2-1888)	125
Lifetime analysis of WWER Reactor Pressure Vessel Internals concerning material degradation (2-1893)	128
Evaluation of J-Integral for surface cracked plates under biaxial tensile/bending loading using extended reference stress method (2-1899)	131
Application of leak before break assessment for pressure tube in case of delayed hydride cracking (2-1915)	132

Failure behavior for nuclear piping using compact pipe specimen (2-1928)	135
Warm pre-stressing tests for WWER materials (2-1948)	138
Fracture energy and size effect studies for nuclear concrete structures (2-1978)	140
A suggestion to make Gurson damage model mesh independent numerically (2-1985)	142
Overview of fracture mechanics research studies in the UK (2-1987)	144
Ascertaining the micromechanical damage parameters using the small scale test specimens (2-1997)	147
Effect of surface finish and loading conditions on the LCF behavior of austenitic stainless steel in PWR environment (2-2018)	151
Improvement techniques for stainless steel welds (2-2032)	152
Residual stress distribution and guidelines for crack inspection in pipe bends (2-2046)	155
Structural integrity of main heat transport system piping of AHWR (2-2499)	157
Structural integrity assessment of a rupture disc housing with explicit FE-simulation (2-2503)	160
3. Applied Computations, Simulation and Animation	163
Phase field modeling of microstructure evolution in nuclear materials (3-1585)	165
Equivalent material properties of perforated structure for free vibration analysis (3-1600)	166
Interoperability between analysis and detailing software for reinforced concrete (3-1628)	167
Dynamic model of a simple supported RC rectangular plate for spreadsheet application. Part I. Motion in elastic domain (3-1645)	168
Dynamic model of a simple supported RC rectangular plate for spreadsheet application. Part II. Motion in elasto-plastic domain (3-1646)	171
The protection of containers for fresh and spent fuel at extremal transportation operating modes in and around a Nuclear Reactor's Portal (3-1649)	174
Numerical welding simulation on a 14" narrow gap dissimilar metal weld (3-1673)	175
FE analysis of heat exchanger NTIW tubesheets according to new ASME VIII 2007 Div 2 Code. Methodology and automated analysis tool development (3-1682)	178
Comparative stress analyses of major RCPB components by using a prototype of integrated finite element model (3-1727)	180
Calibration of damage parameters for Y5 and G91 steels in use of genetic algorithm (3-1729)	181
Modeling of thermal hydraulics aspects of top water reflow. Experiment PARAMETER-SF3 using SOCRAT/V2 code (3-1733)	182
Simulating dynamic fracture in oxide fuel pellets using cohesive zone models (3-1775)	183

Complex FEM based system of computer codes to model nuclear fuel rod thermo-mechanical behaviour (3-1814)	186
CFD based numerical modules for safety analysis at NPPs: validation and verification (3-1828)	188
The calculation error analysis on carrying force of active magnetic bearings (3-1845)	190
Flow coefficient determination through CFD for nuclear reactor safety (3-1868)	193
An energetic approach of the fluid-structure interaction governing the dynamic behaviour of tubes immersed in a fluid (3-1879)	194
Pretest analysis of CSF model for simulated loss of coolant accident conditions (3-1880)	196
Numerical studies on post accident hydrogen management using fan (3-1894)	198
Numerical studies on atmospheric dispersion and associated flow behaviour for flat, raised bluff body and deep depression (3-1896)	199
Numerical studies of flow structures for square building in cross wind for aspect ratio and representative blockage ration variation (3-1897)	200
Fluid-structure interaction calculations using a linear perturbation method (3-1898)	201
3D CFD analysis of passive auto catalytic recombiner for H ₂ mitigation (3-1902)	203
A computational fluid dynamics study of a buoyant plume at a slope cross wind condition (3-1906)	204
An evaluation of methods for the time-domain simulation of turbulence excitations for tube bundles subjected to non-uniform flows (3-1909)	205
Condensation pool experiments at LUT supporting CFD and structural analysis tool development (3-1913)	207
Experiences from structural dynamic analysis projects of BWR plants within the scope of power uprate projects using FEA (3-1914)	210
Studies on the dynamic behaviour of the Fast Reactor Cores (3-1919)	211
Fluid Structure Interaction models for the dynamic behaviour of tube bundles, application to nuclear structures (3-1920)	212
Solution of random response of structures applied to cylindrical shell in turbulent flow (3-1939)	214
Pressure surges in piping systems induced by transient load pulse (3-1944)	216
“As-Built” site response analysis for nuclear power plants – an improvement to the “State-of-the-Practice” (3-1952)	218
AREVA’s fatigue concept (AFC) – an integrated and multidisciplinary approach to the fatigue assessment of NPP components (3-1962)	220
Investigation of the meso-thermomechanical behaviors of plate-type dispersion nuclear fuel elements (3-1984)	222

Missile impact on reinforced concrete walls: simulation of experiments (3-1989)	224
Research and development of welding process with following local thermocyclice treatment of welding joint of zirconium alloys (3-1992)	226
Comparison of creep life of ORNL plates – RCC-MR VS experiments (3-2007)	227
Guide for verification and validation in computational solid mechanics (3-2010)	229
SPH, MM-ALE & erosion simulation of concrete cylinder perforation (3-2011)	231
Some features of the turbulent flow in tube banks of triangular arrangement (3-2020)	233
Mechanistic modeling of thermal-mechanical deformation of CANDU pressure tube under localized high temperature condition (3-2021)	234
Mesh generation for reactor modeling and simulation: practices, procedures and uncertainties (3-2028)	236
An implicit solution framework for reactor fuel performance simulation (3-2045)	240
Investigations of a long-distance 1000 MW heat transport system with apros simulation software (3-2056)	246
Fatigue relevant temperature fluctuations at the inner pipe surface estimated from the measured outer surface temperatures (3-2106)	247
Application of CFD code PHOENICS for simulating cyclone separators (3-2459)	249
Systematic errors in the numeric analyses of computer programs used for the determination of the flexible structure seismic response (3-2489)	250
Chained computations using an unsteady 3D approach for the determination of thermal fatigue in a T-junction of a PWR nuclear plant (3-2494)	251
Simulation of an impact test with a deformable missile on a concrete wall (3-2502)	260
Thermal and structural analysis of calandria vessel of a PHWR during a severe core damage accident (3-2536)	261
Crack formation and water ingression phenomena in top flooded corium molten pool (3-2537)	262
A statistical uncertainty assessment on a LOFT L2-5 LBLOCA based on ACE-RSM (3-2545)	263
Detailed FEA of locally thinned tight radius pipe bends (3-2575)	265
Modeling of the fluid solid interaction during seismic event (3-2661)	267
Numerical studies on dynamic behaviour of pipelines (3-3141)	268
4. Characterization of Loads	269
Spatial distribution characteristics of seismic ground motion intensities in the Tokyo metropolitan area (4-1584)	271
Residual stress analysis of an overlay weld on a dissimilar metal weld (4-1629)	273

Peak reduction of elastic floor response spectra (4-1657)	275
The influence of non-classical damping on subsystem response (4-1657)	276
How reliable are the ground motion prediction equations? (4-1662)	277
Hazard consistent structural demands and in-structure design response spectra (4-1717)	280
Analytical study of containment behaviour under fire due to aircraft fuel spillage (4-1805)	281
CFD analysis of atmospheric dispersion in a large terrain of Kakrapar atomic power station in presence of structural buildings (4-1869)	283
Studies of medium scale non-axisymmetric aluminium missile impacts (4-1876)	284
Contribution to the design of concrete sections reinforced with externally fiber polymers (4-1886)	286
Validation of aircraft FE model for impact analyses (4-1929)	289
Measurement of residual stresses in the dissimilar metal weld joint of a safe-end nozzle mock-up (4-1938)	290
Validation of Riera loading in LS-DYNA models of missile impact (4-1946)	293
Evaluation of Indian nuclear coastal sites for tsunami hazard (4-1976)	294
On the site specific amplification functions for Center and Eastern United States (4-2029)	296
Sensitivity of PSHA in the region of Peninsular India (4-2041)	298
Survey of tornado load research at Texas Tech: past, present and future (4-2506)	301
Smaller-size NPP for isolated area, and its net-work stability consideration (4-2624)	303
Development, implementation and implications of the enhanced Fujita Scale (4-3136)	304
Structural integrity evaluation of shielding blocks for HANARO's cold neutron guide (4-3137)	306
Analysis of the strong motion records obtained from the 2007 Niigataken Chuetsu-oki earthquake and determination of the design basis ground motions at the Kashiwazaki Kariwa Nuclear Power Plant. Part 1. Outline of the strong motion records and estimation of factors in large amplification (4-3189)	309
Analysis of the strong motion records obtained from the 2007 Niigataken Chuetsu-oki earthquake and determination of the design basis ground motions at the Kashiwazaki Kariwa Nuclear Power Plant. Part 2. Difference of site amplification based on the 2D FEM analysis of the folded structure (4-3190)	312
Analysis of the strong motion records obtained from the 2007 Niigataken Chuetsu-oki earthquake and determination of the design basis ground motions at the Kashiwazaki Kariwa Nuclear Power Plant. Part 3. Determination of the design basis ground motions considering findings from the earthquake (4-3191)	315

5. Modeling, Testing and Response Analysis of Structures, Systems and Components	319
PBMR loop acoustics (5-1577)	321
Frequency-dependent impedances in the time-domain SSI analysis: modification of seismic input (5-1592)	322
Earthquake-induced sloshing effects on seismic qualification of liquid storage tanks (5-1594)	324
Nonlinear impact analysis of pipe whipping onto restraints (5-1595)	327
Seismic response evaluation of safety related nuclear structure with yielding dampers using linearization techniques (5-1597)	330
Seismic stability of glove boxes – experiments and analysis (5-1598)	332
Pipe behaviour under radiolysis gas detonations (5-1601)	334
Missile impact on structural members (5-1603)	336
A model for the hysteresis of concrete to describe the cyclic fatigue of reinforced concrete structures during an earthquake (5-1632)	339
Systematic errors in the numeric analyses of computer programs used for the determination of the flexible structure seismic response (5-1635)	349
On scale effects and mesh independence in dynamic fracture analysis by means of the discrete element method (5-1640)	350
Steam generator tube plugging FEM analysis (5-1641)	352
An optimal solution search under design for a pipeline support system to withstand a seismic excitation (5-1653)	354
Seismic qualification of class II buildings of nuclear power plants on the basis of non-nuclear seismic codes (5-1656)	356
Experiments on gamma-ray shielding performance of cracked reinforced concrete (5-1660)	357
SSI Analysis of PBMR module building to South African high frequency input motions (5-1665)	358
Aircraft crash analysis of PBMR module building (5-1666)	360
More precise definition of Rayleigh damping matrix in dynamic analysis of NPP civil structures on ABAQUS (5-1667)	363
Reducing of spectral accelerations in NPP civil structures at the expense of optimization of their geometry (5-1668)	365
Seismic analysis of reactor building of a NPP including soil structure interaction effects and comparison with two additional sites (5-1669)	367
The effect of cover unit drop on Loviisa NPP primary circuit during maintenance outage (5-1670)	368

Study on the MOX fuel manufacture glovebox containment for earthquakes – deformation and leakage tests for window panels (5-1680)	369
Safety significance of a type of seismic input motions and consequences on nuclear industry practice – results of the IAEA coordinated research project on the “Safety significance of near-field earthquakes” (5-1683)	371
Analysis of behaviour of raft foundations under seismic and impulsive loading (5-1689)	373
Generation of dynamic mechanical model of inertial soil foundation in consideration of NPP structures basement finite stiffness (5-1692)	375
FORTUM Participation in BARCOM Round Robin pre-test simulation: mid-term analysis (5-1696)	377
Damping values for seismic design of nuclear power plant SC structures (5-1697)	379
SMART 2008 project. Experimental tests of a reinforced concrete building subjected to torsion. Part 2: presentation of the tests results (5-1700)	382
FORTUM participation in IAEA EBP benchmark for Kashivazaki-Kariwa NPP unit 7 response in July 2007 event (5-1701)	384
Identification of modal parameters of a containment building using ambient vibration measurements (5-1702)	385
Expansion of the Riera approach for predicting aircraft impact damage to steel and concrete buildings – Part 2 – simplified analysis methodology (5-1711)	388
Experimental study on seismic reduction effectiveness of main control room in N.P.P using 3-directional isolation system (5-1713)	390
Activities of OECD/NEA in the fields of seismic hazard assessment & earthquake engineering (5-1721)	393
Experimental studies of confinement integrity of metal cask subjected to impulsive loads due to aircraft engine crash (Part 1) (5-1730)	395
Amplification of seismic motion at deep soil sites (5-1740)	397
VTT IMPACT program – First phase: Lessons gained by IRSN (5-1746)	398
Conservatism in the use of stick models in dynamic SSI analysis (5-1749)	401
Earthquake fatigue analysis for CANDU® nuclear power plants (5-1772)	402
Case study: seismic Soil-Structure-Interaction analysis for a site with varying soil thickness (5-1776)	404
Verification test for integrity of equipment foundations affected by dynamic load (5-1777)	407
Fuel assembly two-beam dynamic model response to faulted condition loads (5-1780)	409
Analytical study on seismic energy balance of NPP buildings. Part 1. Formulation and validity of lattice model (5-1781)	410
Dynamic interaction between the shaking table and the specimen during earthquake tests (5-1783)	412

Comparison of approximate methods for sliding and rocking evaluation of unanchored platforms (5-1784)	414
Effects of liner degradation on the severe accident consequences at a PWR plant with a reinforced concrete containment (5-1786)	416
High energy pipe rupture effects elimination – experience from projects dealing with WWER 440 V2 NPP piping assessment (5-1787)	418
Stress analysis criteria for piping. RCC-M 2002 rules and validation (5-1790)	421
Vibration tests on nuclear power station stacks equipped with structural control oil dampers (5-1792)	424
Performance based capacity assessment of WWER-1000 containment structure for internal accidents (5-1807)	426
Seismic analysis of WWER–1000 control rod drive system (5-1810)	429
Off-axis underground soil pressures from surface impact loads (5-1811)	430
Modal identification of cabinets of nuclear power plant using experimental test (5-1813)	432
On the floor response spectra due to aircraft impact (5-1816)	433
Structural responses of conventional and base-isolated nuclear power plants for blast loadings (5-1819)	436
Seismic margin assessment of Demineralized Water Reserve Tank (5-1829)	438
Study on non-stationarity of frequency by synthesis method of earthquake motions (5-1830)	439
Generation of an artificial time history matching multiple-damping floor design response spectra (5-1832)	441
Modeling of high viscous dampers in piping dynamic analysis. Different approaches and acceptable limits for simplifications (5-1833)	443
Vibration analysis and fatigue assessment of the RBMK-1000 primary piping considering actual operational conditions (5-1836)	444
Analytical study on seismic energy balance of NPP buildings. Part 2. Verification, application and ultimate state with energy index (5-1838)	445
Heat-mechanics interaction behavior of lead rubber bearings for seismic base isolation under large and cyclic lateral deformation. Part 1. Dynamic loading test of LRB and development of analytical method (5-1839)	447
Heat-mechanics interaction behavior of lead rubber bearings for seismic base isolation under large and cyclic lateral deformation. Part 2. Seismic response analysis of base isolated reactor building subjected to horizontal bi-directional earthquake motions (5-1840)	449

1. Mechanics of Materials

Properties of materials and constitutive laws for monotonic, cyclic and dynamic loadings. Experimental and analytical methods applied to nonlinear behavior of isotropic and anisotropic materials. Effects on behavior of materials and welds of thermal cycling, aging, embrittlement, welding, stress corrosion, residual stress, fatigue, creep, cavitation, and interactions. Development of design rules. Nano materials.

Study of Bree's daigram with nonlinear kinematic hardening model (1-1578)

Ali Nayebi

Mechanical Engineering Department, Engineering Faculty
Shiraz University, Shiraz, Iran
e-mail: nayebi@shirazu.ac.ir

Introduction

Cyclic loading of mechanical parts is an important subject in design of these elements. The behavior of different parts under different loadings is dependent on many factors; such as type of loading, material behavior and structure under loading. The answer of mechanical structures under these parameters can be elastic shakedown, plastic shakedown and ratcheting.

In this research, the Armstrong-Freiderick model was used to model the answer of a thin cylindrical shell under constant mechanical loading and cyclic thermal gradient across the shell wall. The use of the return mapping algorithm permitted to determine the structure behavior under different combination of loading.

The studied pressure vessel was considered as a thin cylinder represented by the mean radius as R and the wall thickness t . It is closed at both ends. The can is subjected to an internal pressure p and a heat flux through its internal surface. The temperature decreases along its wall thickness and it cycled between ΔT and zero. It is assumed that the cylindrical shell is very long and the end effects and the curvature can be neglected.

The behavior of a thin closed cylinder was investigated. Constant mechanical and cyclic loading were applied. Maximum inside pressure (mechanical loading) was not exceeded than yield pressure. So, the incremental loading consists of linearly varying temperature difference distribution across the wall-thickness and increasing from zero. When the linear temperature gradient attains the maximum, the temperature gradient is decreased incrementally until zero gradient is reached, at which point a full thermal stress cycle is completed. The number of loading increments varies in different load cases in the test matrix, as each increment applies less than 1°C in temperature gradient. Up to 100 load increments per cycle are applied in the most severe temperature gradients. In some cases, a steady cyclic state stress-strain plot is attained after the first cycle.

As a function of applied mechanical and thermal loading, different answers were obtained in the inner and outer surface of the thin cylinder. The Bree's diagram is divided to the 6 regions as a function of the first yield situation and the in and outer behavior. These regions are shown in the table 1.

Table 1. Stress regimes for Bree's cylinder behavior.

Region	Inner surface		Outer surface	
	Hoop direction	Axial direction	Hoop direction	Axial direction
A	Elastic	Elastic	Elastic	Elastic
B	Elastic	Elastic	Elastic Shakedown	Elastic Shakedown
C	Elastic Shakedown	Elastic Shakedown	Elastic Shakedown	Elastic Shakedown
D	Plastic Shakedown	Plastic Shakedown	Elastic Shakedown	Elastic Shakedown
E	Plastic Shakedown	Plastic Shakedown	Plastic Shakedown	Plastic Shakedown
F	Ratcheting	Ratcheting	Ratcheting	Ratcheting

Tensile and toughness properties of materials for the RSE-M Code (1-1654)

Patrick Le Delliou¹, Bruno Barthelet², Aurore Parrot¹, Lionel Sainton¹,
Marc Berveiller¹, Sébastien Saillet¹

¹Electricité de France, R&D Division, Moret-sur-Loing, France

²Electricité de France, Nuclear Generation Division, Saint-Denis, France

The RSE-M Code provides the essential rules and requirements for in-service inspection of pressure retaining components of the French NPP. Its scope is close to the scope of ASME B&PV Code Section XI Division 1, except that concrete components and metallic liners are not included.

The Code includes a procedure for determining the acceptability of flaws that have been detected by in-service inspection. The procedure is based upon the principles of fracture mechanics (LEFM and EPFM) and applies to ferritic and austenitic materials of the main components and piping. It makes use of partial safety factors on loading and material mechanical properties, so these properties must rely on a statistical approach. Yield strength and ultimate tensile strength 5% fractiles and dimensionless reference true stress-strain curves are provided by the Code for base metals and welds. For piping materials, the 16% fractiles of $J_{0,2mm}$ and $J-\Delta a$ curves were codified using the relationship $J_{\Delta a} = C\Delta a^n$. Mean values and standard deviations are given for fatigue crack growth rates for the main materials.

Between 2004 and 2006, a project was conducted to improve RSE-M Code flaw evaluation and to reduce unnecessary conservatism. One objective of this project was to better understand the effects of aging and to improve the statistical analysis of the databases from experimental fracture mechanics programs on austenitic stainless steel piping and carbon-manganese ferritic steel piping and associated welds. For austenitic stainless steel welds, the effects of thermal aging on fracture toughness were better determined. Fracture toughness tests were conducted at different temperatures, on aged welds from different weld processes, including gas tungsten-arc weld. For carbon-manganese steels, the effects of strain aging on tensile properties and fracture toughness were studied by fracture toughness tests and theoretical models. Correlations were developed for estimating fracture toughness, tensile properties of carbon-manganese steel from material information of acceptance reports as sulfur content, aluminum content or upper shelf Charpy impact energy.

These results will be useful to add or to improve statistical characteristic values in the next RSE-M Code edition. The new values will be generally higher than the former values.

PACE-1450 – Experimental investigation of the crack behaviour of prestressed concrete containment walls considering the prestressing loss due to aging (1-1671)

Nico Herrmann¹, Lutz Gerlach², Harald Müller³, Christoph Niklasch⁴,
Daniela Kiefer⁵, Yann Le Pape⁶, Christophe Bento⁷

¹Materials Testing and Research Institute, MPA Karlsruhe, Universität Karlsruhe (TH), 76128 Karlsruhe, Germany, e-mail: herrmann@mpa-karlsruhe.de

²Materials Testing and Research Institute, MPA Karlsruhe, Universität Karlsruhe (TH), 76128 Karlsruhe, Germany, e-mail: lutz.gerlach@mpa-karlsruhe.de

³Materials Testing and Research Institute, MPA Karlsruhe, Universität Karlsruhe (TH), 76128 Karlsruhe, Germany, e-mail: hsm@mpa-karlsruhe.de

⁴Züblin AG, 70567 Stuttgart, Germany, e-mail: christoph.niklasch@zueblin.de

⁵Schöck Bauteile GmbH, 76534 Baden-Baden, Germany
e-mail: daniela.kiefer@schoeck.de

⁶EDF R&D, 77250 Moret-sur-Loing, France, e-mail: yann.le-pape@edf.fr

⁷EDF R&D, 78401 Chatou, France, e-mail: christophe.bento@edf.fr

Different civil engineering R&D programs dedicated to the analysis of nuclear power plant containments behaviour have been performed in the last decades. The crack initiation and the leakage through the prestressed concrete containment walls are some of the matters of particular interest. Experimental investigations under loading conditions which also include the limit state under containment overpressure are the basis for new constitutive laws for concrete and techniques of modelling which have to be implemented in finite element codes. The models and the methodology have to be verified by comparing their performances with experimental results. These results are normally gained by performing simple tests on small sized specimens which are sometimes not representative regarding the behaviour of structural members of realistic dimensions. In order to determine the capability of the simulations to predict the structural behaviour of realistic and representative structural parts more complex tests are indispensable. A test facility of this kind will be presented in this paper.

As an intermediate sized experiment the “PACE 1450 - Experimental Campaign” aims to investigate the behaviour of a curved specimen which is representative for a 1450 MW nuclear power plant containment under accidental loading conditions. The specimen with the dimensions of 3.5 m in length, 1.8 m in width and 1.2 m in height represents a cut-out of the cylindrical part of a prestressed reinforced concrete containment. Due to experimental boundary

conditions for the tensile load the total length of the specimen has to be larger than the observation area of a length of 2 m standing for the representative part of the containment. The reinforcement layout is very similar to the original geometry and consists mainly of meshes of reinforcement bars near the inner and outer surface and four prestressing cables with each of them consisting of 37 strands within ducts in the circumferential direction. In the orthogonal direction one duct which represents the original vertical prestressing is installed but remains passive.

During the tests the specimen is loaded by air pressure with the help of a pressure chamber placed on the top of it which simulates the internal containment pressure of up to 7 bars absolute. The resulting ring tensile stress in the cylindrical part of the containment which is the consequence of the internal pressure is applied externally by eight hydraulic jacks with each of them being capable of introducing a force of up to 10 MN. With the help of these hydraulic jacks a tensile stress of up to 18 MPa can be applied to the specimen in the circumferential direction. An initial prestressing of the specimen of 12 MPa in this direction is realised in such a way that decreasing the prestressing force for the purpose of simulating the aging of the structure is possible. The prestressing of 1 MPa in the orthogonal direction is realised by external cushions. The decrease of the prestressing force is performed in steps of 20% of the original force. Within the test series consisting of a pre-test (RUN0) and the following four tests (RUN1 to RUN4) the prestressing is kept at 100% for RUN0 and RUN1. RUN2 is performed with 80%, RUN3 and RUN4 with 60% of the original prestressing force.

In order to obtain information about the behaviour of the containment wall segment under the chosen conditions, the specimen is equipped with embedded optical fibre strain and temperature sensors and a sound detection system to record the initiation of cracks. Additionally the displacement of the edges is measured by non-contact Laser sensors and inductive sensors. The paper will explain the setup in detail and will present results of the test series.

Acoustic emission monitoring of slow strain rate tensile tests of 304L and 316L stainless steels in supercritical water environments (1-1674)

Dušan Prchal, Radek Novotný, Kristián Máthis, Peter Hähner, Luigi Debarberis
European Commission, JRC-Institute for Energy
P.O. Box 2, NL-1755 ZG Petten, The Netherlands

Two experimental set-ups have been built and qualified, in order to perform slow strain rate tensile tests (SSRT) on 304 L and 316 L stainless steels in supercritical water (SCW) condition (550°C, 250 bar and 300 bar, respectively). In the first case the supercritical water has been circulated inside internally pressurized tubular specimens mounted into a universal mechanical test rig and heated by electromagnetic induction. The second set-up is based on a miniaturized SSRT rig integrated into an SCW autoclave which is fed by a recirculation loop with full control of the water chemistry. Both set-ups enable *in-situ* monitoring of acoustic emission and electrochemical potential during the SSRT. The SCW environment is found to significantly influence the mechanical performance of the specimens. A correlation between the acoustic emission response and the change of electrochemical potential as a result of corrosion processes is revealed. The advantages and potentialities of both set-ups are also discussed.

Prediction of fracture toughness for nuclear piping using curved wide-plate test (1-1676)

Soo Park¹, Hong Sun Park², Sung Keun Cho², Jae Mean Koo³, Chang Sung Seok⁴

^{1,2} Graduate School of Mechanical Engineering, Sungkyunkwan University
300 CheonCheon-dong, Jangan-gu, Suwon, Kyeonggi, 440-746, Korea
e-mails: roonasis@skku.edu, sungkny@skku.edu

^{3,4} School of Mechanical Engineering, Sungkyunkwan University
300 CheonCheon-dong, Jangan-gu, Suwon, Kyeonggi, 440-746, Korea
e-mails: kjm9000@daum.net, seok@skku.edu

For estimate crack of real pipe based on elastic-plastic fracture mechanics, first of all we must measure correct fracture toughness from pipe. But in case of fracture resistance test by using real pipe, it takes much time and expense. Also the test is very difficult. For reason of these weak points, many researchers have been performing fracture resistance test by using standard specimens, instead of real pipe. Because of standard specimen test is easy to test. Typical example of standard specimen is Compact Tension Specimen and Three Point Bending Specimen. But fracture toughness from these standard specimens are conservative than fracture toughness from real pipe because difference of constraint effect between real pipe and standard specimen. So for correct crack evaluation estimate, we need new specimen which can express constraint effect of real pipe. [1]

According to these facts, many researchers proposed non-standard specimen for express constraint effect of real pipe. Specimens which researcher has proposed are not collected from real pipe. For example, non-standard specimens are DENT, SENT and CCT. [3] Recently researchers proposed non-standard specimens which can collect directly from real pipes. And fracture resistance test from these specimens are progressing.

There are x specimen, ring specimen and curved-wide plate specimen which collect directly from pipe. X and ring specimens [5, 6] can apply to thin and small diameter pipes only. So these specimens can't apply to nuclear power plant pipe. But curved-wide plate specimen can apply to thick and large diameter specimen like nuclear power plant pipe. Also it is easy to collect from pipe and we don't have to machining. [4] Today the research for curved-wide plate specimen is estimated about limited crack length ratio. But its applicability was not verified perfectly.

So proposal of this study are suggestion of fracture resistance test method with curved-wide plate specimen and verification of new test method. For this study, we performed finite element analysis and fracture resistance test about various crack length ratio. And then we calculated J-integral.

For acquisition of mechanical property, we performed tensile test. The specimen was collected from real pipe. From the tensile test result, we could acquire Ramberg-Osgood parameter and we used Ramberg-Osgood parameter for elastic-plastic finite element analysis. We calculated J-integral using finite element analysis, and then extracted η equation which is very important factor for plastic element of J-integral. So fracture resistance test of curved-wide plate specimen became easy.

We performed fracture resistance test using 25 ton UTM. At this time, we used DCPD method for crack length measurement. From the test result, J-integral was calculated and compared with J-integral from real pipe test.[2] And we verified applicability of curved-wide plate specimen.

From this result we can obtain conclusion as follows.

- (1) We performed elastic-plastic finite element analysis and suggested η equation which is important factor for plastic element of J-integral. From this, fracture resistance test became easy.
- (2) J-integral values from curved-wide plate specimen and real pipe were compared. Results of fracture resistance test from real pipe and curved-wide plate specimen were showed similarly. Thus we established applicability about curved-wide plate specimen.

Reference

1. ASTM, 2001. Standard Test Method for Measurement of Fracture Toughness. ASTM Standard E1820-01.
2. Park, J.S., Seok, C.S. 2002. A Study on the Evaluation of the Pipe Fracture Characteristic (II). Proceedings of the KSME Spring Meeting. Pp. 436–441.
3. Kim, J.S., Cho, S.M., Kim, Y.J., Kim, Y.J. 2003. Specimen Thickness and Crack Depth Effects on J Testing and Crack Tip Constraint for Non-standard Specimen. KSME, Vol. 2, 7 No. 9, pp. 1531–1538.
4. Huh, N.S., Kim, Y.J., Choi, J.B., Kim, Y.J., Lim, H.S., Chung, D.Y. 2004. Prediction of Failure Behavior for Nuclear Piping Using Curved Wide-Plate Test. KSME, Vol. 28, No. 4, pp. 352–361.
5. Hsu, H.H., Chien, K.F., Chu, H.C., Kuo, R.C., Liaw, P.K. 2001. An X-Specimen Test for Determination of Thin-Walled Tube Fracture Toughness. Fatigue and Fracture Mechanics 32nd Vol.
6. Arsene, S., Bai, J. 1996. A New Approach to Measuring Transverse Properties of Structural Tubing by a Ring Test. Journal of Testing and Evaluation, Vol. 24, No. 6, pp. 386–391.

Development of constitutive models for fast reactor design – strategy of the study and results in the first half stage (1-1677)

Kazuyuki Tsukimori¹, Koji Iwata², Nobuchika Kawasaki³,
Hiroki Yada⁴, Naoto Kasahara⁵

¹Advanced Nuclear System Research and Development Directorate
JAEA, 1, Shiraki, Tsuruga-shi, Fukui-ken, 919-1279, Japan
e-mail: tsukimori.kazuyuki@jaea.go.jp

²Visiting Researcher, JAEA, 4002, Narita, O-arai, Ibaraki-ken, 311-1393, Japan
e-mail: koji.iwata@ctc-g.co.jp

³Advanced Nuclear System Research and Development Directorate
JAEA, 4002, Narita, O-arai, Ibaraki-ken, 311-1393, Japan
e-mail: kawasaki.nobuchoka@jaea.go.jp

⁴Advanced Nuclear System Research and Development Directorate
JAEA, 1, Shiraki, Tsuruga-shi, Fukui-ken, 919-1279, Japan
e-mail: yada.hiroki@jaea.go.jp

⁵ Visiting Researcher, JAEA / Professor, University of Tokyo
7-3-1, Hongo, Bunkyo-ku, Tokyo, 113-8656, Japan
e-mail: kasahara@n.t.u-tokyo.ac.jp

R&D to enable a practical fast breeder reactor plant is proceeding in Japan. One of the key issues of R&D is to realize a reasonably small reactor vessel by eliminating the thermal liner which is installed inside the vessel in order to reduce thermal loading in the conventional design. Most important concern is the amount of the inelastic strain of the vessel accumulated around the liquid sodium surface which moves up and downward cyclically with start-up and shut-down. If we apply the existing design method, there is the possibility that the estimation of the strain amount becomes too conservative and exceeds the strain limit of the rule. The aim of this study is to develop rational constitutive models that enable prediction of this kind of complex inelastic behaviors precisely and to prepare the design guide based on inelastic analysis.

The requirements for the target constitutive models are as follows.

- (1) can express the nonlinearity of stress-strain relation of the material (316FR stainless steel in this study)
- (2) can be applied to cyclic loading conditions in the elastic plastic region
- (3) can predict the stress- strain behavior properly under the temperature changing conditions (~ 600 deg. C)
- (4) can be applied to non-proportional multi-axial behaviors
- (5) can guarantee conservativeness of the analysis results for design evaluation.

In order to develop the constitutive models that satisfy these requirements, we are proceeding a project consisting of the following five parts.

(i) Simulation analyses of the inelastic stress-strain behavior of the reactor vessel made of 316FR by using the existing analysis methods; The aim is to understand the mechanism of the strain accumulation in the liquid surface traveling region including the effect of the primary stress and grasp the characteristic stress-strain-temperature behaviors and their ranges to be covered by the constitutive models roughly.

(ii) Development of candidate constitutive models; The formulation of some constitutive models was implemented and basic check was done partially by comparing with the existing studies and the verification tests mentioned later. We are preparing two kinds of models considering practical use, one is a simple and convenient model and the other is a detailed and precise model. Concerning the expression of the nonlinearity of stress-strain relation, two methods were tried, i.e., the multi-linear approximation based on the multilayer back stress model¹⁾ and the smooth curve approximation based on the two-surface model²⁾.

(iii) Incorporation of candidate constitutive models into the general purpose structural analysis system; Since large scale analyses are needed in the practical design, the incorporation of the constitutive models and the study of effective numerical procedures are proceeded simultaneously.

(iv) Material property tests: These tests were conducted to get the basic property data of the target material and to determine the constants of constitutive models.

(v) Verification tests for the validity of the constitutive models; Uniaxial tests with strain and temperature controlled under monotonic / cyclic loadings, biaxial tests with non-proportional loadings and structural element tests are conducted. The uniaxial and the biaxial tests were composed by introducing the characteristic behaviors obtained from the above simulation analyses of the reactor vessel. The structural element tests aim at verification of the constitutive models, focusing on the ratcheting phenomena.

This R&D started from late 2006FY and will finish at the end of 2009FY. In this paper, the framework and strategy of the R&D and the results in the first half stage, especially the development of MK-SRR (Multilinear Kinematic hardening model with Stress Reversal-on Resetting) which is in the category of the simple and convenient model, are introduced.

Present study is the result of “Development of elevated temperature structural design method for fast reactor vessels” entrusted to JAEA by the Ministry of Education, Culture, Sports, Science and Technology of Japan (MEXT).

References

1. N. Ohno, J.-D. Wang, *Int. J. Plasticity*, 9(1993), pp. 375–390.
2. K. Iwata, *NED*, 139(1993), pp. 319–326.

Modeling the pseudoelastic response of shape memory alloy cylindrical shells using a nonlinear finite element formulation (1-1690)

M. Shakeri, M. Sadighi

Mechanical engineering department, Amirkabir University of Technology
Tehran, Iran
e-mail: shakeri@aut.ac.ir

Shape memory alloys (SMAs) have recently been considered in many areas of applications due to their unique ability in generating relatively large inelastic deformations and high stresses. The distinctive properties of SMAs are caused by their ability of changing crystallographic structure by solid state transformation between a high symmetry parent phase (austenite) and a low symmetry phase (martensite) in response to mechanical and/or thermal loadings. This state transformation between two stable phases, which is called martensitic phase transformation results in unique properties for structures made of SMAs such as the ability of recovering the original shape after large deformations by applying appropriate thermal procedure. Due to their exclusive characteristics, SMAs are widely used in various applications such as biomedical [1], aerospace [2] and mechanical engineering [3, 4]. As a result of martensitic phase transformation and according to the specific way that the transformation occurs, SMAs exhibit two significant macroscopic phenomena which are called the shape memory effect (SME) and pseudoelasticity.

The solid-to-solid phase transformation in SMAs results in highly non linear coupled material response which causes significant challenges for introducing constitutive relations in stress-temperature space. Many researches are carried out on implementing the finite element method in conjunction with macroscopic phenomenological constitutive models for simulating various SMA structures ranging from trusses [5] to beams and plates [6] subjected to thermomechanical loadings. However, to the authors' knowledge, no research on the nonlinear finite element formulation of SMA cylindrical panels based on shell theories has been reported in the literature. In this paper, a general incremental finite element formulation capable of modeling material nonlinearities based on the first order shear deformation theory (FSDT) is developed for modeling the pseudoelastic response of cylindrical shells. The Boyd-Lagoudas's polynomial hardening model [7] in conjunction with 3D incremental convex cutting plane explicit algorithm is implemented for preparing the SMA constitutive model in the finite element formulation. Some numerical examples are considered for demonstrating

the performance of proposed finite element formulation in modeling the pseudoelastic response of cylindrical SMA panels under loading-unloading cycles in different temperatures.

References

1. Petrini, L., Migliavacca, F., Massarotti, P., Massarotti, S., Dubini, G., Auricchio, F. Computational studies of shape memory alloy behavior in biomedical applications. *Journal of Biomechanical Engineering*, 2005; 127: 716–725.
2. Hartl, D.J., Lagoudas, D.C. Aerospace applications of shape memory alloys. *Journal Aerospace Engineering, Proc. IMechE Part G*. 2007; 221: 535–552.
3. Paine, J.S.N., Rogers, C.A., Smith, R.A. Adaptive composite materials with shape memory alloy actuators cylinders and pressure vessels. *Journal of intelligent material systems and structures*, 1995; 6: 210–219.
4. Birman, V. Review of mechanics of shape memory alloy structures. *Applied Mechanics Reviews*, 1997; 50(11): 629–645.
5. Bandeira, E.L., Savi, M.A., Monteiro, P.C.C., Netto, T.A. Finite element analysis of shape memory alloy adaptive trusses with geometrical nonlinearities. *Arch Appl Mech*, 2006; 76: 133–144.
6. Liew, K.M., Ren, J., Reddy, J.N. Numerical simulation of thermomechanical behaviours of shape memory alloys via a non-linear mesh-free Galerkin formulation. *International Journal for Numerical Methods in Engineering*, 2005; 63:1014–1040.
7. Boyd, J.G., Lagoudas, D.C. A thermodynamic constitutive model for the shape memory alloy materials. Part I. the monolithic shape memory alloy. *International Journal of Plasticity*, 1996; 12: 805–842.

A mixed yield surface for modeling the anisotropic creep behavior of Zirconium alloys (1-1695)

Mathieu Priser^{1,2}, Jean-Marc Cloue², Philippe Pilvin¹, Dominique Poquillon³

¹LIMATB, Université Bretagne-Sud,
rue Saint-Maudé, F-56321 Lorient cedex

²AREVA, AREVA NP

10 rue Juliette Récamier, F-69456 Lyon cedex 06

³CIRIMAT, CNRS/UPS/INPT

118, route de Narbonne, F-31077 Toulouse cedex 04

Internal variable constitutive models have been extensively improved during the past decade mainly for industrial purposes. In this paper, a new yield criterion is proposed to model the anisotropic behavior of textured zirconium alloys. A polycrystalline model which was developed in previous studies (Geyer *et al.* [1], Onimus *et al.* [2]) is widely used in this paper. This micromechanical model which is based on the description of microscopic plasticity mechanisms is very reliable and is considered as a reference in this study. The main idea of this paper is to use the numerical results given by this polycrystalline model to develop a macroscopic model. Using information provided by numerical yield surfaces, this study shows that zirconium alloys exhibit very different mechanical behaviors according to loading paths. However, these observations can be reproduced by a non quadratic mixed yield surface criterion (Bron *et al.* [3]) which is detailed in this paper. An application of this approach for Zircaloy-4 cladding tubes is presented.

References

1. P. Geyer, X. Feaugas, P. Pilvin. Modeling of the anisotropic viscoplastic behavior of fully annealed zircaloy-4 tubes by a polycrystalline approach. Plasticity'1999, Cancun, January 1999.
2. F. Onimus, I. Monnet, J.L. Béchade, C. Prioul, P. Pilvin. A statistical TEM investigation of dislocation channeling mechanism in neutron irradiated zirconium alloys. Journal of Nuclear Materials, Vol. 328, Issues 2–3, 1 July 2004, pp. 165–179.
3. F. Bron, J. Besson. A yield function for anisotropic materials. Application to aluminum alloys. International Journal of Plasticity, Vol. 20, Issues 4–5, April–May 2004, pp. 937–963.

Local failure criteria for wall-thinning defect in piping components based on simulated specimen and real-scale pipe tests (1-1703)

Jin Weon Kim^{1*}, Jong Sun Park¹, Sung Ho Lee²

^{1*}Department of Nuclear Engineering, Chosun University
375 Susuk-dong, Dong-gu, Gwangju, 501-759, Republic of Korea
e-mail: jwkim@chosun.ac.kr

²Nuclear Power Laboratory, Korea Electric Power Research Institute
103-16 Munji-dong, Yuseong-gu, Daejeon, 305-380, Republic of Korea
e-mail: kslee@kepri.re.kr

Local wall-thinning due to flow accelerated corrosion is considered as a main degradation mechanism of carbon steel piping system in nuclear power plant (NPP). Thus, the integrity evaluation of piping components containing local wall-thinning has become more important in maintaining the reliability of nuclear piping system. Several analytical and experimental studies have been conducted to develop a integrity evaluation procedure and acceptance criteria for a pipe with a wall-thinning defect. These revealed that the results of an integrity evaluation of wall-thinned piping component depend on the defect geometry, the failure criterion, and the type of loading. Of special note, the failure criterion directly affects the result of the integrity evaluation and it is influenced by the characteristics of the material and stress state at wall-thinned area. Thus, it is important to develop a reliable failure criterion that is reflected these characteristics of wall-thinning defect in the piping component and to employ it to the evaluation. The objective of this study is to develop a reliable local failure criterion for a wall thinning defect in the piping components.

In this study, therefore, a series of tensile tests was performed using specimens with different stress states, including smooth and notched round bar specimen, and finite element (FE) simulations were performed on these specimens to find the stress and strain states at maximum load and final failure. From these results, we proposed local failure criteria to be able to predict the maximum load and final failure of specimen as form of equivalent stress and equivalent strain, respectively, including local stress state. To verify the proposed failure criteria, tensile test using grooved plate specimens, i.e. simulated specimens, that have different groove radius and burst test using real-scale pipe specimens with a local wall-thinning defect were performed, and the failure load and failure pressure for each specimen were obtained. First of all, the maximum load and final failure of grooved plate specimens were estimated

applying the proposed local failure criteria to the finite element analyses results. It showed that the proposed equivalent stress and equivalent strain criteria accurately estimate the maximum load and final failure of grooved plate specimens, respectively. These criteria also used to predict the failure pressure of wall-thinned pipe specimens. The results showed that the equivalent stress criterion accurately predicted the failure pressure of local wall-thinned pipe, but the equivalent strain criterion overestimated the failure pressure. Therefore, it is demonstrated that the proposed both criteria reliably predict the maximum load carrying capacity and final failure of specimen under tensile load, and in particular the equivalent stress is an accurate criterion for failure pressure prediction of a wall-thinned piping component.

Simulation of roll expansion on Steam Generator tubes (1-1720)

Messier Julien^{1*}, Cano Valérie¹, Geniaut Samuel¹,
Hasnaoui Frédéric², Sellali Nabila¹

¹EDF R&D, 1 avenue du Général de Gaulle, B.P. 408, F-92141 Clamart Cedex

²EDF R&D, 6 quai Watier, B.P. 49, F-78401 Chatou Cedex

*Contact person: julien.messier@edf.fr

Context and object

Steam Generators tubes constitute critical PWR components owing to their heat exchange function as well as their function of safety barrier between primary and secondary circuits.

Among the actual Steam Generator tubes, many crack networks can be observed in the transition roll expansion area. These cracks can have many causes, but they are essentially linked with:

- fabrication process (residual stresses due to mechanical roll expansion)
- operating loads (thermal and hydraulic cyclic solicitations, primary and secondary corrosion).

In order to understand these phenomena aiming to obtain safety margin assessment, and to be able to optimize the fabrication process, we need to evaluate, by numerical simulation, the residual stress field due to the roll expansion.

Indeed, a thorough knowledge of these stress fields is essential in order to understand and predict crack phenomena.

Method and hypotheses

In the early '90, experimental and theoretical works have given a good evaluation of this residual stress field on the inner surface of the tube in its main directions.

Nevertheless, the great improvements of calculation means allow us today to make this result more complete and, particularly, to obtain a full evaluation of the stress field in the whole structure through a realistic representation of contact between the tool and the tube.

Code_Aster [1], Open Source FEA software developed at EDF R&D, is appropriate to solve non-linear mechanical analyses such as roll expansion simulation.

It combines different non-linearities:

- Geometrical ones idealized by contact algorithm which transforms displacements of the rolling tool into load inside the tube,
- Material ones idealized by the material constitutive model of the structure that allows the plastic expansion of the tube inside the tube-sheet.

The tube material constitutive relation is identified using characterization experiments (tensile and cyclic tests) on same material and geometry.

Taking into account calculation constraints, the best fitting relation is a Von Mises law with a combined work-hardening including both linear kinematic and isotropic parts.

The numerical model is made of three components: rolling tool, tube-sheet and tube in a zone where cracks can occur: the expansion transition zone.

Only the outer surfaces of rolling tool are idealized and keep their shape during the load.

The whole thickness of the tube is idealized and can expand under the tool pressure.

The tube-sheet constitutive model is elastic-plastic in the neighborhood of the tube and elastic homogenized in a further domain.

Contact surfaces are defined between rolling tool and tube and between tube and tube-sheet.

The maximal tool displacement is adjusted to satisfy fabrication criterion: tube thickness should present a thinning rate around 4% at the end of the process.

Numerical simulations have been successively validated on different models:

- 2D-Axi-symmetric,
- 2D in a radial-transverse section, allowing to specifically study the effects of the tool rotation,
- 3D with radial load in order to reproduce in 3D the 2D-Axi-symmetric results,
- 3D with the complete tool realistic rotational motion. The great supply of this 3D model is to be able to catch the effects of the tool displacement in terms of eventual stress singularities on every point of the structure and thus, to predict their consequences in presence of cracks.

Results and perspectives

The quality of the obtained results is evaluated through a comparison with previous experimental and numerical works.

1. Mechanics of Materials

Their sensitivity with mesh refinement and with the order of the finite elements has been studied.

3D numerical simulation of roll expansion process gives reliable results leading to a fine description of the residual stress field and brings a significant improvement to estimate the contribution of the fabrication process on crack phenomena in PWR operating conditions, as well as primary circuit hydraulic pressure test conditions.

Reference

1. <http://www.code-aster.org>.

Estimation of the Residual Stresses impact on the J parameter calculation in welded joint (1-1735)

C. Gourdin¹, Y. Kayser¹, C. Delaval², F. Mermaz², V. Klosek³, L.O. Chidwick⁴

¹CEA, DEN, DM2S, SEMT, Laboratoire, F-91191 Gif-sur-Yvette, France

²IRSN, France, DSR, BAMB, B.P. 17 92262 Fontenay aux Roses Cedex

³CEA, LLB, F-91191 Gif-sur-Yvette, France

⁴Veqter Ltd, Bristol, UK

This paper presents recent works on the understanding of residual stresses impact in structure integrity analysis proposed by nuclear standard codes such as A16 Appendix of RCC-MR.

The main objective of this study is to produce experimental data in order to evaluate the effect of the residual stresses on the fracture analyzes, and in particular on the values of the K and J parameters as well as the associated criteria.

This action involves several scientific disciplines and called upon various competences resulting of collaboration between various organizations:

- The Laboratory Léon Brillouin, in charge of CEA Orphée reactor exploitation, carried out residual stress measurements by neutron diffraction on the welded joint before the mechanical tests.
- Veqter Ltd performed residual stress measurements by the method of the hole on a similar testing welded joint.
- The LISN was responsible of the mechanical tests as well as their interpretation.
- The IRSN, National French Institute of Radioprotection and Nuclear Safety, which supported this action.

To study the impact of the residual stresses on the crack propagation, a classical welded joint used in the nuclear industry has been considered. The component was girth welded C-Mn ferritic steel pipe section of french material classification TU42C. The pipe was 200 mm long and 16 mm thick with an external diameter of 220 mm. A “V type” weld of 52° between inner surface and interface has been manufactured in the middle of the pipe and hasn’t been flushed after welding process.

Considering residual stresses measurements two different methods have been used and have given similar results (cf. figure 2). A particular experimental program has been used to support this study.

1. Mechanics of Materials

The first test was carried out in the frame of brittle fracture under monotonous growing loading (four point bending) at -150°C (cf. figure 1).

The second was carried out under fatigue conditions considering a four point bending moment with a load ratio equal to 0.1 at room temperature (25°C).

A mechanical analysis has been performed to estimate the influence of the residual stresses on the crack growth. A description of the numerical work on the experimental tests using the results of the measurements of the residual stresses will be presented in this paper. The influence of the residual stresses on the calculation of the fracture parameter (K and J) will be assessed and a formulation to take into account the residual stresses in the A16 appendix will be proposed.



Figure 1. Experimental fracture of the specimen.

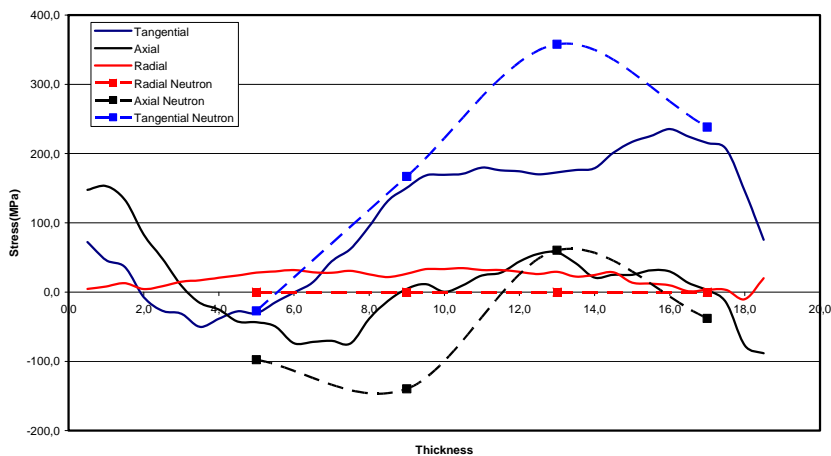


Figure 2. Comparison between two kinds of residual stresses measurements.

Development of raman spectroscopy analysis technique for the oxides forming on Hastelloy-XR at elevated temperatures in coolant helium (1-1743)

Yoichi Takeda

Fracture and Reliability Research Institute, Graduate School of Engineering
Tohoku University, 6-6-01, Aoba, Aramaki, Aoba-ku, Sendai, Japan
e-mail: takeda@rift.mech.tohoku.ac.jp

Gas Cooled Reactors (GCR), namely the Very High Temperature Reactor (VHTR) and the Gas-cooled Fast Reactor (GFR) are selected to be promising nuclear power systems by the Generation IV International Forum. In these reactors, the temperature of coolant helium at the vessel outlet is typically in the range of 900 to 1000°C. Subjects relating to heat resistant alloys with the relevant structural integrity aspects naturally became the most critical issues in the development.

Material degradation mode in high temperature helium environment is strongly influenced by the surface oxidation and decarburization near the surface. For instance, the considerable degradation mode in the structural alloys in the environment is creep damage associated with surface oxidation and decarburisation. For understanding those reaction behaviors in certain environment, it is desirable to apply the in-situ technique to the surface. Due to the high temperature gas, direct access, i.e., connecting the wires and electrodes, into the reacting surface is unlikely. Among noncontact analysis techniques, Raman spectroscopy is plausibly possible to be applied into the surface in-situ. This technique is likely to obtain the information of the surface oxides forming at high temperature.

This paper represents the design of the optical paths for in-situ Raman spectroscopy analysis. In order to correct scatter light selectively from the specimen surface and avoid the background light from furnace heaters, a condensing lens was installed into optics to focus the specimen surface in high temperature. In addition, confocal optics was used by using a spatial pinhole to eliminate out-of-focus light.

Selection of the incident laser beam wave length was made. When the wavelength of the lights emitting from heated specimen due to black body radiation is close to incident laser beam of Raman spectroscopy, a scatter light could sink and it might result in enormous noise in the measurement. Ideal calculation was made to estimate emission light strength by Planck's law of black body radiation and laser wave length was selected to 325 nm and 442 nm.

1. Mechanics of Materials

Using above mentioned optics, composition of the oxides forms after the exposure of Hastelloy-XR in high temperature helium environment at 950°C was successfully identified to Cr_2O_3 and MnCr_2O_4 in ex-situ. In-situ analysis during creep damage of Hastelloy-XR at 950°C in helium was also performed. It exhibited that the formation ratio of Cr_2O_3 and MnCr_2O_4 was changed during creep. A transport model for alloying elements was proposed and it demonstrated the creep manner associated surface reactions.

Using spatial statistical analysis of Taylor factors to characterize material susceptibility to intergranular stress corrosion cracking (1-1779)

Mikko I. Jyrkama¹, Mahesh D. Pandey¹, Edward M. Lehockey²

¹Department of Civil and Environmental Engineering, University of Waterloo
200 University Avenue West, Waterloo, Ontario, N2L 3G1, Canada
e-mail: mjyrkama@uwaterloo.ca, mdpandey@uwaterloo.ca

²Ontario Power Generation, 889 Brock Road, Pickering, Ontario, L1W 3J2, Canada
e-mail: edward.lehockey@opg.com

Studies have shown that variations in the Taylor factor from one grain orientation to the next can help predict failure in materials. For example, grains with low Taylor factors next to grains with relatively high Taylor factors are more susceptible to large stress concentrations, and hence intergranular cracking. The Taylor factor distribution among a large sampling of grains from a particular sample may exhibit a very bi-modal distribution, thereby resulting in a higher likelihood of encountering adjacent grains having large differences in Taylor factor. While describing the material susceptibility to cracking in a general sense, the sampling distribution provides no information at the local grain scale where the differences in Taylor factor are most critical.

In this study, the spatial variability in Taylor factors is correlated with crack behaviour and failure potential using spatial statistical analysis. The spatial correlation of Taylor factors is characterized through variogram analysis, which describes the dissimilarity in Taylor factor across the sample as a function of lag distance. The lag vector represents the separation between two spatial locations and provides directional dependence (e.g., transverse versus radial direction) for the computed variograms. Therefore, the spatial correlation structure embodied in the variogram describes the variability of Taylor factors not only as a function of scale (i.e., from intra-granular to multiple grain sizes), but also in terms of direction.

The proposed methodology is applied to the statistical analysis of Taylor factors from archive and ex-service samples of carbon steel feeder piping used in CANDU® reactors. The spatial distribution of Taylor factors were characterized across the samples in regular intervals through Orientation Imaging Microscopy (OIM). The results of the study demonstrate how the variogram provides a quantifiable measure of variability that is consistent across samples at different scales. While identifying the material susceptibility to intergranular cracking, the analysis also shows how the variogram also provides additional information regarding material texture.

CANDU is a registered trademark of Atomic Energy of Canada Limited.

Experimental study of the effect of radiation exposure to concrete (1-1891)

Kazushige Fujiwara¹, Masanobu Ito¹, Miwa Sasanuma², Hideo Tanaka²,
Kiyoshi Hirotsu³, Kunio Onizawa⁴, Masahide Suzuki⁴, Hiroo Amezawa⁴

¹The Japan Atomic Power Company, 1-1 Kanda-Mitoshiro-cho, Chiyoda-ku,
Tokyo 101-0053, Japan, e-mail:kazushige-fujiwara@japc.co.jp

²Tokyo Electric Power Company, Japan

³Tohoku Electric Power Company, Japan

⁴Japan Atomic Energy Agency, Japan

Concerns over aged nuclear power stations are mounting in Japan today, 40 years are going to pass soon since the nation's oldest Light Water Reactor type of nuclear power stations started operation. Concrete, which offers the functions of both compressive strength and radiation shielding, is used for the main materials of the structural members of nuclear power stations. Since the concrete structure is difficult to replace, we must have proper information on the effect of radiation exposure to concrete which is located close to the reactor core. However, there exists a limited number of experimental studies to date regarding the effect of radiation exposure to concrete.

We have then conducted neutron irradiation tests on concrete specimens (50 mm dia. × 100 mm height) to examine the effect of long-term radiation exposure to the basic material characteristics of concrete. Irradiation tests were done at the Japan Materials Testing Reactor (JMTR). The target neutron fluence was set at values that exceed 3.0×10^{18} n/cm² (E>0.1 MeV), which is equivalent to total fast neutron fluence assumed to be exposed to the concrete located at the exterior of a reactor pressure vessel for a typical BWR by 60-year operation. The irradiation temperature is to be kept below 65 deg. C, which is the limiting value stipulated in the design standard for nuclear power stations in Japan.

The irradiation tests were conducted by varying exposure dose to three different steps. The irradiation conditions aimed were satisfactory attained. Specimens were subjected to approx. 4,000 hours of radiation exposure for the longest test. Irradiation temperature was less than 65 deg. C, and the maximum fast neutron fluence was 12.0×10^{18} n/cm² (E>0.1 MeV). Post-irradiation experiments using irradiated concrete specimens were performed at the JMTR Hot Laboratory. Compressive strength of the irradiated concrete specimens was roughly equivalent to that of concrete specimens cured for the same duration under the basic environment (20 deg. C, 60%RH). Also, changes in compressive strength with increasing neutron fluence were not detected. Furthermore, by measuring water content of irradiated specimens, no changes after irradiation were observed as for the chemically bound water content.

As shown above, it was confirmed that radiation exposure does not significantly affect the basic material characteristics of concrete within the range of doses adopted in this test.

Nuclear reactor structure materials study (Survey of relevant ISTC programs) (1-1916)

L.V. Tocheny¹, A. Ballesteros², M. Deffrennes³, W. Gudowski¹, M. Hugon⁴

¹ISTC - International Science and Technology Center, Moscow, Russia
Krasno proletarskaya 32-34, P.O. Box 20, 127473 Moscow, Russian Federation
e-mail: tocheny@istc.ru

²Tecnatom S.A., Materials and Life Management
Avda. Montes de Oca, 1, San Sebastian de los Reyes, 28703 Madrid, Spain
e-mail: aballesteros@tecnatom.es

³European Commission, DG RTD, 1050 Brussels, Belgium
e-mail: marc.deffrennes@ec.europa.eu

⁴European Commission, DG RTD, 1050 Brussels, Belgium
e-mail: Michel.Hugon@ec.europa.eu

Introduction

The ISTC is an international organization created in Moscow in 1994 by Russia, EU, USA, and Japan. Later Korea and Canada, and several CIS countries as well acceded to ISTC. The basic idea when establishing the ISTC was to support non-proliferation of the mass destruction weapons technologies by re-directing former Soviet weapons scientists to peaceful research thus preventing the drain of dangerous knowledge and expertise from Russia and other CIS countries. After nearly 15 years of operation it is a good time to have a look on the past experience in the fields covered by the SMIRT20 Programme.

Presently, the ISTC now has about 40 member countries (including the 27 Member States of the EU), representing the CIS, Europe, Asia, and North America.

The partner list includes over 200 organizations and leading industrial companies from all ISTC parties.

Concept

Challenge of the World Nuclear Community is to prove to Public over the World, that nuclear power is safe and effective.

The only acceptable method, which is trusted and accepted by Public, is basic-type and demonstration-type Experiment, in advance of computer or paper-type arguing. (This should be reworded and clarified a bit.)

Important that results of these experiments are available for international analysis and validation.

In this sense the ISTC clients (first of all – “nuclear-related” institutes in Russia and CIS) have all set, ready, licensed, and equipped unique nuclear installations, high-skilled personnel, good cooperation. Essential, that the ISTC projects:

- Are managing internationally
- Have plans and results, available for international collaborators
- Results may be passed to international centers for further international benchmarking.

As for today – a set of demonstration and basic-type experiments, which fit closely with IAEA/ INPRO and GIF program, and with EURATOM Research Framework Program – has been done or are ongoing in the frame of ISTC projects and programs with active international collaboration. The ISTC – as a unique international tool – is ready to take part and manage further this activity.

Among five thousand project proposals submitted to ISTC, there are about five hundred related to different aspects of nuclear technologies and Nuclear Fuel Cycle (NFC), first of all – to safety issues.

Approaches

- International cooperation for the further safe operation of existing power plants (Gen III), as well as in future (GenIII+, GEN-IV) is important contributor to the development of safe nuclear power over the World, in particular in plant lifetime management, fuel performance, and the corresponding safety analysis means and tools (numerical and experimental).
- A special attention might have to be paid to international cooperation in research supporting harmonisation of the regulatory aspects.
- International cooperation is also an excellent channel to foster the transfer of competence between generations. The nuclear community is facing a major challenge on this specific aspect in the year to come. Exchanging experiences and expertise, offering fellowships to young scientists of other countries, can only help disseminate knowledge and good practices.

International management

Considering that the importance of the nuclear fission energy to the overall energy supply and the consequent number of NPPs in activity as well as their increasing age, the technical perspectives of applicability offered by the

improvement of phenomenological knowledge in reactor structure materials behavior and particularly – for safe and effective operation and plant life assessment, that international co-operative research is one key element for the ultimate success of the research on Residual Plant Life Assessment and Management and its applicability, on Nuclear Safety and Severe Accident Management, and in order to achieve the highest possible integration of scientists and engineers of beneficiary countries concerned by the ISTC Agreement and to optimize ISTC project management - the Contact Expert Groups for ISTC projects on Residual Plant Life Assessment and Management (CEG PLIM) and on Severe Accident Management (CEG SAM) were formed by the European Union as the ISTC Financing Party, that decided to support its activities.

Survey of the ISTC project results

The following information will be included in the review, with special attention on details of corresponding projects and programs:

- Nuclear Power Plant life management (Reactor pressure vessel and internals monitoring, etc.)
- Severe accident study (Corium modelling, Quench-effect)
- Barrier materials (Catcher, containment and other barriers)
- Protection materials for RAW storage
- Innovative reactor engineering systems – experimental and computer modelling (steam-generators, etc.)
- Study of innovative reactor concepts, corresponding to GIF:
 - Fast reactors (Sodium-, Lead-and Lead-Bismuth-cooled)
 - Supercritical Pressure Water aspects; HTGR (Engineering aspects).
 - Molten salts
- Fusion (First wall, blanket)
- Regulatory aspects.

Some examples of ISTC projects:

- # 2048, “Improvement of Steels Corrosion Resistance in Pb-Bi”, NIIIEFA, IPPE, PROMETHEY
- #0797.2, “WWER-1000 Reactor Pressure Vessel Safe Operation Lifetime Evaluation”, ENES, PROMETHEY, NIKIMT, VNIIEF
- #2378, “Residual Resource Evaluation for Power Equipment”, MGTU, KIAE

1. Mechanics of Materials

- #2864, “Analytical Methods of Hydrogen and Helium Embrittlement”, KIAE, Tomsk TU
- #3420, “Lifetime Extension of VVER-1000 Reactor Pressure Vessels”, KIAE
- #3635, “VVER Vessel in Severe Accident” MPEI (TU), GIDROPRESS
- #0065, “Technique for loads forecasting on nuclear reactor containment during severe accident conditions”, IVTAN
- #3690, “Study of Fuel Assemblies under Severe Accident Top Quenching Conditions in the PARAMETER-SF”, LUCH, GIDROPRESS, IBRAE
- #A-1492, “Safety of Armenian NPP with ageing effects”, NRSC of ANRA, Arm NPP.

Resume

The presentation addresses some outcomes of the ISTC projects and programs, related to nuclear science and technologies, as well as methods and approaches employed by the ISTC to foster close international collaboration and joint manage projects towards fruitful results.

References

The ISTC Annual Reports – ISTC, Moscow, 1996–2007.

Web-site: www.istcinfo.ru.

Two scale damage model for HCF uniaxial and biaxial 304L steel tests (1-1917)

Barbier Gregory^{1,2}, Desmorat Rodrigue¹,
Sermage Jean-Philippe², Courtin Stephan³

¹LMT Cachan, ENS Cachan/CNRS/Université Paris 6/PRES UniverSud Paris
France, e-mail: barbier@lmt.ens-cachan.fr

²EDF R&D / LaMSID, 1 av. Gal de Gaulle, Clamart, France

³AREVA NP, Tour AREVA, 92084 Paris La Défense Cedex, France

A two scale damage model [1–4] has been developed to handle High Cycle Fatigue where mainly elastic materials and structures responses nevertheless lead to damage and cracking. The model is incremental, i.e. it is written in a rate form, the damage rate being obtained by evolution laws. The two scales considered are

- the mesoscopic scale of the representative volume element of classical continuum mechanics of yield stress σ_y ,
- the defects scale, or microscale; the defects responsible of the micro-crack initiation are gathered into a weak inclusion, of same plastic properties at mesoscale but of yield stress taken equal to the asymptotic fatigue limit.

A post processor called DAMAGE solves the model equations (plasticity coupled with damage at microscale, Eshelby-Kröner scale transition law). The mean stress effect is included in the modelling, not directly, as in classical amplitude laws, but by time integration of the constitutive equations.

In this incremental two scale damage model, the two main causes responsible for this effect are [4]:

- the modelling of micro-defects (or micro-cracks) closure by means of a micro-defects closure parameter h in the expression of the energy density release rate [5].
- the consideration of the first stress invariant in the microscale plasticity criterion.

First, the DAMAGE post processor is used here to compare theoretical number of cycles to ruptures to experimental ones on a EDF database made of HCF uniaxial tests on AISI 304L stainless steel. The fatigue tests are strain controlled, made at room temperature.

Then, HCF biaxial tests performed in LMT-Cachan are presented. The tests have been performed on LMT ASTREE triaxial testing machine on a thinned Maltese cross specimen (same material) designed thanks to finite elements

Cast3m code and DAMAGE post-processor. The specimen has a thinned area in its middle part in order to ensure center crack initiation under biaxial loading. The characteristics of the tests are: stress controlled, positive load ratios, room temperature, frequency 10 Hz. Image correlation (speed camera and usual camera devices) are presented: one observes then closely the strains evolution (strain amplitude and plastic strains) and crack initiation in the specimen during the tests. Calculated (DAMAGE) and experimental numbers of cycles to crack initiation are compared.

References

1. Lemaitre, J., Doghri, I. Damage 90: a post-processor for crack initiation. *Comp. Methods Appl. Mech. Engrg*, 115: 197–232, 1994.
2. Lemaitre, J., Sermage, J.P., Desmorat, R. A two scale damage concept applied to fatigue, *International Journal of Fracture*, Vol. 97, pp. 67–81, 1999.
3. Desmorat, R. et al. Two scale damage model and related numerical issues for thermo-mechanical High Cycle Fatigue, *Eur. Jour. of Mech. A/Solids*, Vol. 26, pp. 909–935, 2007.
4. Barbier, G. et al. Mean stress effect by incremental two scale damage model. LCF6 – 6th international conference on low cycle fatigue. 2008.
5. Lemaitre, J., Desmorat, R. *Engineering Damage Mechanics: Ductile, Creep, Fatigue and Brittle Failures*. Springer, 2005.

Concrete shrinkage taken into account as crack width assessment (1-1925)

Etienne Gallitre¹, Pierre Alain Naze², Pierre Labbe³

¹EDF-SEPTEN civil work section manager and reinforced concrete researcher

²EDF-CNEN civil work section manager and reinforced concrete researcher

³EDF-DIN special seismic and civil work expert and IAEA adviser

Context

In very large buildings with connected walls, such as large Nuclear Power Plants, concrete shrinkage strains have to be considered because of elements differential strains, as required in the new European construction code (EC 2). The fastest engineering method consists in considering shrinkage as an equivalent thermal strain, which is in fact computed as internal forces. In EPR, for Flamanville 3 conditions, this first method led to enormous reinforcement ratio in the lower part, so EDF with its partners proposed a new methodology based on crack width assessment.

Methodology summary

At first, we compute the shrinkage differential strains, “ ϵ_s ”, depending on moisture conditions and elements thickness. Then we fix a reinforcement section as a calculation hypothesis in order to estimate the distance “ S_s ” between cracks, which is independent from the loads. Consequently, we can assume that a certain crack width value “ W_s ” is consumed by the shrinkage itself, with $W_s = \epsilon_s S_s R_{ax}$ (R_{ax} restriction factor). So the available crack width for the other loads is the remaining crack width. From cracking theory and according to EC2; we can deduce steel stress σ_d . So the structure design (reinforcement mainly) can be undertaken with this allowable limit value σ_d , in the load combinations where shrinkage has to be considered.

Conclusions

This new methodology is more physical than the one with a thermal equivalent load, so safety requirements are satisfied in focusing on crack width assessment, which is a performance approach. It has allowed EDF to size a reinforcement ratio, which is compatible with concrete technical rules, especially in the areas near the raft. Of course this method remains in accordance with durability hypotheses and other requirements connected to nuclear specificities.

A probabilistic approach for assessing concrete degradation due to leaching (1-1926)

De Larrard Thomas¹, Benboudjema Farid¹, Colliat Jean-Baptiste¹,
Torrenti Jean-Michel^{1&2}, Deleruyelle Frédéric³

¹Laboratoire de Mécanique et Technologie
LMT-ENS Cachan, Secteur Génie Civil
61 av. Président Wilson, 94230 Cachan, France
e-mail: delarrard@lmt.ens-cachan.fr

²Laboratoire Central des Ponts et Chaussée, LCPC Paris, France

³Institut de Radioprotection et de Sûreté Nucléaire, IRSN, DSU, SSIAD, BERIS,
Fontenay-aux-Roses, France

The work presented here is the first step of a project aiming at developing a predictive model based on a probabilistic approach for the mechanical durability of concrete structures under a calcium leaching attack. For this purpose, an important experimental campaign is being carried out simultaneously with the development of a numerical modelling.

The experimental campaign follows two real building sites, thus the samples for the measures have been moulded as long as the building operation lasted. It firstly aims at investigating a correlation between different kinds of measures, some of them being performed in a laboratory as long as they require an important equipment or the use of hazardous chemical products, some others being performed directly on the building sites. This campaign concerns mechanical tests such as compression or tension strength or static and dynamic Young modulus, as well as measures of durability indicators like water porosity and Ammonium Nitrate Accelerated Degradation tests or, concerning the in-situ measurements, electric resistivity. The final objective of this study aims at proposing a few measures that could be performed directly on the building sites to assess the quality of concrete, notably regarding the possible risk of degradation by leaching, without requiring heavy equipment or specific skills in the preparation of the samples.

The second goal of the campaign is to characterise the statistical variability of the mechanical characteristics of the material with the view to deriving probabilistic laws and related parameters (mean value, standard deviation and correlation length). The variability studied here is due to the different times and conditions for mixing the concrete used for building the whole structure. The study aims at finding out a correlation between the properties of the material and the location of the different mixes in the structure.

The results of the above mentioned experimental campaign will be used to simulate the long-term behaviour of the structure by modelling the calcium leaching using a Finite Volume Method and accounting for the variability of the material. Furthermore, inverse analyses could be set up to determine some other characteristics of the material (such as the diffusion coefficient, which is the leading parameter for the modelling of calcium leaching) and their statistical properties that cannot be directly measured but inferred from the results acquired by the former experimental campaign.

Thermal ageing of RPV materials for NPP with VVER (1-1990)

B.T. Timofeev, A.O. Zotova
CRISM “Prometey”, St. Petersburg, Russia

Now the problem of increase of a service life of nuclear power installation is actual. In this connection the especial attention is given a question of probable deterioration of properties of material. Projected at present RPVs are designed for long-term of operation – 60 years with an opportunity of prolongation of service life. The basic requirement showed to materials for such reactors, high resistance thermal embrittlement is. To increase the service life of the light water reactor pressure vessel at present time is one of the most important problems.

There is influence of high temperature and neutron irradiation on material of RPV during operation life. It is a reason of the embrittlement. The embrittlement of a metal expressed in increase of ductile-brittle transition temperature T_{K0} . Under action of operational factors shift ΔT in area of higher temperatures is marked. In case of significant displacement of ΔT value aside positive temperatures, there is a danger of RPV brittle fracture at emergency and hydraulic tests regimes.

Under influence of the elevated temperatures at operation time for RPV steels two forms thermal embrittlement take place. This problem is considered in this paper. There are results of experiments on influence temperature on embrittlement and mechanical properties of various Russian RPV steels. These results were analyzed, that makes it possible to comparison conventional widely applicable Russian RPV steels.

There are attempts to forecast properties after long-term influence of the operative temperatures by translation properties after influence of the elevated temperatures.

Effect of geometrical defects and cracks on the collapse of straight or curved tubes submitted to external pressure (1-1991)

C. Mathon¹, A. Limam²

¹EDF-SEPTEN, Lyon, France

²LGCIE, INSA-Lyon, France

Nuclear power plants sometimes use heat exchanger units with curved tubes. During the manufacturing process the tubes are ovalized, which means that their cross-section becomes elliptical, giving a geometrical imperfection and causing a substantial reduction of the critical buckling pressure compared with that of the perfect configuration. In exceptional cases, it is possible for the tubes to be exposed to a high external pressure. In such cases, an adequate margin of safety against buckling is an important design criterion. The buckling pressure of an oval tube can be estimated conservatively using pressure vessel codes, for example the French RCC-MR code [1] or the German code [2]. Unfortunately for larger ovalization ratios, code results tend to become too conservative so that it is practically impossible to make reliable statements about the true collapse pressure. Other codes yield to similar results, because their most common feature is to provide a simple calculation formula, which of course cannot account for the complex behaviour of an elastoplastic imperfect cross-section. The most complete and reliable procedure for calculating the collapse pressure of the oval tube by FEA is to perform geometrical and material non linear analysis, knowing that both nonlinearities are present and interact in the problem.

This study has been initiated and guided by the need to establish clear and accurate design criteria for the collapse of tubular structures under external pressure for heat exchanger applications. Heat exchangers, for industrial or nuclear plants applications, essentially imply the use of tubes with lower diameter to thickness ratios (D/t) and higher strength materials. D/t ratios as low as 10 to 20 are currently being considered in feasibility studies for heat exchangers. For this range of D/t , the collapse pressure is determined by the inelastic behaviour of the tube material. Extensive numerical studies have been conducted to clarify the buckling of thick cylindrical tubes submitted to lateral pressure or hydrostatic pressure. Straight configuration or curved pipes are considered. Effects of geometrical initial imperfection (initial ovalization) are considered in both configurations for different amplitudes. The obtained design curve is then compared to the RCC-MR code or the German vessel code. Different strain hardenings are considered to gauge the effect of material law on the collapse behaviour. Considering this large parametric numerical study conducted with

1. Mechanics of Materials

different FE codes (CAST3M, ABAQUS, ASTER), the methodology of the design and recommendations are proposed.

In addition, the effect of other imperfections, such as local wall thickness variations associated to corrosion, or cracks due to fatigue induced by vibration, are examined in the light of the strong dependence on the inelastic behaviour associated to material properties and the presence of initial ovalization.

References

1. RCC-MR: Règles de conception et de construction des matériels mécaniques des îlots nucléaires RNR, AFCEN: Association française pour les règles de conception et de construction des matériels des chaudières électro-nucléaires (French code).
2. AD-Merkblatt B6: Cylindrical shells under external pressure (German pressure vessel code), 1995.

Control and exploitation of thermal distortions in welded T-joints (1-1994)

Heikki Keinänen, Jouni Alhainen, Risto Karppi, Martti Verho
VTT Technical Research Centre of Finland, Finland
e-mail: firstname.lastname@vtt.fi

The manufacture by welding generally involves several procedures such as cutting, bending, welding and straightening that trigger thermal distortions. New breakthroughs are still waited for improving the accuracy of thermal cutting for mechanisation of welding in machine shop environments. Shrinkage distortion of welding itself remains a permanent concern of welding machine shops. These distortions adversely affect the component fabrication and all stages of further assembly.

The main objective of the DISCO (Control and Exploitation of Thermal Distortions) project was the creation of an overall concept for the control of thermal distortions. The domain of the project was at this stage limited to structural steels and to the processes most important to the participating industry.

The project explored the possibility to apply the inherent strain method [1] for modelling thermal deformations by establishing an inherent strain database for major arc welding and thermal cutting situations. The project was executed in close co-operation with Osaka University, Japan, Lappeenranta University of Technology and four Finnish enterprises.

The work focused on structural steels representing two strength levels, and GMAW, FCAW, SAW and restrictedly on tandem MAG welding processes. The computational practices were revealed for treating thermal distortions. Further actions included testing and modelling of welded T-joint with various plate thicknesses.

The relationship between plastic strains and angular distortion (out-of-plane deformation with the weld as the axis of rotation) of a fillet welded plate T-joints was studied using numerical analyses [2, 3]. A three dimensional thermo-elastic-plastic analysis incorporating the effects of a moving heat source and non-linear material properties was performed to obtain the plastic strain distributions and hence deformations. Procedures to define a simplified strain distribution (inherent strain) and to compute deformations were presented.

The comparison of detailed thermo-elastic-plastic computation and measurements exhibited a real good correlation. The simplified inherent strain type analysis underestimated somewhat the deformations. The basis for the creation of an inherent strain database was presented.

References

1. Mochizuki, M., Toyoda, M. 1999. Numerical analysis of residual stress in welded structures using inherent strain. Pp. 549–580. Mathematical Modelling of Weld Phenomena Proceedings of the 5th International Seminar on the Numerical Analysis of Weldability. Graz-Seggau, 4–6 October 1999.
2. Keinänen, H. Karppi, R. 2005. Computation of welding deformations of a T-joint. Baseline computation of the DISCO experiments. Research report No. TUO72-055743. VTT, Espoo, Finland. 26 p.
3. Keinänen, H., Karppi, R. 2005. Computation of welding deformations of “DISCO” T-joint and butt welding experiments. Research report No. TUO72-056607. VTT, Espoo, Finland. 26 p.

Experimental and numerical analysis of cyclic thermal shock at the Paul Scherrer Institut (1-1998)

M. Niffenegger, K.G.F. Janssens, K. Reichlin
Nuclear Energy and Safety Research, Paul Scherrer Institut
5232 Villigen, Switzerland, e-mail: Markus.Niffenegger@psi.ch
Phone: +41 (0)563102686

Specific thermo-hydraulic conditions may lead to cyclic thermal shocks in the piping of the primary circuit of light water reactors. In turn this may lead to thermal fatigue damage and, under certain conditions, to cracks running through the wall. While consensus exists concerning the cause of this damage, the exact conditions responsible for macroscopic failures are still unknown. In addition, there is a lack of tools for the reliable prediction of turbulent mixing of fluids, fatigue crack initiation and crack growth under operating conditions. In particular the following questions still need to be answered:

- Under which flow conditions do the thermal fluctuations appear? This is a complex thermo-hydraulic problem.
- What are the critical locations for crack formation in the primary loop of a LWR?
- What are the temperature differences ΔT and frequencies ω of these fluctuations?
- Which conditions (ω , ΔT , mean temperature T_m , pressure) have to be fulfilled for the initiation and growth of thermally induced cracks?
- How deep do these cracks grow? Under what conditions do they arrest?
- What are the differences between different austenitic stainless steels (ASS)?
- What is the difference between unilateral (hot-cold) and bilateral (cold-hot-cold) cyclic thermoshocks?
- What are the reliable mathematical (deterministic and probabilistic) prediction tools for fatigue life prediction?

A research project at the Paul Scherrer Institut (PSI) is dedicated to the analysis of thermo-hydraulic mixing phenomena and to the analysis of crack initiation and growth due to the resulting cyclic thermal shocks on the inner wall of the piping. The project, which includes both experimental investigations and numerical

simulations of the complex behavior of fluid and piping material, aims to contribute to a better understanding of the observations made in nuclear power plants.

In the cyclic thermal shock experiments performed on austenitic stainless steels AISI 321, 347 and 316L, cracks of a length up to a few hundred micrometers were initiated at the tip of a notch with a radius of 0.05 mm and a depth of 1 mm by pure thermal load. The finite element calculations have shown the importance of considering cyclic plasticity for austenitic stainless steels. Precise simulations of hundreds of cycles indicate that local ratcheting can be induced by cyclic thermal shock. It was shown that considering temperature-change induced material softening leads to numerical strain localization, which in turn points at the limitations of a continuum approach, as in reality such strain localization is constrained by microstructural features.

The ongoing research activities at PSI in the field of thermo-mechanical fatigue are discussed. In particular, a cyclic thermal shock facility allowing experiments under well defined loading and boundary conditions is described. Finite element calculations considering cyclic plasticity (with softening/hardening) are used to simulate the thermal shock experiments and to compute the stress strain history. The transient nonlinear cyclic stress/strain calculations are based on computational fluid dynamic calculations of the turbulent mixing phenomena. The number of cycles needed for crack initiation was evaluated based on the local cyclic strain amplitude and the fatigue life curve which was evaluated in extensive fatigue testing. It was found that Smith-Watson-Topper (SWT) correction can be successfully applied to predict the number of cycles to crack formation, if geometry dependent calibration factors are used in the SWT correction. These factors were found in dedicated additional fatigue tests on notched specimens. Furthermore, basic questions regarding the application of such numerical assessment tools are briefly discussed.

Manifestations of DSA in austenitic stainless steels and inconel alloys (1-2013)

Mykola Ivanchenko¹, Yuriy Yagodzinsky¹, Ulla Ehrnstén²,
Wade Karlsen², Hannu Hänninen¹

¹Laboratory of Engineering Materials, Helsinki University of Technology
Puumiehenkuja 3, P.O. Box 4200, FIN-02015 TKK, Finland

e-mail: mykola.ivanchenko@tkk.fi

²VTT Industrial Systems, Kemistintie 3, P.O. Box 1704,
FIN-02044 VTT, Finland

Introduction

Interstitial atoms such as carbon and nitrogen play an important role in the mechanical properties of austenitic stainless steels and Inconel alloys. Strength and creep resistance of these alloys in the environmental conditions of nuclear reactors depend on the amount, state and diffusion mobility of interstitial atoms dissolved in the alloy. Because of the interaction of carbon and nitrogen with mobile dislocations, even a minor content in the solid solution results in dynamic strain aging (DSA) of the alloys at temperatures above 200 °C [1 - 3]. DSA is manifested by negative strain rate sensitivity, and serrated yielding during straining at elevated temperatures and results often in a remarkable degradation of mechanical properties. DSA phenomenon leads to inhomogeneous plastic flow, which results in strain localization that can affect crack initiation and propagation.

Aim of the work

The aim of the present investigation was to examine and compare different types of DSA manifestations in AISI 316 austenitic stainless steel (SS) and Inconel 600 and Inconel 690 alloys by means of slow strain rate tensile testing, mechanical loss spectrometry (internal friction) and transmission electron microscopy (TEM). Another aim was to determine differences in the resulting dislocation structures and internal friction response of materials showing and not showing DSA behaviour.

Essential results

It was found that DSA in nitrogen-alloyed AISI 316L type SS occurs at temperatures above 200°C at strain rates slower than 10⁻⁴ s⁻¹. The apparent

activation enthalpy of DSA in AISI 316NG stainless steel is about 1.24 eV. The value of enthalpy of DSA corresponds well to the enthalpy of nitrogen diffusion in AISI 316NG stainless steel, about 1.45 eV, obtained by the internal friction method. In Inconel 600 and 690 alloys, DSA is observed in the temperature range from 150 to 600°C. The activation energy values for the onset of serrations (about 1.65 eV) are the same for both Inconel alloys, which correspond to activation enthalpy of carbon induced IF peak in Inconel 600 alloy (1.68 ± 0.09 eV). In spite of the fact that the value of activation energy for DSA onset in Inconel alloys is higher than that for AISI 316NG austenitic stainless steel, DSA in Inconel 600 and 690 alloys begins at lower temperatures. The effects of DSA on mechanical properties of these materials were evaluated based on peaks in tensile strength, minimum in ductility and negative strain rate sensitivity in the DSA temperature range. It was also observed that nitrogen suppresses the DSA development in AISI 316L type stainless steels. The onset of DSA serrations shifts to higher values of strain and the amplitude of the flow stress pulses decreases with increasing nitrogen content.

TEM studies of AISI 316NG austenitic SS showed that long-range and short-range planarity was observed in the dislocation structures after pre-straining of the steel at 400°C and 288°C, respectively, when the steel has experienced DSA. After pre-straining at 200°C, which is out of the range of DSA occurrence, the microstructure exhibited cellular dislocations.

Conclusions

Increase in amplitude of the IF peak is probably related to atomic re-distribution during plastic deformation and to the formation of interstitial enriched sub-micron zones dragged by dislocation pile-ups during the DSA.

The peak increase is caused by nitrogen-enriched zones forming by nitrogen-dislocation interactions in the DSA-regime of the material's deformation. Dependence of the nitrogen- and carbon-induced IF-peak decays on time of annealing at the peak temperature reflects the post-pre-straining re-distribution of interstitial atoms at scales of the enriched zones.

Diffusion redistribution of nitrogen in the DSA regime affected the deformation behaviour of the material by restricting cross-slip therefore promoting strain localization and degrading the mechanical performance of the material.

It was shown that DSA is present in commercial AISI 316NG steel and Inconel 600 and Inconel 690 alloys, and occurs at temperatures relevant to nuclear power plant operation.

References

1. R.A. Mulford, U.F. Kocks. *Acta Metall.* 27 (1979), pp. 1125–1134.

2. U. Ehrnsten, A. Toivonen, M. Ivanchenko, V. Nevdacha, Y. Yagodzinsky, H. Hänninen. Dynamic Strain Ageing of Deformed Nitrogen-Alloyed AISI 316 stainless steels. Corrosion Issues in Light Water Reactors. Ed. D. Feron, J.-M. Olive. Cambridge England: Woodhead Publishing, 2007. Pp. 103–118.
3. H. Hänninen, M. Ivanchenko, Y. Yagodzinsky, V. Nevdacha, U. Ehrnsten, P. Aaltonen. Dynamic Strain Aging of Ni-base Alloys Inconel 600 and 690. Proc. of the 12th International Conference on Environmental Degradation of Materials in Nuclear Power System – Water Reactors, 2005. Pp. 1423–1430.

Strength and porosity of concrete incorporating polypropylene and steel fibres subjected to high temperature (1-2024)

Pliya Prosper, Beaucour Anne-Lise, Noumowé Albert
Laboratoire de Mécanique et Matériaux du Génie Civil, L2MGC
Université de Cergy-Pontoise, F-95000 Cergy-Pontoise, France
e-mail: prosper.pliya@u-cergy.fr

Concrete structures in buildings or other constructions may be subjected to accidental conditions such as fire. Then, among many parameters, the safety of the structures depends on the mechanical properties of the concrete. Many research works show that, in some cases, a concrete element subjected to high temperature may present spalling or bursting. These phenomenons seem to be due to the formation of water vapour pressure and thermal stresses during the rise of temperature. Several studies show that concrete thermal stability is improved by incorporating polypropylene fibres to the mix.

The aim of this study is to investigate the effect of polypropylene and steel fibres on the behaviour of concrete subjected to high temperature. Test were carried out on concrete elements subjected to four target temperatures: 150, 300, 450 and 600°C. Three groups of concrete were studied: one group of concrete mixes without fibre, one group of concrete mixes with polypropylene fibres and one group of concrete with steel fibres. The specimens were subjected to heating – cooling cycles from the ambient temperature to 150°C, 300°C, 450°C and 600°C. According to RILEM recommendations for these specimens dimensions, the heating rate was 1°C/min. The amounts of the fibres in the concrete were, for the polypropylene ones 0.11, 0.17 or 0.22% in volume and for the steel ones 0.25, 0.38 or 0.50% in volume. The initial and residual mechanical properties and porosity of the studied concrete mixes were analysed. The evolution of compressive strength, tensile strength, modulus of elasticity and water porosity of the studied concrete mixes are expressed as a function of the temperature.

Many interesting results underlined that the steel fibres improved the concrete residual mechanical properties. Concrete incorporating polypropylene and steel fibres behave better than that incorporating only polypropylene fibres; thermal stability and residual mechanical properties were improved. Porosity tests results permitted to give some explanations of the observed behaviour.

Simulation research of self-healing mechanism for microcapsule composite (1-2054)

Zhang Li¹, Zhang Heng², Dong Xiu-ping¹, Dong Jianling³

¹Faculty of Mechanical and Automation Engineering, Beijing Technology and Business University, Beijing 100048, China, e-mail:zhangli@th.btbu.edu.cn

²Faculty of Mechanical and Electrical Engineering, Zhengzhou University
Zhengzhou Henan 450052, China

³Faculty of Institute of Nuclear and New Energy Technology
Tsinghua University, Beijing, 100084, China

New composite materials which are heated and compressed with matrix resin, reinforced material and fillers have wide potential applications because they are good dampers, fine scream absorbers and with low-pollution and expenses [1]. Under periodic heat or mechanism load, micro-cracks will be produced in matrix resin. Converge of micro-cracks will cause other breakages such as breaks in fibers and matrix or slippage on interfaces [2].

In order to heal the micro-cracks, technology of microcapsule self-healing is applied in this new composite in this paper. Taking integral references and previous works [3] into considering, the detailed recipes for the sample are as follows: inorganic modified resin is applied as matrix and its weight content is 11%. Dicyclopentadiene (DCPD) microcapsules coated with epoxy resins as self-healing capsules are chosen and their weight content is 0.6%. Reinforced fiber weight content is 30%. Total weight content of various fillers is 58.4%. Standard-sized samples of 140*25*34 mm are prepared in certain process. Three-point bending experiments are carried out on LDS-SOP electronic extending tester [4, 5] and yielding and elasticity limit of unsaturated polyester resins and epoxy resins, which are essential for FEA (Finite Element Analysis) calculations, are obtained. Based on the uniform materials' crack criterion, a corresponding self-healing materials criterion is founded.

Crack expanding calculation in such materials with microcapsules is made by means of FEA software ANSYS. Calculations show that the maximum stress appears at the contact spot of crack and microcapsule and the value of it is 8.25 MPa. It exceeds the yielding limit of epoxy resins 7.8 MPa, from which the microcapsule is made, and microcapsule will fracture definitely. The maximum concentrated stress in matrix appears below microcapsule and its value is 6.2 MPa approximately which is below the yielding limit of unsaturated polyester resins 7.37 MPa.

Therefore, when cracks travel through microcapsules, stress is concentrated at the crack end and the microcapsule breaks, and then the encapsulated liquid runs out to fill the crack by the capillary and polymerization with catalyst in the

composite. As a result, the crack is healed. Ultimately, function of self-healing is proved quite feasible. The research of self-healing technology has been applied to steel reinforced concrete structure for healing the cracks.

References

1. Zhang Yang. Development and modal analysis of a new type of composite material auto break pad [D]. Beijing Technology and Business University. 2007.
2. Yang Qingsheng. Micro structure mechanics and design of composite materials [M]. Beijing: China Railway Publishing House, 2000, version 1.
3. E.N. Brown, S.R. White, N.R. Sottos. Microcapsule induced toughening in a self-healing polymer composite[J]. Journal of Material Science, 2004, 39(5):1703.
4. Dang Xudan, Zhang Heng, He Yuejin. A Study of Self-healing Intelligent Composite with Microcapsules. Materials Review. 2005, 19(1):30–32.
5. He Yuejin, Zhang Jun, Dang XUdan et al. Simulation and experimental research on fraction characteristics of self-healing composite material with microcapsule [J]. Function Materials, 2007, 38(5):849–852.

A simplified ratcheting limit method – uniform modified yield (UMY) approach (1-2058)

Jerjes Abou-Hanna, Professor
Bradley University
Peoria, IL

This paper describes the isotropic yield modification (UMY) approach to obtaining ratchet limits for several case studies that are documented and verified in the literature. The ratchet limit is obtained by finite element based limit load analysis of a structure whose yield strength at every point in the structure is modified according to secondary stresses. The approach uses Von Mises yield criterion, based on distortion energy theory. UMY modifies the cylindrical yield surface by reducing its radius according to the Von Mises stress of the secondary stress tensor, and the modification is made at every point in the structure. UMY requires stress classification and clear identification of primary and secondary cyclic load conditions. The approach is very effective. The finite element procedure to implement the UMY approach is extremely fast when compared to conventional numerical schemes such as cyclic elastic plastic finite element simulations, or direct cyclic methods, available in some commercial finite element codes such as ABAQUS. The numerical scheme required the development of a user subroutine that interfaces with the main finite element code to implement the UMY approach. The results of the UMY method are slightly conservative in some cases. However, under certain conditions, especially at high ratio of secondary to primary stress intensities, the approach was found to be overly conservative. The conservatism is caused by the simplifying assumption that the modified yield surface maintains its cylindrical shape. But the true resulting modified yield surface is not cylindrical, and its shape depends on the direction of the principal stresses of the secondary and primary loads. This so called load dependent yield modification (LDYM) approach is reported in another paper in this conference.

References

1. Gokhfeld, D.A., Cherniavsky, O.F. Limit Analysis of Structures at Thermal Cycling, Ploytechnical Institute, Cheliabinsk, USSR, 1980.
2. Ponter, A.R.S., Chen, H. A minimum theorem for cyclic load in excess of shakedown, with application to the evaluation of a ratchet limit. *Eur. J. Mech. A/Solids* 20, pp. 539–553, 2001.
3. Chen, H., Ponter, A.R.S. A method for the evaluation of a ratchet limit and the amplitude of plastic strain for bodies subjected to cyclic loading. *Eur. J. Mech.A/Solids* 20, pp. 555–571, 2001.

Application of CFD Code PHOENICS for simulating CYCLONE SEPARATORS (1-2459)

Anu Dutta, B. Gera, Pavan K. Sharma⁺, R.K.Singh, A.K. Ghosh, H.S. Kushwaha
Reactor Safety Division, Health Safety and Environment Group
Bhabha Atomic Research Centre
Trombay, Mumbai, India- 400085
⁺e-mail: pa1.sharma@gmail.com

Keywords: separator, CFD, IPSA, PHOENICS, two-phase flow

Cyclone separators are widely used in the field of air pollution control, gas–solid separation for aerosol sampling and in many industries like power plants, sand plants etc. In cyclone separators the air flow enters the cyclone through a tangential inlet, generates a swirling flow that forces entrained particles radially outward and leaves via an axial outlet pipe at the top of the cyclone. The rotational fluid motion is generated from the energy obtained from the fluid pressure gradient. This rotational motion causes the particle to separate relatively fast due to the strong acting forces. The cyclone separator is very useful engineering equipment with no moving parts and virtually no maintenance. It enables particles of micrometers in size to be separated from a gas moving at about 15 m/s without excessive pressure-drop.

This work presents a computational fluid dynamics (CFD) calculation to investigate the flow field in a tangential inlet cyclone which is mainly used for the separation of the moisture from an air stream. Three-dimensional, steady state Eulerian simulations of the turbulent gas–droplet flow in a cyclone separator have been performed. Numerical simulation was carried out using CFD code PHOENICS for the given geometry of separators available in literature. The IPSA (Inter-Phase-Slip Algorithm) method has been utilized which entails solving the full Navier-Stokes equations for each phase. The turbulence was modeled with standard k- ϵ turbulence model. The liquid droplet was modeled as particle of size 200 μ and density 1020 kg/m³. The volume fraction of moisture was 1% at inlet and outlet volume fraction was predicted with CFD. The results were in good agreement with the reported results. This knowledge can be further extended for other two phase flow applications in nuclear industry.

Evaluation on the fracture properties of heated concrete by using poly-linear tension softening inverse analysis (1-2531)

Yoshinori Kitsutaka, Koichi Matsuzawa
Faculty of Urban Environmental Sciences
Tokyo Metropolitan University
1-1 Minamiohsawa, Hachiohji, Tokyo 192-0397, Japan
e-mail: kitsu@tmu.ac.jp

Introduction

Concrete structures for nuclear power generation may be subjected to heating action for a long period. Many studies have already reported that the strength of concrete subjected to heating can be retained by maintaining temperature conditions of not more than around 65°C under general control standards for nuclear power generation. The effect of the heating should be considered to discuss the long-term safety and durability of concrete structures, however the fracture properties of concrete under the heating action are not yet to be clarified.

Aim of the work

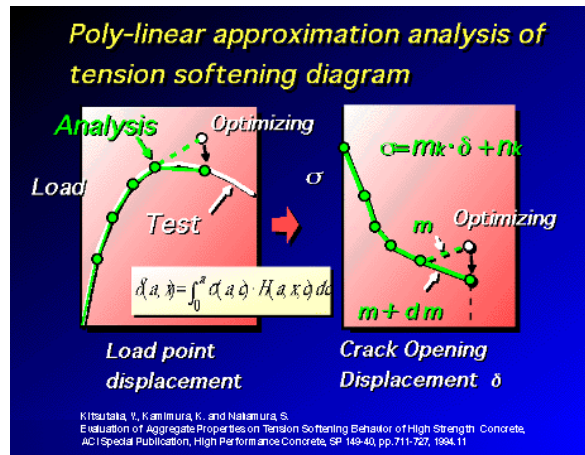
This paper reports on the investigation into the fracture properties of concrete subjected to the effects of heating condition for 60°C by using the poly-linear tension softening inverse analysis.

Essential results

1) Analysis method

In order to evaluate the fracture properties of concrete, a method to determine the tension softening curve of concrete based on the poly-linear approximation inverse analysis (Kitsutaka et al. 1994) is used. The prediction method for the load-displacement relationships of concrete with cracks is developed by means of the fictitious crack model concept (Hillerborg et al. 1976) with the K-superposition method and the constitutive law of the poly-linear tension softening diagram. The nonlinear crack equation was solved by an iteration program for evaluating the optimum softening inclinations of the tension softening diagram. Poly-linear approximation method for calculating the

complete tension softening diagram from the actual load displacement curve was performed by using the stepped inverse analysis. Also the fracture parameters for elastic-plastic materials were estimated based on the calculated tension softening diagram (Kitsutaka 1997).



2) Experiment

The water-cement ratios (W/Cs) of concrete used in this experiment is set to 0.5. Maximum aggregate size was changed for 5 mm and 10 mm. Specimen size was 40 mm × 40 mm × 160 mm. After the 28-day water curing at 20°C, specimens were cured in two temperature conditions of 20°C and 60°C for 90 days in 60%RH. After the curing, three-point bending tests were conducted to measure the load versus crack mouth opening displacement (L-CMOD) curves. The span length was 120 mm, and notch length was 12 mm. Specimen was attached to a loading machine and loaded with constant CMOD speed. Sensitive clip gauges for displacement control (MTS-632.02) were used for the CMOD measurement. The tension softening diagram was determined by poly-linear approximation analysis method based on the obtained load-CMOD curves. Fracture parameters, such as fracture energy, R-curve and cohesive strength were evaluated from the obtained tension softening diagram. Specimens cured at 60°C tend to develop a higher fracture energy than those cured at 20°C. Specimen of maximum aggregate size 10 mm tends to show high energy consumption to compared with specimen of maximum aggregate size 5 mm because of the crack deflection effect.

Summary

- 1) Poly-linear approximation method for calculating the tension softening diagram from a load-displacement curve based on the stepped inverse analysis was introduced.

- 2) Tension softening diagrams of concrete subjected in the heating were analyzed and the fracture parameters were evaluated.
- 3) Specimens cured at 60°C for 90days tend to develop a higher fracture energy than those cured at 20°C for 90days.
- 4) Specimen of maximum aggregate size 10 mm tends to show high energy consumption to compared with specimen of maximum aggregate size 5 mm.

References

- Hillerborg, A., Modeer, M., Petersson, P.E. (1976). Analysis of crack formation and crack growth in concrete by means of fracture mechanics and finite elements. *Cement and Concrete Research*, 6(6), 773–782.
- Kitsutaka, Y., Kamimura, K., Nakamura, S. (1994). Evaluation of aggregate properties on tension softening behavior of high strength concrete. *High Performance Concrete*, American Concrete Institute, ACI SP 149-40, 711–727.
- Kitsutaka, Y. (1997). Fracture parameters by polylinear tension-softening analysis. *J. Engrg. Mech., ASCE*, 123(5), 444–450.

Study on strength development properties of the internal characteristics of mass concrete (1-2559)

Koichi Matsuzawa, Yoshinori Kitsutaka
Faculty of Urban Environmental Sciences, Tokyo Metropolitan University
1-1 Minamiohsawa, Hachiohji, Tokyo 192-0397, Japan
e-mail: matsuzawa-kouichi@tmu.ac.jp

Introduction/background

Concrete members used in the reinforced concrete structures for nuclear power plants are massive. The main characteristic of mass concrete is a large size of the section. And the hydration heat of cement which was produced by hardening process influences the strength development properties of concrete. The hydration heat generated in a typical section size concrete member is easy to make a vending effect for a concrete member. However, the hydration heat generated in the mass concrete does not make a vending deformation for a concrete member because of the large section size. Internal hydration heat will be remained in the mass concrete, and concrete may be exposed at the temperature condition of over 80°C in a hardening process. There are some reports pointed out that the strength development of a concrete cured in high temperature is smaller to compare to the concrete cured in normal temperature in hardening process. In addition, internal heat of mass concrete by the hydration heat causes the difference of the thermal expansion between the inside and outside, and this difference produces the stress distribution in the section of the mass concrete. It is also assumed that the movement of moisture may easily occur in mass concrete because of the temperature gradation between the inside and outside of the concrete.

From the above considerations, in the hardening process of mass concrete, the hydration heat of cement, the stress by the temperature difference between the inside and outside of the concrete, and the movement of moisture in concrete will affect the strength properties of mass concrete.

Aim of the work

The purpose of this study is to clear the effect of multi-axial stress, temperature and humidity on the strength development of the early age concrete.

Essential results

1) Preparation of specimen

Specimen size was 40 mm cube. The water-cement ratios of concrete used in this experiment was set to 0.5. The cement was ordinary portland cement, aggregates were crushed sand and crushed stone of 10 mm maximum size. Approximately 6 hours after casting, the specimen was demolded.

2) Examination method

The specimen was demolded and jigs were put to 6 surface of the specimen. The jigs size were 38 mm × 38 mm section with no obstruction of moisture transfer of the specimen. The concept of the jigs is shown in Fig. 1. The specimen with jigs was set up in the test machine that could control the multi-axial stress, the temperature and humidity, and reproduced the temperature change, the stress change (when compression stress was generated), and the moisture movement in mass concrete. After the controlled curing by this test apparatus, the compressive strength and pore size distribution of the specimen were measured.

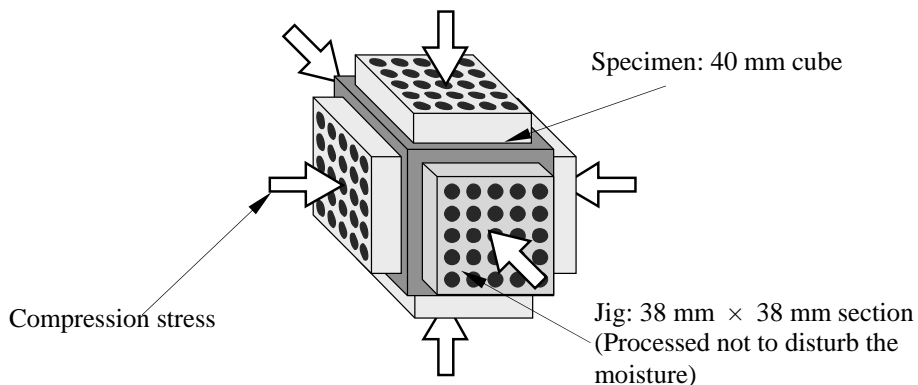


Figure 1. Outline of specimen.

Summary/conclusions

- 1) When concrete is subjected to the different conditions of temperature, and humidity in the young age, strength development properties of concrete is also different.
- 2) Multi-axial stress, temperature, and humidity in the early age concrete affect the total pore volume and pore size distribution of concrete.

Reference

Architectural Institute of Japan. (2000). Recommendation for Practice of Hot Weather Concreting.

Fatigue curve and stress strain response for stainless steel (1-3135)

Jussi Solin¹, Gerhard Nagel², Wolfgang Mayinger²

¹VTT Technical Research Centre of Finland

P.O. Box 1000, FI-02044 VTT, Finland e-mail: jussi.solin@vtt.fi

²E.ON Kernkraft GmbH, Tresckowstrasse 5, DE-30457 Hannover, Germany

e-mails: gerhard.nagel@eon-energie.com,

wolfgang.mayinger@eon-energie.com

Background and aim of the work

Applicability of ASME, KTA and RCC-M fatigue design curves for stainless steels is an issue of current debate. Laboratory data have shown environmental effects in coolant waters, but applicability of the proposed new design criteria to current plant components has been questioned. In a Regulatory Guide for new designs, the US NRC endorsed also a new air curve for stainless steels. Aim of the current study is to test applicability of the existing and proposed design criteria.

Solution annealed Niobium stabilized austenitic stainless steel (X6CrNiNb1810 mod) samples were extracted round the circumference of a $\phi 360 \times 32$ mm pipe, which fulfils all KTA material requirements for primary components in BWR and PWR. An experimental strain life fatigue curve was determined as a base line for component specific evaluations and for comparison with the Langer and Chopra curves, which are the basis of the ASME III and NRC RG 1.207 design criteria [1–3]. Monotonic and cyclic stress strain responses were carefully analysed to clarify the deformation and fatigue mechanisms.

Strain life curve

The Langer and Chopra curves are not much different for LCF and our data lie within a common scatter band in between. The curves deviate in HCF regime, and Chopra curve becomes more conservative. HCF lives for this material were longer than Chopra curve predicts and even an extrapolation of Langer curve becomes conservative at low amplitudes ($\epsilon_a < 0,19 \dots 0,18\%$). This is where the slope of strain life approaches zero and an endurance limit for 10 million cycles is obtained for this alloy in RT air (25 °C).

Stress strain response

Austenitic stainless steels are known for strain hardening and ability to generate large internal stresses. Tensile tests gave yield stress $R_{p\ 0,2\%} = 235 \dots 245$ MPa and tensile strength $R_m = 535 \dots 555$ MPa depending on strain rate, but the true stress strain response reached 1900 MPa stress at 175% strain in necking before break. The elastic modulus was $E = 197$ GPa, but unloading – reloading modulus is not constant. The apparent elastic modulus reaches a maximum just when yielding starts at about 0,1% total strain and then gradually decreases by about 5% until 1% strain and by about 15% until 10% strain (in true stress basis – even more for nominal stress). At high strains, changes of grain orientations may contribute, but at low strains the changes must be mainly due to internal stresses.

Consistent and well repeatable cyclic stress strain responses including initial hardening, softening and secondary hardening were observed. Dislocation density and internal stresses are increased during the first 10 to 50 hardening cycles, which are building up driving force for the following dislocation structure optimization and softening. At low strain amplitudes the final phase is secondary hardening. It is not clear, how onset of secondary hardening is determined, but it is astonishingly well predictable after 10^4 to 10^5 softening cycles – as a function of amplitude – and hardening will continue until fracture or passing of the run-out criterion.

Inelastic strains are notable even in HCF. In a test run at endurance limit, inelastic strain was initially more than one third of the total ($\varepsilon_a = 0,185\%$), but secondary hardening eliminated most of the plasticity before fracture at $1,2 \cdot 10^7$ cycles. Such prominent secondary hardening correlates with the endurance limit behaviour of this material.

Conclusions

Our fatigue data for Niobium stabilized austenitic stainless steel is in better agreement with the Langer curve than some newly proposed air curves. This means that the original basis of ASME 3 and KTA design criteria is valid for this material batch, which is completely relevant for primary loops in certain operating PWR's. Applicability of NRC RG 1.207, which is based on different fatigue data, should be investigated also for new designs utilising this kind of material.

References

1. Criteria of the ASME Boiler and Pressure Vessel Code for design by analysis in sections III and VIII division 2. Pressure Vessels and Piping: Design and Analysis, A Decade of Progress, Vol. One ASME 1972. Pp. 61–83.

1. Mechanics of Materials

2. Chopra, O., Shack, W. 2007. Effect of LWR Coolant Environments on the Fatigue Life of Reactor Materials, Final Report. NUREG/CR-6909, ANL-06/08, Argonne National Laboratory. 118 p.
3. U.S. Nuclear Regulatory Commission Regulatory Guide 1.207. 2007. Guidelines for evaluating fatigue analyses incorporating the life reduction of metal components due to the effects of the light-water reactor environment for new reactors. 7 p.

Effect of hardening model on the weld residual stress field in pipe girth welds (1-3142)

Jonathan Mullins, Jens Gunnars

Inspecta Technology AB, Lindhagensterrassen 1, Stockholm, Sweden
e-mails: jonathan.mullins@inspecta.com, jens.gunnars@inspecta.com

Accurate estimates of weld residual stress fields in welded components are necessary for conducting structural assessments where stress corrosion cracking and/or fatigue are of interest. The aim of the study is to determine whether finite element simulations of the weld residual stress field give the best agreement with experimental measurements if an isotropic, kinematic or mixed material hardening model is used. Two girth weld geometries are considered with thicknesses of 19 mm and 65 mm and radius to thickness ratios of 10.5 and 2.8, respectively.

Welding simulations were conducted using isotropic, kinematic and mixed hardening models. The isotropic hardening model gave the best overall agreement with experimental measurements. The mixed hardening model gave good agreement for predictions of the hoop stress but tended to under predict the magnitude of the axial stress. The kinematic hardening model consistently under predicted the magnitude of both the axial and hoop stress. The conclusions need to be confirmed by further simulations and measurements for other geometries.

Two sensitivity studies were also conducted. In the first the effect of using bilinear isotropic and kinematic hardening models with a saturation strain of 0.01 was evaluated. Neither of these models was capable of accurately predicting the weld residual stress field.

In the second sensitivity study, the effect of defining a viscoplastic model was evaluated. The viscoplastic model was found to give slightly lower stress peaks, although the effect was sufficiently small that the increased complexity and computational cost of defining such a model probably outweighs the benefits.

Theoretical model for the hydrogen-material interaction as a basis for prediction of the material mechanical properties (1-3145)

Dmitriy A. Indeitsev¹, Vladimir A. Polyanskiy², Alexander A. Sukhanov²,
Alexander A. Belyaev²

¹Professor, Director of the Institute of Problems in Mechanical Engineering of
Russian Academy of Sciences
199178, Bolshoy pr. V.O., 64, St.-Petersburg, Russia
e-mail: ind@director.ipme.ru

²Professor, State Polytechnic University of St.-Petersburg, 195294
Polytekhnicheskaya, 29, St.-Petersburg, Russia
e-mail: info@electronbeamtech.com

The natural law concentration of hydrogen inside the materials has a distribution over the different binding energies. This distribution is changing under the mechanical tension. The model of interaction of the small hydrogen concentration with materials provides one with an instrument for modeling the materials fatigue and destruction, as well as the prediction of material properties during exploitation.

The well-known models are of the phenomenological nature. However if one takes into account the physical mechanism then one obtains an accurate model and the instrument for the reliable prediction.

The two-continuum model of the solid material [1] is a substantiation for the present report. This model describes the interaction between the low concentration of hydrogen and the material. The redistribution of the hydrogen between the different binding energies levels is taken into account, too.

E.g., under slow uniaxial tension the stress-deformation curve has a maximum and a zone of instability well corresponding to the super plasticity of zirconium alloys. The model describes the complex process of accumulation and redistribution hydrogen inside the material.

One prediction methodology is constructed on this model. This methodology gives an ability of calculation of the degradation of material properties under mechanical tensions in the hydrogen contained environment. The methodology was applied to the investigation of the mode deformation steel tube with high pressure gas.

In the present report we described the results of the modeling with time-dependent mechanical properties, as well as the mechanical stresses in the tube.

Two-continuum model was applied also to the nanomaterial and the report will contain the derived equation and some results of modeling.

The parameters of model can be determined in the experiments on high temperature vacuum-extraction of hydrogen from the specimen.

Concluding we state that we developed a new physical model of the hydrogen-solid material interaction, this model providing one with a new substantiation for performing the methodology tests and prediction procedures.

Reference

1. Indeitsev, D.A., Semenov, B.N. About a model of structural-phase transformations under hydrogen influence. *Acta Mechanica*, Springer Wien–New York, Vol. 195, No. 1–4, 2008, pp. 295–304.

2. Fracture Mechanics and Structural Integrity

Experimental and theoretical results on brittle and ductile fracture of metallic, non-metallic and concrete materials. Cracks in welds and crack propagation by creep or fatigue. Local approach of fracture mechanics. Dynamic fracture. Fatigue issues including thermal and environmental effects. Simplified methods. Assessment of steel components (reactor vessels, piping systems, etc.). Leak before break assessment. Crack arrest.

The demonstration of warm pre-stress effect on RPV steels: experimental results and interpretation by engineering models (2-1579)

Moinereau Dominique

EDF R&D, Materials and Mechanics of Components Department
77818 Moret-sur-Loing, France, e-mail: dominique.moinereau@edf.fr

The reactor pressure vessel (RPV) is an essential component liable to limit the lifetime duration of PWR nuclear power plants. According French RCCM (Design) and RSEM (In Service Assessment) Regulatory Codes, the assessment of defects and flaws in RPV subjected to hypothetical PTS transients doesn't account the beneficial effect of load history (warm pre-stress WPS) on the brittle resistance of the material. Numerous R&D actions have been conducted by EDF, in collaboration with several organizations, in order to sufficiently give elements to demonstrate, to model and to validate the beneficial WPS effect regarding the risk of brittle failure in a RPV integrity assessment.

An extensive experimental work has been conducted covering a large range of experimental conditions, including WPS type experiments on fracture mechanics specimens and large scale components on usual RPV steels. Among these experiments, one PTS type transient experiment has been performed (by MPA Stuttgart) on a large cracked cylinder. Additional experiments have been made on irradiated material, using 1/2T CT specimens from EDF RPV surveillance programme.

All experimental results are available and confirm the beneficial effect of warm pre-stress on the resistance of RPV steels, with a significant increase of the material resistance regarding the risk of brittle failure. No fracture occurred during unloading, confirming thus the 'WPS conservative principle'.

The experiments have been analysed with fracture mechanics, using both engineering (mainly the Wallin model) and more refined models based on local approach to fracture. The WPS engineering models have been applied to all WPS database in order to predict effective fracture toughness induced by WPS.

Following a short description of the warm pre-stress concept, the paper summarizes the main experimental results, describes the engineering models to account WPS and their applications towards the experiments. The capability of such models to simulate WPS and predict the fracture toughness increase is demonstrated on this extensive WPS database.

NESC VII: a European project for application of WPS in RPV assessment including biaxial loading (2-1580)

Moinereau Dominique¹, Gilles Philippe², Chapuliot Stéphane³

¹EDF R&D, 77818 Moret-sur-Loing, France

e-mail: dominique.moinereau@edf.fr

²AREVA NP SAS, 92084 Paris La Défense, France

e-mail: philippe.gilles@areva.com

³CEA, 91191 Gif-sur-Yvette, France

e-mail: stephane.chapuliot@cea.fr

The Reactor Pressure Vessel (RPV) is an essential component liable to limit the lifetime duration of PWR plants. The assessment of defects in RPV subjected to PTS transients made at an European level do not take necessary into account the beneficial effect of load history (warm pre-stress WPS) on the resistance of RPV material regarding the risk of brittle failure. A 4-year European Research & Development program – SMILE – has been successfully conducted between 2002 and 2005 as part of the Fifth Framework of the European Atomic Energy Community (EURATOM).

The objective of SMILE project ('Structural Margin Improvements in aged-embrittled RPV with Load history Effects') was to give sufficient elements to demonstrate, to model and to validate the beneficial WPS effect in a RPV integrity assessment. Numerous experimental, analytical and numerical results have been thus obtained which confirm the beneficial effect of warm pre-stress on RPV steels, with an effective significant increase of the material resistance regarding the risk of brittle failure.

In addition to SMILE, a new project dealing with WPS - NESC VII - has been launched in 2008 (in link with the European Network of Excellence NULIFE) with the participation of numerous international organizations (involving R&D, Utilities and Manufacturers). Based on experimental, analytical and numerical tasks, the project is focused on topics generally non covered by past experience on WPS: biaxiality of loading on large-scale specimens, effect of irradiation, applicability to intergranular fracture, modeling (including analytical and numerical models) ... Among these tasks, some new original WPS experiments will be conducted on large scale cruciform bend bar specimens in order to study the influence of biaxial loading on WPS effect, using a fully representative RPV steel (18MND5 steel similar to A533B steel).

A full description of the NESC VII project is presented in this paper with the corresponding organization, including the present status of the project.

Primary stress index B_2^* for the evaluation of postulated or detected circumferential flaws at the connection straight-pipe / bend (2-1583)

Wieland Holzer, Werner Wolf
TÜV SÜD Industrie Service GmbH, Munich, Germany

At different locations of piping systems often postulated or detected circumferential flaws have to be evaluated. It has to be decided if the postulated or detected circumferential flaws are acceptable or if the component has to be exchanged or repaired. In this paper the focus is on possible evaluation methods of postulated or detected circumferential flaws at the connection straight pipe/bend.

For detected or postulated circumferential flaws at the weld connecting the straight pipe and the bend the first step of the common evaluation procedures is the determination of the stress distribution. Therefore the common piping calculation programs can be used. In these programs for calculating the primary and secondary stresses and the check if the primary and secondary stress limits are satisfied the following well-known equations (1) and (2) are implemented.

$$B_1 \frac{PD_0}{2t} + B_2 \frac{D_0}{2l} M_i \leq 1.5S_m \quad (1)$$

$$C_1 \frac{PD_0}{2t} + C_2 \frac{D_0}{2l} M_i + C_3 E_{ab} |\alpha_a T_a - \alpha_b T_b| \leq 3S_m \quad (2)$$

The primary membrane and bending stresses have to be considered in the evaluation procedures for circumferential flaws. One example for an evaluation procedure is given in [1]. The important issue is the determination of the primary bending stress for the connection straight pipe/bend. Therefore an appropriate but conservative factor B_2 has to be used.

If the factor $B_2=1$ is used, the calculated bending stress is neither correct nor conservative for the connection straight pipe/bend. But if the factor $B_2 = 1,3xh(-2/3)$ given in the codes and safety standards [2], [3] and [4] for 90°-bends is used, the calculated bending stress seems to be overly conservative for the connection straight pipe/bend. So in this paper it's investigated if the factor $B_2^* = 0,7xh(-2/3)$ which is well established for the evaluation of wall thickness reductions at the connection straight pipe/bend can be used for the evaluation of detected or postulated circumferential flaws at this connection. The development of B_2^* and the evaluation method for wall thickness reductions at the connection straight pipe/bend using B_2^* is described in [5]. To check if B_2^* is appropriate but

2. Fracture Mechanics and Structural Integrity

conservative for the evaluation of circumferential flaws at the connection straight pipe/bend a parametric finite element study is carried out. In the parametric study it's investigated if for the factor B_2^* the following equation is met:

$$B_2^* \leq \frac{J_{StraightPipe/Bend}}{J_{StraightPipe}} \quad (3)$$

Because for the straight pipe and for the connection straight pipe/bend for the local part of the circumferential flaw the same finite element mesh is used, it's not necessary to put the focus on the evaluation of the J-Integral.

The results of the parametric finite element study show that B_2^* can be used for common evaluation procedures and that for very expanded flaws the flaw size should be taken into account.

References

1. ASME Code Section XI, Division 1, Appendix H.
2. ASME Code Section III, Division 1, Subsection NB (Class 1 Components) and Subsection NC (Class 2 Components).
3. KTA 3201.2, Komponenten des Primärkreises von Leichtwasserreaktoren, Teil 2: Auslegung, Konstruktion und Berechnung.
4. KTA 3211.2, Druck- und aktivitätsführende Komponenten von Systemen außerhalb des Primärkreises, Teil2: Auslegung, Konstruktion und Berechnung.
5. Wieland Holzer, Robert Kauer, Christian Hüttner, Assessment of local decreases in wall thickness reductions at the connections straight-pipe/bend using stress concentration factors, SMiRT 16, Washington, 2001.

Dynamic crack growth and arrest simulation with cohesive zone models, during a pressurized thermal shock in a RPV (2-1596)

Debruyne Gilles

EDF, Research and Development Division, Acoustic and Mechanic Analysis
Department, 1 Avenue du Général de Gaulle 92141 Clamart, France
e-mail: gilles.debruyne@edf.fr

The aim of this work is to make prospective investigations concerning the growth and arrest of an initial subclad flaw, into a RPV shell submitted to an hypothetical pressurized thermal shock. The analysis is based on a 2D axisymmetric torus geometry (to take into account the closed end effect) with a negligible curvature (a bending radius of 100 meters is prescribed), including an axial flaw, which ensures conservative results with respect to actual 3D semi-elliptical flaws. A preliminary non linear transient thermal analysis is achieved, before mechanical computations. Due to the severe loading involving strong temperature gradients, combined with temperature and embrittlement dependence for fracture properties, inertial effects could arise and dynamical investigations may be required to assess crack velocity and arrest. Furthermore, a scenario, where a heterogeneous zone is embedded ahead of the crack tip, is also considered, which likely to enhance the dynamic features. A mesh of classical isoparametric finite elements covers the body while a midpoint Newmark scheme is used for time discretization. For Fracture modeling, Cohesive Zone Models (CZM) with or without initial stiffness, including temperature dependent properties (surface energy and critical tensile strength) are set all along the prospective crack path, on the side of the base metal in ferritic alloy steel, but also on the side the austenitic steel cladding. Both materials are considered either elastic or elasto-visco-plastic. Besides, a quasi-static analysis with a loading path following algorithm to match unstable propagation stages, is performed. The main results are the following:

- The crack onset predicted with CZM is in a good accordance with a Griffith criterion, estimated with a classical J integral (particularly for the elastic behavior). It always occurs towards the base metal owing to the cladding ductility.

2. Fracture Mechanics and Structural Integrity

- The crack kinematics, including velocity and arrest length is very few sensitive to the CZM critical tensile strength (in the range considered for steels) and to the cohesive law (the opening stress-displacement jump relation is considered here either linear or exponential).
- Plasticity effects tend to less or more crack growth stability, depending of the growth stage.

Further outlooks concerning 3D extension and cohesive models numerical improvement, are also considered.

Numerical study of 3-D constraint effects in ferritic steels (2-1602)

Claudio Roberto Soares¹, Paulo de Tarso Vida Gomes²,
Emerson Giovanni Rabello³

¹Nuclear Technology Development Center, P.O. Box 941, Brazil
e-mail: roberto@cdtn.br

²Nuclear Technology Development Center, P.O. Box 941, Brazil
e-mail: gomespt@cdtn.br

³Nuclear Technology Development Center, P.O. Box 941, Brazil
e-mail: egr@cdtn.br

In standard fracture toughness testing, the specimens configurations should comply with size requirements regarding the initial crack length and the thickness of the specimen. These restrictions are mainly to ensure a plane strain condition at the crack tip, and thus to obtain a plane strain toughness. However, to obtain relevant material toughness for assessing real structures with shallow cracks and/or small thickness, is necessary to understand and take into account the in-plane and out-of-plane constraint effects from experimental data.

Different approaches have been proposed to quantify constraint and to describe the effects of constraint variations on engineering fracture toughness characterized by J-Integral or equivalently the Crack Tip Opening Displacement, CTOD. This paper presents the results of a numerical investigation, in which single-edge cracked bars in three point bend SE(B) specimens, with different relative crack lengths and thickness, were systematically studied via detailed three-dimensional finite element analyses.

A J estimation scheme for surface cracks in piping welds (2-1672)

Stéphane Marie¹, Patrick Le Delliou², Yann Kayser¹, Bruno Barthelet³,
Philippe Gilles⁴, Hubert Deschanel⁵

¹Commissariat à l'Énergie Atomique (CEA) DRN/DMT/SEMT/LISN
91191 Gif sur Yvette, France

²EDF R&D, Département MMC, Les Renardières
77818 Moret s/Loing Cedex, France

³EDF Industry, Nuclear Power Operations, Site Cap Ampère
93282 St Denis Cedex, France

⁴AREVA NP, Tour AREVA, 92084 Paris La Défense Cedex 16, France

⁵AREVA NP, 10 rue Juliette Recamier, 69456 Lyon Cedex 6, France

The RSE-M and RCC-MR Codes provide respectively rules and requirements for in-service inspection of French Pressurized Water Reactor power plants, and for the design of high temperature nuclear components. The Codes give non mandatory guidance for analytical evaluation of flaws (Appendices 5.3 and 5.4 for RSE-M and Appendix A16 for RCC-MR). Flaw assessment procedures rely on fracture mechanics analyses based on simplified methods (i.e. analytical). Analytical methods are available to calculate the J integral in various cracked piping components (straight pipe, tapered transition, elbow and pipe-to-elbow junction), submitted to mechanical loading (in-plane bending moment, pressure, torsion moment), thermal loading as well as for combined loading. However, for the analysis of cracks in welds, they use the tensile properties of the weakest material between the base material and the weld material. This induces some conservatism on the estimated J values.

A cooperative program between EDF, CEA and AREVA NP was launched in 2004 to develop a J estimation scheme which takes into account the strength mis-match effects. The scheme relies on the definition of an 'equivalent' stress-plastic strain curve, as proposed in the R6 rule. This curve is then used with the analytical methods for homogeneous cracked components. In a first step, the method is developed for circumferential surface cracks in straight butt-welded pipes submitted to mechanical loading. It takes into account the geometry of the weld joint (V-shaped), as well as the location of the crack within the weld.

This paper recalls the background of the method, provides the detailed formulae needed to apply the J-estimation scheme and finally presents the validation work, based on a large finite element database.

Influence of welding process on fatigue crack propagation properties in structural steel (2-1638)

Geraldo de Paula Martins¹, Emerson Rabello², Jefferson José Villela³, Daniel Januário Cordeiro Gomes⁴, Mariana Pimenta⁵, Leonardo Barbosa Godefroid⁶, Carlos Alberto Cimini Jr⁷

¹Centro de Desenvolvimento da Tecnologia Nuclear (CDTN/CNEN), Av. Presidente Antônio Carlos, 6627, Pampulha, Belo Horizonte, Minas Gerais, Brasil
e-mail: gpm@cdtn.br

²Centro de Desenvolvimento da Tecnologia Nuclear (CDTN/CNEN), Av. Presidente Antônio Carlos, 6627, Pampulha, Belo Horizonte, Minas Gerais, Brasil
e-mail: egr@cdtn.br

³Centro de Desenvolvimento da Tecnologia Nuclear (CDTN/CNEN), Av. Presidente Antônio Carlos, 6627, Pampulha, Belo Horizonte, Minas Gerais, Brasil
e-mail: jjv@cdtn.br

⁴Universidade Federal de Minas Gerais, Av. Presidente Antônio Carlos, 6627, Pampulha, Belo Horizonte, Minas Gerais, Brasil; Departamento de Engenharia Mecânica
e-mail: danieljanuário@yahoo.com.br

⁵Universidade Federal de Minas Gerais, Av. Presidente Antônio Carlos, 6627, Pampulha, Belo Horizonte, Minas Gerais, Brasil; Departamento de Engenharia Mecânica
e-mail: maripimenta@yahoo.com.br

⁶Universidade Federal de Ouro Preto, Minas Gerais, Brasil Departamento de Metalurgia; e-mail: Leonardo@em.demet.ufop.br

⁷Universidade Federal de Minas Gerais, Av. Presidente Antônio Carlos, 6627, Pampulha, Belo Horizonte, Minas Gerais, Brasil; Departamento de Engenharia Mecânica
e-mail: cimini@demec.ufmg.br

Keywords: fracture mechanics, fatigue crack propagation, fracture in welds, fatigue crack propagation models.

On this work, the crack propagation resistance of the SAC 50 steel welded joints by the shielded metal arc weld (SMAW), gas tungsten arc weld (GTAW) and gas metal arc welding (GMAW) were studied. The crack propagation tests were accomplished using compact tension (CT) specimens with notch localized at the base metal (BM), heat affected zone (HAZ) and at the melting zone (MZ). Equations for Colliepriest, Priddle and Paris models for the several specimens tested were obtained and comparisons of the crack propagation properties for the three welding processes were made using the three models of crack propagation: Paris, Colliepriest and Priddle. It was concluded that the specimens with notch localized at the HAZ and at the MZ of the welding joints by the SMAW resulted in better crack propagation results. It was also concluded that for all situations, the Colliepriest model were the more near of the test data results.

Thermal fatigue analysis of a NPP steam generator injection nozzle model subjected to thermal stratification (2-1710)

Luiz Leite da Silva¹, Carlos Alberto Cimini Junior², Tanius Rodrigues Mansur³

^{1,3}CNEN/CDTN, Av. Presidente Antônio Carlos, 6627 – Campus UFMG
Pampulha, Belo Horizonte, MG, CEP 30123-970

e-mail: silvall@cdtn.br, tanius@cdtn.br

²UFMG, Av. Presidente Antônio Carlos, 6627 – Campus UFMG, Pampulha
Belo Horizonte, MG, CEP 31270-901, e-mail: cimini@ufmg.br

The study of thermal fatigue damage in AISI 304L stainless steel pipe under thermal stratification was the main purpose of this work. Pipe material damage was quantified comparing results of fatigue tests from specimens from the preserved pipe portion and specimens made of the pipe thermal stratification experimental section. Strains measured during thermal stratification experiments were used as parameters to carry out the fatigue tests. A numerical model was developed to simulate the pipe behavior under thermal stratification phenomenon in order to predict its time life. The experimental section simulates the steam generator (SG) injection nozzle of a Pressurized Water Reactor (PWR) nuclear power plant (NPP). This is a NPP component where thermal stratification frequently happens, mainly during NPP start up and shutdown. Because of thermal stratification loads, thermal fatigue sometimes damages this component and through wall cracks may appear. The main components used to simulate the SG injection nozzle are a 2 m long horizontal pipe, a 90° elbow, a 0.5 m vertical pipe. The whole experimental section is a reduced model made of a pipe with outside diameter of 0.1412 m and wall thickness of 0.0095 m. As in the SG injection nozzle, the experimental section is thermally insulated. The reduced model is made of AISI 304L stainless steel with seven different temperatures and strains measuring positions. Five of these positions are in the horizontal pipe, one of them in the elbow and the last one in the vertical pipe. Outside and inside temperatures are measured in three out of this seven measuring positions. Strains are measured just outside the pipe in all seven measuring positions. The water thermal stratification temperatures are measured inside the pipe by thermocouples probes. Each thermocouple in the probe is positioned at a different level along the inside pipe diameter. A different number of thermocouples are mounted in each probe. Outside wall temperatures are measured by thermocouples brazed in the same positions as the probes. Circumferentially, the outside thermocouples are distributed in such a way that they stay in the same level as the inside ones. Extras thermocouples were brazed at the upper and lower three measuring positions. The strains were measured by

rectangular rosettes in all seven measuring positions and the amount of them is different in each one. Strain gages rosettes were attached in positions where a previously numerical simulation indicated that major strains could be present. Despite of the experimental section not be an injection nozzle scaled model, it is possible to obtain on it similar range of Froude number as in the real PWR NPP injection nozzle. Froude number is the hydraulic parameter commonly used to model thermal stratification phenomenon. This is a parameter that relates the flow velocity, acceleration due to gravity, difference of fluid density and the pipe inside diameter. The Froude number range acquired in the real injection nozzle and in the experimental section is from 0.02 to 0.2. Numerical simulations of stresses and strains were carried out using a coupled analysis in the ANSYS code with temperatures and pressure inputs taken from thermo stratification experimental results. To perform the coupled analysis the tetrahedral SOLID98 element from the ANSYS code library was used. It was possible to conclude that thermal stratification will happen in the experimental section and that numerical and experimental results were in agreement in the pipe region where they were compared, showing that thermal stratification induces considerable thermal stresses and strains in the experimental section. It could also be concluded that thermal stresses due to thermal stratification phenomenon reduce the pipe material life time.

Structure integrity assessment of pressurizer (2-1723)

Nenad Gubelj¹, Jelena Vojvodič-Tuma², Jožef Predan¹, Milan Kljajin³

¹University of Maribor, Faculty of Mech. Eng.
Smetnova 17, 2000 Maribor

²Institute for Metals and Technology-IMT Ljubljana
Lepi pot 11, 1000 Ljubljana

³University of Osijek, Faculty of Mech. Engineering Sl. Brod
35000 Sl, Brod

In regular service of nuclear power plant, the pressurizer has main role to ensure steam's pressure and dumping of pressure caused by water level changes in primary pipe-line system. The most loaded is lower spherical section of pressurizer. This part was made from two material clad and substrate. Lower spherical section and noodle for pipeline are connected by welded joint. It has been found that in vicinity of weld joint is locally highest stress caused by internal pressure and thermodynamic load.

Aim of the work

Considering the strength mis-match effect of materials to stress strain distribution and internal pressure the structure integrity assessment of pressurizer is performed in order to figure out, if easy detectable size is critical in the case of service and overload pressure?

Material characterization

Mechanical properties and fracture toughness testing of substrate pressurizer material is performed on simulated cast with same chemical composition and same production treatment as original material in Nuclear Power Plant [1]. Tests were performed on artificially 2 years aged specimens at service temperature 300°C. The fracture toughness values in term of J-integral=81 N/mm was determined according to ASTM test procedure [2]. Mechanical properties of clad and weld metal are taken from ASME Boiler and Pressure Vessel Code [3].

Numerical analysis

Considering the material and physical properties of pressurizer bottom and internal pressure, the numerical analysis of displacement (Fig. 1) and stress

distribution through the thickness was performed (Fig. 2). Figure 2 shows that stress gradient is highest in region of substrate-clad fusion line, where the maximum stresses are close to yield stress of substrate material. The structure integrity assessment of pressurizer bottom part has been performed considering interaction of all three material properties. The structure integrity is performed for pressurize with assumed semi-elliptical surface crack with depth $a/W=0.75$, with crack $a = 51.2$ mm and $2c/a=5$. Calculation of J-integral as parameter of fracture mechanics was performed by using ABAQUS Version 6.7 [4]. Figure 3 shows that at service temperature and under service pressure $p=15.51$ MPa, the J-integral is more than eight times smaller than measured fracture toughness. The obtained results of numerical analysis show that maximum internal pressure cannot cause the unstable fracture.

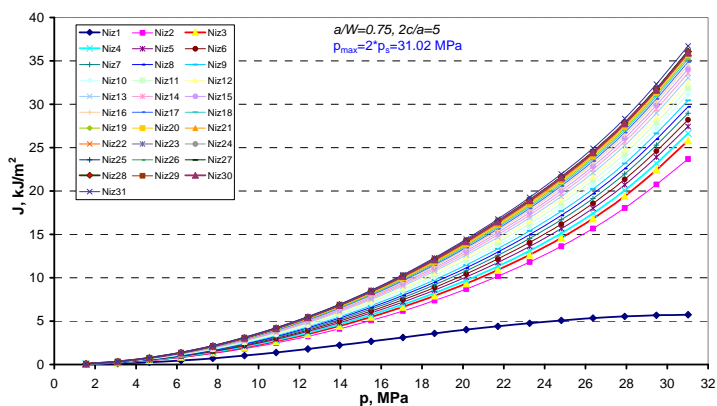
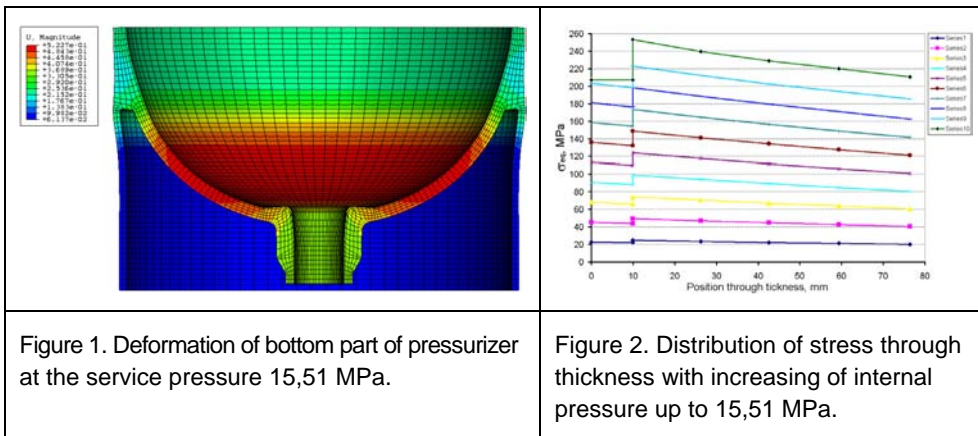


Figure 3. The increasing the crack tip parameter J-integral with increasing internal pressure, (Niz1 is surface point and Niz31 is deepest point of semi-elliptical crack).

Conclusion

Obtained results show, that under constant internal pressure (double than service $p=2 \cdot 15,51=31,02$ MPa, the J-integral value is proportional to crack depth and potentially increasing by pressure. Fracture toughness tests show the minimum material parameter of J-integral $J_{mat}=81$ kJ/m². Since, no any point along the contour of crack achieve this value at deepest crack $a/W=0,75$ (where $a=51,2$ mm), the safe use of pressurizer is ensure.

References

1. Gubelj, N., Vojvodič-Tuma, J., Šuštaršič, B., Predan, J., Oblak, M. Assessment of the load-bearing capacity of a primary pipeline. Eng. fract. mech., Apr. 2007, Vol. 74, Iss. 6, ss. 995–1005.
2. ASTM E-1820 01 Standard Test Method or Measurement of Fracture Toughness, Vol. 03.01, ASTM International, W. Conshohocken, PA, 2004.
3. ASME Boiler and Pressure Vessel Code, Section II, Part D, Edition 1992.
4. ABAQUS Version 6.7-EF1, <http://www.simulia.com>.

Bond behavior between reinforcing steel and concrete under multiaxial loading conditions in concrete containments (2-1734)

Lemnitzer, Laura¹, Schröder, Steffen², Curbach, Manfred³

¹Institute of Concrete Structures, Faculty of Civil Engineering, Technische Universität Dresden, 01062 Dresden, Germany
e-mail: Laura.Lemnitzer@tu-dresden.de

²Institute of Concrete Structures, Faculty of Civil Engineering, Technische Universität Dresden, 01062 Dresden, Germany
e-mail: Steffen.Schroeder@tu-dresden.de

³Head of the Institute of Concrete Structures, Faculty of Civil Engineering Technische Universität Dresden, 01062 Dresden, Germany
e-mail: Manfred.Curbach@tu-dresden.de

Background

Important elements of the safety equipment of nuclear power plants are reinforced and prestressed concrete containments, which generally have been used as protective cover in pressurized-water and boiling-water reactors. For these structures, the leakage rate of hazardous products has to be limited to a maximum allowable rate. Therefore, the verification of integrity and leak tightness of containment structures is of high priority.

During hazardous incidents, the reinforced and/or prestressed concrete containment is exposed to high internal pressure and temperature loads. As a result, tensile loads affect the reinforced concrete structure in the hoop and vertical direction. If the tensile loading exceeds a critical limit, this biaxial stress state could induce a formation of first cracks at a lower level than expected from uniaxial laboratory tests. Additionally, an earlier initial cracking influences the crack formation and therefore the deformation behavior of the reinforced concrete structure.

The deformation behavior of a modern prestressed concrete containment under increasing internal pressure was tested by means of a 1:4 scale model in the Sandia National Laboratories in the USA [1]. Calculations of the load-deformation-behavior with Finite-Element-Analysis show a good agreement between experiment and analysis. However, larger differences between calculated and tested deformations could be observed in the phase of crack formation [2]. For an accurate determination of leakage rates to a given stress state, an improvement of the analytical propagation of the load-deformation-

behavior during the cracking stage is important. Therefore, a precise knowledge of the cracking process is necessary.

Aim of the work

For realistic modeling of the load-deformation-behavior of containment structures, multiaxial loading conditions as well as the interrelation and therefore the specific bond conditions between reinforcement and concrete should be considered. By means of a comprehensive experimental program, the bond properties between reinforcement and concrete under transverse tensile loads have been investigated. Pull-out tests with a short bond length of $2 d_s$ under transverse tension have been carried out. In order to represent the conditions of the primary cracking state, different grades of transverse tension were chosen with the transverse tensile stress lower than the uniaxial mean tensile strength of concrete.

The experimental results can be used in terms of bond-slip-relationships for implementation in the FE-containment model. With this application, a more realistic modeling of the deformations in primary and stabilized cracking can be achieved. Furthermore, the test results can be used for the verification of ultimate limit states, e.g. anchorages and serviceability limit states, e.g. deformations and crack control.

Results

The bond stress could be determined directly from the pull-out test by relating the pull-out load to the embedded lateral surface of the steel bar. The related concrete cover of the specimens is about $c/d_s = 5.75$ so that a pull-out failure is expected for specimens without transverse tension. The influence of an existing transverse tensile load can be described as follows: A pull-out failure with completely sheared of concrete corbels between the ribs occurred for all specimens independent from the transverse tension level. As a result of the confinement action caused by the great concrete cover, no splitting of the concrete cover occurred even for a transverse tensile stress nearly equal to concrete tensile strength. The maximum applicable bond stress shows only a slightly decreasing trend with increasing transverse tension, whereas the corresponding slip values seem unaffected by the transverse tension level. This behavior differs from the test results of Nagatomo/Kaku [3]. They found out that for small concrete covers $c/d_s \leq 3$ the maximum applicable bond stress rapidly decreases with increasing transverse tension level for splitting failure mode.

Conclusion

For the prediction of deformations and cracking processes in reinforced concrete structures, the interrelation between reinforcement and concrete has to be considered. Hereby, multiaxial loading conditions influence the specific bond behavior between these components. Test results show that depending on the concrete cover transverse tensile loads deteriorate the bond properties concerning maximum bond resistance, bond stiffness and failure mode. With the obtained bond stress-slip-relationships from pull-out tests under transverse tension a realistic modeling of multiaxial tensile loaded reinforced concrete structures is possible, e.g. by implementation in FE-Analysis.

Acknowledgement

The authors gratefully acknowledge the financial support of this research from Bundesministerium für Wirtschaft und Technologie (Federal Ministry of Economics and Technology, project no. 1501336).

References

1. Hessheimer, M.F., Klamerus, E.W., Lambert, L.D., Rightley, G.S. Overpressurization Test of a 1:4 Scale Prestressed Concrete Containment Vessel Model (NUREG/CR-6810). Sandia National Laboratories, U.S. Nuclear Regulatory Commission & Nuclear Power Engineering Corporation (Japan), San Diego, 2003
2. Grebner, H., Sievers, J. Structural mechanics simulation of SANDIA large scale experiments on a pre-stressed containment model. In: EUROSAFE – Forum for nuclear safety, Berlin, 2004.
3. Nagatomo, K., Kaku, T. Bond behaviour of deformed bars under lateral compressive and tensile stress. In: Proceedings of international conference “Bond in Concrete – from research to practice. CEB, Vol. 1, Riga, 1992.

Evaluation of the cleavage fracture toughness of SA508 Gr. 4N low alloy steels in the transition region (2-1788)

Min-Chul Kim¹, Ki-Hyoung Lee², Bong-Sang Lee¹

¹Nuclear Material Research Div., Korea Atomic Energy Research Institute,
1045 Daedeok-daero, Yuseong-gu, Daejeon 305-353, Korea
e-mail: mckim@kaeri.re.kr

²Dept. of Materials Science & Engineering
KAIST, 335 Gwahangno, Yuseong-gu, Daejeon 305-701, Korea

Nuclear reactor pressure vessels (RPVs) suffer an increase of tensile strength and a decrease of fracture toughness due to an embrittlement of the materials by a neutron irradiation. Fracture toughness loss causes an increasing ductile-brittle transition temperature, and then a brittle fracture could be occurred. Therefore, RPV steel with higher fracture toughness could enhance the integrity of nuclear power plants. Generally, SA508 Gr.4N low alloy steel has a higher strength and fracture toughness than commercial SA508 Gr.3 by an increase of the Ni and Cr contents. In this study, fracture toughness properties of several SA508 Gr.4N model alloys with different alloying elements contents were evaluated in the transition region. Moreover, effects of alloying elements and impurities on the transition properties of SA508 Gr.4N low alloy steels were investigated based on fractographs and micrographs. Fracture toughness tests were conducted following the ASTM standard E1921-05. All toughness data were size-corrected corresponding to those of 1T specimens. The dependence of the fracture toughness on the test temperature followed the Master Curve trend for all model alloys. Most of the data points were included within 95%, 5% of the theoretical tolerance bound lines. This result means that reference temperature, T_0 , is suitable for parameter characterized transition properties of fracture toughness. The transition behavior of SA508 Gr.4N model alloys was improved by increases of the Ni and Cr contents. These results can be explained by grain size refinement and changes in precipitate behavior as well as intrinsic effects of Ni addition. Higher P content caused a low fracture toughness of SA508 Gr.4N model alloy in the transition temperature region due to a segregation of P into grain boundaries. However, decreasing of the impurities contents improved the transition properties of SA508 Gr.4N model alloys.

An analytical thermal fatigue crack growth approach (2-1796)

C. Gourdin¹, S. Marie¹, S. Chapuliot²
¹CEA, DEN, DM2S, SEMT, Laboratoire
F-91191 Gif-sur-Yvette, France
²AREVA NP, France

This paper presents recent works on the thermal fatigue crack growth approach in structure integrity analysis proposed by nuclear standard codes such as A16 Appendix of RCC-MR. The proposed approach for crack growth is used to study the mechanisms leading to cracking of piping as a result of thermal loading in mixed flow zones.

To accurately determine the mechanical response of a complex component such as a pipe or a mixing zone due to thermal loading, it is necessary to be able to take into account in modelling the effects due to the structure, i.e. the effects due to the boundary conditions, the geometry and the additional loadings (pressure). Figure 1 shows that the mechanical response according to the thickness depends on the geometry. Whereas at the inside wall, the mechanical response is similar in the two cases, the stress profile along the thickness is different and has a substantial impact on the propagation of a crack, for instance. In one case, the crack will be arrested (infinite plate) and the stress will become null. The depth of the crack depends on the frequency of the thermal loading. In the other case, the crack will be continued to grow until it extends all the way through the pipe wall, with considerable membrane stress remaining.

For infinite plates, many thermomechanical analytical models exist in the literature and have been used with varying degrees of success. However, the industrial problems encountered in practice do not correspond to cases involving infinite plates subjected to fluctuations in temperature. This being the case, coefficients depending on the geometry and the boundary conditions are being introduced into “improved” analytical modelling.

The proposed approach for crack consists of two stages, and it is based on fracture mechanics and uses the methodology described in RCC-MR, Appendix A16 [RCC-MR].

The first stage of our proposed approach consists of mathematical analysis of the sinusoidal thermal loading, followed by a mechanical analysis of associated mechanical loading. Furthermore, parameters can easily be set, making it possible to more rapidly begin the study of the local and global responses of the structure. The final objective of this first stage is to determine the critical range of frequency of the thermal loadings for our problem (cf. Figure 2).

The second stage is based on experimental temperature observation with the most realistic smoothing possible between the findings. This thermal loading

2. Fracture Mechanics and Structural Integrity

obviously has little physical reality as it is a mathematical construct, but it offers the advantage of being rapidly set up. We will use the same tools and procedure described on the first stage (analytical model and crack growth calculation). The particularity is the use of spectral temperature fluctuation. Crack propagation rate is determined with the time sequence used, making it possible to estimate the lifespan of the component.

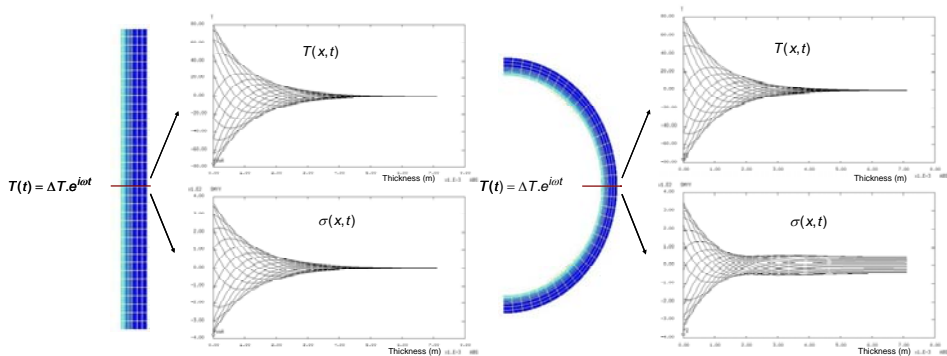


Figure 1. The effect of geometry on mechanical response under the same thermal loading.

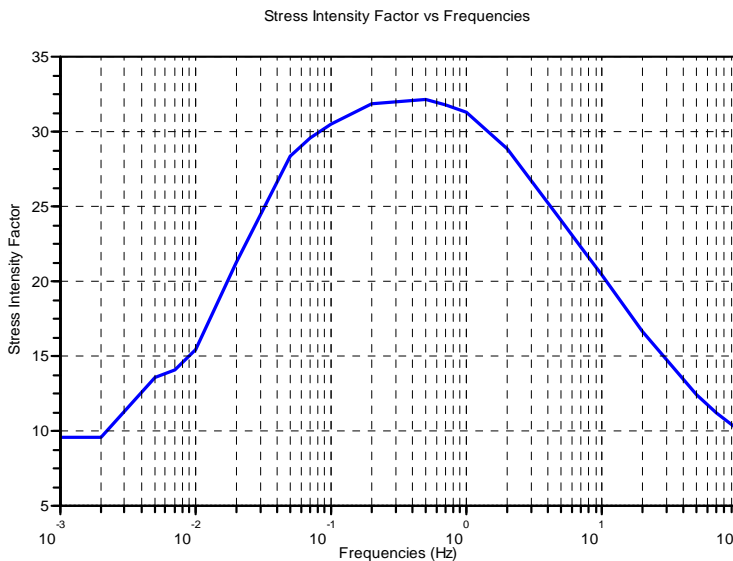


Figure 2. Change in stress intensity factor variation as a function of frequency at the outside surface of the component.

On assessment of initial cracks for RI-ISI analysis purposes (2-1797)

Otso Cronvall

VTT Technical Research Centre of Finland

P.O. Box 1000, 02044 VTT, Finland

e-mail: otso.cronvall@vtt.fi

The assessment of initial cracks for Risk Informed In-Service Inspection (RI-ISI) analyses of Nuclear Power Plant (NPP) piping systems is considered here. In RI-ISI analyses piping component specific risks are assessed based on estimated failure and consequence potentials, and typical analysed locations are welds. In general there exist two main approaches for assessment of piping failure potential in current relevant RI-ISI procedures: qualitative and quantitative. Here discussion concerning assessment of initial cracks connects primarily to quantitative piping failure potential assessment. Estimates of initial cracks are among the most influential input parameters in terms of RI-ISI procedure response, or arguably the most influential ones.

The use of piping degradation data in the statistical assessment of initial cracks is discussed. Then, the use of structural reliability procedures together with statistical estimates and expert judgement as supporting methods is discussed. Only structural reliability procedures can capture in the relative differences of the failure probability results the effects caused by differences in physical characteristics, loading conditions and inspection histories between the analysed piping components. The foremost of the structural reliability procedures for piping components, namely Probabilistic Fracture Mechanics (PFM), is briefly described then. When assessing piping component failure potential the effect of inspections is usually included in the form of Probability Of Detection (POD) functions. The quantitative estimates of piping component failure potential are typically expressed as probability of leak/break.

Typically the relevant needed initial crack estimates for the PFM crack growth simulations are probabilistic density distributions for initial crack depth and length, and for degradation mechanisms causing cracking, probabilistic density distributions for initiation frequency of cracks. All these estimates are dependent of pipe size, material, loads and process conditions as well as considered degradation mechanism.

The uncertainties in the estimation of probabilistic distributions for initial cracks relating to quality, amount, origin and type of available and applicable crack data are discussed next. Because the existing piping crack databases concern only grown cracks the sizes of the initial cracks have to be somehow assessed recursively. Two approaches to recursively calculate estimates for initial cracks are presented: the first and simpler one is mainly based on expert

2. Fracture Mechanics and Structural Integrity

judgement selection of initial crack mean size based on available and applicable crack data, whereas the second one is mainly based on calculating recursively for these data the initial crack sizes using fracture mechanics procedures. Concerning this second procedure, an example involving low-cycle fatigue induced crack initiation in piping components is presented next.

The limitations and associated uncertainties of these two initial crack size assessment approaches are discussed then. Utilisation of the most recent wide scope international crack databases, e.g. OPDE (OECD Piping Failure Data Exchange), to improve problems arising from the lack of crack data is discussed next. The possibilities to develop the two above mentioned approaches for recursive assessment of initial crack sizes are outlined then.

Finally, summary together with conclusions is presented.

On welding residual stresses and their practical inclusion in structural integrity analyses (2-1798)

Otso Cronvall
VTT Technical Research Centre of Finland
P.O. Box 1000, 02044 VTT, Finland
e-mail: otso.cronvall@vtt.fi

This study concerns welding process induced residual stress distributions in Nuclear Power Plant (NPP) reactor circuit component welds. When combined with a degradation mechanism these relatively high stresses, being typically of the scale of material yield stress, can potentially be dangerous to the integrity of the NPP components. Especially, in connection with Stress Corrosion Cracking (SCC) these static stresses are considered to effect in full, whereas in connection with fatigue induced cracking, it is mainly the altering stresses that are considered. There also exist ways to lower the weld residual stresses, in addition it is assumed that several decades of time in plant operation may relieve these stresses to some extent as well. The covered residual stress definition procedures are the ASME recommendations, the British Standard BS 7910: 1999, the R6 Method, Revision 4, the SAQ handbook, the SINTAP Procedure, the API 579 procedure and the FITNET Procedure. The covered weld residual stress types are those in as-welded state and after Post Weld Heat Treatment (PWHT) in circumferential NPP piping welds.

The covered weld residual stress definitions are based both on the available experimental data and Finite Element Method (FEM) based analysis results. In some older ones of the covered weld residual stress definitions, uniform distributions have conservatively been defined to weld residual stresses for some weld types due to lack of data, e.g. those given for parallel to weld for austenitic stainless steel for pipe-to-pipe welds in ASME recommendations.

The published experimental data has a substantial scatter. Consequently the defined weld residual stress distributions have been developed as tensile upper bound solutions based on the data, and are thus often not self-balancing. However, this approach not only lacks consistency for the same type of joints and welding parameters, but can either significantly overestimate the weld residual stress level in some cases, or underestimate it in others.

Over the last decade or so, welding process induced residual stresses have received increasing attention in the pressure vessel and piping research community. The driving force for this interest can be attributed to the fact that application of modern structural integrity assessment procedures for defective welded components, e.g., the British Standard BS 7910: 1999, R6 Method,

Revision 4, SINTAP Procedure, API 579 procedure and FITNET Procedure, require considerably more input data on the weld residual stress state to give a more realistic assessment. The conventional approach for characterising a weld residual stress profile has been to adopt a tensile upper bound solution, as mentioned above.

In this study the weld residual stress distributions are calculated with the above mentioned seven procedures for representative small, medium and large NPP reactor circuit pipe sizes in Finnish Boiling Water Reactor (BWR) NPP units. For these three pipe sizes, weld residual stress distributions through wall are calculated for both ferritic steels and austenitic Stainless Steels (SSs) in both perpendicular and parallel to weld directions. The covered weld conditions in the calculations are as-welded state, and after PWHT. The temperature is set to operational temperature of slightly below 300°C in Finnish BWR NPP units. Then, SCC analyses are carried out using thus obtained weld residual stresses as well as stresses caused by other static system loads to circumferential inner surface crack postulates with fracture mechanics based analysis code VTTBESIT, developed partly at VTT. Analysis results are compared, and conclusions based on them drawn. Also, some recommendations concerning the use of the above mentioned weld residual stress definition procedures are given. Finally, numerical analyses concerning the behaviour of weld residual stresses in the course of several decades of time in plant operation and notable future research aspects are discussed.

Fracture mechanics evaluation of similar and dissimilar welded fracture specimens under plane-strain (2-1803)

I.A. Khan, V. Bhasin, J. Chattopadhyay, K.K. Vaze,
A.K. Ghosh, H.S. Kushwaha*

Reactor Safety Division, Bhabha Atomic Research Centre, Mumbai-85, India

*Director, Health Safety & Environment Group, Bhabha Atomic Research Centre
Mumbai-85, India, e-mails: imran@barc.gov.in, iak_bar@yahoo.com

The classical Upper bound approach of limit analysis is based on the assumption of rigid blocks of deformation that moves between the lines of tangential displacement discontinuity. This assumption leads to considerable simplification but often at the cost of higher estimates of the actual load. Moreover, in many cases, it does not give a correct shape of the plastic field. In order to overcome these limitations a modified Upper Bound approach (MUB) was proposed by Khan and Ghosh [1]. The proposed approach is basically an energetic approach but unlike the classical upper bound approach it is capable of including the presence of statically governed stress field [2]. In this article various applications of this recently proposed MUB approach in the area of fracture mechanics evaluation of similar and dissimilar welded fracture specimens are discussed. Plane strain plasticity problem in rigid elastic-plastic mono-material (homogeneous) was solved to evaluate the useful parameters like limit load, plastic eta functions (η_p) and plastic rotation factor (r_p). For similar and dissimilar welded specimens, limit load solutions are presented. Only deeply cracked specimens were analysed. The proposed theoretical solutions were confirmed by classical Slip-Line Field solutions, wherever available, and by detailed elastic-plastic finite element analysis with Von-Mises yield criterion. Good agreement was found between proposed solutions and the results obtained from classical Slip Line field theory and finite element analysis.

In order to validate the proposed theoretical solutions, limit analyses of similar and dissimilar welded SENB, TPB and CT specimens were performed. All the analyses were performed for plane strain condition. A small geometry change continuum FE model with Von-Mises yield criterion was used. The number of elements and nodes in a typical FE mesh ranges from \approx 900 elements/2600 nodes to 1300 elements/3700 nodes. Standard 8-noded quadrilateral element with reduced integration was used to avoid problems associated with incompressibility. Reasonably fine mesh was used near the crack tip. The analysis was stopped when asymptotic load deflection behaviour was obtained. The corresponding fully plastic limit loads were obtained directly from the FE

solutions. For all cases considered, the FE limit load solutions for standard SENB, TPB and CT specimens (homogeneous) differ from the known SLF solutions by less than 1%, which provides confidence in the present FE calculations for similar and dissimilar welded fracture specimens (see Fig. 1 for configuration).

Detailed finite element analysis of dissimilar welded specimens reveal that the weld slenderness ratio i.e. ($K=h/l$) and mismatch ratio between weld and the weakest base material governs the plastic deformation modes and hence the limit load. Thus, the limit load and plastic η -factor solutions developed for similar welds using MUB approach can also be used for dissimilar welds provided the mismatch ratio between weld and the weakest base material is used. A detailed comparison of the theoretical solutions with results obtained from FEA is provided in this article.

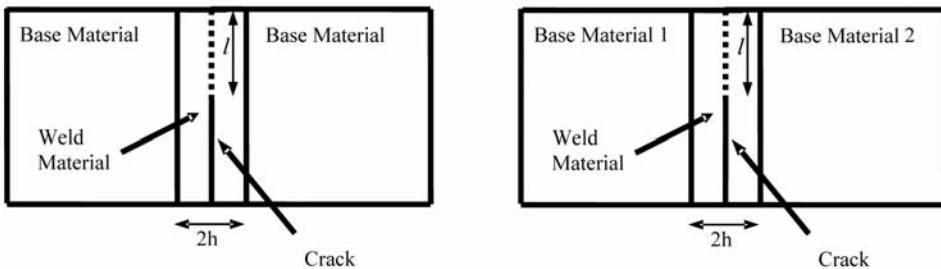


Figure 1. (a) Sketch of similar welded specimen; (b) Sketch of dissimilar welded specimen.

In comparison to detailed SLF analysis the proposed modified upper bound approach is quite simple and can give reasonably accurate upper bound estimate of limit load and other fracture mechanics parameters for both standard homogeneous as well as similar and dissimilar welded fracture specimens under plane strain condition. Due to assumption of rigid blocks of deformation the classical upper bound approach, though simple, when applied to fracture mechanics specimens, subjected to predominant bending load, provides much higher estimate of limit load and plastic rotation factor. The proposed MUB approach is capable of including the presence of statically governed stress field and hence give better results.

References

1. I.A. Khan, A.K. Ghosh. A Modified Upper Bound Approach to limit analysis for plane strain deeply cracked specimens. *International Journal of Solids and Structures*, 44, 2007, pp. 3114–3135.
2. I.A. Khan, V. Bhasin, J. Chattopadhyay, A.K. Ghosh. On the equivalence of slip-line fields and work principles for rigid-plastic body in plane strain. *International Journal of Solids and Structures*, 2008. (In Press.)

Three dimensional damage mechanics analysis of real life reactor piping components under various loading conditions (2-1831)

P.V. Durgaprasad¹, M.K. Sahu, B.K. Dutta
Reactor Safety Division, Bhabha Atomic Research Centre
Trombay, Mumbai, India-400085
e-mail: ¹pvd@barc.gov.in

In order to maintain the structural integrity of safety related components, it is required to determine the fracture behavior of materials at component level at different operating conditions. J-resistance curves are conventionally used for characterizing the elasto-plastic fracture behavior of metallic components. They are usually derived from ASTM standard specimens. However, there is a problem in transferring the specimen J-resistance curves to the components because of the existence of stress triaxiality. The micro-mechanical models are used to overcome this problem and these models help in predicting the fracture behavior of any component with any geometry and loading conditions. In this work, the Gurson-Tvergaard-Needleman (GTN) damage mechanics model [1, 2] is used for the crack growth analysis of real life reactor piping components. The paper also addresses the challenges involved in such analyses.

As a part of component integrity testing, a comprehensive experimental program has been pursued to generate the fracture behavior of reactor piping components. Several real life pipes and elbows with various flaw sizes have been tested under different loading conditions like temperature, pressure, bending etc. In the present work, some of the selected components have been analyzed numerically by using parallel in-house finite element code 'MADAM' with GTN constitutive model. The strength of the micro mechanical models has been demonstrated by comparing the numerical results like load v/s. load-line displacements, J-R curves with the experimental data. It has been demonstrated that micro-mechanical models are useful to limit the total number of experiments to be carried out in future on real life components under any loading conditions.

Damage mechanics analyses of real life components are difficult task due to the large computational time involved. Also, the finite element software may face the convergence problem because of the non-linearity involved in the problems. Thus it requires high performance computing techniques to be used for such analyses. The parallel 'MADAM' code has been used very successfully on a 128 noded parallel computing facility for our analyses of real life

components. The present paper discusses the analysis techniques used, and comparison of the numerical results with experimental data.

References

- Gurson, A.L. 1977. Continuum theory of ductile rupture by void nucleation and growth. Part I. yield criteria and flow rules for porous ductile media. *Journal of Engineering Material Technology, Trans. of ASME*, 9, pp. 2–15.
- Tvergaard, V., Needleman, A. 1984. Analysis of the cup-cone fracture in a round tensile bar. *Acta Metall.*, Vol. 32, pp. 157–169.

Application of the leak before break concept to CANDU feeder piping with service induced cracking (2-1854)

John C. Jin, Raoul Awad, Gerry Frappier

The concept of the Leak Before Break (LBB) had been claimed to be a failure mode of CANDU feeder piping experiencing service induced cracking at Point Lepreau Nuclear Generating Station (PLGS) [1]. The feeders at PLGS have been replaced recently for refurbishment and there has been no cracks discovered in the feeder bends at other CANDU stations. However, due to current limited understanding of the cracking mechanism in terms of root causes, it is not possible to preclude the susceptibility of the same kind of cracking from the feeders at other CANDU stations which have similar operating conditions to those of PLGS. Although the root cause of the cracking is not conclusive yet, it is generally accepted that tensile residual stress plays a critical role in initiating and propagating the service induced cracks [2]. Accordingly, cracking should be considered credible at the feeder bends possessing sufficient level of residual tensile stresses. Once the service induced cracking becomes an active degradation and there is no assurance of prevention of through wall cracking during operation based on crack growth rate estimation and detection limits of the in-service inspection technique, then the LBB should be demonstrated as one of the elements of the fitness for continued service of whole feeder population. Through the LBB assessment, it should be confirmed that a pipe break is an unlikely event even when cracks are missed during the expanded inspection scope and those remaining cracks could grow through wall during operating period.

It has been the regulator's view [1] that the concept of the LBB, if there is sufficient evidence that LBB is the credible failure mode, may be considered as a safety measure for enhancing the defense-in-depth for a prescribed operating period unless it compromises other safety features or is intended to form the basis for continued operation of the feeder with detected service induced cracks. Discovery of a service induced crack at a station will trigger expansion of inspection scope and requires the development of comprehensive ageing management plans.

The feeders at all CANDU stations also experience pipe wall thinning due to flow accelerated corrosion (FAC). The LBB concepts shall not be credited for the FAC wall thinned feeders because there have been a number of actual field experiences showing that the sudden pipe breaks are the final failure modes of the FAC degraded pipes.

2. Fracture Mechanics and Structural Integrity

The capability of leak detection system(s) and the operating response procedure to the leakage are critical elements in crediting the LBB principles. There must be sufficient margin for the leakage from a through wall crack against the capability of the leak detection systems and for the leaking crack size against critical crack size. Operational leak rate limit at each station should be determined based on the LBB assessment. Material characterization will be subjected to regulatory review to ensure that ageing effects on the material properties are appropriately incorporated in the LBB assessment.

Detailed regulatory perspective on the application of LBB to CANDU feeder pipes with active service induced cracking will be discussed in the full paper.

References

1. J. Jin, A. Blahoianu, T. Viglasky. Canadian Regulatory Perspective on LBB Application for CNADU Piping. August 2007, Structural Mechanics in Reactor Technology 19 (SMiRT-19), Toronto, Canada.
2. J. Jin, R. Awad, T. Viglasky. Fitness for Service Assessment of Degraded CANDU Feeder Piping – Canadian Regulatory Expectations. August 2007, Structural Mechanics in Reactor Technology 19 (SMiRT-19), Toronto, Canada.

Evaluation of interaction effect for parallel surface cracks in shell-to-nozzle junction with geometrical discontinuity based on limit load analyses (2-1859)

Chang-Kyun Oh¹, Hyun-Su Kim², Seung-Gun Lee³,
Hag-Ki Youm⁴, Tae-Eun Jin⁵

¹Senior Researcher, Korea Power Engineering Company
e-mail: ckoh@kopec.co.kr

²Senior Researcher, Korea Power Engineering Company
e-mail: hyunsu@kopec.co.kr

³Senior Researcher, Korea Power Engineering Company
e-mail: gun@kopec.co.kr

⁴Senior Researcher, Korea Power Engineering Company
e-mail: hockey@kopec.co.kr

⁵General Manager, Korea Power Engineering Company
e-mail: jinte@kopec.co.kr

When multiple cracks approach one another, the limit load of cracked component is likely to change due to the interaction of the stress field. In ASME Sec. XI, parallel surface cracks are replaced by a coalesced single combined crack if they are located within the distance of half depth of deeper crack. However, the criterion for offset distance is given by an absolute value, although magnitude of the interaction is inevitably dependent on the crack size etc. Results of previous studies for parallel cracks of plates and cylinders describe that evaluations according to ASME Sec. XI may be non-conservative. However, it is important to investigate the interaction effect for parallel surface cracks of components with geometrical discontinuity because these are susceptible to cracking. In this paper, limit load analyses were performed for parallel semi-elliptical axial cracks in shell-to-nozzle junction with geometrical discontinuity under pressure. Based on the elastic-plastic finite element results, the acceptability of the proximity rules provided in the existing guidance was investigated, and the relevant recommendations on a defect interaction for parallel surface cracks of components with geometrical discontinuity were discussed.

Ratcheting-fatigue failure of pressurized elbows made of carbon steel (2-1861)

Suneel K. Gupta, Sumit Goyal, Vivek Bhasin, K.K. Vaze,
A.K. Ghosh, H.S. Kushwaha
Bhabha Atomic Research Center, Reactor Safety Division
Mumbai, 400085, India
e-mail: suneelkg@barc.gov.in

Fatigue ratcheting investigations have been carried out to understand the ratcheting-fatigue failure of low carbon manganese steel (SA 333 Gr. 6). Experiments have been conducted on pressured pipe-elbow assembly subjected to reversible cyclic bending, to assess the failure mechanics of fatigue ratcheting and to evaluate the piping seismic design rules intended for their structural integrity. These investigations have shown a significant influence of the ratchet strain and non-relaxing mean stress on the low cycle fatigue life of material.

Introduction/summary

The earthquake load, an important design basis accident loading, is considered in the design the nuclear power plant structures as well as piping system. During large earthquake events, the pressurized elbows can experience inelastic cyclic excursions and can lead to accumulation of plastic strains, known as ratcheting. In the recent past, a number of investigations [1–3] have been carried out to understand the cyclic plasticity and ratcheting behaviour of materials. However, these have concentrated mainly on material's ratcheting behaviour and its constitutive modelling and the ratcheting-fatigue interaction has not been addressed. However, some investigators [4–5] have shown significant influence of interaction on fatigue life of component. To assess the structural integrity under fatigue-ratcheting, few researchers [6–7] have carried out experimental, analytical and regulatory investigations. The investigations have led to changes in piping seismic design rules of various design codes. However, still there are a lot of uncertainties and unresolved issues related to the failure mechanism. To understand the fatigue ratcheting failure mechanism and to assure the real safety margins vis-a-vis the new design rules related to fatigue-ratcheting, eight number of the ratcheting experiments on 8" NB Sch.100 size pipe-elbow assemblies, made of SA-333 Gr.6 carbon steel, were conducted under constant internal pressure and large amplitude quasi static cyclic displacement loading. The elbows among other piping components exhibit highly strained regions in the piping system and are vulnerable to fail by fatigue ratcheting. The tested elbows have geometrical characteristics and material similar to that used in

Primary Heat Transport (PHT) piping of Indian Pressurized Heavy Water Reactor (PHWR). The experimental setup and instrumentation details for fatigue-ratcheting testing have been shown in figure 1. The pressure applied in different tests ranges from 120 bar to 300 bar which generates nominal hoop stress as $1/3\sigma_y$ to $2/3\sigma_y$, respectively. The displacement is applied in both closing and opening direction and the magnitude of its amplitude is taken such that the corresponding pseudo linear bending moment (calculated based on the elastic stiffness of pressurized pipe elbow test set up) ranges from 0.8 to 2 times of $M_{collapse}$ (based on flow stress). This loading leads to equivalent pseudo linear stress amplitude (ASME Section-III, NB3600, Eq. 9) as $\sim 1.3*\sigma_y$ to $3*\sigma_y$. These limits have been selected to assess the fatigue ratcheting failure and to evaluate the realistic safety margins available vis-a-vis the new and old design rules. In design rule the moment and the stress used are pseudo elastic and evaluated by assuming material elastic formulations.

Results/conclusions

The elbow ratcheting test shows that the gross ballooning (increase in diameter of 45° section of elbow) in initial 10 cycles is quite small (mean value $\sim 1\%$ to 4%) in comparison to local strain accumulation at crown locations (mean value $\sim 3\%$ to 8%). The local strain accumulation is shown in figure-2 for a typical case ERT-2, (pressure stress $\sim 0.58\sigma_y$ and the elastic plastic bending moment amplitude $\sim 0.95M_{collapse}$). The evolution and accumulation of ratchet strain over a number of applied cycles along with presence of non-relaxing internal pressure stress has led to very early fatigue crack initiation on inside surface of crown location. This has been detected using Ultrasonic Testing (UT). The initiated crack, under cyclic loading, further grows to through wall and results in leakage (complete failure). The experiment was stopped on appearance of leakage. In different tests, the cycles for final failure ranges from 62 to 625 cycles (N_f) and for crack initiation from 30 to 210 cycles (N_i). The number of cycles, N_f and N_i depends upon the pressure and cyclic loading amplitudes. The cyclic strain amplitude at crown (in different tests) ranges from 0.5% to 1% . From the classical LCF curve, such strain amplitudes could not lead to crack initiation and to failure in such small number of cycles. These tests clearly point to significant influence of ratchet strain (ductility exhaustion due to local accumulation strain) and sustained non-relaxing pressure stress on the LCF life. Hence, it is instructive to address the influence of ratcheting and pressure stress on fatigue behaviour. Test results have shown that the current design rule provides adequate safety margin against the fatigue ratcheting failure of pressurized elbow. The testing was followed by analytical assessment using the finite element analysis with various kinematic hardening rules and various parameters such as load, load line displacement, ovalization, hoop and axial strains etc. were evaluated and compared with test results.

2. Fracture Mechanics and Structural Integrity

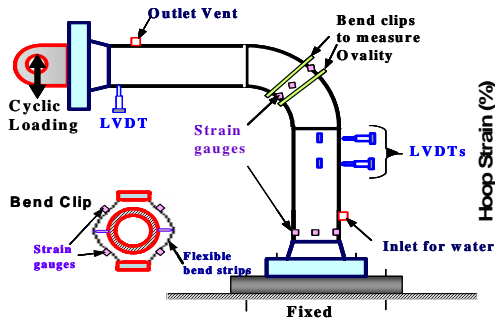


Figure 1. Schematic of Test Setup.

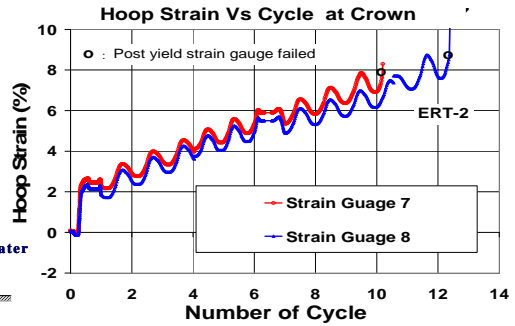


Figure 2. Ratchet Strain Vs. Cycles.

References

1. Ohno, N. et al. 1993. Kinematic hardening rules with critical state of dynamic recovery. Parts I and II. *Int. J. Plasticity* 9, pp. 375–403.
2. Chaboche, J.L. A review of some plasticity and viscoplasticity constitutive theories. *Int. J. Plasticity* 24 (2008).
3. Hassan, T. Influence of non-proportional loading on ratcheting responses and simulations by two recent cyclic plasticity models. *Int. J. Plasticity* 24 (2008).
4. Boussaa, D. et al. Tang H T, Fatigue – Seismic Ratcheting Interactions in pressurized Elbows. *Journal of PVT*, Vol-116, November 1994, pp. 396–402.
5. Weib, E. et al. Simulation of ratcheting and low cycle fatigue. *IJPVP*, Vol-81, 2004.
6. Yahiaoui, K. et al. Response and cyclic strain accumulation of pressurised piping elbows under dynamic in-plane bending. *Journal of strain analysis* Vol. 31–32, 1996.
7. Touble, F. Piping Seismic design criteria: fatigue Ratcheting behaviour under high cyclic loadings. *SMiRT-13*, Brazil, August 13–18, 1995, p. 149, 153.

Cyclic tearing of through wall cracked pipes made of carbon steel (2-1863)

Suneel K. Gupta, Vivek Bhasin, J. Chattopadhyaya, K.K. Vaze,
A.K. Ghosh, H.S. Kushwaha
Bhabha Atomic Research Center, Reactor Safety Division
Mumbai, 400085, India
e-mail: suneelkg@barc.gov.in

Introduction/Summary

The demonstration of Leak before Break (LBB) qualification of the Nuclear Power Plant (NPP) Primary Heat Transport (PHT) piping calls for rigorous fracture assessment of piping components with postulated flaws. In past the research in this area resulted in several publications like NUREG-1061[1] and IAEA-TECDOCs [2, 3], which describe the piping flaw analysis procedures for LBB qualification. The pipe fracture analysis considers the seismic loading as a one time applied load of magnitude equal to peak load at the postulated flaw location during the earthquake event. The assessment of pipe with flaw is based on the monotonic tearing instability or Net Section Collapse (NSC). There is no explicit consideration of the cyclic damage or the number of applied load cycles. However, in India like in many other countries also, the nuclear power plants consider earthquake event, in the design of piping components and other structures. During the typical earthquake event the nuclear power plant piping experiences around 10–20 cycles of large amplitude reversible load. It is a well-known fact that the reversible cyclic loading significantly accelerates the fracture process due to the cumulative damage by the compressive plasticity (i.e. void flattening and crack tip re-sharpening) and low cycle fatigue crack growth (fatigue crack growth under large scale yielding). As a result of combined damage there is significant decrease in the apparent fracture resistance of the material under reversible cyclic loading compared to monotonic loading. Unlike monotonic fracture, in cyclic fracture, the instability depends on the full load history and parameters such as loading ratio, loading range and number of load cycles. A cracked component, which is safe for monotonic load, may fail in limited number of reversible cyclic load of same amplitude. In view of it, a series of seven tests have been conducted [4], on circumferentially through wall cracked straight pipes of 8"Sch100 size, made of SA333Gr.6 Carbon steel and subjected to reversible cyclic bending. All the tests have been conducted in four point bend configuration, at room temperature, under quasi-static i.e. slow loading rates and the dynamic effect is not considered. The tests have been conducted under both the load control conditions and the displacement

controlled conditions. The load-controlled test was carried out with objective of investigating the importance of the number of cycles of loading (comparable to number of cycles in an earthquake) as a function of applied load amplitude (peak dynamic load). The load amplitude was kept constant between 60% and 95% of the predicted monotonic instability load for different tests. For all these tests, the load ratio was kept constant ($R = -1$). The crack growth for these experiments has been plotted versus number of load cycles in Fig. 1. The displacement-controlled tests were carried out to quantify the reduction in the fracture resistance. In displacement-controlled tests, the displacement increment was controlled when the specimen was loaded in the crack opening direction and the load was controlled in the reverse direction loading in order to maintain the constant load ratio.

The results of above cyclic tearing tests have been investigated in detail and a methodology for evaluation of crack growth and instability under fully reversible cyclic loads has been developed. In this study, crack growth by both, fatigue and static fracture have been considered. The fatigue crack growth has been evaluated using, Dowling's ΔJ integral (based on the loading branch of cycle) along with the extrapolated high cycle fatigue law (Paris Law). The static crack growth has been calculated cycle by cycle from the monotonic J-R curve and a new proposed J' -integral which accounts for the cyclic damage. It is evaluated cycle-by-cycle, from area under the positive half of either load versus plastic Load Line Displacement (LLD) curve or load versus plastic Crack Mouth Opening Displacement (CMOD) curve (using CMOD based η and γ factors). The predicted cumulative crack growth has been plotted against number of cycles and compared with corresponding test measured crack growth as shown in Fig. 2 for an experiment. This shows significant contribution of tearing toward the end of test. The proposed cyclic tearing assessment procedure for fully reversible cyclic loading compares well with the experimental results. The load controlled cyclic test results have been compared with the corresponding monotonic pipe fracture test as shown in Fig. 3. It shows that the cyclic tearing instability of the pipe subjected to load controlled fully reversible cyclic, happens when the crack grows to a critical crack size (based on monotonic fracture / plastic collapse assessment for cyclic load amplitude). This point out that cyclic loading has less influence on the load bearing capacity of the material. This also has been observed when experimentally recorded maximum load in the displacement controlled quasi-static cyclic test has been compared with corresponding in quasi-static monotonic test. This may be due to the fact that for SA333Gr6 the load bearing capacity of cracked pipe is governed by plastic collapse / plasticity in remaining ligament [5]. Further the J-R curve has been evaluated from the envelope of displacement controlled cyclic tests and compared with corresponding monotonic tests. It has been observed that there is significant reduction in the fracture resistance under cyclic loading conditions. However, J-R curve evaluation procedure does not excludes the additional crack growth taking place due to fatigue / cyclic loading.

2. Fracture Mechanics and Structural Integrity

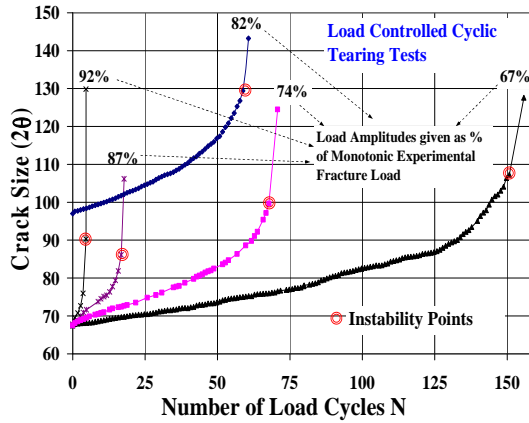


Figure 1. Crack size (degrees) Vs. Number of load cycles for load controlled tests.

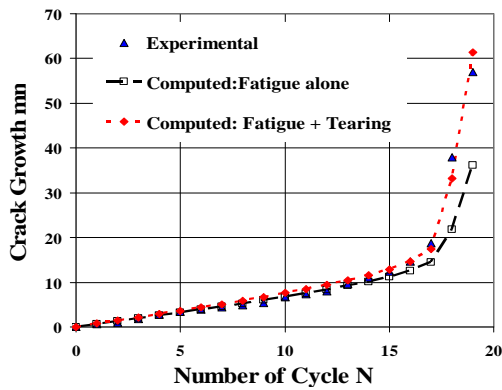


Figure 2. Load Vs. Crack Size comparisons for cyclic tearing and monotonic fracture tests.

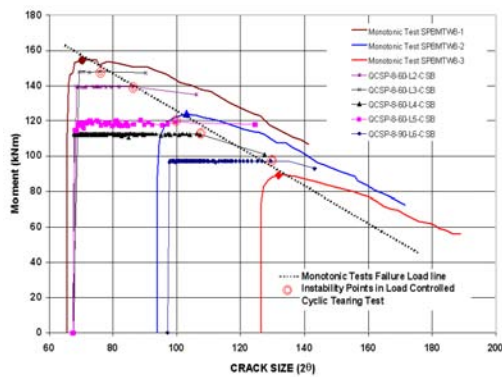


Figure 3. Comparison of Predicted and experimental Crack Growth Vs. Number of load cycles.

References

1. Report No.: NUREG-1061, Vol. 3, (1984). Evaluation of Postulated Pipe Breaks. Report of the U.S. Nuclear Regulatory Commission, Piping Review Committee.
2. IAEA-TECDOC 710, 1993. Applicability of the Leak Before Break Concept.
3. IAEA-TECDOC 774, 1994. Guidance for the Application of the Leak Before Break Concept Saouma V. E., Int. J. Fract. 137:231–249, 2006.
4. S.K. Gupta, V. Bhasin, K.K. Vaze, A.K. Ghosh, H.S. Kushwaha. 2007. Experimental Investigations on Effects of Simulated Seismic Loading on LBB Assessment of High Energy Piping. ASME-JPVT, Vol. 129, February 2007.
5. J. Chattopadhyaya, B.K. Dutta, H.S. Kushwaha. 2000. Experimental and analytical study of three point bend specimens and through wall circumferentially cracked straight pipe. Int. J. PVP, 77, 455–471.

Fatigue crack initiation and crack growth studies for pipes made of carbon steel (2-1864)

Punit Arora, Suneel K. Gupta, P.K. Singh, Vivek Bhasin,
K.K. Vaze, A.K. Ghosh, H.S. Kushwaha
Bhabha Atomic Research Center, Reactor Safety Division
Mumbai, 400085, India
e-mail: punit@barc.gov.in

Introduction

Leak-Before-Break (LBB), a fail-safe design philosophy, is based on fatigue/fracture mechanics concepts and requires rigorous integrity assessment of piping component with postulated part through thickness flaw. It is required to be demonstrated that the unstable tearing will never occur before the crack penetrates through thickness and gives easily detectable leakage. This requires investigation on fatigue crack initiation followed by fatigue crack growth (FCG) of piping components with different postulated part through flaws for the qualification of LBB design criterion. In view of it, six numbers of tests were carried out [1] on 8" Sch.100 straight pipes having circumferential part through wall notch and made of SA333Gr6 carbon steel and subjected to pure alternating bending moment using four point bend setup. The material is similar to that used in primary heat transport (PHT) piping of Indian Pressurised Heavy Water Reactor (PHWR). The notch depth to thickness (a/t) ratio is varied from 0.125 to 0.4. The maximum remote stress is varied from $0.4\sigma_{ys}$ to $0.7\sigma_{ys}$ and the stress ratio (R) is 0.1 and 0.5. The Alternating Current Potential Drop (ACPD) technique has been used for evaluation of crack initiation and growth of notch front. The crack is assumed to be initiated when it grows by 0.1 mm. The cycles to crack initiation in different tests range from 3000 to 320,000 and the cycles for crack to grow through wall fall in the range of 53000 to 869,000.

Analyses were performed for these tests to predict crack initiation life using various procedures available in literature [2–3]. The A-16 guide of RCC-MR [2] provides a procedure based on the pseudo elastic principal stress range ($\Delta\sigma_1$) in the proximity of notch root. The $\Delta\sigma_1$ ahead of notch root generally evaluated using Creager's formulae. Further, the effective elastic strain range is evaluated based on equivalent uniaxial $\Delta\sigma_1$ stress range. The elastic-plastic local strain range amplification is made using Neuber's hyperbola followed by the plastic strain correction to account for effective poisson's ratio. A16 requires calculations to be carried out at characteristic distance (d_i) from the notch root

which is stated to be a material specific parameter by A-16 irrespective of the load applied and notch geometrical parameters. The characteristic distance (d_i) was calculated from experimentally found number of cycles for crack initiation and is evaluated to be 55 μm and 100 μm for two tests whereas rest four tests show d_i to be 70 μm .

In absence of body forces, plane stress and plane strain solutions give identical stress states and hence A-16 procedure will lead to same fatigue initiation life. However, it is known that the strain ranges will be different for the two cases and so as the fatigue lives. Hence, effective stress and effective strain ranges, both should be evaluated from the actual state of stress and strain at the notch tip. In view of it, detailed elastic plastic finite element analyses have been carried out for actual pipes under as tested conditions. One quarter domain of the test specimen was modeled using 20 noded 3D elements, with the finest mesh size of 20 μm near the point of singularity. The stabilized cyclic stress strain data for SA-333 Gr. 6 used for the analysis. The LCF tests were conducted under uniaxial and completely reversible loading conditions. Hence, correction factors for mean stress and multiaxiality have been accounted in the uniaxial $\Delta\varepsilon - N$ curve based on available literature [4]. Thus, the number of cycles to crack initiation (N_i) can be calculated from corrected fatigue-failure curve and elastic-plastic strain amplitude as obtained from FE analysis at different 'd' distances from notch root. The distance at which the number of cycles corresponding to effective elastic plastic strain amplitude matches with the experimental value is basically 'characteristic distance(d_i)'. The characteristic distance is found to be varying between 36 μm to 88 μm with mean value at 60 μm . Further plastic strain range and the tri-axiality factor (T.F., defined as ratio of hydrostatic to von-mises stress), variations with distance from notch root has been studied and also shown in Fig. 1. The higher constraint in the form of T.F. suppresses the plasticity. The T.F. is maximum at around 200 μm and the total equivalent plastic strain range almost vanishes at this distance. The results point to a critical / characteristic distance from the notch root where the material sees maximum damage and causes crack initiation. However, this argument is based on the tests conducted on carbon steel pipes.

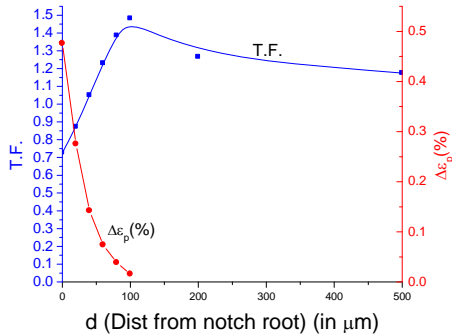


Figure 1. FEA results: Variation of T.F. and % $\Delta\epsilon_p$.

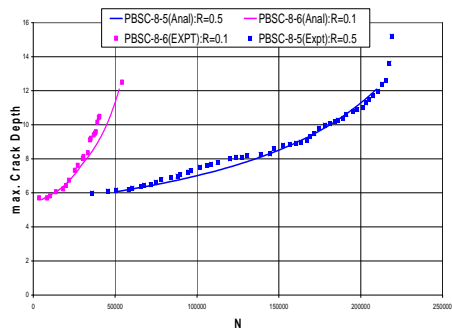


Figure 2. FCG Life Test and Analyses.

After fatigue crack initiation, the fatigue crack growth (FCG) life has been evaluated using Paris law. The Paris law constants for the material were evaluated in previous specimen studies [1] as per the ASTM standard E647, using three point bend (TPB) specimens machined from the same pipe material. The experimental results are in good agreement with growth as predicted by Paris law as can be referred in Fig. 2 above.

References

1. Singh, P.K., Vaze, K.K., Bhasin, V., Kushwaha, H.S., Gandhi, P., Ramachandra Murthy, D.S. Crack initiation and growth behavior of circumferentially cracked pipes under cyclic and monotonic loading. *Int J Pressure Vessel Piping* 80(2003) 629–640.
2. A16 guide for defect assessment and leak before break analysis. Edition 2002.
3. Hoffmann, M., Seeger, T. A generalized method for estimating multiaxial elastic plastic notch stresses and strains. *Transactions of ASME*, Vol. 107(1985), pp. 250–260.
4. Manson, S.S., Halford, G.R. Multiaxial low cycle fatigue of Type 304SS. *Journal of Engineering Material Technology*, (1977), pp. 283–285.

Numerical determination of J-integral value and its crack size sensitivity in case Sub-Clad Flaw for WWER Reactor Pressure Vessel Integrity Evaluation (2-1872)

Szabolcs Szávai^{1, a}, Róbert Beleznai^{1, b}

¹Bay Zoltán Foundation for Applied Research, Institute for Logistics and Production Systems, H-3519, Miskolc-Tapolca, Iglói út 2, Hungary
e-mails: ^aszavai.szabolcs@bay-logi.hu, ^bbeleznai.robert@bay-logi.hu

Introduction

The purpose of this work was to study the effect of the crack size of sub-clad flaws in 4PB specimens in case of WWER-440 reactor pressure vessel steel and determination of the J-integral at cladding interface. The research was performed within the framework of NESC-6 project “WWER Cladged Reactor Pressure Vessel Integrity Evaluation (with Respect to PTS Events)”.

Aim of the work

The main goal of this research was to study the crack front position of sub-clad flaws how influences the J-integral value. Since J-integral values have shown high sensitivity to the distance from the cladding interface, the virtual crack extension method (VCEM) was applied for the calculation.

Essential results

J-integral values were calculated for each crack fronts of the specimens for different integration path. The geometry and material data was provided by NRI, Rez, Czech Republic. Straight crack fronts with average crack lengths were modeled to simplify the analysis. Residual stresses were taken into account in the calculation with the help of stress free temperature method. MSC.MARC 2007r1 FE code was used for the analysis with elastic-plastic material properties. 20 nodes hexahedron elements were applied for generating 3D FE models of specimens. Two different cases were separately examined:

- Upper crack front position has been modified
- Lower crack front position has been modified.

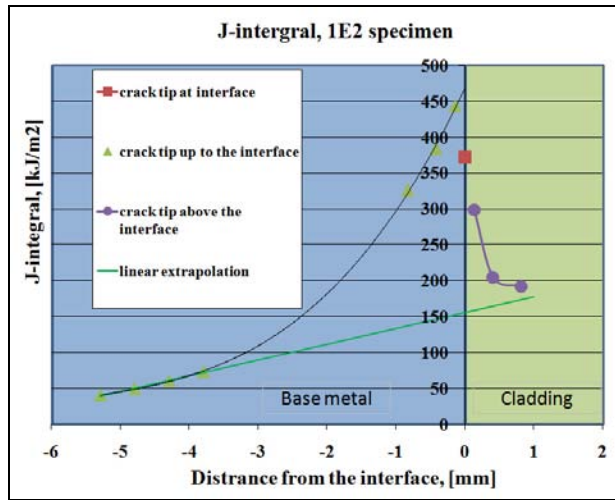
The larger changes in the J-integral values are occurred, when the upper crack front was moved. It has significant effect on result in case upper and lower crack front, as well. The two main reasons are maybe the following: the upper crack front is very close to the fusion line of the cladding so the residual stress has effect on the J integral values, and the tensional stress is higher above the upper crack front, than below the lower crack front due to the bending.

The Crack Propagation Sensitivity Index (CPSI) was also determined and it can be concluded that J-integral at the upper crack front is the most sensitive for the position.

Short crack specimen	J-integral at upper crack front	J-integral at lower crack front	Variation of the crack length	CPSI at upper crack front	CPSI at lower crack front
Upper crack front moving	82.37%	60.25%	11.60%	7.10	5.19
Lower crack front moving	23.57%	12.58%	11.60%	2.03	1.08

Determination of J-values to the interface by extrapolation is not reliable since values obtained by different order polynomials had not converged, so further J-integral calculations were needed close to the interface but it face to difficulties due to the bi-material interface caused discontinues stress field.

If plastic deformation occurs the J-integral path should be out of the plastic zone but the path may cross secondary discontinuity such as the bimetallic interface. In this case the total integral has to be separated into two parts, one caused by the crack as a primary discontinuity and the other one caused by the bimetallic interface as a secondary discontinuity. For calculating the part of the integral caused by the interface a method have been developed based on virtual crack extension method that can be applied with commercial FEM software as well.



Conclusions

J-integral calculation was performed to study the effect of crack size in case of sub-clad flaws. J-integral at upper crack front is sensitive for the crack tip position and conclusion cannot be drawn to the interface, so VCEM has been extended to the cases when the integration domain contains secondary discontinuity. The method has been verified and the J-integral values for the situation when the crack tip is “on” the interface have been determined with the proposed new method. The calculation results show that J-integral has a significant peak at the interface that has to be taken into consideration at the fracture mechanical evaluation.

References

1. Large scale cladded beam specimen tests, Description of the project for NESC, Nuclear Research Institute Rez plc, Division of Integrity and Technical Engineering, Rez, September 2006.
2. Material properties & Residual stresses measurement, Information for NESC, Nuclear Research Institute Rez plc, Division of Integrity and Technical Engineering, Rez, September 2006.

Applicability of Leak-Before-Break (LBB) technology for primary coolant piping to CPR1000 nuclear power plants in China (2-1884)

Li Chengliang, Yang Mengjia

China Nuclear Power Design Company LTD, Shanghai Branch
JIXIE Building, No. 1954 Huashan Road Shanghai, 200030, China

Tel: +86-21-61258203, Fax: +86-21-61258296

e-mail: lichengliang@cgnpc.com.cn

The China Nuclear Power Design Company Ltd. (CNPDC) plans to apply Leak-Before-Break (LBB) technology in the reactor primary coolant piping of CPR1000 nuclear power plants, and has done a lot of comprehensive research, analysis, feasibility studies, aiming at practical application into GUANGDONG YANG JIANG nuclear power plant t Unit 3 before 2010 (It is a new project and construction has not started yet). As a first step, CNPDC has completed the J-R curve test of the Primary Coolant Piping` material under a range of various temperatures and loading rates, including dynamic loading conditions. At the same time, CNPDC has made an extensive research, to develop and verify the evaluation method for fracture behavior of Chinese piping material. In this paper, we reviewed all sub-steps of LBB application based on the LBB design analysis procedure. It is possible for CNPDC to successfully apply LBB technology for primary coolant piping in YANG JIANG nuclear power plant Unit 3.

References

1. USNRC Standard Review Plan 3.6.3. Leak-before-break evaluation procedures. March 2007.
2. NUREG-1061, Vol. 3, Report of the U.S. Nuclear Regulatory Commission Piping Review Committee, Evaluation of Potential for Pipe Breaks. November 1984.
3. Regulatory Guide 1.45. Reactor Coolant Pressure Boundary Leakage Detection Systems.
4. IAEA-TECDOC-710. Applicability of the leak before break concept, June 1993.
5. P. Zanaboni, L. Sokov, N. Garate. Leak Before Break application for Primary Coolant Loop and Surge Line of VVER-1000/320 Plant: TACIS Project R2.09/96. Nuclear Engineering and Design, 235(2005), pp. 1919–1937.

2. Fracture Mechanics and Structural Integrity

6. Leak-before-break Evaluation of the AP1000 piping. AP1000 Design Control Document, Revision 16, 2007.
7. M. Mattar Neto, J.R.B. Cruz, R.P. de Jong. On the structural integrity assessment of cracked piping of PWR nuclear reactors primary systems. *Progress in nuclear energy*, 2008, pp. 1–18.
8. Oh Young Jin, Hwang Il Soon. Review OF dynamic loading J-R test method for leak before break of nuclear piping. *Nuclear engineering and technology*, Vol. 38, No. 7, 2006, pp. 639–656.

Limit load solution for an edge cracked plate under combined independent bi-axial membrane and bending (2-1888)

P. M. James¹, D. G. Hooton¹, D. Dean²

¹Serco, Birchwood Park, Risley, Warrington, WA3 6GA, UK

e-mail: peter.james@sercoassurance.com

²British Energy Generation Ltd., Barnett Way, Barnwood, Glouc., GL4 3RS, UK

Introduction/background

Recent assessment work has shown that a means to estimate the reference stress for a residual stress distribution for a cylinder containing a circumferential crack would be greatly beneficial. More specifically a solution is required to allow for independent biaxial loading which incorporates both membrane and bending stresses; so that generic residual stress distributions can be approximated. A solution for an edge cracked plate is provided within the Miller Compendium of limit load solutions [1] which included both membrane and bending within the crack opening direction, but only membrane in the second axis. It is this solution which has, in the past, been applied to a cylinder under the assumptions that the effects of the cylinders self constraint and of the out of plane bending can be neglected or approximated.

Aim of the work

This paper develops a limit load solution for an edge cracked plate that includes any combination of biaxial bending and membrane loading. This solution will then be compared to the solution within the Miller Compendium [1] and that obtained from Finite Element (FE) analyses. The solutions applicability to a cylinder will also be considered through the use of FE modeling. Through these comparisons it is hoped that the derived limit load solution can be validated and guidance for its applicability to a cylinder provided.

In a real material, a singular secondary (or residual) reference stress, or a combined primary and secondary reference stress, that can be applied to any cracked geometry is difficult to obtain. This is a result of the displacement controlled secondary stress being removed as the resultant stress approaches the materials yield stress. Within this work it is been assumed that the behavior of both primary and secondary stresses is similar as elastic-perfectly-plastic material properties are assumed. This means that the secondary reference stress

can therefore be obtained from a limit load solution derived by assuming primary loads.

The derived limit load solution should provide an improved estimation of a secondary reference stress, for any combination of (membrane and bending) loading, that may be present at a crack resulting from a weld residual or thermally induced stress. Hence this can be used in fracture assessments such as R5 [2] and R6 [3] to reduce conservatism and potentially improve lifetime estimations.

Essential results

The cases considered in validating the derived method discussed above are outlined briefly below, where all combinations of load are used to obtain a limit stress. This limit stress is then compared to the FE model for that combination, as well as to existing alternate methods.

- Three different combinations of out of plane loading are considered; the initial case with no out of plane stress, one with a constant 50 MPa membrane stress and a third with a combination of 50 MPa membrane and 100 MPa bending stresses.
- For each of the different out of plane loads, five different combinations of in plane membrane and bending stress are considered. These five cases consider the full range of cases that encompass a fully tensile load to a pure applied bending moment.
- Also considered are a range of different crack lengths. These range from the un-cracked case through to the limiting crack depth within R6 corresponding to an $a/t = 0.8$.

The suitability of applying the method to a cylinder, to account for both the hoop stress and a through thickness bending which may occur through applying a residual or thermal stress field, is also investigated within this paper. It is also hoped that the effect of a finite length crack, as opposed to a fully circumferential crack, can be investigated and guidance provided.

Summary/conclusions

This paper presents a method for estimating the limit load (and hence the reference stress) of an edge cracked plate subjected to a varying combinations of in and out of plane membrane and bending stresses. The solution has been validated against FE models and compared to other current best estimate solutions available in open literature. The solution has also been compared to thin cylinders to assess the potential range of application. It is envisaged that the solution will be used in future work to provide an improved means to account for the behavior of secondary (or weld residual) stresses within a component.

References

1. A.G. Miller. Review of limit loads of structures containing defects. *International Journal of Pressure Vessels and Piping* 32 (1988), pp. 197–327.
2. R5: Assessment Procedure for High Temperature Response of Structures. British Energy Generation Limited, Revision 3 (2003).
3. R6: Assessment of the Integrity of Structures Containing Defects. British Energy Generation Limited, Revision 4 (2001), with latest updates in 2007.

Lifetime analysis of WWER Reactor Pressure Vessel Internals concerning material degradation (2-1893)

Judit Dudra^{1, a}, Gyöngyvér B. Lenkey^{1, b}, Szabolcs Szávai^{1, c}

¹Bay Zoltán Foundation for Applied Research, Institute for Logistics and Production Systems, H-3519, Miskolc-Tapolca, Iglói út 2, Hungary
e-mails: ^adudra.judit@bay-logi.hu, ^blenkeyne.gyongyver@bay-logi.hu, ^cszavai.szabolcs@bay-logi.hu

Preliminaries

Reactor internals are subject of three principle operation influences: neutron and gamma irradiation, static and dynamic mechanical stresses and coolant chemistry. Design basis for the reactor internals in WWERs did not calculated with any ageing of these structures due to that time unknown mechanisms of degradation.

Aim of the work

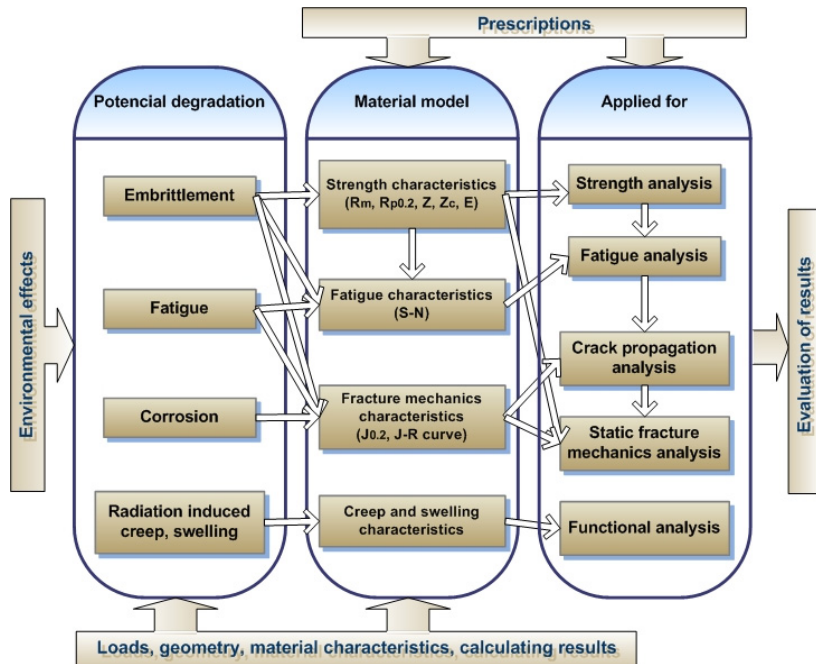
Present study aims at extending the operational lifetime of its WWER 440 type Units. Namely, the purpose of this task is to perform evaluative analysis of presumable changes in material properties of WWER 440 RVI. In line with this objective, making use of this analysis, this study shall determine that are there degradation mechanism, which limits the lifetime of the structural elements.

The subject under consideration, fluence information, evaluation methodology

The subject under consideration of this study are the reactor vessel internals of WWER 440, namely the guide tubes, core barrel, core basket and lower core barrel constructions.

The results of neutron physics calculations, which have done in other project, are concerning the position of the wall of the reactor vessel [1]. The fluence of the test sample estimated for 60 years practically equals with the load of the outer surface of the core barrel, and it is ~12dpa. On the basis of [2] study it can be proved that the fluence value of the core boundary can be multiplied (~5–10) of the value of the core barrel, it can be estimated 35–60 dpa for 60 years operating time.

In the following we shall summarize the possible ageing mechanisms of WWER 440 RVI.



Evaluation of these mechanisms is based on service experience, pertinent laboratory data and relevant experience from other industries.

First step is to define the maximum neutron fluence values concerning 50 and 60 years operating time of the critical place of the RVI. To the calculations to be done the material characteristics suitable for the given maximum fluence values can be used [3], [4], [5].

During the evaluation we examine that the changes of the material characteristics how influence not only the strength and fatigue analysis, but the size of the allowable cracking and the velocity of the crack propagation where in case of an operating or breakdown transient the examined environment loses its stability as well. The austenitic steels, in this way the material of the reactor internals are characterized by ductile fracture mode.

At the same time the effect of irradiation causes embrittlement mechanisms in the material, which can lead to decrease of the toughness of the material. These mechanisms appear at decrease of the Charpy test value, on the other hand causes the decrease of J-R curve (and $J_{0.2}$). To the investigation of the stableness of the crack, of stable crack propagation beside the strength material characteristics, the J-R curve, like the fracture toughness (suitable for express the resistance of the crack propagation) can be applied. For the evaluation of

stability of the crack propagation two parameters Failure Assessment Diagram are applicable.

Conclusions

In the course of lifetime analysis of core internals concerning material degradation in WWER 440 we should consider those changes of material characteristics, which can appear the effect of neutron and gamma irradiation, static and dynamic mechanical stresses and coolant chemistry.

Design basis for the reactor internals in WWERs did not calculated with any aging of the structures due to that time unknown mechanisms of degradation. Nowadays it is a very important research area and instead of that the available literature contains very little information of failures of WWER RVI, the knowledge on the material neutron irradiation degradation has been collected for many years.

References

1. Strength analysis, fatigue analysis and thermal stratification analysis for systems, structures and components (SSCs) – reactor pressure vessel, steam generator, pressurizer, main circulating pump, main gate valve, pipelines, vessels, pumps, heat exchangers and valves – classified into the safety classes 1 and 2. Methodology and criteria documentation.
2. Effect of irradiation on water reactors internals, Ageing Materials Evaluation and Studies (AMES) Report No. 11, Paris (1997).
3. Material characteristics of materials from Greifswald active samples/active material database/core barrel, Hojna, A., Ernestova, M., Keilova, E., Kocik, J., Falcnik, M., Kytka, M., Pesek, P., Rapp, M. Report NRI Rez, DITI 302/419 Rev.3, (2007).
4. CEA, TECNATOM and VTT, Effect of Irradiation on Water Reactors Internals, AMES report No. 11, EUR 17694 EN, European Commission, Brussels–Luxemburg (1997).
5. Regulations for Strength Analysis of Equipment and Piping of Nuclear Power Plants, PNAE G-7-002-87, Energoatomizdat, Moscow (1989).

Evaluation of J-Integral for surface cracked plates under biaxial tensile/bending loading using extended reference stress method (2-1899)

Naoki Miura, Yukio Takahashi
Central Research Institute of Electric Power Industry
2-11-1, Iwado-Kita, Komae-shi, Tokyo, Japan
e-mail: miura@criepi.denken.or.jp

Conventional creep-fatigue crack growth analysis or unstable fracture analysis has been conducted under uniaxial stress condition. However, actual plant components come into various multiaxial stress conditions. Therefore, the evaluation of fracture mechanics parameter of cracked bodies under multiaxial stress conditions is essentially needed for the accurate estimation of crack growth behavior and fracture behavior. In this paper, reference stress solutions for plates with semi-elliptical surface cracks were reviewed, and the applicability of the solutions was examined through the comparison with finite element analysis results under uniaxial loading. Next, an extended reference stress method was newly developed to evaluate J-integral for cracked plates under biaxial tensile and/or bending loading based on an appropriate yielding condition under biaxial loading. It covers bending load perpendicular to crack together with tensile load parallel to crack, and combined tensile and bending loads perpendicular to crack together with tensile load parallel to crack. The accuracy of the method was validated through the comparison with finite element analysis results under biaxial loading.

Application of leak before break assessment for pressure tube in case of delayed hydride cracking (2-1915)

Gintautas Dundulis¹, Remigijus Janulionis², Albertas Grybenas³, Vidas Makarevicius⁴

¹Lab. of Nucl. Inst. Safety, Lithuanian Energy Institute

3 Breslaujos str., LT-44403 Kaunas, Lithuania, e-mail: gintas@mail.lei.lt

²Lab. of Nucl. Inst. Safety, Lithuanian Energy Institute

3 Breslaujos str., LT-44403 Kaunas, Lithuania, e-mail: rjanulionis@mail.lei.lt

³Lab. of Mat. Res.&Test, Lithuanian Energy Institute

3 Breslaujos str., LT-44403 Kaunas, Lithuania, e-mail: agrybenas@mail.lei.lt

⁴Lab. of Mat. Res.&Test., Lithuanian Energy Institute

3 Breslaujos str., LT-44403 Kaunas, Lithuania, e-mail: makarev@mail.lei.lt

Introduction

“Leak Before Break” (LBB) is complex analysis showing that if the started surface crack will grow to the through-wall crack, through this crack some amount of coolant will flow; this leak during definite time can be detected by leak monitoring system and through-wall crack will remain stable under all predictable loading conditions [1].

The application of LBB methodology for Ignalina NPP pressure tube is presented in this paper. Ignalina NPP contains RBMK-1500 type reactor. RBMK reactor are graphite-moderated with a water-cooled reactor core [2]. The pressure tube is important of the piping system for safe operation of reactor. The pressure tubes are piping system into which the fuel element assembly is inserted and through which the coolant flows. A guillotine rupture of one pressure tube is dangerous for structural integrity of graphite blocks and pressure tube adjacent to ruptured pressure tube. As a constructional material for manufacturing of pressure tubes zirconium alloys are used. Zirconium alloys can pick up hydrogen during operation as a consequence of corrosion reaction with water and delayed hydride cracking (DHC) failures may occur. DHC is a phenomenon where a crack can propagate in stepwise fashion as a result of hydrogen redistribution ahead of the crack tip under stress level below the yield stress. The formation of hydrides under certain conditions can reduce resistance to brittle fracture and cause the initiation and development of hydride cracks. Therefore the evaluation of the influence of hydrides on the fracture of pressure tube and possible application of LBB for these tubes with DHC cracks is important.

Analysis approach

The paper presents analysis of LBB application on RBMK-1500 pressure tube. The influence of hydrides on the fracture parameters was evaluated. In these experimental investigations the sections of the pressure tube were hydrided to produce required hydrogen concentration using an electrolytic method and diffusion annealing treatment [3]. Hydride crack formation conditions were investigated and DHC velocity was measured at different temperatures. It has been determined that the DHC velocity is approximately $2 \cdot 10^{-9}$ m/s in RBMK TMT-2 tubes at temperature 250°C.

Deterministic analysis of the pressure tube employing LBB concept was carried out. The critical length of through-wall cracks, the function of crack opening and the leak rate through these cracks was calculated. The stability analysis of crack growth was carried out too. The influence of the hydrogen concentration was evaluated using tested material properties and fracture parameter of the zirconium alloys with different hydrogen concentrations.

The prognosis of DHC crack growth was calculated at 70 ppm hydrogen concentration. The critical cracks length in zirconium alloy without hydrogen and containing 70 ppm hydrogen and the prognosis results of the DHC crack growth in time at the decreasing temperature and pressure during reactor shutdown are presented in Figure 1.

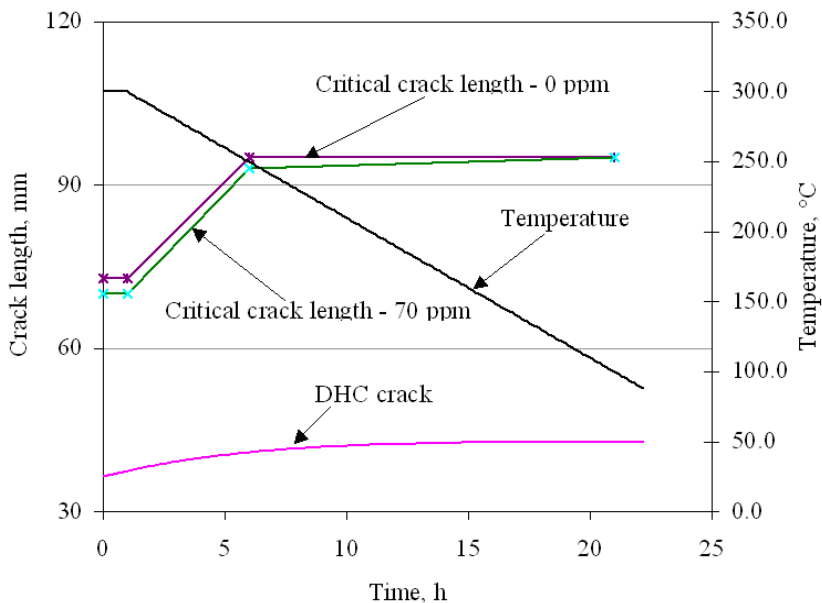


Figure 1. LBB assessment results for emergency reactor shutdown procedure.

Conclusions

According to LBB requirements the leak through the postulated through-wall crack should 10 times exceed the leak, which can be detected by leakage monitoring systems in 1 hour of normal operation, and the length of the postulated defect should not exceed half of critical through-wall crack length. Analysis confirmed, that the length of postulated crack, at which necessary leak rate is reached, is less than half-length of critical through-wall crack.

One of the important requirements of the LBB methodology is that the response time of leak detection systems, including reactor shutdown, should be less than the time of crack propagation from initial (postulated) length up to the critical sizes. The performed analysis shows that the possible intersection of the growing crack curve due to DHC process with a critical crack size curve could not be reached. Performed deterministic LBB analysis confirms that the pressure tube complies with LBB requirements. Therefore the LBB methodology can be used for structural integrity assessment of pressure tube in case of DHC.

References

1. Wilkowski, G. Leak-Before-Break: What Does It Really Mean? *Journal of Pressure Vessel Technology*, 2000, Vol. 122, Issue 3, pp. 267–272.
2. Almenas, K., Kaliatka, A., Uspuras, E. Ignalina RBMK-1500. A Source Book. Lithuanian Energy Institute, pp. 1998–198.
3. Lepage, A.D., Ferris, W.A., Ledoux, G.A. Procedure for Adding Hydrogen to Small Sections of Zirconium Alloys. AECL Report No. FC-IAEA-03, T1.20.13-CAN-27363-03, 1998 November 5.

Failure behavior for nuclear piping using compact pipe specimen (2-1928)

Sung-Keun Cho^{1,a}, Dae-Jin Km^{1,b}, Jung-Hun Choi^{1,c},
Chang-Sung Seok^{1,d}, Jae-Mean Koo^{1,e}

¹School of Mechanical Engineering, SungKyunKwan University
300, Cheoncheon-dong, Jangan-gu, Suwon, Gyeonggi-do, Korea

e-mails: ^asungkny@skku.edu, ^bdaeji76@empal.com, ^cwhvlfwo@hanmail.net,
^dseok@skku.edu, ^ekjm9600@hanmail.net

Introduction

To apply the LBB concept, a crack instability evaluation based on elastic-plastic fracture mechanics should be performed. In practice, the crack instability evaluation requires two steps. The first step is to estimate the crack driving force in terms of the elastic-plastic J-integral [2]. The second step involves measurement of fracture toughness of the material, for instance, in terms of the J-resistance curve. This is typically performed by testing cracked specimens, extracted from the pipe, according to standard fracture toughness testing methods. The crack instability is then evaluated by comparing the crack driving force with fracture toughness, of which methods are well established, see Refs. [3, 4]. To increase the accuracy of the estimated crack driving force in terms of the J-integral, detailed elastic-plastic finite element analyses can be conducted for a full-scale pipe, which is rather straightforward these days. On the other hand, increasing the accuracy of the measured J-resistance curve is rather difficult. It is well known that the fracture toughness could be strongly affected by the specimen size and the loading mode and thus the J-resistance curve from small standard fracture toughness specimen could be lower than that from full-scale pipe. To overcome above-mentioned problem associated with crack-tip constraint, fracture toughness test using full-scale pipe specimen should be performed in principle, which often requires expensive testing equipment and long period of testing time. Another possibility is to determine experimentally constraint-dependent J-resistance curves using non-standard toughness testing specimens, see for example Refs. [5, 6]. This method, however, is still difficult to apply in practice, as the crack-tip constraint conditions, in terms of the h-stress for instance, should be quantified for both testing specimens and full-scale pipes. In this context, a new nonstandard fracture toughness test method is still desirable.

Aim of the work

In this paper, a compact pipe test is proposed to measure J-resistance curve of material of interest considering crack-tip constraint of full-scale pipe.

Essential results

1. Experimental

In this section, experimentally measured J-resistance curves from three different tests are compared to investigate the relevance of the measured toughness. These tests include a full-scale pipe test, a standard fracture toughness test, and a finally curved wide-plate test. Brief descriptions of the tests are given below.

1.1 Full-Scale Pipe Test

1.2 Standard CT Test

1.3 Proposed Compact Pipe Specimen

1.4 Comparison of J-Resistance Curves

2. Constraint Analysis Based on FE Analysis

It has been shown that J-resistance curve from standard CT specimen test underestimate that from full-scale pipe test. On the other hand, the J-resistance curve from the proposed compact pipe test is similar to that from full-scale pipe test, suggesting that the proposed test provides relevant fracture toughness in flaw assessment of nuclear piping. Such phenomenon is related to crack-tip constraint. Therefore, to solidify the relevance of the proposed compact pipe test to failure assessment of full-scale pipes, crack-tip constraint analysis via detailed three-dimensional FE analyses is performed.

2.1 3D Finite Element Analysis

2.2 Analysis Results.

Conclusion

1. Comparison of fracture toughness testing results shows that the J-resistance curve from the full-scale pipe test is similar to that from the compact pipe test. On the other hand, the J-resistance curve from the CT specimen is lower than that from the full-scale pipe test, implying that the use of the toughness data from CT specimen is conservative.
2. Investigation of crack-tip stress fields using the h-stress via detailed three-dimensional FE analysis show that the crack tip constraint condition in the compact pipe specimen is similar to that in the full-scale pipe under bending.

Reference

1. USNRC, 1984. Evaluation of Potential for Pipe Break. NUREG 1061, 3.
2. Rice, J.R. 1968. A Path Independent Integral and the Approximate Analysis of Strain Concentration by Notches and Cracks. *J. Appl. Phys.*, 35, pp. 379–386.
3. Hutchinson, J.W., Paris, P.C. 1979. Stability Analysis of J-Controlled Crack Growth. *ASTM STP-688*, pp. 37–64.
4. Kumar, V., German, M.D., Shih, C.F. 1981. An Engineering Approach for Elastic-Plastic Fracture Analysis. EPRI Report, NP-1931, EPRI, Palo Alto, CA.
5. Kirk, M.T. Dodds, Jr., R.H. 1993. J and CTOD Estimation Equations for Shallow Cracks in Single Edge Notch Bend Specimens. *J. Test. Eval.*, 21(4), pp. 228–238.
6. Kim, Y.J., Budden, P.J. 2001. Plastic h-factor Solutions of Homogeneous and Bi-Material SE(T) Specimens for Toughness and Creep Crack Growth Testing. *Fatigue Fract. Eng. Mater. Struct.*, 24, pp. 751–760.

Warm pre-stressing tests for WWER materials (2-1948)

Vladislav Pistora, Dana Lauerova, Milos Kytka
Nuclear Research Institute Rez
plc., 130 Husinec-Rez, 250 68 Rez, Czech Republic
e-mail: pis@ujv.cz

Introduction/background

Warm pre-stressing (WPS) effect is a well known effect described as follows: after loading of a specimen or component containing a crack at relatively high temperature (warm pre-stressing), the specimen (component) can withstand higher loading at low temperature than corresponds to original (virgin) fracture toughness prediction for the low temperature. A large national project funded by the Czech regulatory body (State Office for Nuclear Safety) was established to validate the WPS effect for WWER reactor pressure vessel (RPV) materials.

Aim of the work

The aim of the project was validation of WPS effect for materials 15Kh2MFA (base material of WWER 440 RPV) and 15Kh2NMFA (base material of WWER 1000 RPV) in as-received, artificially aged and irradiated states. The final aim was improving (reducing the conservatism) of the WPS approach in the procedure for RPV integrity assessment included in Unified Procedure VERLIFE [1].

Essential results

The following regimes were tested:

LUCF	Load – Unload – Cool – Fracture,
LPUCF	Load – Partial Unload - Cool – Fracture,
LTUF	Load – Transient Unload– Fracture,
LPTUF	Load – Partial Transient Unload – Fracture,
LCF	Load – Cool – Fracture.

The tests were performed for different levels of K_I at pre-stressing and for different temperatures at pre-stressing and at final fracture. Most of the tests were performed for pre-cracked Charpy size specimens loaded by three-point-bending; limited number of tests was performed for 1T-CT specimens. Small (pre-cracked Charpy size) specimens had to be used, since significant part of

them were planned to be irradiated in experimental reactor. About 300 specimens were tested in as received state; about 100 specimens in artificially aged state (by heat treatment) and about 200 specimens in irradiated state.

The experimental results were statistically treated and compared with predictive models of Chell [2] and Wallin [3]. The comparison proved relatively good agreement between prediction and experimental results for all states of the material. For some WPS regimes (mainly for LUCF) conservativeness of the predictive models was proved, while for other regimes (mainly for LCF) the predictive models seem to be (only) realistic. Results for 15Kh2MFA material for initial state are discussed in detail in the paper.

Summary/conclusions

WPS effect was proved for WWER RPV materials in as-received, artificially aged and irradiated states. Chell's and Wallin's predictive models can be used for these materials for assessment of WPS. An updated procedure for RPV integrity assessment taking into account benefit of WPS effect (in less conservative way than in the current version) can be established based on the project results.

References

1. Unified Procedure for Lifetime Assessment of Components and Piping in WWER NPPs VERLIFE. Version 2008, Report Number: COVERS-WP4-D4.10, COVERS Project, 6th Euratom framework program, 2008.
2. Chell, G.G., Haig, J.R. The Effect of Warm Prestressing on Proof Tested Pressure Vessels. *Int J Pres Ves & Piping* 23 (1986), pp. 121–132.
3. Wallin, K. Master Curve implementation of the warm pre-stress effect. *Engng Fract Mech*, 2003; 70, pp. 2587–2602.

Fracture energy and size effect studies for nuclear concrete structures (2-1978)

R.K. Singh^{1*}, S.M. Basha², Rajesh K. Singh³

¹Reactor Safety Division

²Architecture and Civil Engineering Division

Bhabha Atomic Research Centre, Trombay, Mumbai 400 085, India

³Department of Civil Engineering

Indian Institute of Technology Bombay, Mumbai 400076

*Corresponding author e-mails: rksingh@barc.gov.in,

rksingh175@rediffmail.com

The design, analysis and testing of large size nuclear concrete structures pose problems due to varying sizes of the test specimens, models and prototype structures and exhibit the structural size effect. In this paper the structural size effect law for such structures is revisited and is explained through nonlinear fracture mechanics description. The new experimental programme of material characterization for softening behavior of concrete in compression and tension are described. The fracture energy evaluation on notched/unnotched, plain and reinforced Three Point Bend (TPB) beam specimens using conventional instrumentation, acoustic b-value analysis and high resolution image processing systems is presented. Further, a few case studies are presented with numerical finite element cohesive crack and crack band models to illustrate the issues of mesh sensitivity as observed in the classical strength/strain based non-linear finite element theories.

The size effect in plain and reinforced concrete structures have been earlier addressed by many investigators with an aim to quantify its effect on the structural strength, which determines the ultimate load carrying capacity based on stress/strain based theories. Many experimental and analytical simulation studies reported earlier though have shown the influence of the size effect on the strength of plain and reinforced concrete structures, still there remain many ambiguities for the interpretation of observed results with regard to tensile, flexure and shear failures. With the evolution of fracture mechanics for quasi-brittle material like concrete, it has been possible to quantify purely in a mechanistic manner the influence of the size effect with the help of brittleness number, characteristic length and fracture energy, which have been shown to be the typical material characteristics in a more rational manner. After defining the size effect laws based on the strength theories, further studies using the fracture energy of concrete have been reported by Bazant et al [1].

In this paper, we propose to present the experimental and finite element simulation studies to address the size effect influence on the fracture energy of beam specimens. The three points bend plain and reinforced concrete beam

specimens used for obtaining the fracture energy is indicated in the test-matrix of Table-1. The measurements during the tests are CMOD, load line displacement and acoustic data for evaluating the fracture process zone. In addition crack growth studies with image processing and strain measurements have also been employed for this experimental study. The fracture energy obtained from the above tests is further compared with the fracture energy constitutive finite element model simulation results for identifying the critical structural and flaw size parameters that influence the maximum load carrying capacity, the softening behaviour and the associated fracture energy. An un-notched and two notched beam specimens of three sizes (Table-1) have been simulated in the present study to highlight the typical results.

Table 1

S.No	Depth (d), mm	Width (b), mm	Span (S= 3d), mm	Total length (L=4d), mm
1	94	47	282	376
2	188	94	564	752
3	750	375	2250	3000

Reference

1. Bazant, Z.P., Qiang, Yu, Goangseup, Zi. 2002. Choice of standard fracture test for concrete and its statistical evaluation. *Int J of Fracture*, 118, pp. 303–337.

A suggestion to make Gurson damage model mesh independent numerically (2-1985)

B.K. Dutta

Reactor Safety Division, Hall-7, Bhabha Atomic Research Centre

Mumbai 400 085, India

e-mail: bk Dutta@barc.gov.in

Introduction

Micro-mechanical modeling of material damage helps to overcome some of the inherent limitations of conventional fracture mechanics. A number of models exist within the frame work of micro-mechanical modelling which address various phenomena of material behavior during material damage ranging from ductile to cleavage fracture. The ductile rupture follows the nucleation, growth, and coalescence of micro-voids with significant plastic deformation. This consumes much more energy due to plastic deformation. The modelling is done using two independent methodologies. The model of Rice & Tracey for ductile crack initiation is based on a critical cavity growth [1, 2]. On the other hand, the “coupled” constitutive models of Gurson and Rousselier affect the yield behavior. The specific material subroutines are required to perform FE analysis. In order to account for the effects of void nucleation and coalescence, and to obtain better agreement between the experimental results and numerical simulations, the original Gurson model was modified and extended into a semi-phenomenological form. The material input parameters of the micro-mechanical models should be obtainable from metallurgical observations. However, the determination of damage parameters is still predominantly a phenomenological fitting procedure and is done by combining test results and numerical simulations.

Background

Present author was earlier involved in computing fracture J-initiation and J-Resistance (J-R) curve for carbon steel materials. A difficulty was experienced to obtain a set of Gurson parameters which can compute J-initiation as well as entire J-R curve close to the measured values. It was then found that a phenomenological form of q_2 parameter, used in Gurson constitutive model, based on experimental observation helps to overcome this difficulty. The new form of q_2 has an exponential spatial variation near the crack tip and has two-constants. These additional constants help analysts to compute complete J-R

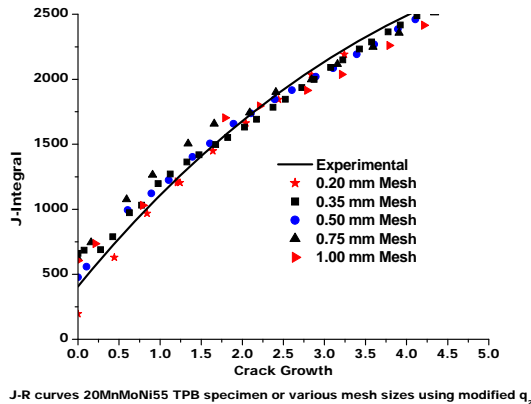
curve (including J-initiation) close to experimental data. The same set of constants was also found to be useful for other fracture specimens and materials [3].

Aim of the work

During the present study, an attempt has been made to overcome mesh dependency of the Gurson model by using exponential form of q_2 described above. The analyses have been carried out on TPB and CT specimens made up of 20MnMoNi55 material for various a/w ratios, for which experimental data are available. Various sizes of crack tip elements ranging from $0.2 \text{ mm} \times 0.2 \text{ mm}$ to $1.0 \text{ mm} \times 1.0 \text{ mm}$ are employed. A strong mesh dependency of load-displacement and J-R curves is seen. Various alternatives are tried to reduce mesh dependency numerically. The most viable alternative is to modify asymptotic value of exponential form of q_2 away from crack tip. This asymptotic value has been found to be a function of crack-tip mesh size to overcome mesh dependency.

Results

A sample result is shown below.



References

- Dutta, B.K., Kushwaha, H.S. 2004. A modified damage potential to predict crack initiation theory and experimental verification. *Engineering Fracture Mechanics*, Vol. 71, pp. 263–275.
- Dutta, B.K., Saini, S., Arora, N. 2005. Application of a Modified Damage Potential to Predict Ductile Crack Initiation in Welded Pipes. *International Journal of Pressure Vessels and Piping*, Vol. 82, Issue 11, pp. 833–839.
- Dutta, B.K., Guin, S., Sahu, M.K., Samal, M.K. 2008. A phenomenological form of q_2 parameter of Gurson model. *International Journal of Pressure Vessels and Piping*, Vol. 85, Issue 4, pp. 199–210.

Overview of fracture mechanics research studies in the UK (2-1987)

John Sharples¹, Mark Jackson², Peter Budden³

¹Serco, Birchwood Park, Risley, Warrington, WA3 6GA, UK
e-mail: john.sharples@sercoassurance.com

²Rolls-Royce plc, Derby, PO Box 2000, DE21 7XX, UK
e-mail: M.Jackson@rolls-royce.com

³British Energy Generation Ltd., Barnett Way, Barnwood, Gloucester, GL4 3RS, UK
e-mail: peter.budden@british-energy.com

Introduction/background

Research associated with the development of the R6 defect assessment procedure [1] has been carried out in the UK for many years. More recently, a further large and long-term research programme has been launched in the UK, a significant part of which is aimed at developing and improving fracture mechanics based methods for assessing the structural integrity of metallic engineering structures and components. This fracture mechanics part of this research programme is strongly linked to developments in R6.

Aim of the work

The main aim of the fracture mechanics studies is initially to develop a better understanding of the levels of conservatism (and possibly non-conservatism) inherent in current methodologies, primarily focusing on the R6 method. Following on from this, the intention is then to develop improved guidance on relevant aspects so as to reduce over conservatism and remove any non-conservatism, as appropriate.

The technical issues being addressed in the UK include the following:

- Deriving alternative methods for the treatment of combined primary and secondary stresses in fracture evaluations that are less conservative and easier to apply than the current methods.
- Assessing the effects that overloads and crack growth (i.e. load history effects) have on crack driving force parameters in the presence of residual stress fields so that the significance of ignoring these aspects (as in conventional fracture mechanics methodologies) can be evaluated.
- Assessing the significance of residual stresses on crack tip constraint such that the potential for using enhanced fracture toughness in fracture

assessments of welded structures may be fully realized by allowing for constraint effects.

- Extending the crack opening area solutions for the leak-before-break guidance within R6 by way of undertaking finite element analyses for such aspects as straight-fronted cracks under combined loading, converging/diverging cracks whereby the length on one surface is different to that on the other surface, weld strength mis-match effects and component features effects.
- Assessing the characterisation rules for multiple defects, particularly in terms of situations where they currently may be non-conservative.
- Developing guidance on the most relevant way of quantifying and dealing with weld residual stresses for fracture mechanics evaluations.
- Developing guidance on the most relevant way of dealing with crack closure effects and random load cycles in fatigue crack growth calculations.

The paper presents an overview of the research work being undertaken and provides an outline of progress made to-date in terms of some of the key technical results obtained, with particular reference to the first four bullet points listed above.

Essential results

The studies being undertaken are leading to a better understanding being gained of the levels of conservatism in some of the current fracture mechanics methodologies and are identifying suitable ways forward of improving guidance in order to reduce any over conservatism. For example, based on developments involving detailed elastic-plastic finite element analyses, a proposed alternative way of treating combined primary and secondary stresses is being shown to have good potential in terms of being less conservative and somewhat simpler to use than the current methods. Finite element analyses have also highlighted the potential benefit of allowing for reduced values of crack driving force resulting from overloads reducing the intensity of residual stress fields. In addition, the potential has been highlighted for developing methodology that allows for the fact that crack driving force may be significantly lower for growing cracks than for stationary cracks in the presence of residual stresses. The work on assessing the significance of residual stresses on crack-tip constraint is leading to better understanding and confidence that constraint-corrected fracture toughness may be able to be considered when such stresses need to be taken into account when assessing the integrity of welded structures and components. More accurate crack opening area solutions have been developed that can be used for leak-before-break considerations for some complex load and geometrical situations. Conversely, where potential non-conservatism of the current procedures have

been identified, in terms of characterising multiple flaws, both analytical and experimental studies undertaken within the programme have led to a better understanding of the situation and resulted in revised guidance being proposed.

Summary/conclusions

The paper presents an overview of fracture mechanics research work being undertaken in the UK and provides an outline of progress made to-date in terms of some of the key technical results obtained. This is with particular reference to studies on the treatment of primary and secondary stresses, load history effects, influences of residual stresses on crack-tip constraint and more accurate crack opening area solutions for leak-before-break assessments.

References

1. R6: Assessment of the Integrity of Structures Containing Defects. British Energy Generation Limited, Revision 4 (2001), with amendments to 2007.

Ascertaining the micromechanical damage parameters using the small scale test specimens (2-1997)

N. Naveen Kumar¹, P.V. Durgaprasad², B.K. Dutta², G.K. Dey³

¹Ph.D. Student, HBNI, RSD, BARC, Trombay, India-400085

e-mail: naveenm@barc.gov.in

²Reactor Safety Division, Bhabha Atomic Research Centre

Trombay, India-400085

³Material Science Division, Bhabha Atomic Research Centre

Trombay, India-400085

Introduction/background

The materials used in Fission and fusion reactors undergo high energy particle irradiation, which results change in material properties. This can be attributed to the evolution of defects and microstructure during and after irradiation. To understand the irradiation effects, post irradiation material testing is carried out on the samples taken from reactor surveillance capsules. The limited availability of the irradiated material in both reactors and accelerators resulted in evolution of innovative testing methods such as small punch testing technique [SPTT]. In the last decade, several experimental studies of SPT are devoted to un-irradiated and irradiated materials. The authors also reported numerical studies of SPTT on unirradiated material. Some of the studies reported the effect of geometric parameters of SP specimen on load displacement curve [Campitelli (2005), Wang (2008)]. Numerical studies of irradiated materials are reported only in few literatures. Campitelli (2005) did the numerical study to assess the irradiation hardening behavior of the material. Jia (2003), Kim (2005) demonstrated that small punch test (SPT) technique can be utilized to determine the shift in DBTT, change in YS after irradiation etc. They given correlations to relate the standard material properties e.g. YS, charpy energy, with the SP load displacement curve parameters such as yield load, small punch energy.

Objective of the present paper is to ascertain the damage parameters and stress strain behaviour of material under irradiated condition. To achieve this goal, following methodology is employed; a) Elastic-plastic and micro-mechanical analysis of small punch test is carried out. From the elastic plastic analysis, friction factor between the ball and specimen is found. From micro mechanical analysis, Gurson damage parameters are calibrated by comparing simulation results with experimental result of unirradiated material, b) load-displacement behaviour of small punch tests are obtained by assuming the damage parameters are unchanged due to irradiation and with approximate shift in the stress strain

curve [Tanguy (2006)], c) Comparing the above small punch results with experimental load displacement data of irradiated sample, the stress-strain data of irradiated samples is obtained. At the next stage, the fracture properties like J-R curve can be evaluated for standard CT specimens by employing the calibrated micromechanical damage parameters and stress strain data.

Aim of the work

Finite element simulation of small punch test is carried out for ferritic/martensitic steels. A methodology is demonstrated to ascertain a) micro mechanical damage parameters and b) stress strain behaviour of irradiated materials using SP test results. Such material data can be further used for structural integrity evaluation.

Essential results

The simulated load displacement results along with the experimental ones are shown in Fig 1 and 2 for unirradiated materials and the Fig 3 shows for irradiated material. From the experimental data it is seen that due to irradiation the peak load of the SP test increases and the displacement at peak load decreases. The increase in peak load corresponds to increase in UTS by considering the correlation in Milicka (2006). From the Fig. 2 and 3 it can be seen that, in the elastic bending region the simulation results diverge from experimental result and, between yield load to peak load the simulation result converge to experimental result. This pattern is observed in both irradiated and unirradiated F82H material. But this is not observed in the simulation of P91 material. This may be due to two reasons, 1] heat treatment conditions of the F82H material (refer Table1), 2] Presence of the machine compliance in measurements of load displacement data of the F82H material.

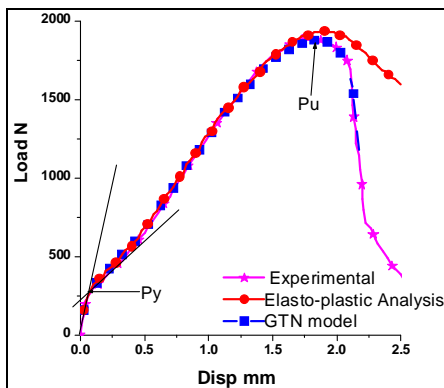


Figure 1. Load displacement curve of P91.

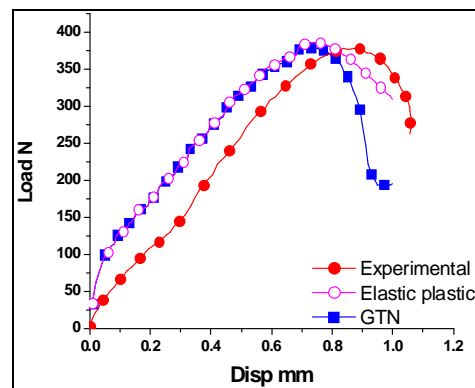


Figure 2. Load displacement curve of unirradiated F82H.

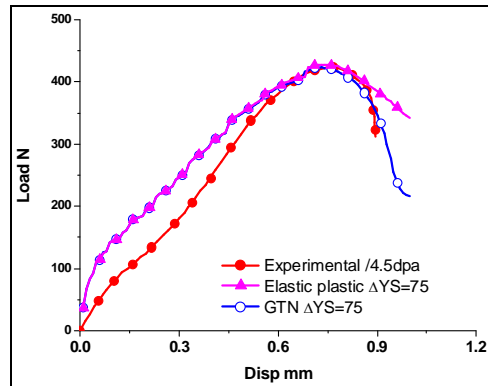


Figure 3. Load displacement curve of irradiated F82H.

Summary/conclusions

The finite element model of the small ball punch test is validated with P91 steel. For F82H material, damage parameters and stress strain data are ascertained by comparing the experimental load displacement curve with corresponding simulated load displacement curves. From the results, it can be concluded that the methodology mentioned in this paper can be successfully utilized in the determination of the damage parameters and stress strain data of the irradiated materials. The present technique is capable of estimating the YS and flow stress curve with reasonable accuracy.

References

- Al Mundheri, M., Soulat, P., Pineau, A. 1989. Irradiation embrittlement of a low alloy steel interpreted in terms of local approach of cleavage fracture. *Fatigue fracture Engineering Materials structure*, Vol. 12:1, pp. 19–30.
- Byun, T.S., Farrell, K. 2004. Irradiation hardening behavior of poly crystalline metals after low temperature irradiation. *Journal of Nuclear Materials*, Vol. 326, pp. 86–96.
- Byun, T., Farrell, K. 2004. Plastic instability in polycrystalline metals after low temperature irradiation. *Acta Materialia*, Vol. 52, pp. 1597–1608.
- Chang, Y.-S., Kim, J.-M., Choi, J.-B., Kim, Y.-J., Kim, M.-C., Lee, B.-S. 2008. Derivation of ductile fracture resistance by use of small punch specimens. *Engineering fracture mechanics*, Vol. 75, pp. 3413–3427.
- Campitelli, E.N., Spatig, P., Bonade, R., Hoffelner, W., Victoria, M. 2004. *Journal of Nuclear Materials*, Vol. 335, pp. 366–378.

2. Fracture Mechanics and Structural Integrity

- Campitelli, E.N., Spatig, P., Bertsch, J., Hellwig, C. 2005. Assessment of irradiation-hardening on Eurofer97' and Zircaloy 2 with punch tests and finite-element modeling. *Materials Science and Engineering A*, Vol. 400–401, pp. 386–392.
- Farrell, K., Byun, T.S. 2000. Hardening of ferritic alloys at 288C by electron irradiation. *Journal of Nuclear Materials*, Vol. 279, pp. 77–83.
- Gurson, A.L. 1977. Continuum of ductile rupture by void nucleation and growth: Part I – Yield criteria and flow rules for porous ductile media. *Journal of Engineering Materials Technology*, Vol. 99, pp. 2–55.
- Jia, X., Dai, Y. 2003. Small punch test on martensitic/ferritic steels F82H, T91 and Optimax-A irradiated SINQ Target-3. *Journal of Nuclear Materials*, Vol. 323, pp. 360–367.
- Karel, M., Ferdinand, D. 2006. Small punch testing of P91 steel. *Int. J. Pressure vessel and piping*, Vol. 83, pp. 625–634.
- Kim, M.-C., Yong, J.O., Lee, B.-S. 2005. Evaluation of ductile brittle transition temperature before and after neutron irradiation for RPV steels using small punch tests. *Nuclear Engineering Design*, Vol. 235, pp. 1799–1805.
- Margolin, B., Gulenko, A., Nokolaev, V., Ryadkov, L. 2003. A new engineering method for prediction of fracture toughness temperature dependence for RPV steels. *International journal of pressure vessel and piping*, Vol. 80, pp. 817–829.
- Spatig, P., Bonade, R., Hoffelner, W., Victoria, M. 2004. Assessment of constitutive properties from small ball punch test: experiment and modeling. *Journal of Nuclear Materials*, Vol. 335, pp. 366–378.
- Tanguy, B., Bouchet, C., Bugat, S., Benson, J. 2006. Local approach to fracture based prediction of ΔT_{56j} and ΔT_{KIC100} shifts due to irradiation for an A508 Pressure vessel steel. *Engineering Fracture Mechanics*, Vol. 73, pp. 191–206.
- Wang, Z.-X. et al. Small punch testing for assessing the fracture properties of the reactor vessel steel with different thickness. *Nuc. Eng. Des.* (2008), doi:10.1016/j.nucengdes.2008.07.013.

Effect of surface finish and loading conditions on the LCF behavior of austenitic stainless steel in PWR environment (2-2018)

Jean Alain Le Duff¹, André Lefrançois², Jean Philippe Vernot³

¹AREVA NP – Plants Sector, Materials and Corrosion Section
Tour AREVA – 92084 Paris La Défense – France

²AREVA NP – Plants Sector, Materials, Technology & Chemistry Department
Tour AREVA – 92084 Paris La Défense – France

³AREVA NP – Product and Technology Division
Fluids & Structural Mechanic Department
Porte Magenta, 71205 Le Creusot – France

During mid 2006, ANL issued a NUREG/CR-6909 report that is now applicable in the US for evaluations of PWR environmental effects in the fatigue analysis of new reactor components.

In order to assess the conservativeness of the application of this NUREG report, low cycle fatigue (LCF) tests were performed by AREVA NP on austenitic stainless steel specimens in a PWR environment.

The selected material exhibits in an air environment a fatigue behavior consistent with the ANL reference “air” mean curve. Tests were performed in PWR environment for two various loading conditions: for fully reverse triangular signal (for comparison purpose with tests performed by other laboratories with same loading conditions) and complex signal, simulating strain variation for actual typical PWR thermal transients. Two surface finish conditions were tested: polished and ground.

The paper presents the comparison of environmental penalty factors (F_{en}) as observed experimentally with the ANL formulation (considering the strain integral method for complex loading), and the actual fatigue life of the specimen with the fatigue life predicted through the NUREG/CR-6909 application. Low Cycle Fatigue test results obtained on austenitic stainless steel specimens in PWR environment with triangle waveforms at constant low strain rates gives F_{en} penalty factors close to those estimated using the ANL formulation (NUREG report 6909). On the contrary, it was observed that constant amplitude LCF test results obtained under complex signal reproducing an actual sequence of a cold and hot thermal shock exhibits significantly lower environmental effects when compared to the F_{en} penalty factor estimated on the basis of the ANL formulations.

It appears that the application of the NUREG/CR-6909 in conjunction with the F_{en} model proposed by ANL for austenitic stainless steel provides excessive margins whereas the current ASME or RCC-M approaches seem sufficient to cover significant environmental effect for components.

Improvement techniques for stainless steel welds (2-2032)

Gary B. Marquis¹, Stephen J. Maddox²

¹Helsinki University of Technology, Espoo, Finland, gary.marquis@hut.fi

²TWI Ltd., Cambridge, United Kingdom, stephen.maddox@twi.co.uk

Introduction

In structural applications where environment and temperature effects are negligible, the fatigue strength of welded components fabricated from stainless steels is similar to that of C-Mn steels [1]. Welded austenitic and higher strength duplex stainless steel welds have similar fatigue properties [2]. It is well established that the fatigue strength of C-Mn steel fillet welds can be improved by controlled welding processes that produce both a good weld profile and small defects [3] or by post weld improvement techniques [4]. This paper summarizes some of the results of an investigation funded in part by the Research Fund for Coal and Steel and performed at six European laboratories and universities [5]. The goal of the investigation was to study methods for improving the fatigue performance of fillet welded stainless steels by means of optimizing the welding processes or the application of post-weld improvement techniques. Fatigue tests were performed on fillet-welded joints in 10 mm thick 304L austenitic and S31803 duplex. The fatigue performance of MAG welds was compared with welds improved by toe grinding, TIG or plasma dressing and ultrasonic impact treatment (UIT).

Aim of the work

The aims of the project were to establish methods for improving the fatigue resistance of fillet welded joints in austenitic and duplex stainless steels by the suitable choice and control of welding process or the application of a post-weld improvement technique. Practical guidance on the application of the techniques and their benefits in real welded stainless steel structures were produced and the benefit achievable from high-strength duplex by the use of improvement measures was quantified.

Essential results

All four of the weld toe improvement techniques investigated improved the fatigue performance of the fillet welds. The effect was essentially the same as observed in the application of the same techniques to welded C-Mn steels.

Initially it had been hoped to achieve a 60% improvement in fatigue strength, but 30% proved to be more realistic. However, the improvement generally increased with decrease in applied stress and the increase in the fatigue limit could be much higher, 100% or more.

One expectation had been that the benefit gained from the application of an improvement technique would have been greater in the higher strength duplex steel. However, this was not the case and the only advantage of using the higher strength steels was that the fatigue strength was still improved at stress ranges above the yield strength of the austenitic steel. However, this is only relevant to relatively low-cycle fatigue conditions. Improvement techniques are particularly effective in the high-cycle regime, approaching the fatigue limit, and there was no difference between the benefit obtained from the different strengths of steel in that regime.

A feature of improvement techniques that rely on the presence of beneficial compressive residual stress is that their fatigue performance depends on the applied mean stress, or more particularly the maximum applied tensile stress. In general, the closer the maximum tensile stress is to yield, the less the benefit. To a lesser extent, it can also be expected that the fatigue behaviour of welds treated to improve their profiles will also depend on applied mean stress. For the reasons already discussed in relation to the effect of applied mean stress, there is also the possibility that improvement techniques will be less effective under variable amplitude spectrum loading than under constant amplitude loading. A further reason for this is the fact that the beneficial effect of any of the improvement techniques tends to decrease with increase in applied stress range. Consequently, the benefit seen under spectrum loading is likely to be less than the maximum seen under constant amplitude, the difference depending on the nature of the applied stress spectrum.

Summary

Results are summarized in the following table.

Method	Weld and steel	Fatigue strength improvement		
		Constant amplitude R = 0.1	Constant amplitude high mean stress	Spectrum loading
Toe grinding	Transverse duplex	Better than x1.3, x2.5 near fatigue limit	N/I	N/I
	Transverse 304L	x1.3, or x2 near fatigue limit, but limited by potential plate failure	N/I	N/I

2. Fracture Mechanics and Structural Integrity

TIG dressing	Transverse duplex	x1.3	x1.3	N/I
	Transverse 304L	x1.3, or x2 near fatigue limit, but limited by potential plate failure	x1.3 or more in high-cycle regime provided $S_{max} < yield$	x1.3, or x2 near fatigue limit, limited by potential plate failure
	Transverse with flaws	None; failure from flaws	N/I	N/I
Plasma dressing	Transverse duplex	Better than x1.3	N/I	N/I
	Transverse 304L	None due to sharp plasma dressed weld toe profile	N/I	N/I
	Longitudinal duplex	x1.3 but limited by potential failure from weld root	N/I	N/I
	Longitudinal 304L	x1.3 if $S_{max} < yield$	N/I	N/I
UIT	Transverse duplex	x1.3	Reduced or even lost at low stresses if high R	x 1.3
	Transverse 304L	x1.3 but limited by potential plate failure	Benefit lost if $S_{max} > yield$	Benefit lost if S_{max} in spectrum $> yield$
	Longitudinal duplex	Better than x1.3, up to x3 near fatigue limit	N/I	N/I
	Longitudinal 304L	Better than x1.3, up to x3 near fatigue limit	N/I	N/I

References

- Hobbacher, A. 2008. Recommendations for fatigue design of welded joints and components. International Institute of Welding, Paris, IIW-1823-07. 148 p.
- Branco, C.M., Maddox, S.J., Sonsino, C.M. Fatigue design of welded stainless steels. Report No. EUR 19972, ECSC Steel Publications, European Commission, Brussels, 2001.
- Nykänen, T., Marquis, G., Björk, T. A simplified fatigue assessment method for high quality welded cruciform joints. International Journal of Fatigue, Vol. 31, Issue 1, January 2009, pp. 79–87.
- Haagensen, P.J. IIW's Round Robin and Design Recommendations for Improvement Methods, Proc. IIW 50th Annual Assembly Conference. (Eds.) S.J. Maddox, M. Prager, 1997.
- ECSC report 'Improving the fatigue performance of welded stainless steels' Contract No. 7210-PR-303, ECSC Steel Publications, European Commission, Brussels, 2006.

Residual stress distribution and guidelines for crack inspection in pipe bends (2-2046)

Metin Yetisir

Atomic Energy of Canada Limited, Component Life Technology Branch
Chalk River Laboratories, Chalk River, Ontario, K0J 1J0
e-mail: yetisirm@aecl.ca

Background

Root cause investigation of feeder pipe cracks detected in one CANDU^{TM1} station indicated that the residual stress had a significant role in these failures. As a result, numerous residual stress measurements of pipe bends were obtained and numerical models were developed for various bending processes.

This paper provides a comprehensive review of pipe bend residual stress data and provides guidelines for crack inspections. Residual stress data, generated since 1997 as part of CANDUTM feeder cracking investigation, was compiled and presented for the quick dissemination of information. This information is summarized in quick lookup tables where likely crack locations are identified for pipe bends manufactured using various fabrication techniques.

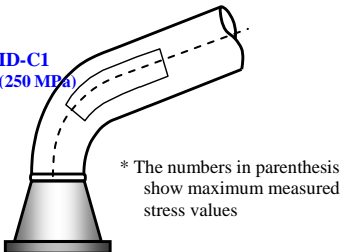
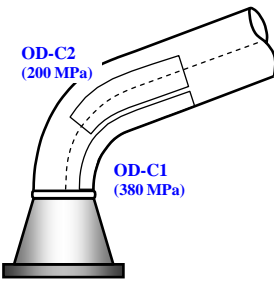
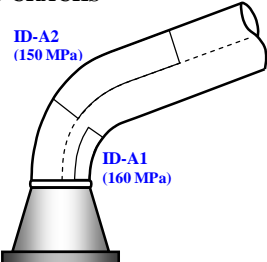
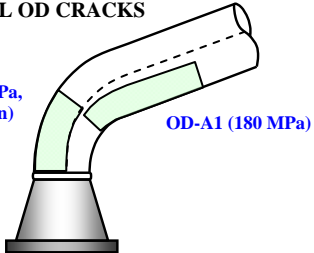
Results and conclusions

Residual stresses were measured for three different manufacturing processes and inspection guidelines are provided based on the locations of peak tensile residual stresses. The considered manufacturing techniques were: (1) intrados-heated draw bending, (2) compression-boost draw bending, and (3) hot forming. In addition, the effects of various parameters, such as pipe diameter, pipe r/D ratio where r is the bend radius and D is the nominal pipe diameter, and bend angle are discussed.

As an example for crack inspection guidelines, likely crack locations for bends manufactured using the compression-boost draw bending technique is given in Table 1.

¹ CANDUTM (Canada Deuterium Uranium) is a trademark of Atomic Energy of Canada Limited

Table 1. Compression-Boost Bend With No Stress Relief.

<i>Possible ID Cracks</i>	<i>Possible OD Cracks</i>
<p>ID-C1. Circumferential crack at the cheeks: search for 60° to 120° (and -60° to -120°) circumferentially, and from the bend mid-section to past the downstream tangent line axially by one feeder diameter.</p> <p>ID-A1. Axial crack at the intrados: search for -60° to 60° circumferentially, and from prior to the upstream tangent line to the bend mid-section axially.</p> <p>ID-A2. Axial crack at the downstream cheek: search for 90° to 180° (and -90° to -180°) circumferentially, and from the bend mid-section to past the downstream tangent line axially by one feeder diameter.</p>	<p>OD-C1. Circumferential crack at the intrados - search for -45° to 45° circumferentially, and from prior to the upstream tangent line to past the downstream tangent line axially by one feeder diameter.</p> <p>OD-C2. Circumferential crack at the cheek: search for 60° to 120° (and -60° to -120°) circumferentially, and from the bend mid-section to past the downstream tangent line axially by one feeder diameter.</p> <p>OD-A1. Axial crack at the intrados: search for -60° to 60° (via 0°) circumferentially, and from the bend mid-section to past the downstream tangent line axially by one feeder diameter.</p> <p>OD-A2. Axial crack at the upstream extrados: search for -90° to 90° (via 180°) circumferentially, and from prior to the upstream tangent line to the bend midsection axially.</p>
<p>CIRCUMFERENTIAL ID CRACKS</p> 	<p>CIRCUMFERENTIAL OD CRACKS</p> 
<p>AXIAL ID CRACKS</p> 	<p>AXIAL OD CRACKS</p> 

Structural integrity of main heat transport system piping of AHWR (2-2499)

P.K. Singh, V. Bhasin, K.K. Vaze, A.K. Ghosh, H.S. Kushwaha
Health Safety & Environmental Group
Bhabha Atomic Research Centre, Mumbai-400085, India

Introduction/Background

Advanced Heavy Water Reactor (AHWR) is a 920 MWth, 300 MW vertical pressure tube type reactor, with boiling light water as a coolant in a high-pressure main heat transport (MHT) system. Structural integrity of the MHT system piping is of concern considering the life of 100 years for which experience and material data are not available. Failure of austenitic stainless steel piping of boiling water reactors due to Intergranular Stress Corrosion Cracking (IGSCC) has been reported extensively in the available literature. Prevention of IGSCC in the operating plant and new plant is of great challenge to the design and material engineers. In view of this it was planned to address all the issues related to structural integrity of the MHT system piping, which are of concern to the long life of the plant. Issues covered under this article are listed below:

1. Selection of material
2. Life limiting material degradation mechanism
3. Optimization of welding process
4. Leak Before Break design criteria.

Aim of the work

In this article, various factors considered for selection of material for MHT system piping is described. Life limiting material degradation mechanism such as Low Temperature Sensitization (LTS) that will lead to IGSCC and Low Temperature Embrittlement (LTE) leading to reduction in toughness were considered. Welding is one of the widely used joining process used in the fabrication of piping system and improper selection of welding process and techniques may lead to higher residual stress and deterioration in material properties. The advantages and disadvantages of existing welding process such as Gas Tungsten Arc Welding (GTAW) and Shielded Metal Arc Welding (SMAW) along with newer hot wire GTAW have been brought out. The use of narrow gap welding technique and high deposition rate welding leading to lower residual stress is also demonstrated. This also helps in reducing the material

susceptibility to sensitization because of higher cooling rate. Occurrence of IGSCC in austenitic steel piping is deterrent in demonstration of Leak Before Break (LBB) design criteria. In view of the improved material specification and welding process optimization, the chances of IGSCC will reduce significantly and help in demonstrating the LBB criteria. The defect tolerance of the piping was demonstrated by carrying out a component test programme showing compliance with LBB criterion.

Summary

Among the various low carbon grades of austenitic stainless steels viz. SS 304L, 316L, 304LN and 316LN, choice of SS 304LN is based on its satisfactory low temperature sensitization behaviour and superior low temperature embrittlement behaviour which are important for targeted life of 100 years. The IGSCC resistance is further improved by adopting high deposition rate (hot wire GTAW) process and narrow gap technique, which has shown reduced residual stresses compared to conventional welding. Further during welding, the margin on sensitization in terms of time temperature (cooling rate) is higher in case of hot wire GATW. Gas Tungsten Arc Welding gives much better fracture resistance compared to Shielded Metal Arc Welding. A combination of narrow gap technique and hot wire GTAW will provide an added assurance against failure due to IGSCC/fatigue/fracture. Number of cycles for crack initiation in AHWR piping is considerably higher than the number of cycles anticipated during the design life. The use of the fatigue crack growth curve given in ASME Section XI will produce a conservative result where as Paris constants determined for this material using CT specimen gives good prediction. Crack growth in depth direction is more than that in length direction. Aspect ratio ($2C/a$) at the point of through thickness lies in the range of 3 to 4 irrespective of the initial notch aspect ratio, thus favouring Leak-before-break. The load carrying capacity of a through-wall cracked pipe is higher than the maximum credible loading due to a Safe Shutdown Earthquake. Thus, AHWR piping has been shown to satisfy the Leak-before-break criterion. Suitable multiplication factor has been suggested for prediction of limit load of pipe welds (GTAW and SMAW) based on flow stress of the base material.

References

1. Selection of material for main heat transport system piping of AHWR. Internal report of material selection committee of AHWR 2005
2. Danko, J.C. Effect of residual stress on the stress corrosion cracking of austenitic stainless steel pipe weldments. Practical application of residual stress technology, Conference proceedings, Indianapolis, Indiana, USA, 15–17 May 1991.

3. Sandusky, D.W., Okada, T., Saito, T. Advanced Boiling water reactor materials technology. Material Performance, January 1990
4. Material specification. ASME Boiler and Pressure Vessel Code, Section II, New York 1992.
5. Shankar, V., Gill, T.P.S., Mannan, S.L., Sundaresan, S. Solidification cracking in austenitic stainless steel welds. Sadhna Vol. 28, Parts 3&4, June/August 2003, pp. 359–382.
6. Dutta, R.S., De, P.K., Gadiyar, H.S. The sensitization and stress corrosion cracking of nitrogen containing stainless steel. Corrosion Science, Vol. 34, No. 1, pp. 51–60, 1993.
7. Baboian, R. Corrosion Tests and Standards. ASTM Manual Series: MNL20, PA19103ASTM, Publication code no. (PCN): 28-020095-27
8. Chopra, O.K. Thermal Ageing of cast stainless steels: Mechanisms and Predictions. ASME-PVP publication 1991.
9. ASME Boiler & Pressure Vessel code, Section IX, New York, 1989
10. Rules for In-service Inspection of Nuclear Power Plant Components. ASME Boiler and Pressure Vessel Code, Section XI, New York 1989.
11. Singh, P.K., Vaze, K.K., Ghosh, A.K., Kushwaha, H.S., Pukazhendi, D.M., Murthy, D.S.R. Crack resistance of austenitic stainless steel pipe and pipe welds with circumferential crack under monotonic loading. Fatigue and Fracture of Engineering Material and Structures, Vol. 29 (11), November 2006, pp. 901–915.

Structural integrity assessment of a rupture disc housing with explicit FE-simulation (2-2503)

R. Trieglaff, C. Bergler

TÜV Nord SysTec GmbH & Co. KG, Große Bahnstraße 31, Germany

e-mail: rtrieglaff@tuev-nord.de

Introduction/background

Low pressure turbines of PWR power plants are generally equipped with rupture discs to avoid a pressure overload that could lead to a damage of the turbine and the condenser.

To avoid an intake of air in case of a defect or imploded rupture disc membrane, a freely supported plate in the rupture disc housing withstands the vacuum forces. In case of a rupture disc burst caused by an excess pressure in the turbine, the plate is accelerated and impacts the clamps mounted on the housing.

Aim of the work

The purpose of the investigation is the assessment of the structural integrity of the rupture disc housing in compliance with essential safety standards. To account for the nonlinear dynamic effects, explicit FE-simulations are carried out using LS-Dyna.

Essential results

Since the influence variables for impact scenarios are manifold, safety factors may not easily be determined based on the current literature and regulations. For the analyzed scenario a safety factor on the impact velocity has been determined to be adequate in accordance with the requirements for a limit load calculation. Beside a purely lagrangian calculation of the structure, a coupled Euler-Lagrange approach for the fluid-structure interaction has been tested. As a result of the simulation, a safety margin is determined, for which the integrity of the structure at nominal burst conditions is maintained.

Summary/conclusions

Explicit FE-Simulation is valid for best estimate calculation of dynamic and highly nonlinear events and for load cases, where conservative assumptions cannot be easily made. For the investigated scenario, safety margins regarding the structural integrity of the structure may be determined.

3. Applied Computations, Simulation and Animation

Development in innovative computational methods for linear and nonlinear (inelasticity, material damage, large deformations) analysis, impact, creep damage, vibrations, turbulence, fluid dynamics, flow-induced vibrations, thermal hydromechanics, fluid-structure interaction. Computer-aided engineering and information technology. Multi-scale modeling. Computer software and control of errors. Verification and validation .

Phase field modeling of microstructure evolution in nuclear materials (3-1585)

S.Q. Shi

Department of Mechanical Engineering
The Hong Kong Polytechnic University, Hung Hom, Kowloon, Hong Kong

Keywords: microstructure evolution, phase field model, nuclear materials

Microstructure evolution is common during material processing. Since many properties of materials are determined by the microstructure of materials, in recent years much effort was made to develop computational methodologies for predicting the evolution of microstructure of materials. One of these methodologies is the phase field method (PFM). PFM describes a microstructure using a set of conserved and nonconserved field variables that are continuous across the interfacial regions. The temporal and spatial evolution of the field variables is governed by the Cahn-Hilliard nonlinear diffusion equation and the time-dependent Ginzburg-Landau (TDGL) equation. With the fundamental thermodynamic and kinetic information as the input, PFM is able to predict the evolution of arbitrary morphologies and complex microstructures without explicitly tracking the positions of interfaces. PFM has been successfully applied to various materials processes including solidification, solid-state structural phase transformations, grain growth and coarsening, domain evolution in thin films and smart materials, pattern formation on surfaces, dislocation microstructures, crack propagation, and electromigration. This paper presents two examples of phase field modeling of microstructure evolution of materials used in nuclear power industry. In the first example, an elasto-plastic phase field model was developed to predict hydrogen diffusion, hydride precipitation and fracture in zirconium at crack and notch tips. In the second example, some preliminary results of our current research on void-lattice formation in irradiated materials will be given.

Equivalent material properties of perforated structure for free vibration analysis (3-1600)

Myung Jo Jhung, Young Hwan Choi
Principal Researcher, Korea Institute of Nuclear Safety
19 Guseong-dong, Yuseong-gu, Daejeon 305-338 Korea
e-mail: mjj@kins.re.kr

For the perforated structure such as circular plate or cylindrical shell, it is very difficult to develop a finite element model due to the necessity of the fine meshing of the structure especially if it is submerged in fluid. This necessitates the use of solid structure with equivalent material properties. Unfortunately the effective elastic constants suggested by the ASME code for the circular plate are found to be not valid for the modal analysis, and those for cylindrical shell are not found anywhere. Therefore in this study, the equivalent material properties of perforated plate and cylinder are suggested by performing several finite element analyses with respect to the ligament efficiencies.

Interoperability between analysis and detailing software for reinforced concrete (3-1628)

Peter Carrato¹, Michael Gustafson²

¹Principal Civil Engineer and Fellow, Bechtel Corporation, 5275 Westview Drive, Frederick, Maryland, USA, e-mail: pcarrato@bechtel.com

²Product Manager – Engineering, North America, Tekla Inc., 114 Town Park Drive, Kennesaw, Georgia, USA, e-mail: Michael.Gustafson@tekla.com

Software interoperability allows data to be exchanged among various applications. Exchanging data that is common to multiple applications, rather than inputting the same data several times provides significant efficiency in the design process. Sharing common data not only minimizes the design effort but it virtually eliminates errors associated with the shared data set. The sharing of data also facilitates design evolution by allowing multiple potential solutions to be evaluated rapidly, as well as ensuring a more holistic design, specifically between the processes of structural analysis, structural design and construction.

In the design of reinforced concrete structures, such as those in a nuclear power plant, a significant amount of data can be shared between the analysis software and software used to detail the reinforcing steel. Specific data that is common to both applications are neat line dimension of the concrete and required reinforcing ratios to resist both shear and tension. This paper demonstrates the concept of interoperability between analysis and detailing software by flow charting the appropriate flow of common data. An application of the proposed data flow is provided to validate the concept. Data is shown to pass in both directions between software applications, ie not only from analysis to detailing but also from detailing back to analysis.

The full scale application of the proposed interchange of data is discussed. Conclusions related to potential challenges and rewards associated with developing fully functioning interoperability between analysis and detailing software for reinforced concrete are provided.

Dynamic model of a simple supported RC rectangular plate for spreadsheet application. Part I. Motion in elastic domain (3-1645)

Jean-Mathieu Rambach
 Institut de Radioprotection et de Sûreté Nucléaire
 Fontenay-aux-Roses, France
 e-mail: Mathieu.Rambach@irsn.fr

The contribution of this paper (Part I) and its companion paper (Part II) is aimed to provide the civil engineers with a simple modeling tool to be run on current spreadsheet code. Such a tool allows them to perform the resolution of the dynamic motion of an elastic (Part I) and elastoplastic (Part II) simply supported thin rectangular plate, made of reinforced concrete, when submitted to any variable loading, namely an impact loading.

The expression of the motion of a plate, when neglecting the shear deformation, is given by

$$\rho \cdot h \cdot \left(\frac{\partial^2 W}{\partial t^2} + 2 \cdot \xi \cdot \omega \cdot \frac{\partial W}{\partial t} \right) + \frac{\partial^2 M_x}{\partial x^2} + 2 \cdot \frac{\partial^2 M_{xy}}{\partial x \cdot \partial y} + \frac{\partial^2 M_y}{\partial y^2} - Q = 0$$

with usual notations:

- W: displacement of the point (x,y)
- ρ and h : volumic mass and height of the plate
- ξ and ω : viscous damping coefficient and pulsation of 1st modal response
- M_x , M_y and M_{xy} : component of the bending moment tensor
- Q: external loading applied transversally.

The resolution of the above equation of motion in elastic domain is based on the modal analysis: the displacements, bending moments and applied loadings are expressed in the eigen mode basis, for instance

$$W = \sum_{m=1}^{\infty} \sum_{n=1}^{\infty} W_{mn} \cdot \sin(m \cdot \pi \cdot \frac{x}{a}) \cdot \sin(n \cdot \pi \cdot \frac{y}{b}),$$

W_{mn} being the weight of the real displacement of the plate on the modal surface

$$S_{mn}(x, y) = \sin(m \cdot \pi \cdot \frac{x}{a}) \cdot \sin(n \cdot \pi \cdot \frac{y}{b}).$$

The decomposition of the loading $Q(x,y)$ on the modal basis is expressed by:

$$Q_{mn} = \frac{4}{a.b} \int_0^a \int_0^b Q(x,y) \cdot \sin(m.\pi.\frac{x}{a}) \cdot \sin(n.\pi.\frac{y}{b}) \cdot dx \cdot dy,$$

a and b being the lateral plate dimensions.

The pertinent variables for solving the equation of motion are the velocity V and the structural response

$$F_s = \frac{\partial^2 M_x}{\partial x^2} + 2 \cdot \frac{\partial^2 M_{xy}}{\partial x \cdot \partial y} + \frac{\partial^2 M_y}{\partial y^2}.$$

In the modal basis the fundamental equation of motion is then superseded by infinity of equations:

$$\frac{dV_{mn}^t}{dt} + 2 \cdot \xi \cdot \omega \cdot V_{mn}^t + \frac{1}{\rho \cdot h} F_{s_{mn}}^t = \frac{1}{\rho \cdot h} Q_{mn}^t,$$

m and $n \in \mathbb{N}^*$.

After classical finite difference approximation

$$V_{mn}^t = \frac{W_{mn}^{t+\Delta t} - W_{mn}^t}{\Delta t},$$

and according to semi-implicit scheme, the value of V_{mn} and $F_{s_{mn}}$, in modal basis, may then be directly computed at time step $t+\Delta t$ from their value and from Q_{mn} loading value at time step t according to following iterative relations:

$$(1 + \xi \cdot \omega \cdot \Delta t + \frac{\Delta t^2}{4 \cdot \rho \cdot h} D_{mn}) \cdot V_{mn}^{t+\Delta t} = (1 - \xi \cdot \omega \cdot \Delta t - \frac{\Delta t^2}{4 \cdot \rho \cdot h} D_{mn}) \cdot V_{mn}^t - \frac{\Delta t}{\rho \cdot h} (F_{s_{mn}}^t - \frac{Q_{mn}^{t+\Delta t} + Q_{mn}^t}{2})$$

$$(1 + \xi \cdot \omega \cdot \Delta t + \frac{\Delta t^2}{4 \cdot \rho \cdot h} D_{mn}) \cdot F_{s_{mn}}^{t+\Delta t} = (1 + \xi \cdot \omega \cdot \Delta t - \frac{\Delta t^2}{4 \cdot \rho \cdot h} D_{mn}) \cdot F_{s_{mn}}^t + \Delta t \cdot D_{mn} \cdot V_{mn}^t + \frac{\Delta t^2}{4 \cdot \rho \cdot h} \cdot (\frac{Q_{mn}^{t+\Delta t} + Q_{mn}^t}{2})$$

where

$$D_{mn} = \frac{E \cdot h^3}{12 \cdot (1 - \nu^2)} \cdot \left(\left(\frac{m \cdot \pi}{a} \right)^2 + \left(\frac{n \cdot \pi}{b} \right)^2 \right)^2$$

with E : Young's modulus and ν : Poisson's ratio of plate.

After each step, the velocity V_{mn} computed in modes space is brought back in the real space after basis change and the displacement, in real space, is deduced from the velocity through the classical finite difference approximation:

$$W^{t+\Delta t} = W^t + \Delta t \cdot \left(\frac{V^{t+\Delta t} + V^t}{2} \right).$$

The components of the bending moment tensor, in the real space, can be directly deduced from the curvature through the classical bending moment law for a plate:

$$M_x = D \left(\frac{\partial^2 W}{\partial x^2} + \nu \frac{\partial^2 W}{\partial y^2} \right) \quad M_y = D \left(\frac{\partial^2 W}{\partial y^2} + \nu \frac{\partial^2 W}{\partial x^2} \right) \quad M_{xy} = D \cdot (1 - \nu) \cdot \frac{\partial^2 W}{\partial x \partial y}.$$

The second order derivation of W with respect to x and y may be simply deduced from finite difference approximation by:

$$\frac{\partial^2 W}{\partial x^2} \approx \frac{W(x + \Delta x, y) - 2W(x, y) + W(x - \Delta x, y)}{\Delta x^2},$$

$$\frac{\partial^2 W}{\partial y^2} \approx \frac{W(x, y + \Delta y) - 2W(x, y) + W(x, y - \Delta y)}{\Delta y^2} \quad \text{and}$$

$$\frac{\partial^2 W}{\partial x \partial y} \approx \frac{W(x + \Delta x, y - \Delta y) - W(x - \Delta x, y + \Delta y) - W(x + \Delta x, y + \Delta y) + W(x - \Delta x, y - \Delta y)}{\Delta x \Delta y}$$

The computational procedure developed in this article considers the discretization of a rectangular plate into $30 \times 30 = 900$ elements: such discretization level is appropriate to capture the deformations during the motion with sufficient accuracy. The modal basis dimension may be 900 or may be reduced, when the higher modes are not solicited.

The changes of basis from real space into modes space and back are operated through matrices products. The value of the projections of the loading Q on the modal basis involves integrals that can be computed by Simpson's rule and can be operated through the same matrices of basis change.

The implementation on current spreadsheet software (like Excel®) is easy and allows calculating the structural response of the plate within few seconds on any current personal computer.

Dynamic model of a simple supported RC rectangular plate for spreadsheet application. Part II. Motion in elasto-plastic domain (3-1646)

Jean-Mathieu Rambach
 Institut de Radioprotection et de Sûreté Nucléaire
 Fontenay-aux-Roses, France
 e-mail: Mathieu.Rambach@irsn.fr

Introduction

The contribution of this paper (Part II) and of its companion paper (Part I) is aimed to provide the civil engineers with a simple modeling tool to be run on current spreadsheet code. Such a tool allows them to perform the resolution of the dynamic motion of an elastic (Part I) and elastoplastic (Part II) simply supported thin rectangular plate, made of reinforced concrete, when submitted to any variable loading, namely an impact loading. A criterion is proposed for a RC plate with reinforcement that may differ in both main directions and on each face. The dominant rupture mode is supposed to be the rupture by flexion, the rupture by shearing is neglected.

Method

The motion of the plate in the elastic domain is simulated by the method developed in Part I. The limit of the elastic domain is characterized by a global criterion of Johansen's type with a correction factor k_2 in order to keep the consistency of the law, either in its global or local expression and a coefficient k_1 in order to avoid some mathematical singularities. When the reinforcement is not isotropic nor symmetric, when defining the limiting bending moment in x and y directions for face I and face II, respectively by \bar{M}_x^I , \bar{M}_y^I , \bar{M}_x^{II} and \bar{M}_y^{II} , the criterion may be improved by:

$$f^I(\vec{M}) = \frac{M_{xy}^2}{k_2^2} + k_1^2 - (\bar{M}_x^I - M_x) \cdot (\bar{M}_y^I - M_y) = 0$$

$$\text{or } f^{II}(\vec{M}) = \frac{M_{xy}^2}{k_2^2} + k_1^2 - (\bar{M}_x^{II} - M_x) \cdot (\bar{M}_y^{II} - M_y) = 0$$

with

$$0 < k_2^2 = \frac{(\bar{M}_x^I - \bar{M}_x^{II} + \bar{M}_y^I - \bar{M}_y^{II})^2}{4(\bar{M}_x^I - \bar{M}_x^{II})(\bar{M}_y^I - \bar{M}_y^{II})} \text{ and}$$

$$0 \leq k_1 \ll \sqrt{(\bar{M}_x^I - \bar{M}_x^{II})(\bar{M}_y^I - \bar{M}_y^{II})}$$

The relevance of the expression f^I or f^{II} for the criterion depends on the position, in (\bar{M}_x, \bar{M}_y) plane, of the (\bar{M}_x, \bar{M}_y) point with respect to the segment joining the point $(\bar{M}_x^{II}, \bar{M}_y^I, 0)$ to $(\bar{M}_x^I, \bar{M}_y^{II}, 0)$. When $k_1 = 0$, the elastic domain, in the space $(\bar{M}_x, \bar{M}_y, \bar{M}_{xy})$, is the volume comprised between 2 opposite cones whose summits are on the point $(\bar{M}_x^I, \bar{M}_y^I, 0)$ and $(\bar{M}_x^{II}, \bar{M}_y^{II}, 0)$ and intersecting along an ellipse.

With $k_1 > 0$, there is no more mathematical singularities represented by the cones summits. The elastic domain is then the volume comprised between 2 opposite sheets of hyperboloids whose preceding cones are their asymptotic surface. If $f^I(\vec{M})$ or $f^{II}(\vec{M}) < 0$, the deformation due to the bending moment tensor represented by the vector \vec{M} is in elastic domain. If either $f^I(\vec{M})$ or $f^{II}(\vec{M}) > 0$, it means that the deformation is beyond elastic limit and a correction $\Delta\vec{M}_c^p$ is to be applied to the bending moment vector \vec{M} whose value shall be considered as the trial value: the corrected value of the bending moment is given by

$$\vec{M}_1 = \vec{M} - \Delta\vec{M}_c^p \text{ with}$$

$$\Delta\vec{M}_c^p = \frac{f(\vec{M}) \cdot [K^p] \cdot \vec{\text{grad}}(f(\vec{M}))}{\vec{\text{grad}}(f(\vec{M})) \cdot [K^p] \cdot \vec{\text{grad}}(f(\vec{M}))}$$

and $[K^p]$ the tangent elasticity matrix for a plate giving the relationship between the bending moment and the resulting curvature during the plastic deformation.

Essential results

The plastic curvature tensor is deduced from the correction of bending moment and from the consumption of the incremental elastic energy into energy dissipation due to the plastic deformation, essentially in the hinges.

The motion of the plate is computed by using the fundamental equation of motion of a thin plate:

$$\rho \cdot h \cdot \left(\frac{\partial^2 w}{\partial t^2} + 2 \cdot \xi \cdot \omega \cdot \frac{\partial w}{\partial t} \right) + \frac{\partial^2 M_x}{\partial x^2} + 2 \cdot \frac{\partial^2 M_{xy}}{\partial x \cdot \partial y} + \frac{\partial^2 M_y}{\partial y^2} - Q = 0$$

and by decomposing the displacements in the modes space. The pertinent variables are the velocity V and the structural response

$$F_s = \frac{\partial^2 M_x}{\partial x^2} + 2 \cdot \frac{\partial^2 M_{xy}}{\partial x \cdot \partial y} + \frac{\partial^2 M_y}{\partial y^2}.$$

The computation is performed by finite differences, by incrementation with step time and according to a plate discretization into 30×30 elements. At the end of each step time, a new value of velocity V is deduced from the ratio of the variation of displacement (including plastic displacement) during the step time Δt and a new value of the structural response F_s is obtained from the second derivation of the bending moment components (once corrected). These values of V and F_s are then decomposed in modal basis into V_{mn} and $F_{s,mn}$ and substituted to their trial value for the following step.

Results comparison with those ones from commercial FE code shows good agreement, for reasonable computing time.

Conclusion

The motion of a simply supported elasto-plastic RC plate when submitted to a variable loading can be simulated on current spreadsheet software. The dominant rupture mode is by flexion. The accuracy is sufficient for pre-sizing a RC slab or wall against impact loading or for checking an order of magnitude of permanent deflections coming from more sophisticated non linear computation code.

References

- Rambach, J.-M. Dynamic model of a simple supported RC rectangular plate for spreadsheet application – Part I: Motion in elastic domain, in SMiRT 20 Proceedings, Espoo, Finland, 9–14 August 2009.

The protection of containers for fresh and spent fuel at extremal transportation operating modes in and around a Nuclear Reactor's Portal (3-1649)

Akop Sargsian, Andrey Grishin
Atomenergoproekt, Podolskih Kursantov ul., 1, Moscow, Russia
e-mail: gandrey24@gmail.com

The certified containers for fresh and spent fuel (further the containers) are able to survive dropping from a distance of 9 meters on a concrete table top.

In present-day nuclear power plants the hoisting height of the containers at cargo handling is up to 40 meters. Possible fall of the containers on a concrete table top will probably result in its destruction.

The goal of the paper is the substantiation of a new shock-absorbing gravel-sand cushion that is designed to be installed under a Nuclear Reactor's Portal. Furthermore, there are determined the physical and mechanical specifications and the dimensions of the new shock-absorbing gravel-sand cushion. A new construction of shock-absorbing gravel-sand cushion must absorb the kinetic energy of a container so that the unabsorbed kinetic energy would not exceed the value corresponding to its fall from a distance of 9 meters on a concrete table top.

The shock-absorbing cushion mounting (composed of asphalt, gravel and sand) under portal crane of a Reactor Building will insure structural strength and impermeability of the containers in case of its fall from the maximum possible height at all transportation operating modes.

At the beginning of the paper the possible trajectories, positions and kinematical parameters of the containers are determined from a fall from the distance of up to 40 meters. These calculations are made for the cases of crane failures.

In a 3-D space, by means of FEM contact problems of the container and the shock-absorbing cushion interaction are solved. The kinematical parameters determined earlier are used as an initial condition.

It was shown that the overload coefficients for the containers do not exceed the admissible values at possible impacts of the containers with the shock-absorbing cushion.

Numerical welding simulation on a 14" narrow gap dissimilar metal weld (3-1673)

S. Courtin¹, Ph. Gilles¹, V. Pasquier¹, C. Ohms², X. Ficquet³

¹AREVA NP SAS, Tour AREVA, 92084 Paris La Defense, France

²European Commission Joint Research Centre, Institute for Energy
The Netherlands

³VEQTER Ltd, University Gate East, BS1 5UB Bristol, UK

Welding remains a key process in joining metallic pieces. In nuclear reactors, ferritic low alloy steel heavy section components have to be connected with austenitic stainless steel piping systems. Special manufacturing procedures are required to ensure a good resistance of the Dissimilar Metal Weld (DMW). In the field, AREVA NP has developed narrow gap weld techniques to perform these junctions.

In parallel, numerical welding simulation shows, years after years, its relevance to predict residual stress fields in welded components and becomes more and more a real support for industrial design engineers [1–2].

This paper presents computations performed by AREVA NP on a 14" narrow gap DMW configuration (see Fig. 1). Considering 2D axisymmetric hypotheses, the analysis simulates each elementary step of the mock-up manufacturing procedure. Multipass welding simulation reproduces the deposit of each bead by thermo-metallurgical and mechanical calculations. The main remarkable points of the work are:

- The choice of non linear kinematic hardening models to describe material behaviors,
- The use of strain annealing and phase transformation techniques to reproduce physical process,
- The proposal of a simplified approach to model the cladding welding,
- The simulations of the machining process and the post weld heat treatment (PWHT) by elasto-viscoplastic computations.

For validation, the numerical results are compared to measurements obtained by two different ways: neutron diffraction and deep hole drilling [3] techniques. The residual stress fields are observed at various locations from the weld centerline, in the depth of the pipe (see Fig. 2 to 4 for instance). It can be seen that the numerical results are in a very good agreement with measurements and they have totally caught the trend of the residual stress fields.

The narrow gap DMW configuration had to be investigated for AREVA NP applications. This work enables to give another evidence of the relevance of the

numerical welding simulation to predict residual stress fields in welded components. It highlights the capability for AREVA NP to perform, with success, such a kind of analyses.

This paper gives also some elements to have a look on the validity of both numerical and experimental techniques. This work will be the source, in the future, for sensitivity analyses studying mesh quality, material description, machining and PWHT effects.

References

1. S. Courtin, Ph. Gilles, Detailed Simulation of an Overlay Repair on a 14" Dissimilar Material Weld, ASME PVP Conference, 2006, Canada.
2. S. Courtin, Ph. Gilles, Multipass Welding Simulation on a Dissimilar Metal Weld and Overlay Design, International Seminar of Numerical Analysis of Weldability 2006, Austria.
3. X. Ficquet et al. Measurement of residual stresses in large industrial components using the deep hole drilling technique, ASME PVP Conference 2005, USA.

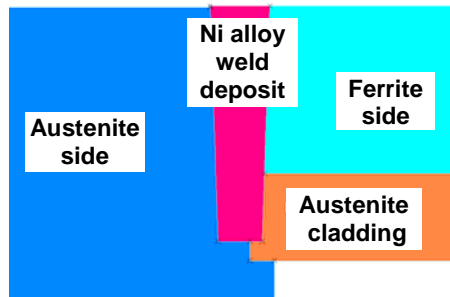


Figure 1. Narrow gap dissimilar metal weld configuration.

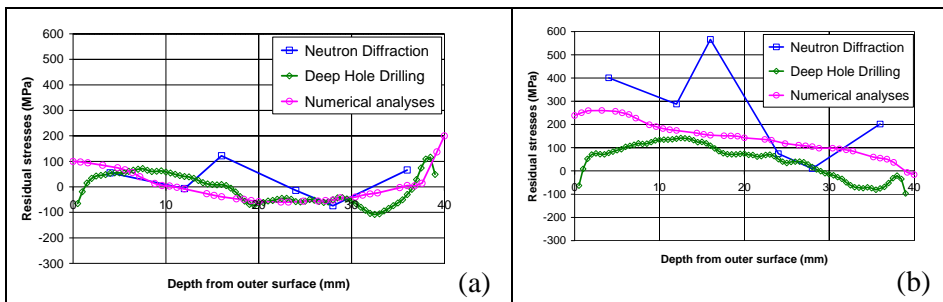


Figure 2. Axial (a) and hoop (b) residual stresses at the weld centerline. Measurements and numerical results.

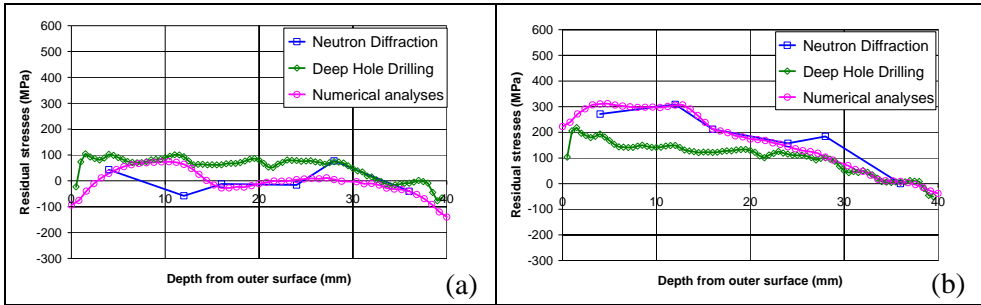


Figure 3. Axial (a) and hoop (b) stresses at 9 mm from the centerline in the austenite side. Measurements and numerical results.

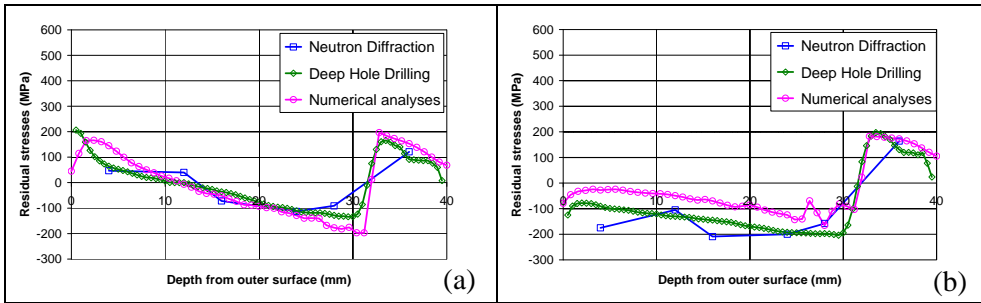


Figure 4. Axial (a) and hoop (b) stresses at 9 mm from the centerline in the ferrite side. Measurements and numerical results.

FE analysis of heat exchanger NTIW tubesheets according to new ASME VIII 2007 Div 2 Code. Methodology and automated analysis tool development (3-1682)

Julio A. Guirao Guijarro, Silvia Iglesias Benéitez,

Angel Bayón Villajos, Joaquín Polo Ruiz

Numerical Analysis TEChnologies (NATEC INGENIEROS)

C/ Marqués de San Esteban 9, 4th floor D, 33206 Gijón, Spain

e-mail: julio@natec-ingenieros.com

Numerical Analysis TEChnologies (NATEC INGENIEROS)

C/ Marqués de San Esteban 9, 4th floor D, 33206 Gijón, Spain

e-mail: silvia@natec-ingenieros.com

IBERDROLA INGENIERÍA, División de Generación Nuclear, Av/ Manóteras

20 Edf. C, 2nd floor, 28050 Madrid, SPAIN, e-mail: abv@iberdrola.es

IBERDROLA INGENIERÍA, División de Generación Nuclear, Av/ Manóteras

20 Edf. C, 2nd floor, 28050 Madrid, SPAIN, e-mail: jpriu@iberdrola.es

In Heat Exchangers (HEX) design, one of the most complex and critical parts to analyze is the tubesheet. The high diversity in tubesheet constructive configurations as well as the uncertainty in the resistant characteristics of a perforated plate make the analytical approach of these components very difficult. One of the most widely deployed analytical methods in the design of tubesheets is the one proposed in ASME Sec VIII Div. 1 in the UHX subsection. This method, consisting in analytical formulas, is based on the consideration of equivalent characteristics in the perforated zone, depending on the effective ligament efficiency, a geometric parameter based on the tubesheet configuration and which characterizes the bending stiffness of the plate in the perforated zone. The application of this method is not intuitive due to the high number of complex formulas whose physical sense and interpretation is not clear. On the other hand, the method given in UHX is based on certain hypotheses (consideration of a uniform circular perforated zone) which are not respected by some of the common configurations for HEX tubesheets (No tubes in window NTIW). Other codes (EN, RCC-MR, BS, CODAP, AD Merck...) don't reference alternative methods to overcome these situations. A usual approach in these cases consists in an analysis of the component through the Finite Element Method (FEM) (DBA "Design By Analysis). Nevertheless, for complex equipment or components with a high number of tubes, the detailed model of the tubesheet requires high computational capacity and complex geometry which

highly increases the difficulty of these analyses. The usual alternative to this complex and time consuming analysis is to use a plate with equivalent mechanical properties based on UHX method. This option, not enough justified, presents also some problems like the pressures acting in these perforated zones and the consideration of the additional stiffness given by the tube bundle. In ASME Sec. VIII Div, 2 Ed. 2007, in its 5th Appendix, for the first time it is presented a systemized methodology for a design by analysis approach and particularly Appendix 5E references the case of perforated plates without any limitation on the perforated zone pattern or axially symmetric pattern contrary to the restrictions imposed by UHX. In the mentioned reference the calculation and applications conditions are established for an orthotropic equivalent material in the perforated zone, as well as the acting pressures in each side of the plate to take into account the reduction in pressure acting area due to perforations. It also establishes an exhaustive methodology to validate the stresses including an assessment for cyclic loads (fatigue). However, its application is quite complex and still lets some undefined points such as the way in which tube bundle additional stiffness should be considered, the inclusion of thermal dilatation effects of the tube bundle or the general treatment of thermal loads. In the present paper a complete methodology for the general treatment of problems related to tubesheet analyses through Appendix 5 of ASME Sec. VIII Div. 2 Ed. 2007 and taking into account all the aspects previously mentioned is presented. In the same way its application through a parametric tool (programmed with APDL and Tcl Tk inside the ANSYS Finite Element Code) which, once given all the geometric characteristics of the component as well as the mechanical properties of the materials and the working conditions (pressures and temperatures), builds automatically the FE model, solves the coupled thermo mechanical analysis and checks the stresses generated in the tubesheet according to the design code. Finally, some application examples of this tool are presented. These examples correspond to several HEX designed for EDF's Flamanville 3 NPP (Nuclear Power Plant) in France according to ASME Sections III or VIII depending on the component location in the plant.

Comparative stress analyses of major RCPB components by using a prototype of integrated finite element model (3-1727)

Shin-Beom Choi¹, Yoon-Suk Chang¹, Jae-Boong Choi¹, Young-Jin Kim¹,
Myung-Jo Jung², Young-Hwan Choi²

¹School of Mechanical Engineering, Sungkyunkwan University
Suwon 440-746, Korea

²Korea Institute of Nuclear Safety, Daejeon 305-338, Korea

Since oppositions against new construction of nuclear power plants are getting stronger despite rapidly rising electric power demand, safe operation of existing plants until the optimum life becomes more important. In this context, during the last two decades, lots of efforts have been devoted for development of efficient structural integrity assessment techniques required to prevent unanticipated failures due to primary water stress corrosion cracking for instance and further re-evaluations often needed to fulfill current licensing bases as well as to eliminate over-conservatism for continued operation beyond their design lives. The objective of this paper is to introduce a prototype of integrated stress analysis model conceived to assist synthetic fatigue evaluation and management of major RCPB (Reactor Coolant Pressure Boundary) components. Complex three-dimensional geometries are modeled for the reactor coolant system of OPR1000 (1000 MW Optimized Power Reactor) and finite element analyses are carried out employing both representative design transients and selected monitoring histories, respectively. Resulting stress components at critical locations are compared with those obtained from previous finite element analyses by the authors for each major RCPB component; the vessel, pressurizer, steam generator and main pipes. Lessons learned to determine optimized mesh and numerical analysis conditions are fully discussed from exactness and cost efficiency points of view. Also, ongoing activities in conjunction with an aging monitoring system being developed under web environment are briefly described.

Calibration of damage parameters for Y5 and G91 steels in use of genetic algorithm (3-1729)

Yoon-Suk Chang¹, Jae-Uk Jeong¹, Shin-Beom Choi¹, Jae-Boong Choi¹,
Young-Jin Kim¹, Min-Chul Kim², Bong-Sang Lee²

¹School of Mechanical Engineering, Sungkyunkwan University
Suwon 440-746, Korea

²Korea Atomic Energy Research Institute, Daejeon 305-600, Korea

Determination of fracture toughness is prerequisite to perform elastic-plastic fracture mechanics assessment, for instance, leak-before-break analyses of nuclear piping systems and integrity evaluation of low upper-shelf reactor vessels. However, sometimes, there are lacks of fracture toughness data especially for old vintage nuclear power plants and it is not easy to extract standard specimens from archival materials or installed components. In these cases, damage mechanics is applicable as one of alternative approaches because several efficient models have been suggested to simulate ductile fracture behavior during the last couple of decades. In the present paper, a multi-island genetic algorithm is adopted into well-known Rousselier model to resolve variableness and complexity of previous calibration methods since reliability of damage parameters significantly depended on the calibration method – trial and error method, neural network method and so on combined with notched bar tests or small punch (SP) tests – and analyzer's experiences. SP test data of typical nuclear materials such as a low alloy steel (Y5) and a high Cr steel (G91) are used to determine damage parameters and, then, resulting values are applied to predict corresponding fracture toughnesses. Load-displacement curves and fracture resistance curves are compared with those obtained from a conventional estimation method as well as standard fracture tests, which show effectiveness of the proposed method.

Modeling of thermal hydraulics aspects of top water reflood. Experiment PARAMETER-SF3 using SOCRAT/V2 code (3-1733)

Arcadii E. Kisselev¹, Valerii F. Strizhov¹, Alexander D. Vasiliev¹,
Vladimir I. Nalivaev², Nikolai Ya. Parshin²

¹Dept. of Severe Accidents, Nuclear Safety Institute (IBRAE), Moscow, Russia
e-mail: vasil@ibrae.ac.ru

²NPO "LUTCH", Podolsk, Moscow region, Russia
e-mail: dvp@luch.podolsk.ru

The PARAMETER-SF3 test conditions simulated a severe LOCA (Loss of Coolant Accident) nuclear power plant sequence in which the overheated up to 1700÷2300K core would be reflooded from the top and the bottom in occasion of ECCS (Emergency Core Cooling System) recovery. The test was successfully conducted at the NPO "LUTCH", Podolsk, Russia, in September 2008 and was the third of four experiments of series PARAMETER-SF.

PARAMETER facility of NPO "LUTCH", Podolsk, is designed for studies of the VVER fuel assemblies behavior under conditions simulating design basis, beyond design basis and severe accidents.

The test bundle was made up of 19 fuel rod simulators with a length of approximately 3.12 m (heated rod simulators) and 2.92 m (unheated rod simulator). Heating was carried out electrically using 4-mm-diameter tantalum heating elements installed in the centre of the rods and surrounded by annular UO₂ pellets. The rod cladding was identical to that used in VVERs: Zr1%Nb, 9.13 mm outside diameter, 0.7 mm wall thickness.

After the maximum cladding temperature of about 1800 K was reached in the bundle during PARAMETER-SF3 test, the top flooding was initiated.

The thermal hydraulic and SFD (Severe Fuel Damage) best estimate numerical complex SOCRAT/V2 was used for the calculation of PARAMETER-SF3 experiment.

Thermal hydraulics in PARAMETER-SF3 experiment played very important role and its adequate modeling is important for the thermal analysis. The results obtained by the complex SOCRAT/V2 were compared with experimental data concerning different aspects of thermal hydraulics behavior including the CCFL (counter-current flooding limitation) phenomenon during the reflood. The temperature experimental data were found to be in a good agreement with calculated results. It is indicative of the adequacy of modeling the complicated thermo-hydraulic behavior in the PARAMETER-SF3 test.

Simulating dynamic fracture in oxide fuel pellets using cohesive zone models (3-1775)

R. L. Williamson, D. A. Knoll
Idaho National Laboratory
P.O. Box 1625, Idaho Falls, ID 83415-3855, USA
e-mail: Richard.Williamson@inl.gov

Introduction and objectives

It is well known that oxide fuels crack during the first rise to power, with continued fracture occurring during steady operation and especially during power ramps or accidental transients. Fractures have a very strong influence on the stress state in the fuel which, in turn, drives critical phenomena such as fission gas release, fuel creep, and eventual fuel/clad mechanical interaction. These phenomena carry important implications not only for subsequent fuel performance, but also for safety.

A variety of approaches are used to account for pellet fracture in fuel performance codes. The most common and simplest technique employs empirical relocation models, which simply force radial displacement of the fuel as a function of power and burnup. A few codes employ a more mechanistic approach, using smeared-cracking models to locally modify the material behavior and approximate the effects of fracture [1]. These models are reasonably straightforward to implement, since they do not involve the complexities associated with tracking of discrete cracks; only the local constitutive behavior in terms of stresses and strains is modified in any region which undergoes cracking. Recently, interest has been expressed in discrete fracture methods, such as the cohesive zone approach [2]. Such models are attractive from a mechanistic and physical standpoint, since they reflect the localized nature of cracking. The precise locations where fractures initiate, as well as the crack evolution characteristics, are determined as part of the solution. Cohesive zone models also offer the possibility to simulate important phenomena such as crack closure during power reduction and crack healing (re-sintering) in high temperature regions.

This paper explores the use of finite element cohesive zone concepts to predict dynamic crack behavior in oxide fuel pellets during power-up, steady-operation, and power-ramping. The aim of this work is first to provide an assessment of cohesive zone models for application to fuel cracking and explore important numerical issues associated with this fracture approach. A further objective is to

provide basic insight into where and when cracks form, how they interact, and how cracking effects the stress field in a fuel pellet.

Model description

The ABAQUS commercial finite element code, which recently incorporated powerful cohesive zone capability, was used for this study. Fully-coupled thermo-mechanical behavior is employed, including the effects of thermal expansion and fission product swelling. Cohesive surfaces are placed along potential crack paths, as dictated by experimental evidence. Crack initiation is determined by a maximum principal stress criterion, based on measured fracture strengths for UO_2 . Damage evolution is governed by a traction-separation relation, calibrated to data from fracture toughness measurements.

Numerical models are first developed in 2D based on both axisymmetric (to explore transverse cracking) and plane strain (to explore radial and circumferential cracking) assumptions. A 3D model is then developed, permitting simultaneous radial and transverse fractures. Although fuel pellet cracking is clearly three-dimensional, 2D models are of interest since they are simpler to implement, are much less computationally intensive, and have potential application to existing 2D fuel performance codes.

Results

Model results indicate that for typical oxide fuel properties, both radial and transverse cracking occurs during initial heat-up, well before steady-state thermal gradients are established in the pellet. Cracking results in local stress relief and a shift in peak stress locations, leading to the initiation of new cracks. Continued growth of existing cracks, plus the initiation and growth of additional fractures, is observed during steady operation and power ramping. 3D models provide insight into the progressive interactions between radial and transverse cracking.

Cohesive zone models, which exhibit softening behavior and stiffness degradation, often encounter severe numerical convergence difficulties. Viscous regularization of the constitutive equations was needed in ABAQUS to obtain solutions for the low-toughness fuel material. The effects of viscous damping on solution accuracy and efficiency are addressed. Parametric results are also provided showing sensitivity to meshing and iteration convergence tolerance.

Conclusions

Cohesive zone models have been successfully used to study progressive cracking in UO_2 fuel pellets during various stages of reactor operation. Such models are attractive since they provide a mechanistic and physically based description of the fracture process. Radial and transverse fracture occurs during initial heating, with further cracking observed as temperature gradients increase during steady-operation and power-ramping. The stress field is strongly affected by fracture, becoming highly non-uniform after cracking. Results suggest that realistic fuel pellet fracture modeling will likely require a combination of discrete and smeared-crack models. Future models will include the fuel cladding, permitting investigation of the effects of pellet fracture on pellet-clad interaction.

References

1. Michel, B., Sercombe, J., Thouvenin, G., Chatelet, R. 3D Fuel Cracking Modeling in Pellet Cladding Mechanical Interaction. *Eng Frac Mech*, 75, 3581 (2008).
2. Helfer, T., Garcia, P., Ricaud, J.M., Struzik, C., Sidoroff, F., Bernard, L. Modeling the Effect of Oxide Fuel Fracturing on the Mechanical Behavior of Fuel Rods, *Proc. Pellet-Clad Interaction in Water Reactor Fuels*, Aix-en-Provence, France, March 9–11 (2004).

Complex FEM based system of computer codes to model nuclear fuel rod thermo-mechanical behaviour (3-1814)

Mojmír Valach, Martin Dostál*, Jiří Zymák

Nuclear Research Institute, Řež plc, 120 68 Řež-Husinec 130, Czech Republic

e-mail: dostal@nri.cz

*corresponding author

The paper presents long-term effort to establish closed chain of computer codes, which allow computer modeling of the thermo-mechanical fuel rod behaviour from the 1D representation to the 3D detailed problem description. The whole complex uses the same FEM based mathematical approach. The principle of this modular approach is to handle boundary and initial conditions by the similar transfer independent on the complexity of solved problem.

The goal of our modeling work was to develop model (FRA – Fuel Rod Analyser) capable of computing the spatial distribution of temperature and stress-strain in the fuel and cladding especially during power transients. Developed local models (FRA_local) of nuclear fuel rod can be mainly used for modeling the stresses and deformations in the pellet-cladding contact point. The margin to possible failure of cladding, that may appear as a consequence of large power changes, can be predicted by this way. Global model (FRA_global) enables effectively calculate detailed temperature distribution in the whole fuel rod (including end plugs and spring).

The development was performed in the COSMOSM FEM software product of S.R.A.C. California, U.S.A. The FRA_TFM versions are using nonlinear thermal solver (HSTAR), static mechanics solver (STAR) and nonlinear (NSTAR) mechanics COSMOSM solver. All materials, thermophysical properties as well as mechanical properties are prepared in the form of COSMOSM library – functions and material curves with temperature dependence and time (expressing burn-up process).

Recently we have combined the FEMAXI integral code (1-2D axisymmetrical approach) to the full 2D r-z global model of fuel pin ending at 2D (r-z, r- ϕ) and 3D local detailed submodels. The system of codes is connected (coupled) by data transfer. All the submodels are stand-alone. The same is valid for the material data properties.

To illustrate the whole approach the exact chain of the simulation is as follows: RODBURN, FEMAXI-6, FRA-TF(thermo-physical)_global, FRA-TFM(thermo-physical mechanical)_r-z/r- ϕ _local and FRA-TFM_3D_local (one pellet and two pellet contact configuration, one half cracked pellet-clad contact in 3D).

Paper concludes our long term effort in 2D and 3D modeling of nuclear fuel rod thermo-mechanical behavior. 3D fuel rod simulator was installed successfully and tested by our industrial sponsor.

References

- Belac, J., Valach, M., Zymák, J. 2005. Influence of azimuth and radial neutron and thermal sources anisotropy on contact problem simulation in real fuel pellet-cladding configuration using FEM. SMiRT-18, Beijing, China, August 7–12, 2005.
- Belytschko, T., Liu, W.K., Moran, B. 2000. Nonlinear Finite Elements for Continua and Structures. J. Wiley & Sons Ltd.
- COSMOSM 2.8 for Windows – online manuals, SRAC 2003.
- Dostál, M., Valach, M., Zymák, J., Svoboda, R. 2006. 3D FEM Based Fuel Rod Simulator FRA-TF. TopFuel 2006: International Meeting on LWR Fuel Performance, Salamanca, Spain, October 22–26, 2006.
- Hughes, T.J.R. 1987. The Finite Element Method: Linear Static and Dynamic Analysis. Prentice Hall, Inc., Englewood Cliffs, New Jersey.
- Suzuki, M., Saitou, H. 2005. Light Water Reactor Fuel Analysis Code FEMAXI-6 (ver. 1). Japan Atomic Energy Agency – Data/Code 2005-003, Japan.
- Uchida, M., Saito, H. 1993. RODBURN: A code for calculating power distribution in fuel rods. Japan Atomic Research Institute, JAERI-M, 93-108, Japan.
- Valach, M., Zymák, J. 2004. 2D Pellet-Cladding Modelling using FEM at NRI Rez plc. International seminar on pellet-clad interactions with water reactor fuels, Aix-en-Provence, France, 9–11 March 2004.
- Valach, M., Zymák, J., Dostál, M. 2005. 2D Pellet-Cladding Modelling using FEM at NRI Rez plc. – High Burnup Fuel Simulation. 2–3 March 2005, Fuel Safety Research Meeting 2005, Tokio, Japan.
- Valach, M., Zymák, J., Dostál, M., Hejna, J., Svoboda, R. 2005. First attempts to simulate contact problem using FEM based system COSMOS/M for analyses of three pellets in non-symmetrical oxidized cladding in 2D and 3D configuration. 2005 Water Reactor Fuel Performance Meeting, Kjoto, Japan.

CFD based numerical modules for safety analysis at NPPs: validation and verification (3-1828)

Chudanov V.V.^a, Anna Aksenova, Valerii Pervichko
Nuclear Safety Institute (IBRAE), Russian Academy of Sciences
52, B. Tulsкая, Moscow, 115191, Russia
e-mail: ^achud@ibrae.ac.ru

Recent IAEA activities in support of safety assessment capabilities are directed at increasing of the role of CFD methods in safety assessments of NPPs [1]. Use of computer codes of the best estimate for the accident analysis does not justify itself. These codes are typically one dimensional approximation of phenomena and plant systems. These methods are not adequate for some applications, particularly where modeling local flow and heat transfer phenomena is important to safety. Therefore there is interest in the application of 3D CFD codes for safety analysis as a supplement to or in combination with system codes. The CFD codes are capable of calculating local parameters. Due to this capability they provide insights into many problems, contribute to a deep understanding of fluid flow physics, and thus may lead to better designs at reduced cost and/or to more precisely quantified safety margins. Verification and validation is an important part of qualifying analysis software for nuclear safety and engineering applications.

During some years in IBRAE a set of 3D unified numerical modules for safety analysis of the operated Nuclear Power Plants (NPPs) is developing [2]. These modules are based on the developed algorithms with small scheme diffusion, for which the discrete approximations are constructed with use of finite-volume methods and fully staggered grids. They were successfully used for solving of thermohydraulics problem at modeling of corium retaining in a reactor vessel, modeling of molten core concrete interaction and spreading of the molten corium together with filling of core catcher.

The developed modules were validated [2] on a series of the well known numerical tests in a wide range of Rayleigh numbers from a range 10^6 - 10^{16} and Reynolds numbers from a range 10^3 - 10^5 . The developed software has been applied to the simulation of the RCW test conducted in the frames of MASCA Project [3] and to the simulation of the SURC-4 MCCI test [4]. As a result of numerical modeling of aforementioned experiments qualitative and quantitative agreement with experimental data was obtained including the diffusion of the components between phases and relocation of more dense phase due to Rayleigh-Taylor instability. New area of software application appeared with the development of core catcher a device for melt retention and coolability. The core

catcher is used for the ex-vessel melt retention in the concrete cavity. The appropriate design-basis measures are foreseen in order to prevent lower head failure and melt ejection at high pressures. In case of a severe accident, the effective heat removal from molten corium is performed by passive safety means cooling water stored in the containment. The software has been applied to the simulation of the phenomena in the core catcher designed for VVER-1000 reactor [5].

In this paper the examples of use of the developed software for modeling of a fuel assembly, namely, for research of a hydraulic resistance factor of a spacer are demonstrated. The calculations are carried out on a sequence of condensed grids with an amount of nodes from a range 10^7 – 10^8 , for which the convergence was obtained. Moreover, the attention of this paper is focused on validation and verification of software with usage of such tests as: full turbulent flow of water in a round pipe, backward-facing step (BFS) flow.

References

1. Modro, S., El-Shanawany, M., Lee, S. Recent IAEA activities in support of safety assessment capabilities. Proc. of ICONE-14 International Conference on Nuclear Engineering, Miami, Florida, USA. CD-disk. Paper ICONE-89828. 2006.
2. Chudanov, V.V., Aksenova, A.E., Pervichko, V.A. Methods of direct numerical simulation of turbulence with use DNS and LES approaches in thermalhydraulics of fuel assembly. *Izvestiya Rossiiskoi Akademii Nauk. Seriya Energetica*, №6, 2007.
3. Chudanov, V.V., Aksenova, A.E., Pervichko, V.A., Strizhov, V.F. The analysis of the large scale RCW test. Proceedings of the MASCA Seminar 2004, Aix-En-Provence, pp. 217–240.
4. Bolshov, L.A., Chudanov, V.V. CFD approach to modeling of Core-Concrete interaction. Transactions, SMiRT-19, Toronto, August 2007. CD-ROM. Paper 2545. 2007.
5. Asmolov, V.G., Bechta, S.V., Berkovich, V.M. et al. Crucible-type core catcher for VVER-1000 reactor. Proceedings of the International congress for Advances in nuclear power, ICAPP 05, Seoul, KOREA, May 15–19, 2005. Paper 5238.

The calculation error analysis on carrying force of active magnetic bearings (3-1845)

Sun Zhuo, Shi Zhengang

Institute of Nuclear Energy Technology, Tsinghua University, Beijing, China
e-mail: sunzhuo@tsinghua.edu.cn

Introduction

The carrying force is a very important parameter of active magnetic bearing (AMB). There are many methods to calculation carrying force. But it is difficult to calculate accurately due to the nonlinearity of the electromagnet components. In the 10 MW high temperature gas-cooled reactor of Tsinghua University (HTR-10), the spare main helium circulator [1] will adopt active magnetic bearings. The carrying force of AMBs in spare main helium circulator was calculated and then was measured in experiments. The calculation errors are analyzed based on theory calculation and proved by the experimental results.

Structure of helium circulator

The electrical motor of helium circulator is vertical type, 380 V/160 kW, and its rated speed is 5000rpm. One axial bearing and two radial bearing control five degrees of freedom. The position sensors are inductance differential displacement sensors.

The simplified structure of axial bearing is shown in Fig. 1. All the analysis results are for axial bearing in this paper.

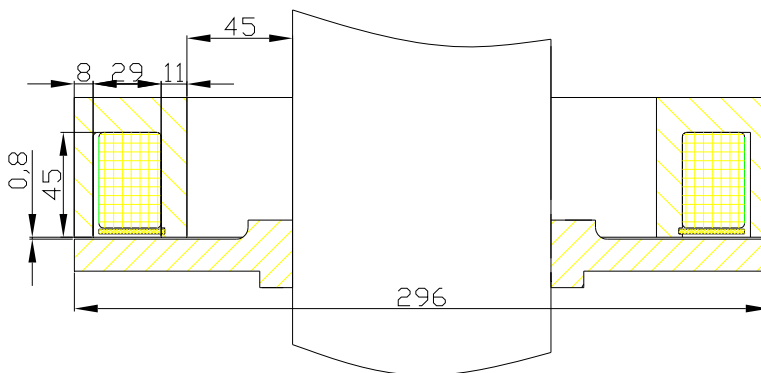


Figure1. The simplified structure of axial bearing in HTR-10 helium circulator.

There are two methods to calculate the magnetic force, method of virtual work and Maxwell stress tensor. Assuming that the leakage magnetic flux is zero and the magnetic reluctance of magnetic material is also zero, two calculation methods are identical, that is:

$$F = \frac{(Ni)^2 \mu_0 S}{4\delta^2} \quad (1)$$

where

- F : magnetic force
- N : number of turns
- i : current in coil
- μ_0 : space permeability
- S : area of magnetic pole
- δ : gas length.

Besides leakage magnetic flux and magnetic reluctance of magnetic material, the area of magnetic pole may cause calculation errors, too. In fact the area of magnetic pole is not equal to the area of magnetic circuit. The area of magnetic circuit should be used in equ.1 instead of area of magnetic pole. Most of the researchers neglect this fact.

Experimental results

The carrying force of axial bearing was calculated by equ.1 and finite-element method. And then the real axial force was measured by dynamometer. The calculation and experimental results are shown in Fig. 2.

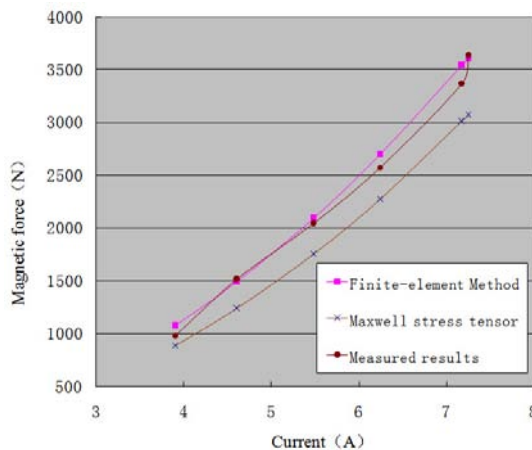


Figure 2. Carrying force obtained by different ways.

The carrying force calculated by finite-element method is near to the real axial force, but it is larger than the results calculated by Maxwell stress tensor (Eq. 1). The reason is that the area of magnetic circuit is larger than the area of magnetic circuit.

Conclusions

Leakage magnetic flux, magnetic reluctance of magnetic material and the area of magnetic pole cause calculation errors. Most of the researchers neglect the difference between the area of magnetic pole and the area of magnetic circuit. Experimental results and simulation results proved the analysis.

References

1. Sun Zhuo, Shi Zhengang, Xu Yang, Zhao Lei. Study of Active Magnetic bearing for Helium Circulator in HTR-10. 19th International Conference on Structural Mechanics in Reactor Technology (SMiRT 19), Aug. 12–17, 2007, Toronto, Canada.

Flow coefficient determination through CFD for nuclear reactor safety (3-1868)

Pavan K. Sharma⁺, B. Gera, Anu Dutta, R.K. Singh, A.K. Ghosh, H.S. Kushwaha
Reactor Safety Division, Health Safety and Environment Group
Bhabha Atomic Research Centre, Trombay, Mumbai, India- 400085
⁺ e-mail: pa1.sharma@gmail.com

Keywords: loss coefficient, CFD, pressure drop, PHOENICS

The availability of sophisticated Computational Fluid Dynamics (CFD) codes on cheaper and powerful computers gives the opportunity to study the detail of the complex phenomena in nuclear safety. In the nuclear industry the use of CFD codes has been devoted to the study of the buoyant Containment thermal hydraulics occurring during the hypothetical accident simulations. The distribution of hydrogen in the containment in the case of a severe accident and fire simulation for nuclear application etc are some of the examples. An interesting applied aspect through CFD is the evaluation of pressure drop coefficients and flow coefficients piping or multiple compartment containment configurations in simple and complex configurations, changes of flow area and abrupt modifications of the geometry.

The present work is focused in the analysis of the flow coefficients across the junction in different configuration by means of CFD code. The broader objective of the work is to show which are the parameters affecting the pressure drop in this simple/complex configuration geometry along with various flow conditions. However the present paper focuses on the flow coefficient determination for a) Flow in a bend b) Flow through sudden contraction c) Flow through sudden expansion d) Flow through T junction, e) Flow coefficient in a oscillating ceiling junction f) Flow coefficient in a large vertical opening in bidirectional flow g) Flow coefficient for a valve. Applicable forward (K_{fwd}) and reverse (K_{rev}) flow energy loss coefficient (used as input in system thermal hydraulic codes such as RELAP5, CONTRAN) are later on calculated from the CFD result by bidirectional flow. A first attempt to investigate which are the main parameters affecting the concentrate flow coefficient by mean of a CFD code in few configuration/situation has been presented and could be considered as a starting point for a more systematic assessment and an additional comparison with experimental data in future.

An energetic approach of the fluid-structure interaction governing the dynamic behaviour of tubes immersed in a fluid (3-1879)

Marion Duclercq¹, Daniel Broc²

Laboratoire d'Etudes de Mécanique Sismique

CEA Saclay, 91191 Gif-sur-Yvette, France

e-mails: ¹marion.duclercq@cea.fr, ²daniel.broc@cea.fr

This paper deals with a vibratory problem of fluid-structure interaction. It is a part of the development of a model of the seismic behaviour of nuclear reactor cores, such as pressurized water reactor cores (PWR) or fast reactor cores. The final objective is to build a homogenized model of the dynamic behaviour of tubes bundles immersed in a fluid and submitted to a seismic excitation. It can be observed that tubes motions are strongly influenced by the presence of the fluid. The main modifications are a decrease of eigen-frequencies and an increase of damping and dissipation. In order to describe accurately those physical modifications, the final homogenized model must be based on the general Navier-Stokes equations for the fluid.

That is why this paper focuses on the numerical resolution of the Navier-Stokes equations as a contribution to the efforts to understand the physical phenomena governing the fluid-structure interaction. The part of the problem regarding the homogenisation is not presented here, but can be found in [1]. The key point of the present paper is the development of an energetic approach based on the mean power balance.

As a first step, the paper considers the two-dimensional case of a rigid, smooth and circular cylinder undergoing transverse sinusoidal oscillations and immersed in a viscous fluid otherwise at rest. Our work is focused on the in-line force acting on the cylinder in unsteady laminar flow. The aim is to understand the variations of the force with time according to the configuration of the physical system. That system can be characterized by two non-dimensional numbers: the Reynolds number (R_e) compares the importance of the fluid viscosity to its inertia, and the Keulegan-Carpenter number (K_c) measures the amplitude of the cylinder displacement compared to its diameter.

First the incompressible Navier-Stokes equations are solved numerically by means of a finite elements method. The flow structure is analyzed by determining the evolution with time and throughout the computational domain of flow quantities, such as pressure field, vorticity field or stream lines. We also calculate the values versus time of the different terms occurring in the mean

force balance and power balance. Those two types of results (the flow structure and the power balance) are compared and interpreted with energetic considerations for several pairs (K_c , R_e) of “extreme” values. Thus it appears three characteristic configurations: the inertial Euler case ($K_c \ll 1$ and inviscid fluid [4]), the Stokes case ($K_c \ll 1$ and viscous fluid [2, 6, 7]) and the drag case ($K_c \gg 1$ and viscous fluid [5]). For these three reference configurations the physical mechanisms operating in the system are identified. But in intermediate cases, particularly when $K_c > 1$, every mechanisms interact. Consequently the evolution of the force acting on the cylinder versus time is more complex and its interpretation becomes less straightforward. That is why a quantitative energetic analysis is carried out. We define coefficients measuring the dissipative energy and the kinetic energy present in the flow. Then we compare the values of those coefficients for different cases throughout the map (K_c , R_e).

References

1. Broc, D., Duclercq, M. Toward a global model for FSI in tube bundles, Pressure Vessel and Piping paper PVP2008-61570.
2. Cobbin, A.M., Stansby, P.K. The hydrodynamic damping force on a cylinder in oscillatory, very-high-Reynolds-number flows. Applied Ocean Research, 17, pp. 291–300, 1995.
3. Duclercq, M., Broc, D. Physical and numerical study of the interaction between a fluid and an oscillating cylinder, Pressure Vessel and Piping paper PVP2008-61036.
4. Fritz, R.J. The Effect of Liquids on the Dynamic Motion of Immersed Solids. Journal of Engineering for Industry, 94, pp. 167–173, 1972.
5. Morison, J.R, O'Brien, M.P., Johnson, J.W., Schaaf, S.A. The forces exerted by surface waves on piles. Petroleum Transactions, AIME, 189, pp. 149–157, 1950.
6. Sarpkaya, T. Hydrodynamic damping and quasi-coherent structures at large Stokes numbers. Journal of Fluids and Structures, 15, pp. 909–928, 2001.
7. Sarpkaya, T. On the force decomposition of Lighthill and Morison. Journal of Fluids and Structures, 15, pp. 227–233, 2001.

Pretest analysis of CSF model for simulated loss of coolant accident conditions (3-1880)

I. Thangamani, Vishnu Verma, R.K. Singh, A.K. Ghosh
Reactor Safety Division, Bhabha Atomic Research Centre, Mumbai, India
e-mail: tmi@barc.gov.in

An experimental facility for the purpose of research and development in the area of nuclear reactor containment thermal hydraulics has been set up at BARC. The experimental set up, called Containment Studies Facility (CSF) consists of a containment model and a Primary Heat Transport Model (PHTM) system which includes a pressure vessel and associated piping system for blowdown experiments. The containment model is approximately 1:250 volumetrically scaled down model of a 220 MWe Indian Pressurized Heavy Water Reactor (IPHWR) containment system. A suite of instrumentation system has been included for monitoring the containment system thermal hydraulic parameters for the test blowdown experiments.

This facility is primarily designed for safety experiments related to the existing 220 MWe/540 MWe IPHWR. However, additional studies with regard to the features of new reactor such as spray system in a typical 700 MWe IPHWR can also be studied.

Like the containment system of IPHWR, the containment model is also divided into V1 volume (dry well) and V2 volume (wet well). The V1 volume is further divided into many compartments to simulate the various rooms such as pump room, fuelling machine vault etc. present in actual reactor containment. The V2 volume is connected to V1 volume through vent pipes and suppression pool.

In pressure vessel, DM water is maintained at prescribed pressure and temperature and then it is allowed to blowdown into V1 volume by rupturing the rupture disk.

As part of CSF project thermal hydraulic analysis, a pretest analysis was carried out using in-house containment thermal hydraulic code CONTRAN for simulating loss-of-coolant accident (LOCA) conditions. In pretest analysis, the obtained blow down mass and energy discharge data, using RELAP code, for different blow down conditions were used as inputs to CONTRAN code for simulating LOCA or main steam line break (MSLB) conditions in containment model.

The pressure and temperature transients in containment model were obtained for the blow down conditions ranging from 10 bar to 100 bar. The effect of condensation models such as Tagami, Uchida and Diffusion model on peak

pressure and temperature were also studied. A number of parametric studies were conducted to assess the influence of a large number of thermodynamic and geometrical parameters which are known to affect the transients and alter the peak pressure and temperature values. The thermodynamic parameters are containment initial temperature, initial relative humidity etc. and the geometrical parameters are V1/V2 ratio, vent pipe area, submergence depth of vent pipe, suppression pool, etc. The details of the studies conducted are presented in this paper.

Numerical studies on post accident hydrogen management using fan (3-1894)

Pavan K. Sharma, R.K. Singh, A.K. Ghosh, H.S. Kushwaha*
Reactor Safety Division
*Health Safety & Environment Group
Bhabha Atomic Research Centre, Mumbai, India
e-mail: pa1.sharma@gmail.com

Hydrogen transport behaviour in the containment of NPPs is an extremely complex phenomenon and must be properly understood for the assessment of the overall plant safety under accident conditions. A study has been carried out to predict the hydrogen concentration profile in the multi-floor multi-compartment geometry of Kaiga Indian Pressurised Heavy Water Reactor (IPHWR). A CFD computer code FDS has been used for conducting these studies. The results indicate a strong possibility of stratification of the lighter gas within as well as across the compartments during both the injection and post injection phases. After the momentum effects due to the convective currents die down, stratification was noted to be more or less stabilized. Molecular diffusion was seen to have insignificant diffusion. It was proposed to use fans to mix the hydrogen in Fueling Machine (FM) Vault atmosphere with the pump room as one of the arrangement apart from the proposed passive recombiners. To evaluate the efficacy of the fan for limiting the hydrogen concentration values to regulatory limits CFD studies have been carried out. The rate of hydrogen generation in a design basis accident and fan discharge into the FM vault is considered as a boundary condition. The analysis was performed with and without the proposed fan system. The hydrogen concentration is considerably reduced in this calculation in the case in which fan system is credited.

Numerical studies on atmospheric dispersion and associated flow behaviour for flat, raised bluff body and deep depression (3-1896)

Pavan K. Sharma, R.K. Singh, A.K. Ghosh, H.S. Kushwaha*

Reactor Safety Division

*Health Safety & Environment Group

Bhabha Atomic Research Centre, Mumbai, India

e-mail: pa1.sharma@gmail.com

The transient transport and dispersion of airborne pollutants in the atmosphere and understanding of such pollutant transport will facilitate the assessment of the risk to occupants from such release. Research on air flows and pollutant transport in urban spaces using Computational Fluid Dynamics (CFD) is an emerging field. The atmospheric dispersion and associated flow behaviour a) in a simple terrain; b) in presence of features i.e. a bluff body; c) a deep depression (cavity) has been carried out. The parametric studies have also been carried out for the cavity simulation by changing the incoming horizontal wind and its effect on generation of vertical component of velocity inside the cavity. The dense scalar (SF₆) dispersion simulation has also been carried out with variation in source height and distance from the cavity. Depending on the applied velocity which is a horizontal velocity, a velocity component develops inside the cavity along with the recirculation patterns. The upward velocity component developed inside due to applied velocity is generally below 30% in magnitude of the velocity at the edge of the cavity. Some other important observations noted were a) Obstructions play a dominant role in atmospheric dispersion of pollutant; b) There is a time lag in pollutant concentration built-up with increased number of obstructions on the path; c) Presence of complex terrain results in the fall in the pollutant concentration due to turbulent mixing.

Numerical studies of flow structures for square building in cross wind for aspect ratio and representative blockage ration variation (3-1897)

Pavan K. Sharma, B. Gera, R.K. Singh, A.K. Ghosh, H.S. Kushwaha*

Reactor Safety Division

*Health Safety & Environment Group

Bhabha Atomic Research Centre, Mumbai, India

e-mail: pa1.sharma@gmail.com

Flow past a square building block in a free stream is numerically investigated by three dimensional Large Eddy Computation Fluid Dynamic (CFD) Simulations. The main objectives of this study are to identify and capture the features of flows past a square building in an infinite domain with the use of CFD. The CFD results obtained are in good agreement with earlier studies qualitatively. The well-known Korman vortex shedding is observed. These studies being a part of street canyon flows for atmospheric dispersion and the major objective is to assess the effect of additional scalar mixing because of the blockage in free stream. A square block shape building has been studied in terms of representative blockage ratio (RBR: the ratio of cross-stream length to height of the domain) and aspect ratio (ratio of stream wise length to cross stream length) as a function of Reynolds No. The Strouhal number was the quantified output. The mean wind flow was varied (variation of Reynold No. for a given aspect ratio or RBR) between 0.5 m/s to 10 m/s and the vortex shedding was found to get affected. The velocity components in the wake regions were processed by FFT analysis to find out the frequency and then the Strouhal number. The wind has been modeled as a power law profile. It was shown different patterns of vortex shedding alternately occur for the different value of aspect ratio and RBR. The following conclusions were drawn. At very low Reynolds Number there is no wake formation, but as the Reynolds number increases the formation of wake can be observed at critical Reynolds number (300). Vortex shedding was found to be independent of RBR. Increasing the aspect ratio has a stronger influence on the shedding frequency. At low Reynolds number there was absence of formation of a low pressure region and there is absence of reattachment of vortex circulation. Increasing the aspect ratio has a profound effect on the shedding frequency. The upstream distance was directly proportional to the shedding frequency. The paper also present a brief review of the vortex shedding due to flow past a square cylinder along with the details and salient results of the parametric studies carried out.

Fluid-structure interaction calculations using a linear perturbation method (3-1898)

Antti Timperi

VTT Technical Research Centre of Finland, P.O. Box 1000, FI-02044 VTT, Finland
e-mail: antti.timperi@vtt.fi

Introduction

An explicit Fluid-Structure Interaction (FSI) coupling scheme is numerically unstable in some applications. In these cases, stable calculations may be achieved with an implicit scheme where boundary data is exchanged between the fluid and structure several times during iteration inside a time step (Vierendeels et al., 2005; Sigrist and Abouri, 2006). With some commercial codes, however, only the explicit scheme is available.

If the structural displacements are relatively small, it may be sufficient to use only one-way mapping of fluid pressure to the structure. However, often the presence of the fluid still affects frequency of the structural motion considerably through the added mass effect.

During a hypothetical Loss-Of-Coolant Accident (LOCA) in a boiling water reactor, a large amount of steam and non-condensable gas would be injected into the pool water which causes pressure loads on the pool walls. Two-way coupled FSI calculations of a scaled-down condensation pool test facility have been numerically unstable with explicit coupling (Kauppinen et al., 2006).

Aim of this work is to present and validate FSI calculations by using a linear perturbation method (Huber et al. 1979; Sonin, 1980) and commercial Computational Fluid Dynamics (CFD) and structural analysis codes. Star-CD is used for CFD calculations and ABAQUS for structural analysis. The external MpCCI code is used for coupling the CFD and structural analysis codes.

Results

Basis of the method is first examined mathematically with an order of magnitude analysis similar to that in Sonin (1980). The flow field is separated into two components: flow field that would occur if the walls were rigid and flow field due to wall motion. It is shown that as certain conditions are met, these two flow fields can be solved separately and superposed afterwards in order to account for FSI.

Second, the method is validated against numerical data by using a simplified model of a condensation pool. Two-way coupled FSI calculations are carried out

with a sufficiently small time step in order to prevent numerical instability. Wall pressure and displacement obtained with the perturbation method and with two-way coupling are in good agreement whereas in one-way coupled calculations absence of the added mass effect is clearly seen.

Third, validation is carried out against scaled-down condensation pool experiments made at Lappeenranta University of Technology (Laine and Puustinen, 2008). In the experiments, air was injected into the pool through a submerged pipe and the resulting wall pressure and displacement were monitored. A reasonable agreement in wall pressure and displacement is found between the experiment and calculation with the perturbation method. Calculation with one-way coupling shows qualitatively incorrect results for the wall pressure. In addition, the structural displacements are smaller compared to the experiment and to those obtained with the perturbation method.

Conclusions

The method has certain restrictions, the most important being that the structural motion has to be sufficiently small. These restrictions do not seem to be too limiting for modeling the considered test facility or a real condensation pool. The method may have significance also in other applications because only small structural motion is often encountered.

References

- Huber, P.W., Kalumuck, K.M., Sonin, A.A. 1979. Fluid-structure interactions in containment systems: small-scale experiments and their analysis via a perturbation method. 1st International Seminar on Fluid-Structure Interaction in LWR Systems, held in conjunction with the 5th International Conference on Structural Mechanics in Reactor Technology, Berlin, Germany, August 13–17, 1979.
- Kauppinen, P., Sarkimo, M., Timperi, A., Kinnunen, P. 2006. Integrity and life time of reactor circuits. In: SAFIR The Finnish Research Programme on Nuclear Power Plant Safety 2003–2006, Final Report. Eds. by Rätty, H., Puska, E.K. VTT Research Notes 2363, Espoo. Pp. 81–87.
- Laine, J., Puustinen, M. 2008. Steam line rupture experiments with the PPOOLEX test facility. Research report CONDEX 2/2007, Nuclear Safety Research Unit, Lappeenranta University of Technology. 23 p. + app. 7 p.
- Sigrist, J.F., Abouri, D. 2006. Numerical simulation of a non-linear coupled fluid-structure problem with implicit and explicit coupling procedures. ASME 2006 Pressure Vessels and Piping Conference, PVP2006-ICPVT-11-93107.
- Sonin, A.A. 1980. Rationale for a linear perturbation method for the flow field induced by fluid-structure interactions. *Journal of Applied Mechanics*, Vol. 47, pp. 725–728.
- Vierendeels, J., Dumont, K., Dick, E., Verdonck, P. 2005. Analysis and stabilization of fluid-structure interaction algorithm for rigid-body motion. *AIAA Journal*, Vol. 43:12, pp. 2549–2557.

3D CFD analysis of passive auto catalytic recombiner for H₂ mitigation (3-1902)

B. Gera, Pavan K. Sharma⁺, R.K. Singh, A.K. Ghosh, H.S. Kushwaha*
Reactor Safety Division, *Health Safety and Environment Group
Bhabha Atomic Research Centre
Trombay, Mumbai, India- 400085
⁺e-mail: pa1.sharma@gmail.com

Keywords: recombiner, CFD, hydrogen, containmnet

Resolving hydrogen related safety issues, pertaining to nuclear reactor safety have been an important area of research world over for the past decade or so. The studies on hydrogen transport behavior and development of hydrogen mitigation systems are still being pursued actively in various research labs, including BARC, in India. The passive autocatalytic recombiners (PARs) are one of such hydrogen mitigating device consisting of catalyst surfaces arranged in an open-ended enclosure. In the presence of hydrogen with available oxygen, a catalytic reaction occurs spontaneously at the catalyst surfaces and the heat of reaction produces natural convection flow through the enclosure. The present study aims for some of the engineering considerations governing the design of such a device and some of the salient features of the simplified CFD model being developed at BARC. 3D CFD code has been developed to study the mechanism of catalytic recombination and has been used to simulate one reported recombiner assembly. Conjugate heat transfer modeling has been done between the solid plate and surrounding gas mixture. Reaction has been modeled as one step reaction. The source term for energy and water vapour and corresponding sink term for hydrogen and air mass has been applied in the very first fluid cell near the solid plate. The paper explained the salient features of CFD code and results obtained. The model will help to arrive at the optimum design of the recombiner. Results of the present model calculations are presented in the paper.

A computational fluid dynamics study of a buoyant plume at a slope cross wind condition (3-1906)

Pavan K. Sharma, B. Gera, R.K. Singh, A.K. Ghosh, H.S. Kushwaha*

Reactor Safety Division

*Health Safety & Environment Group

Bhabha Atomic Research Centre

e-mail: pal.sharma@gmail.com

A computational study has been carried out for predicting the behaviour of a buoyant plume rising above a fire source at a sloping plane in presence of crosswind using a field model based CFD code. Time dependent velocity and temperature fields in the form of animations are predicted along with the resulting changes in the plume trajectory and its width for different speeds of cross wind. The analysis has been carried out with uniform velocity profiles. The predicted swaying angles of the plume by the current analysis are generally in good agreement with reported experimental data. The studies have demonstrated the utility of field model based tools to model this particular separate effect phenomenon and validate the experimental data. The use of modified plume behaviour on sloping plane in presence of crosswind have several applications in situations such as ventilated room fires, wildland fires, smoke or ash disposal etc. The present study uses the advanced Large Eddy Simulation (LES) turbulence model. The paper presents brief description of the code, details of the computational model along with the discussions on the results obtained under these studies.

An evaluation of methods for the time-domain simulation of turbulence excitations for tube bundles subjected to non-uniform flows (3-1909)

Jose Antunes¹, Philippe Piteau², Xavier Delaune², Laurent Borsoi²

¹Instituto Tecnológico Nuclear (ITN) – Applied Dynamics Laboratory (ADL)
Sacavem, Portugal

²Commissariat a l’Energie Atomique (CEA) – DM2S/SEMT/DYN Laboratory
Saclay, France

Introduction

The predictive dynamical analysis of gap-supported tubular bundles subjected to turbulence-induced vibrations is of practical significance, in particular when addressing nuclear power-plant facilities. It is a multi-disciplinary work which resulted in a number of computational tools, mostly based on time-domain numerical simulations of the flow-excited nonlinear systems – see, for instance, Sauv e and Teper (1987), Axisa et al (1988), Fisher et al (1989), Haslinger and Steininger (1995) or Hassan et al (2003). The present paper addresses the problem of achieving adequate modelling of the turbulence excitations when performing such time-domain computations.

Aim of the work

In most published work, the details on time-domain implementations of turbulence excitations are seldom supplied, as if such modelling aspects were obvious or non-important. Actually, providing adequate time-domain force functions – which rightly account for the spectral properties, the space correlation, as well as the local magnitude of the flow velocity field – is a nontrivial task. Indeed, numerical simulations are often performed by exciting the tubes with random forces which account in a very crude manner, or not at all, for the partial space correlation of the flow turbulence. For instance, a common approach is to excite the system through a number of random forces assuming full correlation within each tube span and none beyond – see, for instance, Hassan et al (2003). Such oversimplified approaches may lead to inadequate modelling of the excitation, and hence to unreliable predictive analysis. In the present paper, our developments addressing this issue are presented and discussed.

Results

We recently proposed a simple but consistent method to simulate the continuous space-correlated flow force field, using a finite set of uncorrelated discrete random forces located along the structure – see Antunes et al (2008). These are computed from the turbulence spectrum and the space correlation of the original turbulence field, accounting for the flow velocity profile, based on the theoretical formulation for the linear modal responses of the excited tube. Our approach was validated on a number of test cases, consisting on linearly multi-supported tubes. On the other hand, sample computations suggested that such computationally efficient approach is also effective when dealing with the nonlinear vibro-impact responses of gap-supported tubes subjected to non-uniform flows, as intended. However, a thorough analysis of this essential aspect was needed and is offered in the present paper. Here, illustrative nonlinear tube response computations using our simple excitation method are compared with those obtained by modelling the turbulence through a partially correlated random field, computed using the general techniques developed by Shinozuka (1971) and co-workers.

Summary

The results presented stress the effectiveness of both techniques, as well as their merits and drawbacks in terms of computational efficiency and versatility.

References

- Antunes, J., Delaune, X., Piteau, P., Borsoi, L. 2008. A Simple Consistent Method for the Time-Domain Simulation of Turbulence Excitations Applied to Tube/Support Dynamical Analysis Under Non-Uniform Flows. 9th International Conference On Flow-Induced Vibrations (FIV2008), 30 June – 3 July 2008, Prague.
- Axisa, F., Antunes, J., Villard, B. 1988. Overview of numerical methods for predicting flow-induced vibrations. *ASME Journal of Pressure Vessel Technology*, 110: 6–14.
- Fisher, N., Olesen, M., Rogers, R., Ko, P. 1989. Simulation of tube-to-support dynamic interaction in heat exchange equipment. *ASME Journal of Pressure Vessel Technology*, 111: 378–384.
- Haslinger, K., Steininger, D. 1995. Vibration response of a U-tube bundle with anti-vibration bar supports due to turbulence and fluidelastic excitations. *Journal of Fluids and Structures*, 9: 805–834.
- Hassan, M., Weaver, D., Dokainish, M. 2003. The effects of support geometry on the turbulence response of loosely supported heat exchanger tubes. *Journal of Fluids and Structures*, 18: 529–554.
- Sauvé, R., Teper, W. 1987. Impact simulation of process equipment tubes and support plates – a numerical algorithm. *ASME Journal of Pressure Vessel Technology*, 109: 70–79.
- Shinozuka, M. 1971. Simulation of multivariate and multidimensional random processes, *Journal of the Acoustical Society of America*, 49: 357–367.

Condensation pool experiments at LUT supporting CFD and structural analysis tool development (3-1913)

Markku Puustinen¹, Antti Räsänen¹, Jani Laine¹, Heikki Purhonen¹,
Timo Pättikangas², Antti Timperi²

¹Lappeenranta University of Technology

P.O. Box 20, FI-53851 Lappeenranta, Finland

e-mails: markku.puustinen@lut.fi, antti.rasanen@lut.fi, jani.laine@lut.fi

²VTT Technical Research Centre of Finland

P.O.Box 1000, FI-02044 VTT, Finland

e-mail: antti.timperi@vtt.fi

Introduction

Nuclear power plant safety has been experimentally investigated at Lappeenranta University of Technology (LUT). Thermal hydraulic test facilities have been constructed and operated over 30 years. In addition to the thermal hydraulic studies it has been beneficial to add instrumentation for structural measurements into the tests facilities as well. This way running tests aiming to solve thermal hydraulic problems can also serve other purposes such as producing data for developing tools for structural analysis.

At VTT, Computational Fluid Dynamics (CFD) modeling of the pressure loads has been performed. In addition, coupling of commercial CFD and structural analysis codes has been done for analyzing Fluid-Structure Interaction (FSI), where the deformations of the structure are accounted for in the flow solution [1]. One-way coupled calculations, in which only the pressure is transferred to the structure, were first carried out with an in-house code. Later the commercial middleware MpCCI developed at the Fraunhofer Institute has been used for analyzing also two-way FSI.

The main goal of the work at LUT has been to gather data of structural loads from thermal hydraulic tests. Coupled CFD and structural analysis codes can then be validated against measured structural loads related to thermal hydraulic phenomena such as rapid condensation, gas bubble formation and detachment.

Experiments and related instrumentation

Using thermal hydraulic experiments for development of coupling of the codes requires additional instrumentation. Sophisticated instruments are available in

the market, but basic instruments like strain gauges and movement transducers will also serve this purpose.

In POOLEX (open pool) and PPOOLEX (closed pool) facilities several experiments of BWR condensation pool behavior have been performed [1, 2]. The test arrangements in the facilities do not represent prototypical situation in a real BWR with respect to materials because steel structures are used in the experimental facilities while condensation pool of a BWR is made of concrete. However, this does not effect on the validity of the structural data gained from the tests.

Typical transient that is used for validating structural analyses tools is a blowdown test either with compressed air or steam. Instrumentation (pressure and strain gauges) are needed especially in the bottom and in the section connecting the cylinder wall to the bottom part of the facility as the loads there are of interest.

After the first analyzed test cases POOLEX open pool steam blowdown test STB-36-05-02 and PPOOLEX closed pool gas injection test SLR-05-02 were preliminarily selected as test cases for further coupled code analysis.

Results

STB-36-05-02 was an open pool steam blowdown test with 1.5 MPa steam generator pressure. Initially the blowdown pipe (214.1 mm) was filled with air when steam blow was started. Steam mass flux was 40 kg/m²s in the blow. Maximum recorded strain caused by the steam blow was 250 μ S located few centimeters below the joint of the cylinder wall and the bottom part.

SLR-05-02 was a closed pool thermal stratification test for containment drywell with gas injection into the upper drywell. Structural data are gained as side effect of the test in addition to the main purpose of the test. As gas is injected into the drywell, increased pressure pushes gas from the upper drywell to the condensation pool through a blowdown pipe causing loads in the wall structures. The strains are mainly due to increased pressure of the system, but also from the gas bubble formation and detachment from the blowdown pipe (214.1 mm) outlet. Strain caused by bubble behavior was about 10 μ S and about 70 μ S by static pressure increase. Initial pressure of gas accumulator was 1.2 MPa and maximum gas mass flow was 800 g/s.

An overview of the numerical work on loads and FSI in condensation pools is presented. Pressure loads caused by the injection of steam or air have been considered in the CFD calculations. CFD calculation of an experiment with air blowdown is presented. The bubble dynamics are studied and temperatures in the dry and wet wells are compared with the experiment. FSI calculations by using a linear perturbation method and coupling of CFD and structural analysis codes have also been validated [3].

References

1. Rätty, H., Puska, E.K. (Eds.). 2006. SAFIR The Finnish Research Programme on Nuclear Power Plant Safety 2003–2006, Final Report. VTT Research Notes 2363, Espoo.
2. Laine, J., Puustinen, M. 2008. Steam line rupture experiments with the PPOOLEX test facility. Research report CONDEX 2/2007, Nuclear Safety Research Unit, Lappeenranta University of Technology. 23 p. + app. 7 p.
3. Timperi, A. 2009. Fluid-Structure Interaction calculations using a linear perturbation method. SMiRT 20, August 9–14, 2009, Espoo, Finland.

Experiences from structural dynamic analysis projects of BWR plants within the scope of power uprate projects using FEA (3-1914)

Björn Svärd¹, Jan-Anders Larsson²

¹Scanscot Technology AB, Lund, Sweden, e-mail: svard@scanscot.com

²Scanscot Technology AB, Lund, Sweden, e-mail: larsson@scanscot.com

During recent years, power-uprate projects have been executed at several BWR-units in Sweden. As part of these projects, structural verification of the safety-related buildings as well as the new and old internal parts of the reactor pressure vessel has been performed.

In this document, some experiences will be presented from structural dynamic verification, using finite element analysis, FEA, within the scope of these power uprate projects. Examples where FEA-applications have been used are; global vibration analyses, structural verification of safety-related buildings, structural verification of RPV internals and design of new RPV internals.

Three-dimensional FEA-models of all safety-related buildings, including the reactor containment, have been used in global vibration analyses for calculating in-structure design response spectra for structural verification of components mounted in the structure. In-structure design response spectra have been calculated for Safe Shutdown Earthquake, pool dynamic loads, e.g. chugging and pipe-break events. For the analyses of pipe-break events a load application methodology has been developed, transferring results from thermohydraulic calculation programs to take into account two-phase effects of the fluids inside the reactor pressure vessel.

In the model of the reactor containment, a detailed description of the reactor pressure vessel with internals has been included in order to simulate the behavior of these parts as accurate as possible. Focus has also been put on modeling the fluid-structure interaction inside the reactor pressure vessel, since this has a significant effect on the response of certain parts.

The detailed modeling of the reactor pressure vessel implies that in-structure design response spectra in various positions on the internals, as well as stresses in the internals for subsequent ASME-evaluation can be determined.

From this work, a number of conclusions can be drawn. Global models with dense meshes can successfully be used for a broad range of applications. Large FEA-models can today be used efficiently if suitable dynamic analysis methods are used. There can be strong dynamic interactions between the containment, fluids, the RPV and internals. Stress calculation and evaluation can be executed efficiently on large models. The structural models can with advantage be re-utilized in future projects.

Studies on the dynamic behaviour of the Fast Reactor Cores (3-1919)

Daniel Broc

CEA Saclay, 91 191 Gif/Yvette France, e-mail: dbroc@cea.fr

The core of a Fast Reactor is a tubes bundle constituted of Fuel Assemblies (or FA) in the centre, and Neutronic Shields (or NS) at the periphery. The FA are hexagonal tubes and contains the fuel. The NS are steel cylindrical tubes. They are arranged in an hexagonal array, and immersed in the primary coolant (sodium).

Under a seismic excitation the assemblies will move, with changes in the volume of the core and impacts between the assemblies. It is necessary to check that the volume variations will not change the reactivity of the core, and that the impacts will not lead to damages for the structures.

A key point for the dynamic behaviour of the core is the interaction between the assemblies and the sodium. The study of such effects, called Fluid Structure Interaction (or FSI) is a wide scientific topic. Depending of the conditions (fluid at rest, fluid flow, amplitude of the movement of the structure), the fluid may lead to inertial effects (lower natural frequencies), dissipative effects (damping) or even instabilities.

In the case of the Fast Reactor Cores, the fluid is at rest, at least in the tubes bundle (the primary coolant flow is inside the Fuel Assemblies) and inertial and dissipative effects will take place. FSI is characterized by the high confinement (the assemblies are separated by very thin sodium spaces) and the complex geometry of the fluid structure system, due to the high number of assemblies. The size of the numerical simulations (by using the Navier Stokes or Euler equations for the fluid) may be very large.

Homogenization methods have been studied and developed in the last decades to take into account the FSI phenomena with lower computer times.

The paper presents a finite element model for the dynamic behaviour of a whole fast reactor core, taking into account Fluid Structure Interaction by homogenization techniques and impacts between the assemblies. This model is used in for dynamic studies in the frame of the GEN IV program.

References

- P. Buland, B. Fontaine, F. Gantenbein, C. Pedron. Symphony experiment Mock up. SMIRT 13, August 1995, Porto Allegre.
- D. Brochard et al. Fluid Structure interaction in tube bundles. ASME PVP 1995.
- J.F. Sigrist, D. Broc. Dynamic analysis of a tube bundle with fluid structure interaction modeling using a homogenization methods. Computer methods in applied mechanics and engineering.

Fluid Structure Interaction models for the dynamic behaviour of tube bundles, application to nuclear structures (3-1920)

Daniel Broc, Marion Duclercq
CEA Saclay, 91 191 Gif/Yvette France
e-mails: dbroc@cea.fr, marion.duclercq@cea.fr

It is well known that a fluid may strongly influence the dynamic behaviour of a structure. Many different physical phenomena may take place, depending on the conditions: fluid flow, fluid at rest, little or high displacements of the structure. Inertial effects can take place, with lower vibration frequencies, dissipative effects also, with damping, instabilities due to the fluid flow (Fluid Induced Vibration). In this last case the structure is excited by the fluid.

The paper deals with the vibration of tube bundles under a seismic excitation or an impact. Such structures are very common in the nuclear industry, for example in the reactor cores and the steam generators. In this case the structure moves under an external excitation, and the movement is influenced by the fluid. The main point in such system is that the geometry is complex, and could lead to very huge sizes for a numerical analysis.

Many works has been made in the last years to develop homogenization methods for the dynamic behaviour of tube bundles. The size of the problem is reduced, and it is possible to make numerical simulations on wide tube bundles with reasonable computer times. Such methods consider a perfect fluid. Following the Fluid mechanics theory, this hypothesis is valid only for “little displacements” of the structure: in this case, only “inertial effects” will take place, with globally lower frequencies. It is well known that dissipative effects due to the fluid may take place, even if the displacements of the tube are not so high. Such effects may be described in the Euler homogenized models by using a Rayleigh damping, but the basic assumption of the model remains the “perfect fluid” hypothesis.

Examples are presented on the use of such homogenization methods to describe the dynamic behaviour of industrial tube bundles.

A next step in the building of models for tube bundles is, in order to get a best description of the physical phenomenona, to build a model, with a more general equation for the fluid. Instead of a perfect fluid equation, a homogenized equation for the fluid flow in the tube bundles has to be used. This fluid equation has to be coupled to the solid equation. The paper considers the most important key points to build such models.

References

D. Brochard et al. Fluid Structure interaction in tube bundles. ASME PVP 1995.

F. Axisa, J. Antunes. Fluid Structure Interaction. Elsevier 2007.

J.F. Sigrist, D. Broc. Dynamic analysis of a tube bundle with fluid structure interaction modeling using a homogenization methods Computer methods in applied mechanics and engineering.

Solution of random response of structures applied to cylindrical shell in turbulent flow (3-1939)

Kuželka Václav

VIDIA-C, s.r.o., Hrabáková 1970, CZ-148 00 Prague, Czech Republic

Introduction

In engineering practice there are many cases where structure failures result from to vibrations of fluidodynamic origin. Vibrations induced by fluid flow are generally very complex phenomena. The problem of mutual interaction of vibration bodies surrounded by flowing fluid has an interdisciplinary character and belongs to several scientific fields.

Aim

This paper concentrates on the explanation of the mathematical model of the vibrational response of structures to random exciting forces and to its application to cylindrical shell-core barrel in turbulent flow of a reaktor.

Results

The model assumes that the structure behaves like an r -degree of freedom system. However, an i -th element of the system is regarded as a continuum. The equations of motion are being solved using the modal analysis and Fourier transforms. The relations for numerical solution of the response are expressed in matrix form. The model was applied to the solution of the response of a cylindrical shell-core barrel excited by a turbulent flow. The core barrel was represented by a system with 24 to 2 400 degrees of freedom. A computation code was developed for this purpose. The velocity vector forms the basis for the description of the fluidodynamic excitation through coherence function of the fluctuating surface pressure in circumference and axial directions. The first stage involves calculations of generalized quantities and spectral compliance (frequency response functions), the second stage processes spectral loads (acceptance integral) of a core barrel and, finally, there are computations of power spectral displacement densities and of r.m.s. values of displacement and stress distributions. The obtained result of generalized spectral compliances show that by applying a modal matrix of basic dimension we get considerably disfigured

values. With increasing dimensions of the modal matrix, the generalized masses and the spectral compliances are converging to independent values. From the courses of generalized spectral loads can be inferred that they are significantly dependent on fluid flow parameters, such as mean velocity, correlation pressure length, turbulent velocity dependent on frequency. The results of the power spectral density of the radial displacement, or r.m.s. values of this displacement, indicate that the damping and the flow parameters have a considerable influence on the magnitude as well as characters of the response of cylindrical shell-core barrel.

Conclusions

The application of numerical method in solving the vibration response of cylindrical shell-core barrel in turbulent flow makes it possible to evaluate its stochastic behaviour including to compute m.s. amplitudes of the stress and displacement distributions of the core barrel. It has been proved, at the same time, that the amplitudes of random displacements must be attributed mainly to what is called joint terms. In solution, this permits of neglecting the cross terms, which results in a substantial cut of the computing time.

References

- J. Acoust. Soc. Am. 30 (1958) Am. On the fatigue failure of structures due to vibrations excited by random pressure field.
- Proc. Seventh Internat. Conf. on Structural Mechanics in Reactor Technology, Chicago (North- Holland, Amsterdam, 1983) paper B8/11. The influence of thickness and viscosity of liquid annular layer on dynamic behaviour of cylindrical shell.
- Prog. Nucl. Energy 4 (1979) 25–49. Flow-induced vibration in nuclear reactors.
- Nuclear Engineering & Design 238 (2008) 1316–1331. Core analysis at Paks NPP with a new generation of VERONA.
- Nucl. Engineering & Design 238 (2008) 890–903. Flow-induced vibration and fretting-wear prediction of steam generator helical tubes.

Pressure surges in piping systems induced by transient load pulse (3-1944)

Lineu J. Pedroso, Carlos A.E. Melo, Vicente G.O. Júnior, Paulo M.V. Ribeiro
University of Brasília, Faculty of Technology, Department of Civil and
Environmental Engineering, CEP: 70904-970. Brasília, Brazil
e-mail: lineu@unb.br

The study of accidents that may occur during extreme conditions in nuclear reactors is advisable for improving the safety of them. These accidents may be hypothetical because they suppose successive and simultaneous failure of systems that are usually very reliable.

A sudden depressurization, the effects of the sodium-water reaction in fast neutron reactors, the rupture of safety membranes, the pressures due to cavitation bubble collapse, the stoppage or reversal of pumps, the vibration of deformable parts, and predicted or accidental activities cause perturbation in the system which are cause or consequence of the transient phenomena.

To predict the capability of the structure to resist these transients, it is necessary to calculate the response of the associated fluid-structure systems to these loads.

Before the study of the fluid-structure interaction, which is a much more complex problem, it is essential to know the evolution of the transient responses, which allow the determination of the loads and behavior of the system structure under these effects.

The model developed here is not intended to duplicate or improve the work in others codes, but instead of it, to illustrate the kind of analysis that can be used to complete the overall picture of transients in piping networks.

The aim of this work is to compare the results of Finite Element (FEM) and Finite Difference (FDM) Methods, and Method of Characteristics (MOC) for a pipe conveying fluid under different sorts of transient load pulse applied to the system, such as rectangular, half-cycle sine, symmetrical triangular, and others.

For the Finite Element Analysis is used an unsymmetrical formulation (U-P), which uses only the pressure as the variable in the fluid, and a symmetrical potential formulation (U-Ø-P), which uses the velocity potential. For these analyses, the programs used were ANSYS (U-P formulation), FEDYFE (U- Ø -P formulation), and TRANSPETRO (MOC 1D). The last two programs were developed by the Group of Dynamics and Fluid-Structure of University of Brasília. The comparison of the results from these programs presented a good agreement between them.

References

- Barbosa, A.N. 1998. Uma Formulação Potencial Simétrica para o Cálculo Estático e Dinâmico de Problemas de Interação Fluido-Estrutura. Master Thesis. University of Brasília.
- Bathe, K.J., Nitikitpaiboon, C., Wang, X. 1995. A mixed displacement-based finite element formulation for acoustic fluid-structure interaction. *Computers & Structure*, Vol. 56, No. 2/3, 225–237.
- Hansson, P., Sandberg, G. 2001. Dynamic finite element analysis of fluid-filled pipes. *Computer Methods in Applied Mechanics and Engineering*. 190 (2001) 3111–3120.
- Nascimento, C.M.B.M. 2002. Estudo de Transientes em Dutos de Derivados de Petróleo. Master Thesis. University of Brasília.
- Sreejith, B., Jayaraj, K., Ganesan, N., Padmanabhan, C., Chellapandi, P., Selvaraj, P. 2004. Finite Element Analysis of Fluid-Structure Interaction in Pipeline Systems. *Nuclear Engineering and Design*. 227 (2004) 313–322.
- Streeter, V.L., Wylie, E.B. 1967. *Hydraulic Transients*, McGraw-Hill Company.
- Zienkiewicz, O.C., Newton, R.E. 1969. Coupled vibrations of a structure submerged in a compressible fluid. *Symposium on Finite Element Techniques*, Stuttgart.

“As-Built” site response analysis for nuclear power plants – an improvement to the “State-of-the-Practice” (3-1952)

Antonio Fernández-Ares, P.E., Ph.D.¹, Jose Enrique Blanco, Ph.D.¹, Dr. Enrique Bazán², Julio A. García, Ph.D.¹, Dr. Jacobo Bielak³

¹Employer – Paul C. Rizzo Associates, Inc., 105 Mall Boulevard, Suite 270E, Monroeville, PA, USA 15146, e-mail: antonio.fernandez@rizzoassoc.com

¹Employer – Paul C. Rizzo Associates, Inc., 105 Mall Boulevard, Suite 270E, Monroeville, PA, USA 15146, e-mail: jose.blanco@rizzoassoc.com

²Employer – DiGioia and Associates, Inc., 11 Wisteria Drive, Pittsburgh, PA 15235

¹Employer – Paul C. Rizzo Associates, Inc., 105 Mall Boulevard, Suite 270E, Monroeville, PA, USA 15146, e-mail: julio.garcia@rizzoassoc.com

³Professor – Carnegie Mellon University, 5000 Forbes Avenue, Pittsburgh, PA 15213, e-mail: jbielak@cmu.edu

The current “state-of-the-practice” for site amplification analyses involves the use of methods that do not provide clear guidance for the dynamic analysis of Nuclear Power Plants (NPPs). It is not clear how the results of such methods compare with each other and with what the actual response at the site might be. The methodologies do not incorporate complete representations of the site conditions, since they assume elastic response of horizontally layered models under the excitation of vertically propagated shear waves. In addition, the effect of the containment is accounted on a later stage during the Soil Structure Interaction (SSI) analysis. The SSI model usually comprises an accurate three dimensional representation of the structure. However, the soil model and the seismic excitation are rather crude, with limited representation of the three-dimensional nature of both the soil geometry and the seismic ground motion. Soil geometry is incorporated by the use of strain-dependant properties obtained from the site response analysis and seismic ground motion from Foundation Input Response Spectra (FIRS) matching time histories. Additionally, the Structure to Structure Interaction (StSI) effects are incorporated only by using simple spectral factors that quantify the impact of the containment facility on other adjacent buildings, after the completion of its SSI analysis.

This study presents a methodology to incorporate the results of a Probabilistic Seismic Hazard Analysis (PSHA) into a significantly improved site amplification analysis procedure. This technique is known as the Domain Reduction Method (Bielak, 2001), consisting in a Finite Element Method (FEM) based approach that is capable of preserving the three-dimensional nature of seismic waves that originate from an earthquake. The Domain Reduction Method (DRM) also furnishes a more accurate representation of the soil conditions and of the seismic

input when performing the SSI, the SSSIS (Soil Structure Soil Interaction), and the StSI Analyses in one single step. As such, the procedure reduces the levels of epistemic uncertainty in the site analysis, eliminates numerous requirements of information exchange between analysts, and eliminates controversies surrounding the approaches to develop foundation input ground motion. This study also shows how the DRM methodology can be incorporated into existing FEM computer codes, making it available for industry use.

AREVA's fatigue concept (AFC) – an integrated and multidisciplinary approach to the fatigue assessment of NPP components (3-1962)

Jürgen Rudolph, Steffen Bergholz, Wilhelm Kleinöder, Nikolaus Wirtz
AREVA NP GmbH, Paul-Gossen-Straße 100, 91052 Erlangen, Germany
e-mail: rudolph.juergen@areva.com

Keywords: AFC (AREVA Fatigue Concept), fatigue monitoring system, realistic fatigue usage factors, identification of fatigue locations

The prevention of fatigue damages is to be considered as a crucial issue in the view of changing boundary conditions: modification of the code based approaches, lifetime extension, new plants with scheduled operating periods of 60 years (e.g. EPR, SWR1000) and improvement of disposability. The AREVA fatigue concept provides for a multiple step and multidisciplinary process (process engineering, fatigue monitoring, fatigue analyses etc.) against fatigue before and during the entire operation of nuclear power plants. Fatigue analyses are based on the real operational loads measured continuously on site in the plant. The entire process of fatigue design is based on an installed fatigue monitoring system. Qualified fatigue usage factors can be determined for the whole lifetime of the plant. Locations of potential fatigue failure are reliably identified and all efforts can be concentrated on these fatigue critical components.

The direct processing of the measured temperatures is immediately used for a first fast fatigue estimation. This procedure is highly automated and allows for a rough online estimation of the recent usage factor as well as the qualitative comparability of the data.

In the framework of the Periodic Safety Inspection (PSI) a detailed fatigue check conforming to the code rules is carried out in order to determine the current state of the plant. This fatigue check is based on the real loads (specification of thermal transient loads) and finite element analyses in connection with the local strain approach to design against fatigue. The finite element analyses always include transient thermal determination of the temperature field and subsequent determination of (local) stresses and strains. The latter analyses might be simplified elastic or fully elastic plastic.

One peculiarity is the additional check against progressive plastic deformation (ratcheting) which is demanded by the design code. In the case of the elastic plastic approach much care has to be taken with respect to the application of an appropriate material law. Advanced nonlinear kinematic material laws of the

Ohno & Wang type are favored at AREVA at the present time. The implementation of these material laws within commercial finite element codes is still to be considered as non-standard use (especially for non-isothermal conditions).

As a conclusion, one essential benefit for the customer to apply the AREVA fatigue concept can easily be identified. Locations of potential fatigue failure are reliably identified and all efforts can be concentrated on these fatigue critical components. Thus, expensive costs for inspection can be essentially reduced. Of course, one presumption is the application of the temperature measurement system FAMOS in the power plant.

In the future, it is planned to integrate direct measurements of fatigue damage, more sophisticated analyses concepts for fatigue damage (application of short crack fracture mechanics to fatigue crack growth) and realistic ratcheting simulations in the integral AREVA concept.

Investigation of the meso-thermomechanical behaviors of plate-type dispersion nuclear fuel elements (3-1984)

Shurong Ding¹, Yongzhong Huo²

Department of Mechanics and Engineering Science

Fudan University, Shanghai 200433, China

e-mails: ¹dsr1971@163.com, ²yzhuo@fudan.edu.cn

The Reduced Enrichment for Research and Test Reactors (RERTR) program started in 1978 has been tasked with the conversion of research reactors from highly enriched to low-enriched uranium (LEU) with a ²³⁵U content of less than 20%. Many countries have been seeking for technical means to achieve this goal. In order to reach the requisite power density, the needs to raise the density of the exiting fuels must be met. Due to the high uranium density of dispersion nuclear elements, several kinds of dispersion fuels such as U₃Si₂ dispersion fuel are formally qualified for reactor use and a good many research and test reactors have been converted to LEU fuels or were originally built with LEU. However, there remain some reactors that have not been converted to LEU fuels because the initial developed dispersion fuels might not meet the needs of the required high power density. A range of high-density advanced dispersion fuels such as the U-Mo dispersion fuel plates are being developed and a series of irradiation tests are being tested.

Dispersion fuels are composed of fissile particles and metal matrix with fissile particles dispersed in the non-fissile metal matrix. They are similar to particle composites in the configurations and they are designable. The performances of dispersion fuels are affected by several factors, for an example, geometries, sizes, volume fractions and different distribution forms of fissile particles, different material performances of particles and metals etc. The thermal and mechanical behaviors of dispersion fuel elements during their lifetime under different operation conditions need to be evaluated.

In order to design and obtain a kind of ideal dispersion fuel, irradiation tests are necessary. But it is impossible to carry out tests for all the circumstances, more over, it is very time-consuming. As a result, numerical modeling is becoming a measure of importance, which might interpret irradiation experiments of dispersion fuel elements and explain the damage mechanism. Other purposes are to perform parametric studies to identify the more sensible parameters on the performances of fuel elements and to be a support to the fuel design.

In this study, based on the characters of the geometric shape, the three-dimensional finite element model is developed. In this model, the mutual actions among the fuel particles, metal matrix and the cladding of the fuel element are considered, thus the relative meso-thermomechanical behaviors might be investigated. The temperature field and mechanical behaviors induced by thermal effects together with fuel swelling are evaluated with the finite element method. And the interlaminar stresses at the interface between the metal matrix and cladding are especially focused on. The damage mechanism is predicted.

Missile impact on reinforced concrete walls: simulation of experiments (3-1989)

Dino A. Oliveira¹, Nam Ho Lee², Medhat Elgohary³

¹SNC Lavalin Nuclear, ^{2&3}Atomic Energy of Canada Limited

e-mails: ¹Dino.Oliveira@slnuclear.com, ²leenh@aecl.ca, ³elgoharm@aecl.ca

The ability of civil structures to withstand a localized impact from a projectile, launched as a result of an external event, is increasingly becoming a requirement in the design of safety-related civil structures. One key aspect of improving the overall design of such structures is to better understand the response of a reinforced concrete wall due to a high-rate impact event. Thus, this work focuses on the numerical simulation of a benchmark experiment whereby a reinforced concrete wall was exposed to a high-rate impact by a deformable missile, as shown in Figure 1. The development of such a predictive tool provides additional insight into the non-linear and high-rate impact response of reinforced concrete walls, and forms a basis for further development of simulation tools to be used in the design and analysis of full-scale civil structures.

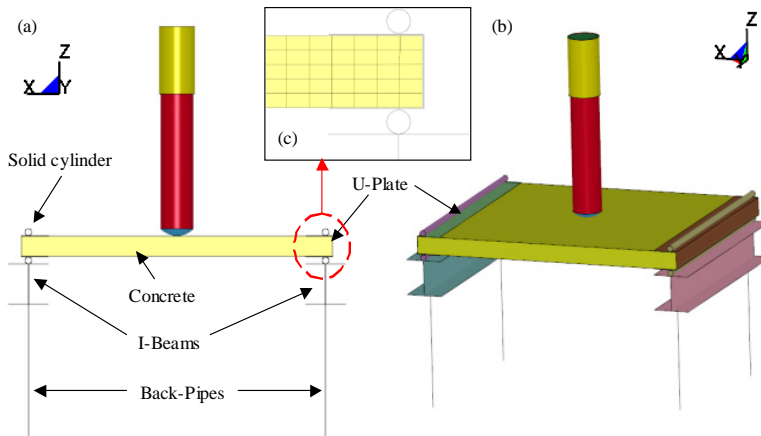


Figure 1. Finite element representation of missile impact onto the concrete wall: (a) front; and (b) isometric views; and (c) close-up view of solid cylinder/U-plate/concrete interaction.

The experiment was simulated using LS-DYNA, an explicit dynamic finite element software code. The concrete and reinforcing bars comprising the wall were represented in a discrete manner using solid and beam elements, respectively, as shown in Figure 2. A three-invariant material representation utilizing three shear failure surfaces, which includes damage and strain-rate effects was adopted for the concrete, while a high strain-rate constitutive model

was employed to represent the response of the reinforcing bars. The predictive ability of the model was assessed based on the following data measured in the experiment: (i) impact load; (ii) deflection of the wall; and, (iii) strain in the reinforcing bars. It is concluded that the finite element model developed in this work is able to predict the highly non-linear dynamic response of a reinforced concrete wall subjected to impact by a missile.

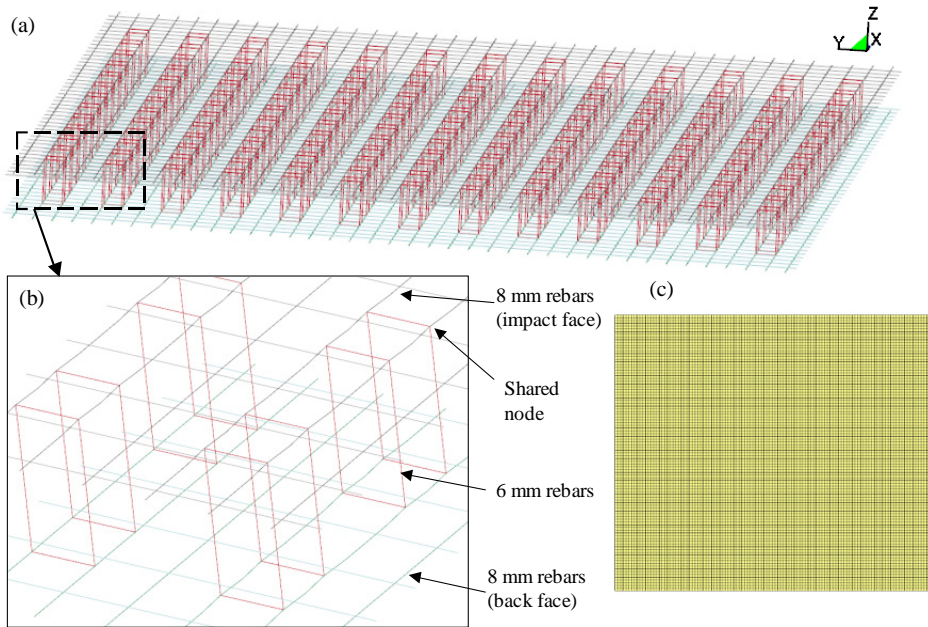


Figure 2. (a) Wall reinforcements; (b) close-up of reinforcing bars; and, (c) finite element discretization of concrete wall.

Research and development of welding process with following local thermocyclice treatment of welding joint of zirconium alloys (3-1992)

V. Melukov¹, A. Korepanov¹, T. Rivkin², A. Semenov², M. Plushevsky²,
M. Shtutza³, I. Vdovenco³

¹Vyatka State University (VyatSU), Kirov

²Research and Development Institute of Power Engineering (RDIPE), Moscow

³Chepetsky Mechanical Plant (ChMP), Glazov

In production of zirconium designs for nuclear power industry, there are problems caused by the increase of the welding process productivity and the need to ensure the strength and corrosion resistance of welding joints. RDIPE in common VyatSU and ChMP has developed the process of electron beam welding and following local thermocyclice treatment of welding joint with the same electron beam. This process provides produce with extensive technical alternatives and new ways for the economic solution of manufacturing problems.

The methods of optimum control and the mathematical modeling of heat conductivity processes was used when developing the technological process of electron beam welding and local thermocyclice treatment. The optimization of heat and hydrodynamics processes of welding and also the optimum control of power density distribution of the thermo cyclic treatment were used in the technological process when forming the welding circumferential joints of nuclear reactor fuel channels.

The optimum control of electron beam welding with following local thermo cyclical treatment of welding joint made possible to reduce the heat treatment in furnace and at the same time to increase the quality of zirconium manufactures.

Developed technological process may be used in industrial production of welding joints of zirconium alloys.

Comparison of creep life of ORNL plates – RCC-MR VS experiments (3-2007)

Kulbir Singh, P. Chellapandi, S.C. Chetal
Nuclear Engineering Group
Indira Gandhi Centre for Atomic Research, Kalpakkam, India
e-mail: pcp@igcar.gov.in

Design code RCC-MR is widely used for design and analysis of fast breeder reactor components. The code gives robust rules to evaluate creep life of components operating at high temperature. The code also provides rules for treating multiaxiality and weldments. The weld reduction factors to be applied on the base metal data of stress to rupture and design fatigue curve are specified for some of the materials including SS316 LN. Accordingly the creep-fatigue damage can be evaluated. A series of high temperature experiments are in progress to understand these effects and evaluate any possible conservatism in the design code procedure.

A number of high temperature tests have been completed on components having multiaxiality features and weldments. One of them is simulation of creep-fatigue damage on ORNL plates with / without welds at the highly stressed location.

The set up (Fig. 1) consists of 10 ton loading frame, split furnace, actuator operated through a motor along with computer and Programme Logic Controller (PLC). There is a load cell and LVDT sensors to measure the load applied on the component and its displacement. Tests have been conducted at 933 K (660°C) in an indigenously developed test set up.



Displacement control tests have been completed with various types of load cycles such as +3mm to -3mm (hold at both extreme) and 0 to 3 mm having hold only at 3 mm etc. The specimens are investigated for crack at critical location at regular intervals by interrupting the tests. However visual inspection is carried out through a viewing window on line. These plates are analysed using CAST 3 M, issued by CEA, France and investigated as per RCC-MR (2002) and RCC-MR (2007).

All the test results are compared with analytical predictions using numerical investigation plus design code procedure. The effect of multiaxiality and weld are brought out. The recent version of RCC-MR (2007) is compared with the earlier version of RCC-MR (2002) with illustration. More results are presented in the paper.

References

RCC-MR, Division 1. (2002&2007), Design and construction rules for mechanical components of FBR for nuclear power plant, AFCEN, Paris.

RCC-MR Section I, Subsection Z. (2002&2007). Technical Appendix A3, AFCEN, Paris.

Guide for verification and validation in computational solid mechanics (3-2010)

Leonard E. Schwer
Schwer Engineering & Consulting Services
6122 Aaron Court, Windsor CA 95492, USA, e-mail: Len@Schwer.net



Reprinted by permission of
The American Society of Mechanical Engineers. All rights reserved.

Preface

The American Society of Mechanical Engineers (ASME) Standards Committee on Verification and Validation in Computational Solid Mechanics (PTC 60/V&V 10) approved their first document (Guide) in July 2006. The Guide has been approved by ASME and the American National Standards Institute (ANSI) for public release. The Guide is available through ASME publications as V&V 10-2006:

Guide for Verification and Validation in Computational Solid Mechanics:
http://catalog.asme.org/Codes/PrintBook/VV_10_2006_Guide_Verification.cfm

Outline of the guide

As stated in the Guide's Abstract, the guidelines are based on the following key principles:

- Verification must precede validation.
- The need for validation experiments and the associated accuracy requirements for computational model predictions are based on the intended use of the model and should be established as part of V&V activities.
- Validation of a complex system should be pursued in a hierarchical fashion from the component level to the system level.
- Validation is specific to a particular computational model for a particular intended use.
- Validation must assess the predictive capability of the model in the physical realm of interest, and it must address uncertainties that arise from both simulation results and experimental data.

The *Guide* contains four major sections:

1. Introduction – the general concepts of verification and validation are introduced and the important role of a V&V Plan is described.
2. Model Development – from conceptual model, to mathematical model, and finally the computational model are the keys stages of model development.
3. Verification – is subdivided into two major components: code verification – seeking to remove programming and logic errors in the computer program, and calculation verification – to estimate the numerical errors due to discretization approximations.
4. Validation – experiments performed expressly for the purpose of model validation are the key to validation, but comparison of these results with model results depends on uncertainty quantification and accuracy assessment of the results.

In addition to these four major sections a Concluding Remarks section provides an indication of the significant challenges that remain. The document ends with a Glossary, which perhaps should be reviewed before venturing into the main body of the text. The Glossary section is viewed as a significant contribution to the effort to standardize the V&V language so all interested participants are conversing in a meaningful manner.

SPH, MM-ALE & erosion simulation of concrete cylinder perforation (3-2011)

Leonard E. Schwer
Schwer Engineering & Consulting Services
6122 Aaron Court, Windsor CA 95492, USA
e-mail: Len@Schwer.net

Simulation of penetration and perforation events requires a numerical technique that allows one body (penetrator) to pass through another (target). Traditionally these simulation have been performed using either an Eulerian approach, i.e. a non-deformable (fixed) mesh with material advecting among the elements, or using a Lagrangian approach, i.e. a deformable mesh with large mesh deformations. The chief criticism of the Eulerian approach has been that the shape of the penetrating body, usually an idealized rigid projectile, becomes ‘fuzzy’ as the penetration simulation proceeds due to the mixing of advected materials in the fixed Eulerian cells. Lagrangian methods require some form of augmentation to minimize or eliminate large mesh distortions. Two often used augmentations for Lagrangian penetration simulations are the so called ‘pilot hole’ technique and material erosion. In the pilot hole technique elements are removed, a priori, from the target mesh along the penetrator trajectory; this technique works (surprisingly) well for normal impacts where the trajectory is know a priori. The material erosion technique removes distorted elements from the simulation, i.e. along the penetrator trajectory, based upon a user supplied criteria; no general guidance exists for selecting such criteria, i.e. they are ad hoc.

The focus of the present work is to perform an assessment of a relatively new class of numerical methods, referred to as meshfree methods, that offer analysts an alternate analytical technique for simulating this class of ballistic problems, without a priori trajectory knowledge, nor resorting to ad hoc criteria. The assessment is made by the comparison of techniques, as applied to a ballistic impact experiment. The techniques compared are the meshfree method known as Smooth Particle Hydrodynamics, an Multi-Material Arbitrary Lagrange Eulerian (MM-ALE) technique that preserves the projectile shape, and Lagrangian with material erosion. Such comparisons inherently have aspects of an apples-to-oranges-to-pears comparison, but an effort has been made to minimize the numerous ancillary aspects of the different simulations and focus on the capability of the techniques. To minimize unintended differences in the simulations, the following three key aspects remain constant:

1. Only one software package (code) is used,
2. The same constitutive model is used,

3. The models were constructed by one analyst with similar levels of experience with the three modeling techniques.

Even with these considerable constraints on the simulation comparisons, it is obvious that the results are subject to the user's knowledge and skills in applying the various analysis techniques to the fragment impact simulation. Thus the reader should not assess the merits of these techniques on the provided 'answers,' but should instead focus on the relative merits of each technique and their applicability to specific simulations of interest to the reader.

Some features of the turbulent flow in tube banks of triangular arrangement (3-2020)

A.V. de Paula¹, L.A.M. Endres², S.V. Möller¹

¹Graduate Program in Mechanical Engineering – PROMEC,
Federal University of Rio Grande do Sul – UFRGS, Porto Alegre, Brazil
e-mail: svmoller@ufrgs.br

²Hydraulic Research Institute – IPH
Federal University of Rio Grande do Sul – UFRGS, Porto Alegre, Brazil

Keywords: turbulent flow, hot wires, tube banks, wavelets, flow visualization

In the present work, some features of the turbulent flow in tube banks of triangular arrangement are discussed. The experimental study is performed by means of hot-wire measurements in an aerodynamic channel, and flow visualizations in a water channel. The tube banks had pitch-to-diameter ratio 1.26 and 1.6, and the Reynolds numbers are in the range from 7.5×10^3 to 4.4×10^4 , computed with the tube diameters and the percolation velocity. The experimental data are analyzed through statistical, spectral and wavelet tools. The results show stable wake patterns after the first row of tubes. Flow visualizations show that the flow emanating from the gaps between the tubes form coalescent jets. In some cases, a changing flow direction occurs. This phenomenon is called in literature as “metastable”. After two rows of tubes, the flows present a transverse vertical component. For $P/D = 1.26$, the flow direction changes at irregular time intervals, called “bistable flow”. For $P/D = 1.6$, the wake pattern is stable. The features of turbulent flow through three, four and five rows of tubes seems to be similar, where the gap flop presents a fast swapping, from one side to another (flip-flop).

Mechanistic modeling of thermal-mechanical deformation of CANDU pressure tube under localized high temperature condition (3-2021)

Farshad Talebi, John C. Luxat
Department of Engineering Physics, McMaster University
Hamilton, Ontario, Canada
e-mails: farshat@mcmaster.ca, luxatj@mcmaster.ca

Thermal strain deformation is a pressure tube failure mechanism. The main objective of this paper is to develop mechanistic models to evaluate local thermal-mechanical deformation of a pressure tube in CANDU reactor and to investigate fuel channel integrity under localized contact between fuel elements and pressure tube. The consequence of concern is potential creep strain failure of a pressure tube and calandria tube. The initial focus will be on the case where a fuel rod contacts the pressure tube at full power with highly cooling condition. Such an event could occur if a fuel element was to become detached from a bundle. Calculations are performed using the finite element method in which the heat and thermal mechanical strain equations are solved, simultaneously. The heat conduction from fuel sheath to the inner surface of the pressure tube with appropriate convective and radiation boundary conditions has been simulated and then the thermal stresses were obtained when the pressure tube is under full operational condition. The contact boundary could be a spot or a small arc contact between the fuel sheath and pressure tube. The vapor pockets are considered in the areas beside the contact region where the convective cooling is drastically decreased. Subsequently, modeling has been extended to the contact of number of fuel elements where, several fuel rods are postulated to contact the pressure tube under fully cooling conditions. It was observed that pressure tube thermal strain will occur if sufficiently high temperature is reached. Sensitivity analysis is performed in order to evaluate the contact conductance, extension of vapor region and contact width. The pressure tube local strain is very sensitive to these parameters where any local strain will act to reduce the contact width, contact conductance and pressure tube thermal strain and therefore, will be self-limiting.

References

1. J.C. Luxat. Mechanistic Modeling of Heat Transfer Processes Governing Pressure Tube to Calandria Tube Contact and Fuel Channel Failure. Proc. 23rd CNS Annual Conf., Toronto, Ontario, June 2002.
2. F. Talebi, G. Marleau, J. Koclas. A model for coolant void reactivity evaluation in assemblies of CANDU cells. *Annals of Nuclear Energy*, Vol. 33, No. 11–12, August, 2006, pp. 975–983.
3. D.B. Reeves, P.S. Kundurpi, G.H. Archinoff, A.P. Muzumdar, K.E. Locke. Analysis of fuel element to pressure tube contact using the MINI-SMARTT computer code. *CNS Proceedings of the Seventh Annual Conference*, 1986, pp. 156–162.
4. G.R. McGee, M.H. Schankula, M.M. Yovanovich. Thermal resistance of cylinder-flat contacts: theoretical analysis and experimental verification of a line-contact model. *Nuclear Engineering and Design*, Vol. 86, No. 3, June 1985, pp. 369–381.
5. R.S.W. Shewfelt, L.W. Lyall, D.P. Godin. A High-Temperature Creep Model for Zr-2.5 wt% Nb Pressure Tubes. *Journal of Nuclear Materials*, Vol. 125, Iss. 2, pp. 228–235, (1984).
6. G.R. McGee, M.H. Schankula, M.M. Yovanovich. Thermal Resistance of Cylinder-Flat Contacts: Theoretical Analysis and Experimental Verification of a Line-Contact Model. *Nuclear Engineering and Design*, Vol. 86, No. 3, pp. 369–381, (1985).
7. D.B. Reeves, P.S. Kundurpi, G.H. Archinoff, A.P. Muzumdar, K.E. Locke. Analysis of Fuel Element to Pressure Tube Contact Using the MINI-SMARTT Computer Code. Proc. 7th CNS Annual Conf. Pp. 156–162, (1986).
8. C. Gerardi, J. Buongiorno. Pressure-Tube and Calandria-Tube Deformation Following a Single-Channel Blockage Event in ACR-700. *Nuclear Engineering and Design*, Vol. 237, No. 9, pp. 943–954, (2007).
9. V.F. Urbanic, T.R. Heidrick. High-Temperature Oxidation of Zircaloy-2 and Zircaloy-4 in Steam. *Journal of Nuclear Materials*, 75, pp. 251–261, (1978).
10. R.S.W. Shewfelt, L.W. Lyall. A High-Temperature Longitudinal Strain Rate Equation for Zr-2.5 wt% Nb Pressure Tubes. *Journal of Nuclear Materials*, Vol. 132, Iss. 1, pp. 41–46, (1985).
11. M.H. Bayoumi, W.C. Muir, P.B. Middleton. Simulation and Analysis of Bearing Pad to Pressure Tube Contact Heat Transfer under Large Break LOCA Conditions. Proc. 17th CNS Annual Conf., Toronto, (1996).
12. W.C. Muir, M.H. Bayoumi. Prediction of Pressure Tube Ballooning under Non-Uniform Circumferential Temperature Gradients and High Internal Pressure. Proc. of the 5th Inter. Conf. on Simulation Methods in Nuclear Engineering, Montreal, (1996).
13. P.M. Mathew, W.C.H. Kupferschmidt, V.G. Snell, M. Bonechi. CANDU-Specific Severe Core Damage Accident Experiments in Support of Level 2 PSA. *Transactions, SMiRT 16*, Washington DC, (2001).
14. R.W.L. Fong, C.K. Chow. High-Temperature Transient Creep Properties of CANDU Pressure Tubes. Proc. 23rd CNS Annual Conf., Toronto, (2002).

Mesh generation for reactor modeling and simulation: practices, procedures and uncertainties (3-2028)

Steven Owen¹, Glen Hansen²

¹Sandia National Laboratories, Albuquerque, New Mexico, USA
e-mail: sjowen@sandia.gov

²Idaho National Laboratory, Idaho Falls, Idaho, USA
e-mail: glen.hansen@inl.gov

Accurate modeling and simulation of nuclear reactors must employ mesh generation tools to accurately discretize complex geometry where multiple scales and multiple physics are represented. Reactor simulation, in many cases can use tools developed for other application areas. Common concerns such as geometry fidelity, mesh quality, adaptivity, anisotropy, element shapes, data structures and scalability are all important aspects of reactor simulation.

Mesh Generation for reactor simulation begins to be more specialized as it is employed as a predictive design and safety analysis tool. The multiphysical nature of the problem and the physics algorithms employed will impose varying requirements and restrictions on the nature of the mesh. This work discusses briefly the current state of meshing technology applied to reactor simulation, including current practices and procedures. We also propose a set of requirements, which will be important in the generation of high-quality reactor mesh generation for today and in the future.

Engineering analysts performing reactor simulation, similar to other disciplines, continue to spend the majority of their time preparing geometry and developing a finite element mesh acceptable for simulation. While the tools for automatic mesh generation have become more powerful, the complexity and scale of problems that are now addressed have also increased. The following are a sample of some of the issues encountered by engineers and their application to reactor simulation.

Procedures and practices

It is often noted that two equally skilled engineers, when given an identical problem, will build analysis models that can differ significantly. Engineering judgment and differing software tools and algorithms can result in widely varying meshes. Many established disciplines such as auto manufacturing employ a common set of industry-wide practices and procedures, which are aimed at reducing these differences. Due to the sensitivity and the non-linear

nature of reactor analysis, small differences in mesh can introduce significant errors. While common procedures and practices would be highly recommended for reactor simulation, the ultimate correctness of the result will rely on many other factors.

Geometry and CAD issues

Geometry models for reactor analysis increasingly are supplied using industry standard CAD and solid modeling software tools. Similar to other disciplines, the CAD model is not designed for analysis; instead, small features and extraneous translation errors can take significant effort to resolve prior to mesh generation. If meshing automation is to be achieved, automatic algorithms for resolving dirty geometry or the ability to employ meshing algorithms in a geometry tolerant manner will be required.

Meshing tools

Reactor analysis requires the ability to resolve several different physics, including structural, fluids, neutronics and others. Each of these physics requires different characteristics of the mesh. CFD, for example requires a highly anisotropic boundary layer, while non-linear structural analysis may require a high quality isotropic hex or tet mesh. Generating a single mesh that satisfies all constitutive models in most cases would be intractable. As each physics domain must transfer computed values between meshes, a robust rezoning method would be employed requiring accurate and conservative mapping between meshes [1]. Alternatively, we propose a common base mesh, known as a *net* [2], in which goal-based adaptivity is employed to satisfy requirements of the geometry and physics.

Current computational tools for reactor simulation may be restricted to all-hexahedral or structured mesh. The ability to automatically generate an all-hexahedral mesh for arbitrary geometry configurations remains a significant research objective [3]. While hex research will continue to develop more sophisticated tools, those developing simulation tools must also consider alternative element formulations to support tet, mixed hex-tet and polygonal elements where meshing algorithms may be more easily automated.

Spatial adaptation

The multi-scale and multi-physics nature of reactor simulation requires the ability to adaptively modify the mesh both temporally and spatially. *h*-adaptation, or the ability to cut elements into smaller pieces to better capture physics can be

employed, but often requires significant changes in element sizes or introduction of hanging nodes, particularly for hexahedral or structured meshes.

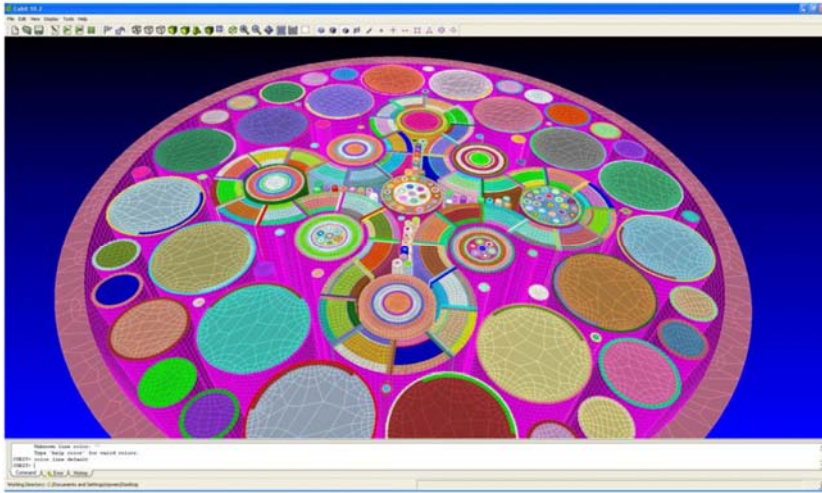


Figure 1. All-hexahedral mesh of the Idaho National Laboratory Advanced Test Reactor (ATR) using the CUBIT Geometry and Meshing Toolkit developed by Sandia National Laboratories.

r -adaptation, or the ability to reposition or smooth nodes based on an error metric should also be employed [4]. p -adaptive refinement may also be necessary to capture geometric curvatures or highly non-linear physics.

Software

Even with highly accurate and reliable meshing tools, the ability to deploy the tools in a manner that can be easily used is also very important. Individuals contributing to decisions regarding design and safety of nuclear reactors must be able to use these tools in a robust and straightforward environment. In addition, the scientific community developing new computational tools for geometry and mesh generation, should also be able to contribute to a common, well-defined tool suite using common APIs or SDKs that have been deployed. This will greatly facilitate the sharing of tools and technology among diverse groups.

There is much we can learn from other disciplines in developing geometry and meshing tools for reactor simulation. It is important to use these technologies where appropriate, however new technologies must be developed to address specific demands of nuclear reactor design and safety.

References

1. Jiao, X., Heath, M.T. 2004. Common-refinement-based data transfer between non-matching meshes in multi-physics simulations. *Int. J. Numer. Meth.* 61(14), 2402–2427.
2. Hansen, G., Owen, S.J. 2008. Mesh Generation Technology for Nuclear Reactor Simulation; Barriers and Opportunities. *Nucl Eng Des Vol.* 238(10), 2590–2605.
3. Staten, M.L., Kerr, R.A., Owen, S.J., Blacker, T.D. 2006. Unconstrained Paving and Plastering: Progress Update. *Proceedings 15th Int. Meshing Roundtable*, 469–486.
4. Hansen, G., Zardecki, A. 2007. Unstructured surface mesh adaption using the Laplace-Beltrami target metric approach. *J. Comput. Phys.* 225 (1), 165–182.

An implicit solution framework for reactor fuel performance simulation (3-2045)

Glen Hansen, Chris Newman, Derek Gaston
Multiphysics Methods Group, Idaho National Laboratory
Idaho Falls, ID 83415-3840
e-mail: Glen.Hansen@inl.gov

Introduction

The simulation of nuclear reactor fuel performance involves complex thermo-mechanical processes between fuel pellets, made of fissile material, and the protective cladding that surrounds the pellets. An important design goal for a fuel is to maximize the life of the cladding thereby allowing the fuel to remain in the reactor for a longer period of time to achieve higher degrees of burnup. This presentation examines various mathematical and computational issues that impact the modeling of the thermomechanical response of reactor fuel, and are thus important to the development of INL's fuel performance analysis code, BISON. The code employs advanced methods for solving coupled partial differential equation systems that describe multidimensional fuel thermomechanics, heat generation, and transport within the fuel.

Aim of the work

BISON is designed for fully coupled steady and transient analysis, and to be efficient on both desktop computers and in massively parallel environments. It employs physics-based preconditioned Jacobian-free Newton-Krylov solution methods and is developed using modern software engineering principles to form a robust, extensible software architecture to provide a predictive capability for fuel performance analysis. This discussion summarizes the current status of *BISON* and demonstrates results on selected three dimensional capabilities that support fuel performance calculations.

Significant progress has been achieved within *BISON* in coupling thermo-mechanics to an oxygen diffusion equation and in creating a base multi-dimensional code that demonstrates these capabilities in UO_2 fuel pellet geometry. The equation set consists of three fully coupled partial differential equations for heat conduction, oxygen nonstoichiometry and linear elastic solid mechanics. Let Ω define the fuel pellet domain. The heat conduction model assumes fission reactions generate heat at a uniformly distributed constant rate, Q ,

$$\begin{aligned}
 \rho C_p T_t - \nabla \cdot k \nabla T - Q &= 0 & T \in \Omega, \\
 T &= T_d & T \in \Gamma^D, \\
 n \cdot \nabla T &= 0 & T \in \Gamma^N, \\
 T(t=0) &= T_0 & T \in \Omega,
 \end{aligned} \tag{1}$$

where T , ρ , C_p and k are temperature, density, specific heat, and thermal conductivity, respectively. Here, Γ^N denotes the top and bottom boundary of the fuel pellet, and Γ^D denotes the outer circumferential fuel pellet boundary. The nonstoichiometric model for oxygen diffusion x , is given by

$$\begin{aligned}
 x_t - \nabla \cdot (D \nabla x + \frac{x Q^*}{FRT^2} \nabla T) &= 0 & x \in \Omega, \\
 x &= x_d & x \in \Gamma^D, \\
 x(t=0) &= x_0 & x \in \Omega,
 \end{aligned} \tag{2}$$

where D is diffusivity of UO_2 , F is the thermodynamic factor of oxygen, Q^* is the heat of transport of oxygen, and R is the universal gas constant. The boundary condition for (2) is a constant Dirichlet condition at the outside circumferential pellet boundary. The linear elastic solid mechanics model for the displacement \mathbf{u} is given

$$\begin{aligned}
 \mathbf{A}^T \mathbf{D} \mathbf{A} \mathbf{u} + \mathbf{f} &= 0 & \mathbf{u} \in \Omega, \\
 \mathbf{u} &= 0 & \mathbf{u} \in \Gamma^D,
 \end{aligned}$$

with

$$\mathbf{A} = \begin{bmatrix} \partial_x & 0 & 0 \\ 0 & \partial_y & 0 \\ 0 & 0 & \partial_z \\ \partial_y & \partial_x & 0 \\ 0 & \partial_z & \partial_y \\ \partial_z & 0 & \partial_x \end{bmatrix}, \quad \mathbf{D} = c_1 \begin{bmatrix} 1 & c_2 & c_2 & 0 & 0 & 0 \\ c_2 & 1 & c_2 & 0 & 0 & 0 \\ c_2 & c_2 & 1 & 0 & 0 & 0 \\ 0 & 0 & 0 & c_3 & 0 & 0 \\ 0 & 0 & 0 & 0 & c_3 & 0 \\ 0 & 0 & 0 & 0 & 0 & c_3 \end{bmatrix},$$

and

$$c_1 = \frac{E(1-\nu)}{(1+\nu)(1-\nu)}, \quad c_2 = \frac{\nu}{(1-\nu)}, \quad c_3 = \frac{(1-2\nu)}{2(1-\nu)}. \tag{3}$$

The coefficients E and ν are Young's modulus and Poisson's ratio. The forcing term \mathbf{f} weakly enforces linear thermal expansion with coefficient Q , ρ , C_p , k , D , Q^* , F are given by strongly nonlinear empirical models and are functions of T , nonstoichiometry x and \mathbf{u} .

The JFNK solution method used in *BISON* begins with writing a weak form of the above system of equations and casting it into a residual function. Further, gap heat transfer terms that arise from the discretization of the heat equation across the gap and contact expressions between the pellet and cladding modify the residual vector,

$$\mathbf{F}(\mathbf{x}) = \mathbf{0}, \tag{4}$$

that is of length N , where N is the number of unknowns in the discrete problem. The Jacobian of this system is a $N \times N$ sparse matrix,

$$\mathcal{J}(\mathbf{x}) = \frac{\partial \mathbf{F}(\mathbf{x})}{\partial \mathbf{x}}. \quad (5)$$

Given the Jacobian in this form, it is straightforward to express the Newton iteration,

$$\mathcal{J}(\mathbf{x}^{(k)}) \delta \mathbf{x}^{(k)} = -\mathbf{F}(\mathbf{x}^{(k)}), \quad (6)$$

and

$$\mathbf{x}^{(k+1)} \leftarrow \mathbf{x}^{(k)} + \delta \mathbf{x}^{(k)}, \quad (7)$$

where the superscript k denotes the iteration count of the Newton iteration. Using Newton's method as shown here amounts to implementing a sequence of steps:

1. Form the Jacobian matrix.
2. Solve the sparse linear system (6) to obtain $\delta \mathbf{x}^{(k)}$.
3. Apply this update (7) to obtain the next iteration of the solution state vector, $\mathbf{x}^{(k+1)}$.

Even for moderately-large grids, the cost of forming the Jacobian is high and typically dominates the computation, making the above algorithm impractical for most situations. Fortunately, Krylov iterative solvers such as the generalized minimum residual (GMRES) algorithm [1], which is used here to solve the Jacobian system, do not require the Jacobian matrix itself but simply the action of the Jacobian matrix on a vector. Approximating this matrix-vector product by differencing, which requires two nonlinear function evaluations, is the basis of the JFNK method. Specifically, to evaluate the matrix-vector product $\mathcal{J}(\mathbf{x}^{(k)})\mathbf{v}$, a finite-difference approach,

$$\mathcal{J}(\mathbf{x}^{(k)})\mathbf{v} \approx \frac{\mathbf{F}(\mathbf{x}^{(k)} + \varepsilon \mathbf{v}) - \mathbf{F}(\mathbf{x}^{(k)})}{\varepsilon}, \quad (8)$$

is commonly used [2, 3]. Here, ε is chosen in an automatic fashion to avoid problems with machine precision.

Using this Jacobian-free approach, the dominant cost of the algorithm shifts from evaluating the Jacobian to the solution of the linear system. Indeed, the solution cost of GMRES for elliptic problems scales quadratically with the number of unknowns in the grid, unless effective preconditioning is used [4].

Essential results

To demonstrate the efficacy of the proposed approach, a calculation published by Ramirez, Stan, and Cristea [5] and reproduced by Shadid and Hooper [6] was extended to three dimensions and to include a linear mechanics model.

The coupled thermomechanics/oxygen diffusion equation system shown in Eqs. (1)–(3) were solved to provide the results in Figs. 1 and 2. These solutions are characterized by strong temperature gradients and by thermal diffusion and oxygen diffusion that operate on significantly different time scales. The impact of coupled oxygen diffusion is clear on both the pellet temperature and thermal expansion. Figure 1(b) shows the effectiveness of the JFNK solver by showing the strong reduction in nonlinear residual with respect to Newton iteration. Figure 2 shows the average pellet temperature and displacement vs. distance from the center of the pellet. While this is a three dimensional calculation, both the geometry and physics of this example are axisymmetric and the results are therefore one dimensional. The temperature and nonstoichiometry (x) results presented here are similar to [5]. This figure also shows the strong impact of the coupled oxygen diffusion model on pellet displacement.

Summary

This discussion explores the effectiveness of a JFNK-based solution of a problem involving three dimensional fully coupled, nonlinear transient heat conduction and including solid mechanics and oxygen nonstoichiometry. These equations are closed using empirical data that is a function of temperature, density, and nonstoichiometry. The method appeared quite effective for the three dimensional fuel pellet configurations examined, with excellent nonlinear convergence properties exhibited on the combined system. In closing, fully coupled solutions of three dimensional thermomechanics coupled with oxygen diffusion appear quite attractive using the JFNK approach described here, at least for configurations similar to those examined in this report.

3. Applied Computations, Simulation and Animation

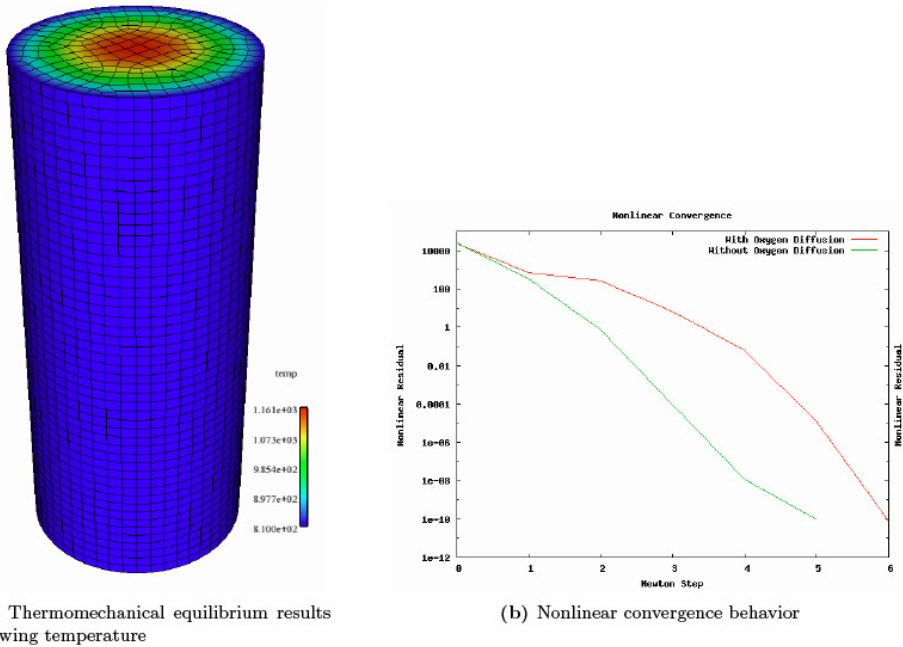


Figure 1. Results of three dimensional JFNK solution of Eqs. (1)–(3). Note the strong convergence behavior of the nonlinear solver on the fully-coupled problem.

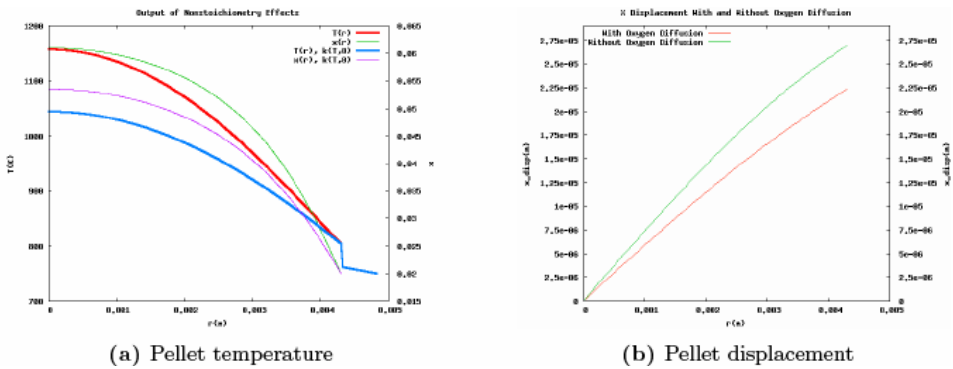


Figure 2. Results of JFNK solution of coupled thermomechanics/oxygen diffusion system. Figure (a) shows pellet temperature as a function of radius from the pellet centerline which essentially duplicates the results by Ramirez [5] (but in 3D). Figure (b) shows the impact of coupled oxygen diffusion on thermal expansion (displacement u) as a function of radius from the centerline.

Acknowledgments

The submitted manuscript has been authored by a contractor of the U.S. Government under Contract No. DE-AC07-05ID14517 (INL/CON-08-15018). Accordingly, the U.S. Government retains a non-exclusive, royalty-free license to publish or reproduce the published form of this contribution, or allow others to do so, for U.S. Government purposes.

References

1. Y. Saad. *Iterative Methods for Sparse Linear Systems*, The PWS Series in Computer Science, PWS Publishing Company, Boston, MA (1995).
2. D.A. Knoll, D.E. Keyes. Jacobian-Free Newton-Krylov Methods: a Survey of Approaches and Applications. *J. Comput. Phys.*, 193, 2, pp. 357–397 (2004).
3. M. Pernice, H.F. Walker. NITSOL: a Newton iterative solver for nonlinear systems. *SIAM J. Sci. Comp.*, 19, 1, pp. 302–318 (1998).
4. D.A. Knoll, W.J. Rider. A Multigrid Preconditioned Newton-Krylov Method. *SIAM J. Sci. Comput.*, 21, pp. 691–710 (2000).
5. J. Ramirez, M. Stan, P. Cristea. Simulations of heat and oxygen diffusion in UO₂ nuclear fuel rods. *J. Nuclear Materials*, 359, 3, pp. 174–184 (2006).
6. J.N. Shadid, R. Hooper. Trilinos Pellet Transport Example Code.
<http://trilinos.sandia.gov>.

Investigations of a long-distance 1000 MW heat transport system with apros simulation software (3-2056)

Matti Paananen, Tommi Henttonen
Fortum Nuclear Services Ltd.
P.O. Box 100, 00048 Fortum, Finland
e-mails: Matti.Paananen@fortum.com, Tommi.Henttonen@fortum.com

This paper presents a computer model and simulation results for a long-distance heat transport system. The modeled system is designed to transport 1000 MW of heat over a distance of 77 km for district heating purposes. This kind of a nuclear CHP option is being investigated as one option within Fortum's new Loviisa 3 NPP project. The heat produced in Loviisa NPP would be utilized for the district heating of Helsinki metropolitan area in Finland. The objective of this study is to carry out simulations to examine the behaviour of such a large-scale heat transport system and to perform safety analyses for the purposes of preliminary planning of a heat transport system between Loviisa and Helsinki. The model was created using APROS (Advanced Process Simulation Environment) simulation software.

The behavior of the heat transport circuit is simulated in both steady state and several transient cases. Several variations of pump trips and leaks from the circuit into the surrounding service tunnel are simulated and their effects in the pipeline are investigated. The safety risks of the transients are analyzed. Major leaks cause the pressure in the circuit to fall drastically. The tripping of pumps can also cause hazardous pressure transients. However, the consequences of the transients can be substantially limited with proper safety systems.

Fatigue relevant temperature fluctuations at the inner pipe surface estimated from the measured outer surface temperatures (3-2106)

Boštjan Zafošnik, Leon Cizelj
"Jožef Stefan" Institute
Jamova 39, SI-1000 Ljubljana, Slovenia
e-mails: bostjan.zafosnik@ijs.si, leon.cizelj@ijs.si

Temperature fluctuations could lead to the fatigue of the of nuclear power plant components. It is therefore important to detect and record at least those temperature fluctuations, which are sufficient to cause stress amplitudes in excess of the fatigue limit.

In many nuclear power plants dedicated systems were installed to measure the temperature of the pipes. On one side, it is clear that the fluid driven temperature fluctuations are affecting the inner surface of the pipes. On the other side, to keep the reactor coolant pressure boundary intact it is usually necessary to measure the temperatures at the pipe outer surface. To estimate the temperature fluctuations at the tube inner surface from the measured temperatures at the tube outer surface remains a not yet completely solved challenge.

A model using closed form solutions for nonstationary heat transfer through cylindrical geometries is proposed. The boundary conditions are prescribed time varying temperatures at the inner surface and zero heat flux (ideal insulation) at the outer surface. The nonstationary temperature distributions through the pipe wall are then calculated, followed by the estimation of the nonstationary thermal stresses. In addition, the pipe stresses due to the internal pressure could be calculated. From these stresses combined, the model predicts the partial fatigue usage factor. The closed form provides very fast and reasonably accurate solutions. Moreover, it conveniently facilitates the development of inverse solutions.

Additional features of the model include provision to account of the accuracy of the thermocouples used to measure the temperatures.

The immediate results of the model given the inside temperature fluctuations are nonstationary temperature fields through the tube wall thickness together with thermal and internal pressure stresses and partial usage factors. Less obvious results include:

1. Estimates of amplitudes of the distinct surface temperature spikes which are masked by the pipe wall and could not be detected by the measurement at the pipe outside surface. Those amplitudes are given as

a function of the duration of the spike and accuracy of the measurement device at the outside surface.

2. Estimate the amplitudes of the periodic inner surface temperature fluctuations which are masked by the pipe wall and could not be detected by the measurement at the pipe outside surface. Those amplitudes are given as a function of fluctuation frequency and accuracy of the measurement device at the outside surface.

Results are presented graphically for a set of typical piping geometries and using the material parameters typical for the austenitic stainless steels. An example for a typical 12" pipe also illustrates the amplitudes, frequencies and partial usage factors of the periodic temperature fluctuations at the inner pipe surface, which could not be detected using outside thermocouples with sensitivity of $0,1^{\circ}\text{C}$.

The variability of the temperature along the circumference of the pipe and introduction of the film coefficient at the inner surface are among the obvious future development directions of the model.

Application of CFD code PHOENICS for simulating cyclone separators (3-2459)

Anu Dutta, B. Gera, Pavan K. Sharma⁺, R.K. Singh, A.K. Ghosh, H.S. Kushwaha
Reactor Safety Division, Health Safety and Environment Group
Bhabha Atomic Research Centre, Trombay, Mumbai, India 400085
⁺e-mail: pa1.sharma@gmail.com

Keywords: separator, CFD, IPSA, PHOENICS, two-phase flow

Cyclone separators are widely used in the field of air pollution control, gas–solid separation for aerosol sampling and in many industries like power plants, sand plants etc. In cyclone separators the air flow enters the cyclone through a tangential inlet, generates a swirling flow that forces entrained particles radially outward and leaves via an axial outlet pipe at the top of the cyclone. The rotational fluid motion is generated from the energy obtained from the fluid pressure gradient. This rotational motion causes the particle to separate relatively fast due to the strong acting forces. The cyclone separator is very useful engineering equipment with no moving parts and virtually no maintenance. It enables particles of micrometers in size to be separated from a gas moving at about 15 m/s without excessive pressure-drop.

This work presents a computational fluid dynamics (CFD) calculation to investigate the flow field in a tangential inlet cyclone which is mainly used for the separation of the moisture from an air stream. Three-dimensional, steady state Eulerian simulations of the turbulent gas–droplet flow in a cyclone separator have been performed. Numerical simulation was carried out using CFD code PHOENICS for the given geometry of separators available in literature. The IPSA (Inter-Phase-Slip Algorithm) method has been utilized which entails solving the full Navier-Stokes equations for each phase. The turbulence was modeled with standard k- ϵ turbulence model. The liquid droplet was modeled as particle of size 200 μ and density 1020 kg/m³. The volume fraction of moisture was 1% at inlet and outlet volume fraction was predicted with CFD. The results were in good agreement with the reported results. This knowledge can be further extended for other two phase flow applications in nuclear industry.

Systematic errors in the numeric analyses of computer programs used for the determination of the flexible structure seismic response (3-2489)

Viorel Serban, Marian Androne

Subsidiary of Technology and Engineering for Nuclear Projects – SITON

At present, the determination of the building seismic response is being done by finite element computer models, by in-time or frequency dynamic response analyses.

For the in-time analyses, the computation is merely the solving of a differential equation system of 2nd degree in the relative displacement variables, x , for which the initial conditions (displacement and velocity at $t = 0$) need to be specified.

All the current computer programs known by the authors, consider $x_0 = 0$ and $\dot{x}_0 = 0$ as initial conditions. The initial relative velocity cannot be zero when the initial displacement is zero and considering it null together with the initial displacement, is introducing errors in the determination of the building seismic response. These errors are important when speaking about flexible buildings such as tall buildings, seismically isolated buildings or buildings where plastic hinges are accepted and when the main eigen periods due to degradation are long.

Some recorded or generated accelerograms, also include harmonic components of long and very long period (which may be due to the measurement instrument or its location or due to the time-history generation process) which alter the calculated seismic response of the structures, especially in respect of seismic isolation issues.

Especially for flexible structure, the response in displacements could be overestimated due to the dependence on the square of long vibration period, while the response in accelerations does not show this type of dependence.

The presence of long periods in accelerograms, even very low in amplitude, leads to high resonance amplifications in the displacements around that long period, proportionally with the period square.

The paper is an evaluation of the computation errors resulted from the computer programs employed today (the examples are based on the results obtained with a well known computer program) in the calculations for structures and it also includes solutions to eliminate such errors. Also, the errors occurring in the determination of the relative displacement response spectra for recorded earthquakes are presented and their influences in the seismic qualification solution are estimated.

Chained computations using an unsteady 3D approach for the determination of thermal fatigue in a T-junction of a PWR nuclear plant (3-2494)

Thomas Pasutto¹, Christophe Péniguel², Marc Sakiz³

¹EDF R&D, Fluid Mechanics and Heat Transfer

6, quai Watier, 78401, Chatou, France

e-mails: ¹thomas.pasutto@edf.fr, ²christophe.peniguel@edf.fr, ³marc.sakiz@edf.fr

Abstract – Thermal fatigue of the coolant circuits of PWR plants is a major issue for nuclear safety. The problem is especially acute in mixing zones, like Tjunctions, where large differences in water temperature between the two inlets and high levels of turbulence can lead to large temperature fluctuations at the wall. Until recently, studies on the matter had been tackled at EDF using steady methods: the fluid flow was solved with a CFD code using an averaged turbulence model, which led to the knowledge of the mean temperature and temperature variance at each point of the wall. But, being based on averaged quantities, this method could not reproduce the unsteady and 3D effects of the problem, like phase lag in temperature oscillations between two points, which can generate important stresses. Benefiting from advances in computer power and turbulence modeling, a new methodology is now applied, that allows to take these effects into account. The CFD tool Code_Saturne, developed at EDF, is used to solve the fluid flow using an unsteady L.E.S. approach. It is coupled with the thermal code Syrthes, which propagates the temperature fluctuations into the wall thickness. The instantaneous temperature field inside the wall can then be extracted and used for structure mechanics computations (mainly with EDF thermomechanics tool Code_Aster).

The purpose of this paper is to present the application of this methodology to the simulation of a straight Tjunction mock-up, similar to the Residual Heat Remover (RHR) junction found in N4 type PWR nuclear plants, and designed to study thermal striping and cracks propagation. The results are generally in good agreement with the measurements; yet, in certain areas of the flow, progress is still needed in L.E.S. modeling and in the treatment of instantaneous heat transfer at the wall.

I. INTRODUCTION

Thermal fatigue of the coolant systems of PWR plants is a major issue for nuclear safety. The problem is especially acute in mixing zones, like T-junctions, where a large difference of water temperature between the two entry branches and the high level of turbulence can lead to large temperature fluctuations at the wall. Civaux N4 class reactor was shut down in may 1998 following a leak of primary coolant from a pipe in the Residual Heat Removal (RHR) system. Cracks have been discovered in the elbow following the T-junction, that were clearly the result of thermal fatigue. Since then, the RHR pipeworks have been redesigned at all four EDF's N4 units and a large research program has been launched to address this issue. One of its contents is a cooperation with CEA and Framatome ANP on the study of a real-scale model of straight Tjunction, based on the RHR junction geometry, on which fine near-wall and in-wall temperature measurements are performed. The aim of

this model is to get a better understanding of the thermal loads seen by the structure in such situation and to evaluate the capacity of numerical simulation to reproduce it. The present paper deals with this last aspect. In order to capture the physics properly, instantaneous thermohydraulic phenomena, thermal coupling between the fluid and the solid, as well as the thermal conduction inside the wall have to be accounted for. These aspects are described in detail in the present paper. Eventually, the 3D instantaneous solid temperature fields obtained by simulation are used to compute the resulting mechanical stresses [1]. But this last aspect is beyond the scope of this paper.

II. NUMERICAL APPROACH OF INSTANTANEOUS THERMOHYDRAULIC PHENOMENA

3. Applied Computations, Simulation and Animation

The characteristics of the flows in mixing zones usually involve a high level of turbulence. Hence, Direct Numerical Simulation is totally out of reach of even the most powerful computers. On the other hand, Reynolds Averaged Navier Stokes models (like $k-\epsilon$ or more advanced models) can deal with such flows rather easily. Yet, they sometimes lack accuracy in specific complex areas of the flow, and most of all they can only yield mean or low order averaged quantities, thereby overlooking any high frequency instantaneous aspects, which are yet essential in thermal fatigue studies. In the last few years, the growing of computer capacity has made mixing zones configuration accessible to a third and intermediate technique : Large Eddy Simulation. In LES, only the smaller scales of turbulence are modeled, whereas the large energy carrying structures are computed directly. Thus, LES provides 3D time dependent solutions, on which any kind of signal processing can be done, at much higher Reynolds numbers than DNS.

I.I.A. The CFD tool Code_Saturne

The EDF finite volume CFD code, *Code_Saturne*, is used to solve Navier-Stokes equations on unstructured meshes. The flow is assumed incompressible and Newtonian and the density is only a function of temperature. Using LES, the filtered Navier-Stokes equations can be written as follows (the filtering operator is omitted used for clarity sake), together with the equation for the temperature.

$$\frac{\partial p}{\partial t} + \frac{\partial \rho U_j}{\partial x_j} = 0 \quad (1)$$

$$\begin{aligned} \rho \frac{\partial U_i}{\partial t} + \rho U_j \frac{\partial U_i}{\partial x_j} = & - \frac{\partial p^*}{\partial x_i} + \frac{\partial}{\partial x_j} \left[\mu_c \left(\frac{\partial U_i}{\partial x_j} + \frac{\partial U_j}{\partial x_i} \right) \right] \\ & - \frac{2}{3} \frac{\partial}{\partial x_i} \left(\mu_c \frac{\partial U_j}{\partial x_j} \right) + (\rho - \rho_0) g_i \end{aligned} \quad (2)$$

$$\rho \frac{\partial T}{\partial t} + \rho U_j \frac{\partial T}{\partial x_j} = \frac{\partial}{\partial x_j} \left[\left(\frac{\lambda}{C_p} + \frac{\mu_t}{\sigma} \right) \frac{\partial T}{\partial x_j} \right] \quad (3)$$

In these equations, U_i are the filtered components of the velocity, p^* stands for the pressure (minus the reference hydrostatic pressure), μ_c represents $\mu + \mu_t$ where μ and μ_t are respectively the molecular and subgrid-scale viscosities. T is the temperature, λ , C_p and σ respectively the fluid conductivity, specific heat and turbulent Prandtl number. It should be noted that in $k\epsilon$ approaches, the turbulent viscosity models the turbulent effects on the whole energy spectrum, whereas in LES the subgrid viscosity only represents the small scale structures (high frequencies). In our computations, both a Smagorinsky model [2] and a more complex dynamic model [3] have been

used to calculate the sub-grid viscosity. Concerning the near-wall modeling, our computations rely on a regular wall function. More details on LES in *Code_Saturne* can be found in [4], [5] and [6].

Before taking on the study presented here, *Code_Saturne* has been tested on a large number of academic and industrial validation cases (homogeneous turbulence, channel flows, tube bundles, T-junction, coaxial jet, ...).

I.I.B. Numerical Technique Used for Solving the Fluid Equations

In the collocated finite volume approach used in *Code_Saturne*, all variables are located at the centers of gravity of the cells (which may take any shape). The momentum equations are solved by considering an explicit mass flux (the three components of the velocity are thus uncoupled). Velocity and pressure coupling is insured by a SIMPLEC prediction/correction method with outer-iterations [7]. The Poisson equation is solved with a conjugate gradient method. The collocated discretisation requires a Rhie and Chow interpolation in the correction step to avoid oscillatory solutions [8]. This interpolation has been used in the present application, although it doesn't seem essential for unstructured meshes. For L.E.S. calculations, second order schemes are used in space (fully centered scheme for the velocity components, centered scheme with slope test for the temperature) and time (Crank-Nicolson with linearised convection). A second order Adams-Bashforth method is used for the part of the diffusion involving the transposed velocity gradient, to keep the velocity components uncoupled.

I.I.C. The Solid Code Syrthes

The solid code Syrthes relies on a finite element technique to solve the following general heat equation where all properties can be time, space or temperature dependent.

$$\rho C_p \frac{\partial T}{\partial t} = \frac{\partial}{\partial x_j} \left(k_s \frac{\partial T}{\partial x_j} \right) + \Phi_v \quad (4)$$

T is the temperature, Φ_v a volumic source or sink, ρ and C_p , respectively the density and the specific heat. k_s (a matrix when the material is anisotropic) designates the conductive behaviour of the medium. Radiation phenomena from wall to wall can also be taken into account. For optimization reasons, only two kinds of elements have been retained (6 nodes triangles in 2D, 10 nodes tetrahedra in 3D). More details on the possibilities of the finite element

code Syrthes can be found in [9]. Like *Code_Saturne*, Syrthes has been checked thoroughly against experimental and analytical test cases proving that it provides very accurate solutions in problems similar to the present one.

II.D. The Solid Code Syrthes

At the interface, every time step, the thermal coupling is performed. Let T_s be the temperature of the solid node at the interface, and T_f the temperature of the corresponding first node in the fluid domain. At the beginning of time step (n), *Code_Saturne* receives from Syrthes the value of $T_s^{(n)}$ and uses it to calculate the exchange coefficient $h^{(n)}$, defining the heat flux at the wall by $\phi = h(T_s - T_f)$ and sends its value to Syrthes. Then, the two codes work separately. *Code_Saturne* calculates $T_f^{(n+1)}$ implicitly considering the heat flux $\phi^{(n+1)} = h^{(n)}(T_s^{(n)} - T_f^{(n+1)})$ whereas Syrthes calculates $T_s^{(n+1)}$, also implicitly, considering the flux $\phi^{(n+1)} = h^{(n)}(T_s^{(n+1)} - T_f^{(n)})$. The system is then ready to perform the next time step.

III. CONFIGURATION AND SIMULATION PARAMETERS

III.A. Physical Parameters

The global geometry of the mock-up is shown on figure 1. In this specific study, the horizontal hot branch and the vertical cold branch are set respectively at a temperature of 204°C and 41°C. The total flow rate is set to 260 m³/h and the velocity ratio between the cold flow branch and the total flow rate is 20%. The physical properties of the fluid and the solid (density, viscosity, diffusivity, ...) are calculated using polynomial approximations that were defined by regressions over a sample of values taken from a in-house database, in the considered range of temperature.

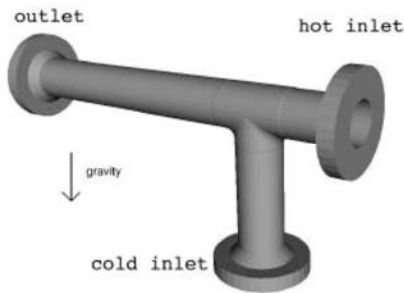


Figure 1: General view of the mock-up

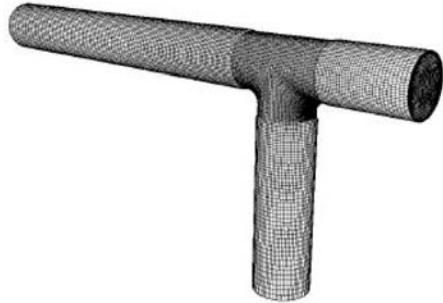


Figure 2: Fluid mesh (500 000 cells)

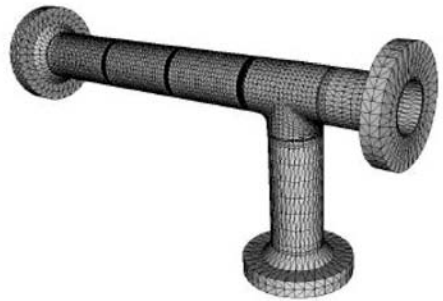


Figure 3: Solid mesh

III.B. Meshes

In order to solve the former equations numerically, the geometry has to be discretised. Here the mesh generators GiBi and Ideas have been used. Two fluid meshes have been generated, containing roughly 500 000 and 1 000 000 hexaedric cells (cf. figure 2). The solid mesh is presented in figure 3. It contains 370 000 nodes and 260 000 tetraedra. Figure 4 presents a close view of the solid mesh to underline how fine the discretisation is, especially near the fluid/solid interface. Previous mechanical studies have determined that an optimal spatial discretisation (for the mechanical stresses computation taking place afterwards) is of the order of 100 µm for the first element, i.e. the first solid node within the wall is only 50 µm away from the interface.

3. Applied Computations, Simulation and Animation

The instantaneous temperature variation of the wall should therefore be well captured.

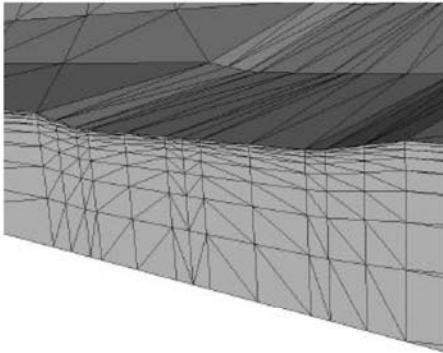


Figure 4: Solid mesh - detail of the discretisation at the fluid interface

III.C. Initial and Boundary Conditions

Initial conditions for the fluid flow present no problem, as they are evacuated very rapidly. It is however not the case for the solid, where at least 30 s of physical time would be necessary to wipe them off, which would be unrealistic to simulate with LES. Therefore a specific strategy is used. First the fluid flow is initialized over a few seconds, without any solid coupling (zero heat flux at the wall). Then, a semi-coupled calculation is started over a few seconds: the fluid temperature and exchange coefficient are calculated by *Code_Saturne* and send to Syrthes, but the effective boundary conditions for the fluid are still zero heat flux. At each point of the fluid/solid interface, the mean temperature and mean exchange coefficient are calculated. These values are then used as boundary conditions for a solid-only thermal computation with Syrthes over two hours of physical time. Hence the temperature field in the solid is in accordance with the fluid flow. After that, the proper fully coupled calculation is started.

Due to mesh limitations, the distance from the wall of the first calculation point in the fluid can be as large as 300 wall units for the coarser mesh, and 170 for the finer. Velocity and temperature boundary conditions therefore use usual wall functions. As for the entry conditions in the fluid, LES method requires to specify the instantaneous velocity. The mean part is estimated from the mean flow rate in each branch, and random drawings are made at each entry point and at each time step, following a centered

gaussian distribution, for the fluctuating part. The RMS value of the distribution is evaluated from the turbulence level expected in such a pipe flow. Other tests have been made using a more physical method of synthetic vortex creation, but it yields limited differences.

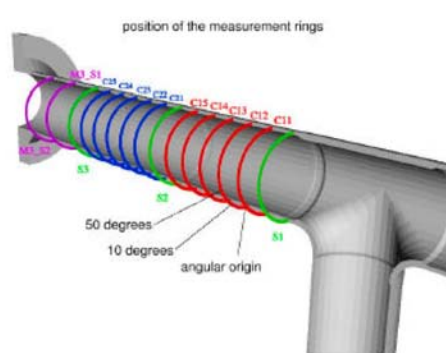


Figure 5: Position of the measurement probes

IV. COMPUTATIONAL RESULTS

These calculations give access to unsteady results on the entire solid and fluid domains. 10 s of physical time have been simulated for the Smagorinsky model on the coarser mesh, which corresponds to an already very large computational effort (around 1000 hours of CPU on a Fujitsu VPP5000 vector machine)¹. Calculations with the dynamic model have been made on 32 parallel Alpha processors. 10 s of physical time have been simulated for a CPU time of 500 hours per processor. Results are mainly presented on different sections and the symmetry plane for which experimental measurements are available on site. These sections are pointed out in figure 5. All thermal results are presented in non-dimensional variables; let T_{cold} and T_{hot} be the cold and hot temperatures in the branches, the non-dimensional temperature and RMS temperature are calculated as:

$$T_{a,dim} = \frac{T - T_{cold}}{T_{hot} - T_{cold}} \text{ which varies between 0 and 1}$$

$$\sigma_{T,dim} = \frac{\sqrt{T''T''}}{T_{hot} - T_{cold}}$$

¹ due to computing limitations, only 2 s of physical time have been simulated with the Smagorinsky model on the finer mesh

Unless specified, the results presented in this paper correspond to the simulation with the coarser mesh and Smagorinsky model.

Figure 6 presents the instantaneous fluid velocity field in the symmetry plane at the physical time $t=10$ s. Figure 7 gives a snapshot of the fluid instantaneous temperature field. One may notice the strong irregularity of the stratification and the turbulent eddies created at the hot/cold interface and convected further away.

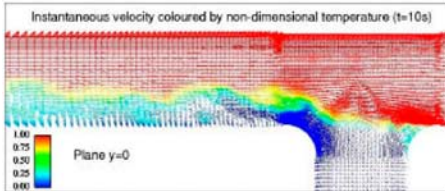


Figure 6: Instantaneous velocity field in the symmetry plane, coloured by the non-dimensional temperature, at time $t=10$ s

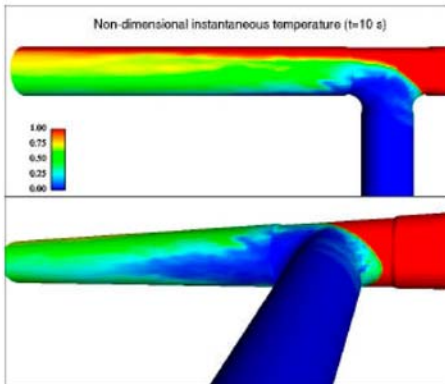


Figure 7: Instantaneous non-dimensional temperature, at time $t=10$ s

Figure 8 presents the mean velocity field in the symmetry plane and shows the recirculation downwind from the junction of the two branches. This recirculation reattaches around section C12.

Figures 9 and 10 respectively present the mean and the RMS temperature (obtained by time averaging of the instantaneous temperature field). Figure 11 shows the instantaneous temperature in the solid, at time $t=10$ s. It is clear that the field is much smoother than in the fluid (cf.

fig. 7), because of the strong attenuation due to the thermal inertia of the wall.

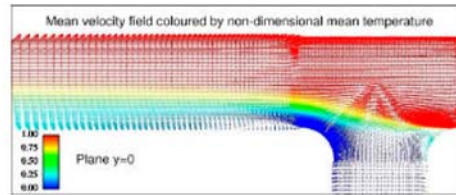


Figure 8: Mean velocity field in the symmetry plane, coloured by the mean non-dimensional temperature

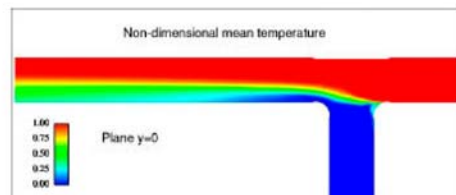


Figure 9: Mean non-dimensional temperature in the symmetry plane

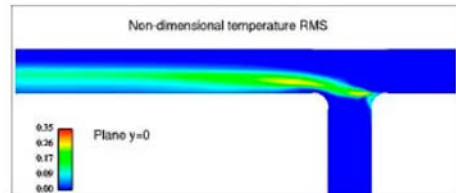


Figure 10: Non-dimensional temperature RMS in the symmetry plane

IV.A. Temperature Evolution at the Fluid/Solid Interface

The focus is put on points located at the fluid/solid interface, corresponding to experimental probes on the mock-up. Figures 12 and 13 point out, on the C12 ring, the strong attenuation of the temperature signal of the wall compared to the very fluctuating temperature signal of the fluid in the near wall region. The angular positions of the probes on the ring are 50 degrees for figure 12 and 10 degrees for figure 13 (cf. fig. 5). These probes will be further

3. Applied Computations, Simulation and Animation

referenced as C1250 and C1210. This attenuation is due to the thermal inertia of the wall and is strongly dependent on the frequency of the fluctuations. This dependence is naturally reproduced by our unsteady simulation, whereas it is totally unreachable through averaged R.A.N.S. based approaches. Also, these figures show the large difference in the level of thermal fluctuations between probe C1210, located in the cold stratification, and probe C1250, closer to the hot/cold interface.

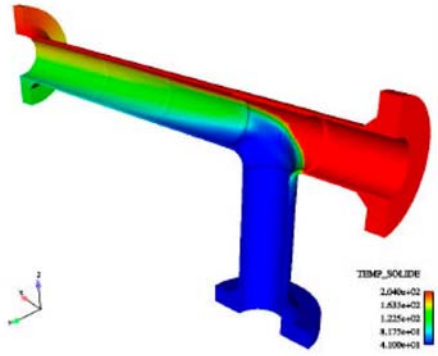


Figure 11: Instantaneous non-dimensional temperature in the solid at time $t=10$ s

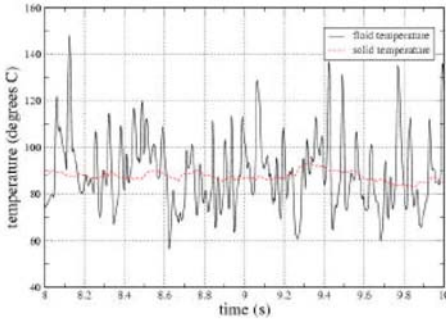


Figure 12: Fluid and solid temperature at the fluid/solid interface, probe C1250

IV.B. Temperature Evolution within the Wall

As expected, the temperature fluctuation are extremely attenuated as soon as one considers points located further inside the wall. To give an overview, figure 14 presents the

RMS temperature decrease through the wall for probes on ring C25 at angle 50 degrees. This confirms the importance of solid mesh refinement at the fluid/solid interface.

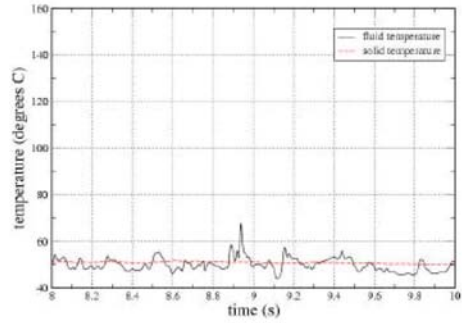


Figure 13: Fluid and solid temperature at the fluid/solid interface, probe C1210

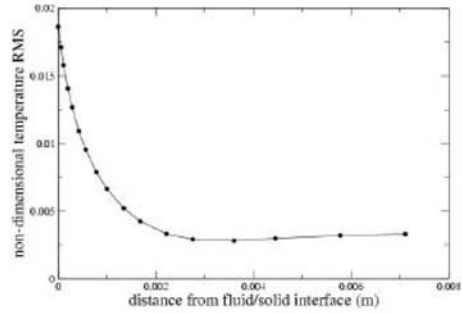


Figure 14: Attenuation of the non-dimensional temperature RMS through the wall thickness

V. COMPARISON WITH EXPERIMENTAL DATA

The results of our simulations will now be compared to experimental data taken from mock-up measurements.

V.A. Mean Temperature along Measurement Rings

Figures 15 and 16 show the comparisons between the measurements and the three simulations for the non-dimensional temperature in the fluid, at the wall on rings C12 and C24. The sensitivity of the mesh refinement and of the subgrid-scale model can clearly be seen. Indeed, on the finer mesh, the Smagorinsky model yields correct results on

ring C12, but the comparison deteriorates along the flow, probably because of the known difficulty of LES models to capture reattaching flows. On the coarser mesh, the Smagorinsky model yields a larger error close to the junction, but the comparison is strangely better towards ring C24. This might be due to error compensations rather than proper increase in precision. The third calculation, with the dynamic model, was proposed to try and get proper results at the junction that would not deteriorate after reattachment. Indeed it does give a more uniform behaviour, with proper comparison with the measurement all along the flow on the side of the pipe. Yet, there is a definite overestimation of the temperature on the lower part of the sections (angle=0).

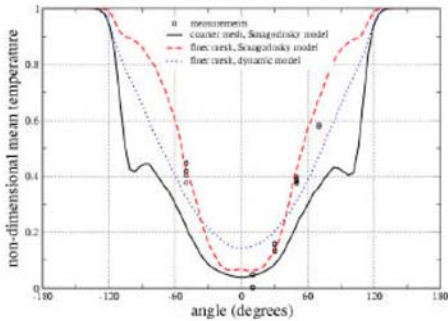


Figure 15: Mean fluid non-dimensional temperature profile at the wall on ring C12

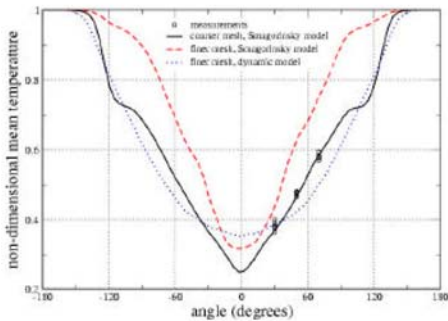


Figure 16: Mean fluid non-dimensional temperature profile at the wall on ring C24

V.B. Time Evolution and Spectral Analysis

Figures 17 and 18 show the evolution of the instantaneous temperature in the fluid at probes C1250 and C1210, over 2 seconds of physical time, taken from experimental data and from the simulation. It shows reasonable agreement between both as far as the temperature RMS and frequencies are concerned. It should be noted that the sampling rate is much larger in the simulation. This is especially visible on probe C1250 (figure 17). Results with the dynamic model are not shown here. They largely overestimate the temperature fluctuations at the wall.

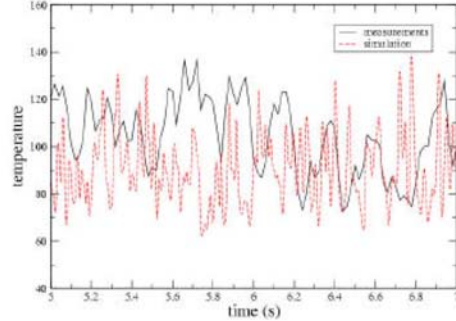


Figure 17: Comparison between measurements and simulation results for the instantaneous fluid temperature at probe C1250

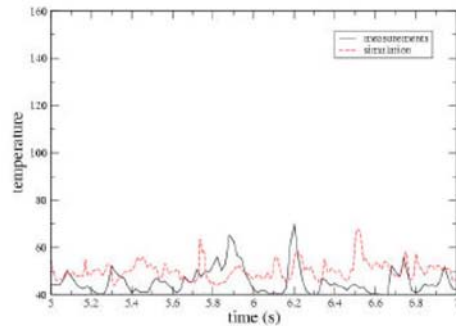


Figure 18: Comparison between measurements and simulation results for the instantaneous fluid temperature at probe C1210

Figures 19 and 20 show the evolution of the instantaneous temperature in the solid at probes C1250 and C1210, over 10 seconds of physical time, taken from

3. Applied Computations, Simulation and Animation

experimental data and from the simulation. If results at probe C1250 still show reasonable agreement, it is not the case at probe C1210, where the simulation greatly underestimates the temperature fluctuations. Since the fluctuations in the fluid are correctly simulated (fig. 18), it shows that the error originates in the treatment of the fluid/solid interaction. Indeed the use of wall functions is not so appropriate for LES computations, and especially in the area of probe C1210, which corresponds to the reattachment point at the end of the recirculation.

These results are corroborated by figures 21 and 22 which show the Power Spectral Density Function for the solid temperature at probes C1250 and C1210. Reasonable agreement is shown on probe C1250, while large underestimation of temperature RMS is predicted at probe C1210.

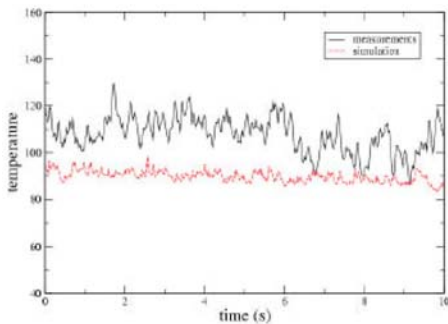


Figure 19: Comparison between measurements and simulation results for the instantaneous solid temperature at probe C1250

VI. CONCLUSION AND PERSPECTIVES

This paper presents a numerical approach able to address thermal fatigue problems occurring in pipeworks and its application to the simulation of a T-junction mock-up. A Large Eddy Simulation turbulent model implemented in EDF's CFD tool *Code_Saturne* yields instantaneous velocity and temperature fields. The thermal coupling with the finite element thermal code *Syrthes* allows to have access to the instantaneous thermal field inside the wall. These solid thermal fields can then be exploited with a mechanical tool to obtain thermally induced stresses. Different meshes and subgrid-scale models (Smagorinsky and dynamic) have been used on this study. As far as the fluid temperature is concerned, the simulation results

compare fairly well with the mock-up measurements. The Smagorinsky model shows difficulties dealing with the reattachment after the recirculation. The dynamic model shows a more uniform behaviour, but largely overestimates the temperature fluctuations at the wall and the temperature in the lower part of the mixing branch.

At the fluid/solid interface, heat transfer from the fluid to the wall is taken into account by standard wall functions. Although they seem to work quite well in some parts of the flow, they strongly overestimate the attenuation of the temperature fluctuations at the fluid/solid transfer in specific areas, like the recirculation zone, leading to a large error in solid temperature fluctuations.

Therefore, further efforts and theoretical developments are still needed for the subgrid-scale model and the near wall modeling. Also, although this methodology seems promising and is becoming more and more affordable as computer power increases, it is still very costly in terms of CPU time and computing memory.

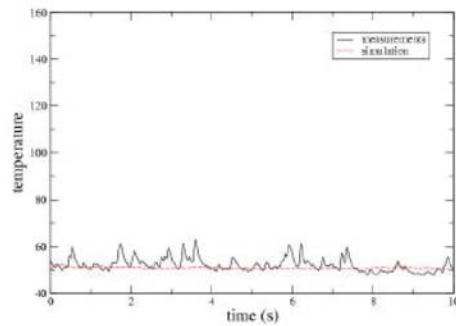


Figure 20: Comparison between measurements and simulation results for the instantaneous solid temperature at probe C1250

REFERENCES

1. J.M. STEPHAN, C. PENIGUEL, P. GENETTE, F. CURTIT, M. SAKIZ, . PASUTTO, S. SZALENIEC, "Evaluation of Thermal Sollicitations and Stresses in Piping's Mixing Zones", Proceedings of ASME PVP05 Conference, Denver, Colorado, USA (2005).
2. J. SMAGORINSKY, "General circulation experiments with the primitive equations, part I: the basic experiment", *Monthly Weather Rev.*, **91**, 99-164 (1963).

3. M. GERMANO, U. PIOMELLI, P. MOIN, W.H. CABOT, "A dynamic subgrid scale eddy viscosity model", *Proceedings Summer Workshop*, Center for Turbulent Research, Stanford, California, USA (1990).
4. S. BENHAMADOUCHE, D. LAURENCE, "LES, coarse LES and transient RANS comparisons on the flow across a tube bundle", *Proceedings of 5th Int Symp on Engineering Turbulence Modelling and Measurements*, W Rodi and N. Fueyo Edts, Elsevier, Mallorca, Spain (2002).
5. S. BENHAMADOUCHE, K. MAHESH, G. CONSTANTINESCU, "Collocated Finite Volume Schemes for L.E.S. on Unstructured Meshes", *Proceeding of the 2002 Summer program*, Center for Turbulent Research, Stanford, California, USA (2002).
6. C. PENIGUEL, M. SAKIZ, S. BENHAMADOUCHE, J.M. STEPHAN, C. VINDERINHO, "Presentation of a Numerical 3D Approach to Tackle Thermal Striping in PWR Nuclear T-Junction", ASME PVP Conference, Cleveland, USA (2003).
7. J.H. FERZIGER, M. PERIC, *Computational Methods for Fluid Dynamics*, Springer, third edition (2002).
8. C.M. RHIE, W.L. CHOW, "A Numerical Study of a Turbulent Flow past an Isolated Airfoil with Trailing Edge Separation", *AIAA J.*, **21**, 1525-1532 (1983).
9. I. RUPP, C. PENIGUEL, "Coupling Heat Conduction, Radiation and Convection in Complex Geometries", *Int Journal of Numerical Methods for Heat and Fluid Flow*, **9** (1999).

Figure 21: Power spectral density function for solid temperature at probe C1250

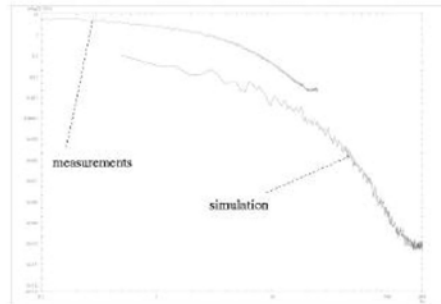
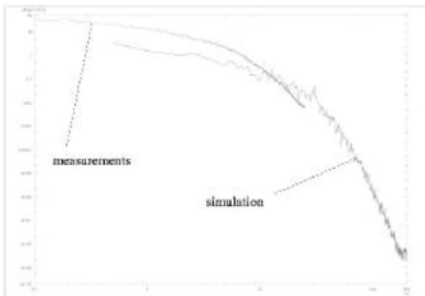


Figure 22 : Power spectral density function for solid temperature at probe C1210



Simulation of an impact test with a deformable missile on a concrete wall (3-2502)

Heckötter Christian, Sievers Jürgen
Gesellschaft für Anlagen- und Reaktorsicherheit (GRS) mbh
Reactor Safety Research – Barrier Effectiveness
Schwertnergasse 1 50667 Cologne, Germany
e-mails: Christian.Heckoetter@grs.de, Juergen.Sievers@grs.de

Reinforced concrete structures are used to protect vital parts and equipment of nuclear power plants. In areas with dense air traffic the external containment buildings have been traditionally designed to resist accidental impact loads. Recent events have shown that also a civil aircraft can be used as weapon for intentional sabotage, emphasizing the need to consider more carefully impact load determination when assessing and designing protective structures of nuclear power plants.

In the framework of the reactor safety research program of the German Federal Ministry of Economics and Technology GRS has started to validate the structure mechanics analysis method based on the nonlinear dynamic software ANSYS AUTODYN with respect to its capability to simulate the impact of deformable missiles on resistant barriers. For the validation of analysis models to determine the mechanical load assumptions and the consequences, small scale tests on the fragmentation of fragile projectiles when impacting on solid targets are performed at different test facilities.

The paper summarizes a study using ANSYS AUTODYN simulations of an impact test with a thin-walled aluminum missile on a reinforced concrete wall performed at the Technical Research Centre of Finland VTT. The comparison of numerical results with measured data shows satisfactory results especially concerning the deformation of the concrete wall and the fragmentation of the missile. Relevant influence parameters on the results are the boundary conditions, the mesh size, strain rate sensitive material properties and the damping which have to be chosen adequately.

Thermal and structural analysis of calandria vessel of a PHWR during a severe core damage accident (3-2536)

S.V. Prasad, R.K. Singh, A.K. Nayak*, M.G. Andhansare,
P.K. Vijayan, D. Saha
Reactor Engineering Division, Bhabha Atomic Research Centre
Trombay, Mumbai 400085, India
*e-mail: arunths@barc.gov.in
Fax: 91-22-25505151

In a hypothetical severe core damage accident in a PHWR, multiple failure of core cooling systems may lead to collapse of pressure tubes and calandria tubes, which may ultimately relocate inside the calandria vessel forming a debris bed. The debris bed which is at high temperature and still generating the decay heat, is cooled by the overlaying heavy water in the debris. However with time this water gets evaporated and what remains after sometime, is the hot dry debris bed generating a lot of heat. The debris ultimately melts down and forms a corium molten pool in the lower head of the calandria vessel. The molten corium pool is surrounded by calandria vault water which works like the ultimate heat sink. However, a few unresolved issues on this phenomenon are;

- i. How long the vault water can act as heat sink and after that how the calandria vessel fails?
- ii. If cold water is continuously required to replenish the evaporating water in the calandria vault as a part of severe accident management safety, then what is the rate at which the decay heat is removed from corium molten pool and nature of the thermal stress pattern built-up in the calandria vessel?

In the present study, a numerical analysis is performed to evaluate the thermal loads and the stresses due to that in the calandria vessel following the above accident scenario. The heat transfer from the corium molten pool to the surrounding is assumed to be by a combination of radiation, conduction through the wall of calandria vessel and convection from calandria vessel wall to vault water. From the temperature distribution in the vessel wall, the transient thermal loads have been evaluated. The strain rate and the vessel failure in the lower head has been evaluated for the above two scenario.

Crack formation and water ingression phenomena in top flooded corium molten pool (3-2537)

Arun Kumar Nayak, Raj Kumar Singh, Parimal P. Kulkarni, B.R. Sehgal*,
P.K. Vijayan, A. Rama Rao, D. Saha, R.K. Sinha
Reactor Engineering Division, Bhabha Atomic Research Centre
Trombay, Mumbai 400085, India
*Royal Institute of Technology, Stockholm, Sweden

During a postulated severe accident in a LWR, the core can melt and the melt can fail the reactor vessel. Subsequently, the molten corium can be relocated in the containment cavity forming a melt pool. The corium melt pool interacts with the concrete basement, which eventually results in significant change in its properties with erosion of concrete and its inclusion into the molten pool. One of the convenient severe accident management strategy is to flood the corium molten pool from the top so as to quench and terminate the severe accident progression. However, the question that arises is to what extent the water can ingress in the corium melt pool to cool and quench it. The extent of water ingression depends on the mechanics of crack formation and the heat generation rate or the limiting dryout heat flux in the melt pool. Cracks can occur in the solidified crust depending on the temperature distribution in it, when the corium melt is quenched at its top due to the overlaying water. However, there are certain unresolved issues. For example, whether the crack formation is sudden and discrete or it occurs at a continuous rate. Why the crack formation stops after certain depth below the top of the pool. What are the important physical properties of the materials which affect the crack formation rate. To reveal that, a numerical study has been carried out using the computer code MELCOOL. The code considers the heat transfer behaviour in axial and radial directions from the molten pool to the overlaying water, crust generation and growth, thermal stresses built-in the crust, disintegration of crust into debris, natural convection heat transfer in debris and water ingression into the debris bed. The predictions of the code were validated with the test data of COMECO (COre MELt COolability). The code was found to simulate the quenching behaviour, nature of crack formation and depth of water ingression quite reasonably. A parametric study was carried out to reveal the effect of physical and mechanical properties of melt on crack formation and water ingression.

A statistical uncertainty assessment on a LOFT L2-5 LBLOCA based on ACE-RSM (3-2545)

Kwang-II Ahn¹, Bub-Dong Chung², John C. Lee³

¹Integrated Safety Assessment, KAERI, Daejeon, Korea
e-mail: kiahn@kaeri.re.kr

²Thermal-Hydraulic Safety Research Division, KAERI, Daejeon, Korea

³Nuclear Engineering & Radiological Science, Univ. of Michigan
Ann Arbor, MI, USA

Introduction

Two alternative methods for a sampling-based uncertainty analysis have been utilized to avoid the problem associated with the size of the relevant statistical samples: one is based on Wilks' formula and the other is based on the conventional nonlinear regression approach. While both approaches provide a useful means to draw a conclusion on the resultant uncertainty with a limited number of code runs, there are also the corresponding limitations. For example, a conclusion based on the Wilks' formula is highly affected by the sampled values themselves and the response surface model (RSM) based on the conventional regression approach requires a priori estimate on functional forms of a regression model (coupled with multivariate nonlinear regression analysis). The above limitation involved in the traditional RSM approach can be greatly reduced by employing the alternating conditional expectation (ACE) method. The ACE method is a generalized regression algorithm that yields an optimal relationship between a dependent variable and multiple independent variables, by maximizing the statistical correlation between the transformed dependent variable and the sum of transformed independent variables.

Aim of the work

Main objective of this paper is to introduce a complementary method (based on the ACE algorithm) to the Wilks' formula and the conventional regression approach for uncertainty analysis and to provide an example application to the OECD BEMUSE Phase III LOFT L2-5 LBLOCA PCT uncertainty analysis.

Results and conclusion

A comparison with the original MARS code results on PCT shows that except for the lower PCT values (subjected to highly nonlinear thermal-hydraulic behaviour), the formulated ACE-RSM Models relatively well trace the original code results, even with a limited number of code runs. The above results indicate that the ACE-RSM models could give an appropriate surrogate model to the original MARS code, although they also show a greater or less dependency on the utilized number of samples as in the conventional RSM yet. Such kind of dependency on the utilized number of samples could be reduced further by employing more efficient sampling schemes like the Latin Hypercube Sampling (LHS) approach.

Detailed FEA of locally thinned tight radius pipe bends (3-2575)

Usama Abdelsalam, Dk Vijay
Operations Engineering, AMEC NSS, Toronto, Ontario, Canada
e-mail: usama.abdelsalam@amec.com

Introduction/background

Carbon Steel pipes experience wall thinning due to the flow accelerated corrosion (FAC) resulting in locally thinned areas (LTA). The local thinning deteriorates the structural integrity of the piping component and fitness for continued service assessments, repair, or replacement is required. Structural fitness for service assessments provide economically sound approach that has been adopted to extend the operational life of nuclear components and equipment.

Aim of the work

This paper presents the structural integrity assessment of tight radius bends under internal pressure loading using the finite element method. The analysis follows the linear elastic rules of the ASME SEC III NB-3221. Both general and local thinning is included in the detailed three dimensional models using parametric thickness profiles. The axial and circumferential thickness profiles provide a lower bound on the measured thicknesses. A location dependent thinning rate function is developed and used to provide the predicted thickness profile at the end of the evaluation period.

Essential results

The finite element analysis is conducted using ANSYS v10.0 and the results are post-processed to show compliance with the ASME SEC III NB-3221 criteria. A comparison between the results obtained from the detailed FEA and the ASME Code Case N-579-2 is also presented.

Summary/conclusions

This paper demonstrates the effectiveness in using detailed FEA to extend the useful life of nuclear components.

References

1. Canadian Standard Association. Design Procedures for Seismic Qualification of CANDU Nuclear Power Plants. CAN3-N-289.3-M81, September 1981.
2. ASME Boiler and Pressure Vessel Code, Section III. Rules for Construction of Nuclear Power Plants, 1998.
3. Usama Abdelsalam and Dk Vijay. Finite Element Modeling of Locally Thinned Short Radius Pipe Bends. Canadian Nuclear Society CANDU Maintenance Conference CMC2008, Toronto, Ontario, November 2008.

Modeling of the fluid solid interaction during seismic event (3-2661)

Jan Vachulka

Stevenson & Associates

Office in Czech Republic, Vejprnicka 56, Pilsen, Czech Republic

e-mail: vachulka@stevenson.cz

The main aim of this paper is to present acceptable method for determining fluid-structure interaction during seismic event using standard finite element code without implemented fluid finite elements. The method is based on assumption that in-vacuum modal shapes of the structure are known and also the modal shapes of the free liquid surface are known. The mode shapes in vacuum are determined by standard finite element code and free surface modes are derived analytically or using boundary element method. The boundary condition on the fluid-structure interface is obtained semi-analytically in form of Fourier or Bessel-Fourier series for simple domains or using boundary element method for complicated fluid domains. The fluid is assumed to be irrotational and incompressible. Applying Galerkin method the system of is obtained. The system of equations is solved in time domain using Newmark integration scheme.

The seismic response of the liquid-filled tank is calculated. The calculated example shows very good agreement with the previously published. The method can be used in nuclear technology design.

References

- M. Amabili, M.P. Paidoussis, A.A. Lakis. Vibrations of partially filled circular tanks with ring stiffeners and flexible bottom. *Journal of Sound and Vibration* 213(2), pp. 259–299, 1998a.
- M. Amabili. Free vibrations of partially filled horizontal cylindrical shells. *Journal of Sound and Vibration* 191(5), pp. 757–780, 1996b.
- M.A. Haroun. *Dynamic analysis of liquid storage tanks*, Pasadena California, 1980.

Numerical studies on dynamic behaviour of pipelines (3-3141)

Kim Calonius

VTT Technical Research Centre of Finland

P.O. Box 1000, Kemistintie 3, Espoo, 02044 VTT, Finland

e-mail: kim.calonius@vtt.fi

Dynamic excitation due to a pipe break can cause pipe to abruptly displace and hit the components, instrumentation and equipment nearby. In order to minimize the extensive damage caused by such pipe whips in a nuclear power plant, different types of restraints and supports are designed for the pipelines.

Here, structural dynamic behaviour of pipelines is studied with finite element method. A relatively short pipe line section with one bend and one restraint and rigidly fixed from its other end is chosen as a test case. The usability of different types of elements provided by Abaqus finite element code in modelling the pipe, restraint and adjacent civil structure is tested.

First, the stiffness of the restraint as well as the flexural stiffness of the pipe cross-section are solved with static analyses with a detailed model using three-dimensional solid and shell elements. After that, the model is substituted with couple of simpler models using special purpose structural elements such as pipe, elbow, spring and pipe support elements having the corresponding stiffness properties.

The eigenmodes of models are calculated and compared with each other. The pipe whip is simulated with nonlinear dynamic analyses. The displacement and stress results of different models are compared with each other and the reliability and adequacy of different element types are discussed. Sensitivity study is made by varying the analysis type, material properties, mesh density and element properties (interpolation, number of integration points and ovalization modes).

The results of the most adequate simple models with the right combinations of special-purpose elements provided by Abaqus corresponded well to the ones of the much larger three-dimensional solid and shell element models. Long pipe runs should preferably be modelled with special-purpose elements in order to save time and prevent errors due to overly large and complicated models.

References

- Calonius, K., 2009. Numerical Studies on Dynamic Behaviour of Pipelines. VTT Research Report VTT-R-01025-09.
- Vörös, G., Zsidi, Z., 2002. Analysis of the effects of postulated pipe rupture. *Gépészet* 2002, Budapest. 307–310.
- Micheli, I., Zanaboni, P., 2003. Transactions of the SMiRT Conference, 2003. Paper #J05-4. An Analytical Validation of Simplified Methods for the Assessment of Pipe Whip characteristics.
- Abaqus Manuals, 2006. Version 6.6. Abaqus Inc.

4. Characterization of Loads

Probabilistic and deterministic definition of design and beyond-design loads and load combinations for critical facilities caused by earthquakes, tornadoes, high winds, floods, aircraft impact, missile impact, impulsive loads, flow-induced vibrations, hydrodynamic loads, fire, blast, temperature and environmental effects, severe accidents (hydrogen/vapor deflagration/detonation, steam generator tube rupture, reactor cavity flooding, etc.).

Spatial distribution characteristics of seismic ground motion intensities in the Tokyo metropolitan area (4-1584)

Tetsushi Kurita¹, Satoru Takahashi², Tadashi Annaka³

¹Tokyo Electric Power Services Co., Ltd.

Higashi-Ueno 3-3-3, Taito-ku, Tokyo 110-0015, Japan

e-mail: kurita@tepsco.co.jp

²Tokyo Electric Power Company

Egasaki-cho 4-1, Tsurumi-ku, Yokohama, Kanagawa 230-0002, Japan

e-mail: takahasi.satoru@tepcoco.jp

³Tokyo Electric Power Services Co., Ltd.

Higashi-Ueno 3-3-3, Taito-ku, Tokyo 110-0015, Japan

e-mail: annaka@tepsco.co.jp

Large damage-causing earthquakes strike cities throughout Japan almost every year. In 2007, the Niigata-ken Chuetsu-oki earthquake (M_j6.8) occurred near the Kashiwazaki-Kariwa nuclear power plant. This reminded people of the importance of seismic load issues to nuclear power plants. By contrast, the Tokyo metropolitan area has not suffered a serious earthquake disaster since the 1923 Great Kanto Earthquake, namely the Tokyo earthquake (M_j7.9). However, the characteristics of seismic ground motion in the Tokyo metropolitan area are important for the field of urban disaster management, since the area is one of the highest electricity-consuming regions in the world. Meanwhile, seismograph networks such as the Japan Meteorological Agency (JMA) network of seismic intensity meters and the K-NET and KiK-net of the National Research Institute for Earth Science and Disaster Prevention (NIED), have been installed all over Japan to observe strong ground motions. More than 2,000 strong-motion seismographs have been installed at intervals of approximately 20 km. In this decade, seismic ground motions across a wide area have been observed by these networks. In this study, we aim to investigate the distribution characteristics of seismic ground motion intensities in the Tokyo metropolitan area based on the seismic records of these various networks.

The spatial distribution characteristics of seismic ground motion intensities are obtained by examining the difference between the observation data compiled from the networks and the standard values of the empirical model. The standard values are the expected seismic intensities derived from the existing attenuation relation of seismic ground motion intensities. The trend is extracted by averaging the differences for many earthquakes and factoring out random components. We use the attenuation relation proposed by Annaka & Nozawa (1988), since it was formulated using the database of seismic ground motion

4. Characterization of Loads

records in the Tokyo metropolitan area. Hereinafter we refer to the observed data as “O,” and the calculated standard value as “C.” The datasets from 72 earthquakes are used to obtain the geometric average of O/Cs or average of O-Cs. Peak ground acceleration (PGA), peak ground velocity (PGV), and JMA instrumental seismic intensity are considered to be indicative of the seismic ground motion intensities. The geometric averaged O/Cs are used to derive the trend components for PGA and PGV, while simple averaged O-Cs are used for the JMA instrumental seismic intensity.

The distribution characteristics of seismic ground motion intensities from the viewpoint of PGV or JMA instrumental seismic intensity can be largely explained by the site amplification factors of the subsurface layers. Regarding the PGA, the geometrically averaged O/Cs in most of the plain field are in close agreement with the average amplification factor between the alluvial ground surface and the engineering base layer. However, it is hard to explain all of the distribution characteristics using the site amplifications. The results of the investigation of the classification of seismic source region suggest that the distribution characteristics of PGA may be influenced not only by the site amplification of subsurface layers, but also by the effect of the seismic source and/or path characteristics.

This study reveals the spatial distribution characteristics of seismic ground motion intensities in the Tokyo metropolitan area. The results of this study could have applications for several different kinds of disaster reduction measures.

Residual stress analysis of an overlay weld on a dissimilar metal weld (4-1629)

Kang Soo Kim^{1*}, Ho Jin Lee¹, Bong Sang Lee¹, I. C. Jung²,
J. G. Byeon², K. S. Park²

¹Korea Atomic Energy Research Institute
150, Dukjin-dong, Daejeon 305-353, Korea

²Doosan Heavy Industries and Construction Co., 555 Gwigok Dong,
Changwon 641-792, Korea, *Corresponding author, kskim5@kaeri.re.kr

In recent years, a dissimilar metal, Alloy 82/182 welds used to connect stainless steel piping and low alloy steel or carbon steel components in nuclear reactor piping system have experienced a cracking due to a primary water stress corrosion (PWSCC) [1]. It is well known that one reason for the cracking is the residual stress by the weld. But, it is difficult to estimate the weld residual stress exactly due to many parameters of a welding. In this paper, the analysis of 3 FEM models is performed to estimate the weld residual stress on a dissimilar metal weld exactly.

3 FEM models were made by ABAQUS/CAE Code [2]. These are the Butt model, Repair model and Overlay model, and the plane-strain 2D model. The thermal analysis and the stress analysis are performed on each model and the residual stresses on each model were calculated and compared respectively.

Butt model

Butt model consists of a SUS316 plate ($33 \times 330 \times 40$ mm) and a SA508 plate ($330 \times 330 \times 40$ mm). The edge of the SA508 plate became the butting by Alloy 182 and the two plates were welded by the filler (Alloy 182). Actually, this specimen was made and the residual stresses were measured by the X-Ray method and the Hole Drilling Technique. These results were compared with the FEM result of the Butt model.

Repair model

The bottom part of the plate was removed and was welded again by the filler (Alloy 182). Actually, this specimen was made and the residual stresses were measured by the X-Ray method and the Hole Drilling Technique. These results were compared with the FEM result of the Repair model.

Overlay model

Overlay model is shown in Fig. 1. The top part of the plate was overlaid by the filler (Alloy 182). Totally, 3 layers were overlaid. Whenever each layer was

4. Characterization of Loads

overlayed, the results were calculated respectively. The analysis results of Overlay model are represented in Fig. 2.

Conclusions

The experimental values by the X-Ray method and the Hole Drilling Technique have the trend which is in agreement with the FEM results. Repair weld elevated the stresses. Therefore, a relaxation of the stress in the welding part is needed. The stress in the thickness direction of the Overlay weld converged to nearly 0 MPa. Overlay weld lowered the stress in the welding part. Therefore, the Overlay weld has good benefits with a view to a stress relaxation and a PWSCC.

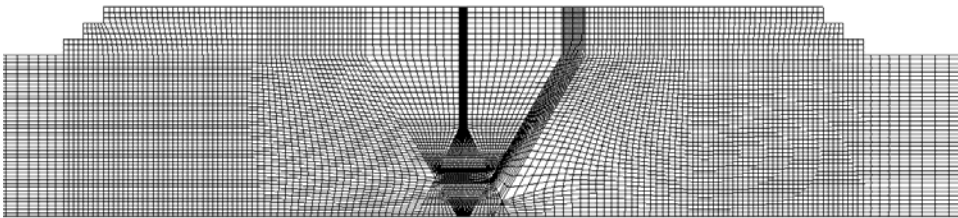


Figure 1. 2D FEM model of Overlay weld.

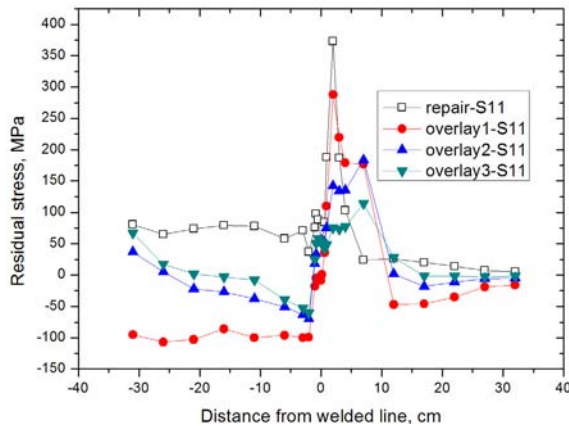


Figure 2. FEM results of Overlay weld (S11).

References

1. C. King, G. Frederick. Technical Basis for Preemptive Weld Overlays for Alloy 82/182 Butt Welds in PWRs (MRP-169). EPRI Topical Report, October 2005.
2. ABAQUS, 2004. Standard User's Manual, version 6.4. ABAQUS Inc., Pawtucket, RI, USA.

Peak reduction of elastic floor response spectra (4-1657)

Fritz-Otto Henkel, Jens Roehner
Woelfel Beratende Ingenieure GmbH + Co. KG
Max-Planck-Strasse 15, 97204 Hoechberg, Germany
e-mail: henkel@woelfel.de

The German Nuclear Design Code KTA 2201 is currently being revised. In the course of this revision questions concerning the design of floor response spectra (Smoothing, Broadening of Peaks, etc.) had to be answered. Many current nuclear design codes still incorporate the provisions of the 1978 USNRC Regulatory Guide 1.122, according to which peaks of floor response spectra at the structural frequencies have to be fully covered and broadened to account for uncertainties in the structural frequencies.

The determination of floor response spectra by deterministic linear modal analyses often results in spectral shapes which show distinct local spikes over narrow frequency intervals. In reality, however, it is usually not possible to measure such local resonance spikes to the same extent. This paper investigates the following phenomena that might be responsible for the observed discrepancy between numerically determined and real amplitudes of such resonance peaks in floor response spectra:

- Non-linear effects
- Coupled / De-coupled analysis
- Numerical pitfalls during the modeling of damping
- Deterministic / Probabilistic calculation of floor response spectra.

Based on the results of this investigation a pragmatic proposal for the reduction of “unrealistic” peaks in numerically determined floor response spectra will be derived.

The influence of non-classical damping on subsystem response (4-1657)

Jens Roehner, Fritz-Otto Henkel
Woelfel Beratende Ingenieure GmbH + Co. KG
Max Planck Strasse 15, 97204 Hoechberg, Germany
e-mail: roehner@woelfel.de

With increasing speed and capacity of modern computer systems a trend to more detailed structural models containing multiple vibrating substructures can be observed. In nuclear design such models usually account for soil-structure-interaction and are often non-classically damped. When analyzed by conventional modal analysis such non-classically damped systems may lead to incorrect results in the case of closely spaced modes with different damping characteristics.

Basic insight into the reasons of such phenomena is developed, based on an analytical investigation of the 2-DOF system. The classical damping types “diagonal approximation” and “composite modal damping” are treated in detail.

Subsequently the theoretical findings of the 2-DOF system analysis are visualized by numerical earthquake response analysis of a 2-DOF and a 3-DOF system. The classical damping types “diagonal approximation”, “composite modal damping” and “Rayleigh damping” are discussed and compared to the exact solutions obtained by complex modal analysis.

It is found that although increased computer capacity may justify more detailed numerical models, it does not necessarily mean that the accuracy of the results is increased. The numerical phenomena that may come along with closely spaced modes in sophisticated, non-classically damped systems must properly be paid attention too.

How reliable are the ground motion prediction equations? (4-1662)

Iztok Peruš, Peter Fajfar

University of Ljubljana, Faculty of Civil and Geodetic Engineering
Jamova 2, Ljubljana, Slovenia

e-mail: iperus@ikpir.fgg.uni-lj.si, pfajfar@ikpir.fgg.uni-lj.si

Introduction

Ground motion prediction equations (GMPEs) are used for the estimation of the ground motion parameters, which are needed for design and evaluation of important structures, including nuclear power plants (NPPs). Seismic hazard may contribute greatly to the total risk of a NPP, therefore the selection of appropriate GMPEs may have a substantial influence on the design and safety evaluation. Recently, new GMPEs were derived by five different teams of US authors within the NGA project [1]. Unfortunately, in spite of starting from the same database, quite large differences (from the engineering point of view) of median values obtained by different models are still present. New GMPEs have been proposed also in other parts of the world. There have been indications that the models developed by using regional data can be transferred to another region.

Aim of the work

An empirical approach, called the CAE (Conditional Average Estimator) method, has been implemented for the estimation of an unknown quantity (e.g. peak ground acceleration) as a function of known input parameters (e.g. magnitude, distance, style-of-faulting, local soil characteristics). The description of the method is given in [2]. The method is based on a special type of multi-dimensional non-parametric regression. The main idea is to predict the ground motion parameters by an alternative approach which does not take into account any a priori information about the phenomenon [3], and to compare the results with the results of existing GMPEs. Using this approach, the influence of different databases, as well the influence of pre-determined functional forms, used for the development of five NGA and one European model [4], were investigated. Also, the applicability of the NGA models for Europe is discussed.

Essential results

There are two main sources of the differences between various GMPEs: the adopted database and the assumed functional form of the GMPEs. Both rely to some extent on judgement. The five NGA teams used different subsets of the original common NGA database. The main source of differences is in the treatment of aftershocks. The models with aftershocks in the database generally predict smaller median values and larger scatter of ground motion parameters. The choice of the functional form has an important influence on the estimated ground motion, especially at short distances, where the data are scarce. The results of the study show that all investigated models, with one exception, are in good agreement with data in the case of $M=6$. In the case of $M=7$, some model predictions are not entirely supported by data. A very good correlation can be observed in the case of two NGA models. The European model is based on a different database. However, the median results of this model are mostly in the range of the NGA results. For the investigated scenario, the differences between the European model and the NGA models are similar to the differences between the NGA models.

Conclusions

For the investigated scenario, significant differences between the predictions of different models can be observed. The fact, that the NGA models differ substantially in spite of starting from the same database, suggests that the available GMPEs, although greatly improved, are not yet fully reliable, especially at short distances from the fault. On the other hand, the fact that the median results obtained by European GMPE fall in the range of the NGA predictions, suggests that the regional differences do not play a major role, at least not in the moderate distance range. As a consequence, the use of worldwide data in a single database seems to be feasible. Such a database should not include aftershocks, which generally decrease the median values and increase the scatter. A problem with combined databases may be the increased scatter, which can exert the dominant influence on the probabilistic seismic hazard analysis for important structures like NPPs.

The CAE method proved to be a simple and powerful research tool. It can also be successfully applied for specific needs at specific sites (e.g. for subsets/compilations of databases, for extended databases with new data, for checking the influence of different input parameters).

References

1. Earthquake Spectra (2008), Special Issue on the Next Generation Attenuation Project, 24(1), 1–341.
2. Peruš, I., Poljanšek, K., Fajfar, P. (2006), Flexural deformation capacity of rectangular RC columns determined by the CAE method. Earthquake Engineering and Structural Dynamics, 35, 1453–1470.
3. Fajfar, P., Peruš, I. (1997), A non-parametric approach to attenuation relations. Journal of earthquake engineering - JEE, 1 (2), 319–340.
4. Akkar, S., Bommer, J.J. (2007), Prediction of elastic displacement response spectra in Europe and the Middle East, Earthquake Engineering & Structural Dynamics, 36(10), 1275–1301.

Hazard consistent structural demands and in-structure design response spectra (4-1717)

Thomas W., Houston, P.E., Michael C., Costantino, P.E., Carl J. Costantino, Ph.D
Carl J. Costantino and Associates
4 Rockingham Road, New York 10977, USA
e-mail: carl@cjassoc.com

Current Soil-Structure Interaction (SSI) analysis procedures, as defined by standards of the U.S. Nuclear Regulatory Commission and the American Society of Civil Engineers, are based on deterministic median plus one-sigma design motions. These procedures are intended to provide an 80th percentile of Non-Exceedance Probability (NEP) for the development of structural demands and in-structure response spectra of a nuclear facility, based on a probabilistic seismic hazard. The concern is the appropriateness of deterministic procedures for a performance or risk-based design. This study compares a set of hazard consistent SSI analysis procedures versus the current methodology to determine the effectiveness of current procedures at meeting performance targets. The hazard consistent procedures are based on probabilistic SSI analyses involving sampling methods for randomized variables of soil shear strength, hysteretic damping of the soil, structural stiffness and structural damping. The analyses are performed for multiple soil site definitions and structures. Complementary deterministic analyses are performed on the same soil site and structure definitions, then structural demands and in-structure response spectra from the deterministic procedures are compared against those of the probabilistic procedures for their target performance goal. The study shows that in several cases current deterministic procedures perform poorly at meeting their target performance goal of 80% NEP, but rather are closer to a median probability. This finding generally relates to deep soil sites consistent with those found in the southeastern U.S. and hard rock sites. The results also show that in some cases current deterministic procedures result in overly conservative estimates of structural demand and in-structure motions. The results of this study are intended to develop updated hazard consistent SSI analysis procedures to meet the target performance goals of nuclear facilities.

Analytical study of containment behaviour under fire due to aircraft fuel spillage (4-1805)

A. Ravi Kiran¹, M.K. Agrawal¹, R.K. Singh², A.K. Ghosh³, H.S. Kushwaha⁴

¹Scientific Officer, Reactor Safety Division
Bhabha Atomic Research Centre, India

²Head, Containment Studies Section, Reactor Safety Division
Bhabha Atomic Research Centre, India

³Head, Reactor Safety Division, Bhabha Atomic Research Centre, India

⁴Director, Health, Safety & Environment Group
Bhabha Atomic Research Centre, India

Aim

Nuclear containment is an important safety related structure which acts as an ultimate barrier against release of radioactivity. In the recent past, safety assessment for Indian PHWR nuclear containment has been carried out for aircraft impact. However, during this assessment, the thermal load generated due to the fuel spillage was not taken into consideration. Recent studies have pointed out that the fire involved during the aircraft impact on WTC (World Trade Centre) towers had a significant effect on their collapse. This has therefore necessitated a study on the behavior of the containment under fire due to the spillage of aircraft fuel. An analytical study is carried out on the containment behavior under fire due to the spillage of the aircraft fuel.

Scope

The cross sectional elevation of Indian 500 MWe PHWR containment building is as shown in Fig. 1. It contains a primary inner containment of pre-stressed concrete construction and a secondary containment of reinforced concrete construction. Fig. 2 shows the Finite Element model of the containment. Concrete portion is modeled using 3-D solid conduction elements and rebars with one dimensional conduction elements. Convective and radiative boundary conditions are applied to the model. To calculate thermal load due to fuel spillage, it is assumed that a commercial aircraft collides horizontally at the dome wall junction of the containment just below ring beam. The heat flux is calculated using typical aviation turbine fuel properties and is applied on the finite element model to the nodes corresponding to the wall portion between ring beam and ground. Due to symmetry, half the flux is applied over a quarter

4. Characterization of Loads

portion of containment model. Transient thermal analysis is carried out to obtain limiting conditions in terms of temperature for different structural members.

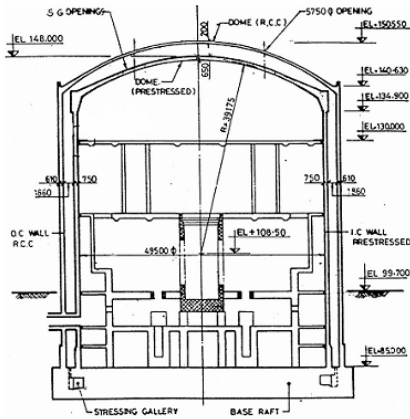


Figure 1. Cross Section of OCW and ICW of 500MWe PHWR.

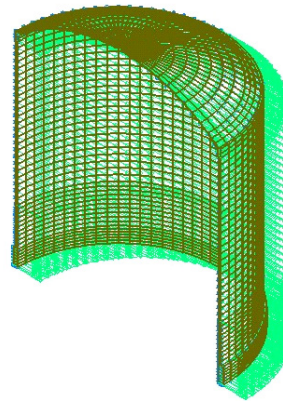


Figure 2. FE model of the outer containment.

Conclusions

An analytical study on thermal behavior of the outer containment under fire due to the spillage of the aircraft fuel is carried out. The heat flux calculations are carried out using typical aviation turbine fuel properties. Transient thermal analysis is carried out and temperature distributions at different locations are obtained. It is observed that the outer concrete cover portion of the OCW will be affected much under thermal load due to fuel spillage. However, the central concrete portion will remain intact under such loading.

References

- Kukreja, M., Singh, R.K., Vaze, K.K., Kushwaha, H.S. (2005). Damage evaluation of 500 MWe Indian PHWR Nuclear containment for aircraft impact. *Nuclear Engineering and Design*, 235, pp. 1807–1817.
- Quintiere, J.G., Di Marzo, M., Becker, R. (2002). A suggested cause of the fire induced collapse of World Trade Centre. *Fire Safety Journal*, 37, pp. 707–716.
- Usmani, A.S., Chung, Y.C., Torero, J.L. (2003). How did the WTC Towers collapse: A new theory. *Fire Safety Journal*, 38, pp. 501–533.

CFD analysis of atmospheric dispersion in a large terrain of Kakrapar atomic power station in presence of structural buildings (4-1869)

B. Gera, Pavan K. Sharma⁺, R.K. Singh, A.K. Ghosh, H.S. Kushwaha*
Reactor Safety Division, *Health Safety and Environment Group
Bhabha Atomic Research Centre, Trombay, Mumbai, India 400085
⁺e-mail: pa1.sharma@gmail.com

Keywords: dispersion, CFD, turbulence, PHOENICS

The transient transport and dispersion of airborne pollutants around large objects is an area of continued scientific and practical interest. An improved understanding of such pollutant transport will facilitate the assessment of the risk to occupants from a release of an airborne toxic (dense/lighter) pollutant in the space, and help identify and evaluate ways to reduce occupant exposures in the event of such release as per regulatory standard. Scientific research on air flows and pollutant transport in large open spaces around buildings using Computational Fluid Dynamics (CFD) is a new emerging field. Most studies of atmospheric dispersion of airborne toxic material released from NPPs are based on Gaussian plume models or on the use of a convection–diffusion equation. Such models, which do not involve solving the flow problem, are inexpensive and can be useful in the atmospheric mesoscale, of the order of 2–2000 km from the NPP. However, they fail to take into account the turbulence generated by the interaction of the wind with buildings, the terrain, and with the convective forces of the released material stream, which are the dominant factors in the local scale, of the order of 0–2 km from the source of emission.

This work presents a computational fluid dynamics (CFD) calculation to investigate the dispersion of SF₆ over terrain of Kakrapar nuclear power plant using the actual meteorological data. Three-dimensional, transient simulations have been carried out using CFD code PHOENICS. The CFD calculation covers a domain of 3.2 km X 3.2 km in plan and 0.5 km in height. Atmospheric dispersion in presence of the structures like Reactor Building, Natural Draft Cooling Tower and Turbine Building has been studied. The SF₆ was released from the stack at a height of 100 m. SF₆ released was considered for 2 hours duration at a rate of 1 gm/sec. This model was used to simulate the transport of SF₆ for 6 hours. The ground level concentration of SF₆ was monitored.

Studies of medium scale non-axisymmetric aluminium missile impacts (4-1876)

Juha Kuutti, Auli Lastunen

VTT Technical Research Centre of Finland, P.O. Box 1000, 02044 VTT, Finland
e-mail: juha.kuutti@vtt.fi

Aircraft impact has been a design consideration for protective structures since the 1960's. Nowadays modern nuclear power plants are designed against aircraft crashes. Besides the damage caused by impact to the protective structure itself, one concern in structural design is to prevent the airplane or one of its components like fuel tanks or fuel itself from penetrating the protective structure. Also, if the protective structure remains intact, fuel spreading outside the structure must be considered. In many cases it is not possible to create a full nonlinear model of impact and simpler evaluation methods and small scale experimental testing is needed. In order to make simplifications reliably, the behaviour of an aircraft in impact must be known in as much detail as possible. Experimental data of various missile impacts against concrete walls are available in literature but tests carried out using complex airplane-like missiles with water included are not available.

VTT Technical Research Centre of Finland has studied medium scale missile impacts against rigid and deformable targets to provide data for the calibration and verification of numerical models of a loading scenario where an aircraft impacts against a nuclear power plant. The testing apparatus provides data for validating these models. Missiles used in most of the tests have been cylindrical aluminium and steel pipes. Recent development in the project is tests with a more structurally complex airplane-like missile. Aircraft fuel is also represented as water. The objective of these tests is to produce an impact loading transient with a changing loading area resembling full scale aircraft impact. The tests are also used to develop and verify models of impact scenarios. The goal is to predict the results of the experiments using a mathematical model and if successful, apply the same methods to other impact scenarios. The assumption is made that if the experimental tests can be simulated with accuracy, the same methodology can be applied to full scale phenomenon.

The models presented in the literature to analyse impact behaviour, e.g. missile deformation, impact loads caused by the missile and protective structure barrier wall damaging, are often developed to predict full scale phenomenon. Experimental testing is usually performed in smaller scale and it is unclear if the methods can be directly applied. Now the medium tests are analyzed with analytical and numerical methods to validate the methodology and results. Riera's method for determining impact loads is presented and impact loads produced by the medium scale missile are compared to the impact loads

produced by a commercial airline using dimensional analysis. It is shown that the missile structure can not be fully scalable within the requirements of experimental tests so that missile impact data can not be directly used to make assumptions of full scale impact.

Experimental results of the missile impact are in agreement with the analytical predictions. Using numerical methods the missile deformation and impact loading can be calculated with reasonable accuracy. Although the analytical and numerical methods predict the current impact scenario accurately, validating the methods to be used in this scale and understanding the full impact phenomenon with wide range of uncontrollable variables require more experimental testing.

Contribution to the design of concrete sections reinforced with externally fiber polymers (4-1886)

Ferran Prats Bella¹, Ramón González Drigo², Adrina Bachiller Saña³

¹Engineer, Westinghouse-Initec Nuclear. Lecturer Professor, RMEE, EUETIB, UPC
e-mail: ferran.prats@upc.edu

²Doctor Engineer, RMEE, EUETIB, UPC
e-mail: jose.ramon.gonzalez@upc.edu

³Engineer, IferCat. Lecturer Professor, ETSECCPB, UPC
e-mail: adrina.bachiller@upc.edu

Introduction

In the design of seismic category 1 buildings in nuclear power plants it is considered, as a normative requirement, its performance under Operating Basis Earthquake (OBE) and Safe Shutdown Earthquake (SEE). During the operational life of a nuclear plant, a seismic phenomenon can occur in the site of a greater intensity than the foreseen, thus modifying the seismic levels of design of seismic category 1 structures, as happened recently in Japan.

An event as the described above requires an evaluation of the damage suffered by the structure during the seism and the viability of its reinforcement, given the case that the damage is not significant, in order to compile with the new seismic requirements.

A similar case can be observed outside the nuclear domain, on the more conventional structural design. As instance, the design of a building initially conceived for as an office building and, later on, adapted for hospital use. This change of use can lead to a change on the seismic requirements which, depending on the code applied can be up to a 50% higher (RCA-02, for example).

Aim of the work

Within this context, this communication presents a study on the viability of reinforcing reinforced concrete buildings with externally adhered polymers. With this objective the work is divided in two phases. On the first phase, an algorithm (and its code) to obtain “momentum-curvature” diagrams of reinforced concrete sections with externally adhered polymers is presented. Based on this curves, the stiffness of the elements according to their stress level can be evaluated. On the second phase of the study, these diagrams are used for a static non-linear analysis.

The obtaining of the “moment-curvature” diagrams is based on the behaviour of each of the materials adding to the already known behaviour of concrete and steel, the elastic behaviour of the polymers. Due to the main objective of the research, it is interesting to obtain a “moment-curvature” diagram for the pillars of a structure, taking into account both the contribution of the reinforcement and the concrete properties and behaviour under confined conditions. Besides, its application is extended to the case of concrete beams. The interaction bending moment-axial force in ultimate limit state is necessary to evaluate the effect of FRP reinforcement.

Once these diagrams are obtained, a standard and widely accepted technique (even with its limitations) can be used to evaluate the seismic capacity of a structure. Among the available analysis methodologies, a static non-linear analysis (or push-over) technique has been chosen.

Finally, an example of application based on a simplified regular reinforced concrete building is presented. Its resistance with and without “FRP” reinforcements is calculated in order to evaluate the improvement on the seismic response of the structure due to the polymer external reinforcements.

Essential results

The externally adhered polymer, changes the behaviour of moment-curvature relationship, as show in Fig. 1. This is obtained for one beam with and without externally adhered polymer. The effect of confinement is not included here.

And, in order to study the behaviour of columns in the ultimate limit state, the interaction bending-axial diagram is obtained in order to check the effect of FRP reinforcement, see Fig. 2.

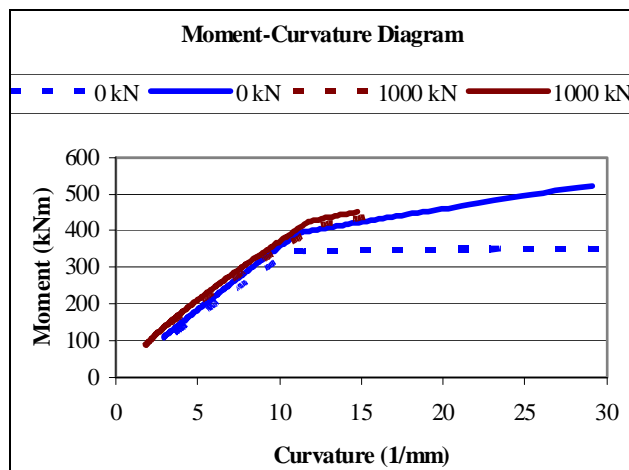


Figure 1. Typical M-C diagram of one section of beam with (full line) and without (dashed) FRP. This figure, shows two cases: without compression force; and with 1000 kN.

4. Characterization of Loads

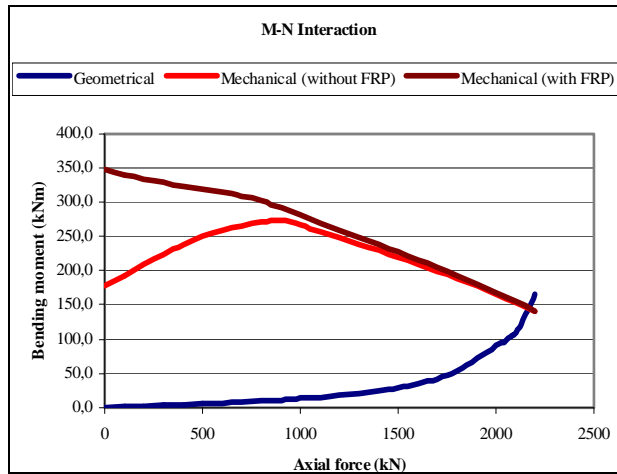


Figure 2. Typical configuration of Geometrical and Mechanical (with and without externally FRP) Bending-Axial diagram. Shows the effect of FRP (brown line) and the conventional reinforced section (red line) in interaction M-N diagram for one beam.

Conclusions

The analysis of one section of conventional reinforced concrete with externally FRP reinforcement is presented. With this analysis, it is possible to obtain MC diagrams of the section and evaluate the MN diagrams in ultimate state. A significant improvement of the performance of conventional reinforced concrete sections is obtained thanks to FRP reinforcement.

Finally, with these diagrams, a standard push-over analysis shows that it is possible to use the externally FRP reinforcement in a concrete building to improve and guarantee its seismic response.

References

- American Concrete Institute, Committee 440, ACI-440.2R-02. Guide for the Design and Construction of Externally Bonded FRP Systems for Strengthening Concrete Structures. 2002.
- FIB bulletin nº 14. Externally bonded FRP reinforcement for RC structures. fédération internationale du béton. 2001.
- National Research Council. Guide for the Design and Construction of Externally Bonded FRP Systems for Strengthening Existing Structures. CNR-DT 200. 2004.
- Instrucción EHE. Instrucción de Hormigón Estructural. Ministerio de Fomento. 1999.

Validation of aircraft FE model for impact analyses (4-1929)

Jan Stepan

UJV Rez a.s. Div. Energoprojekt Praha
Vyskocilova 3/741, Prague, Czech Republic
e-mail: stepan@egp.cz

After tragical experience with terrorist attacks in USA, in which large passenger aircraft have been used, safety of sensitive targets (and therefore also safety of nuclear devices and buildings) has become more important. Request for evaluation of this risk caused incorporation of large aircraft impact into design analyses. The loads caused by aircraft crash can be introduced into the calculation of response of impacted building in several ways. In case of perpendicular hits to relatively rigid structures the published loading curves can be often used, which are determined based on experimental tests or based on simple computing models (e.g. Riera 1968). When the hit structure is not rigid the forces acting between structure and aircraft will differ. In such case it is necessary to use an adequate computing model of aircraft and the task need to be resolved for each case individually as interaction of both bodies.

The paper deals with the comparison of results for calculation based on Riera model and calculation of aircraft impact through FEM interaction of two bodies (aircraft and building). Because it is not possible to create detail and accurate FE model of aircraft due to necessary simplification of the model as well as unavailability of the detail plane structure documentation, the check of adequacy of aircraft model is important. Riera model was chosen because this model is general accepted and has been validated by tests. The comparison demonstrated the possibility to use relatively simple FE model of aircraft instead of external dynamic loading. In this way it is possible to validate FE model of aircraft in global point of view but there is not possible to check the interaction of individual parts of aircraft body with building structure (e.g. interaction of wing with column). Impact tests are usually focused on impact of rigid or flexible body on structure with reference to perforation of structure, the interaction of two flexible bodies including their gradual damage is difficult to get. This could be open challenge for next steps in refinement of these analyses.

Reference

Riera, J. (1968). On the Stress Analysis of Structures Subjected to Aircraft Impact Forces, *Nuclear Engineering and Design* 8/1968, pp. 415–426.

Measurement of residual stresses in the dissimilar metal weld joint of a safe-end nozzle mock-up (4-1938)

Kazuo Ogawa¹, Ed Kingston², Laurie Chidwick³, David Smith⁴

¹Senior Officer, Japan Nuclear Energy Safety Organisation, Tokyo, Japan

²Managing Director, VEQTER Ltd., Bristol, UK

e-mail: ed.kingston@veqter.co.uk

³Project Leader, VEQTER Ltd., Bristol, UK

⁴Professor, Department of Mechanical Engineering, University of Bristol
Bristol, UK

Introduction

Knowledge of the origin, magnitude and distribution of residual stresses generated during the manufacture of nuclear power plants is of vital importance to their structural integrity assessment. The overall aim of this work was to measure welding residual stresses in components prone to primary water stress-corrosion cracking in nuclear reactor pressure vessels. This paper describes the on-site application of the Deep-Hole Drilling (DHD) technique to measure the through-thickness residual stress distributions through a safe-end nozzle component containing a dissimilar metal weld joint at different stages of manufacture.

Scope

The safe-end nozzle component measured was a full-scale, whole mock-up of those typically found on Japanese Pressurised Water Reactors (PWR). Figure 1 shows a PWR and the location of the safe-end nozzle under investigation. Figure 1 also shows a sketch of the safe-end nozzle measured, the weld geometry, the DHD measurement locations and the manufacturing sequence in which the measurements were carried out. The DHD residual stress measurements were undertaken radially through the centreline of the double-'V', alloy 132 weldment joining the low alloy steel nozzle to the stainless steel safe-end. DHD measurements were carried out before and after the stainless steel safe-end was welded to a main coolant pipe.

This paper describes the DHD technique [1] adopted to measure the residual stresses through the double-V weldment and their comparison with results from other measurement techniques and UK based standards, e.g. BS7910 and R6.

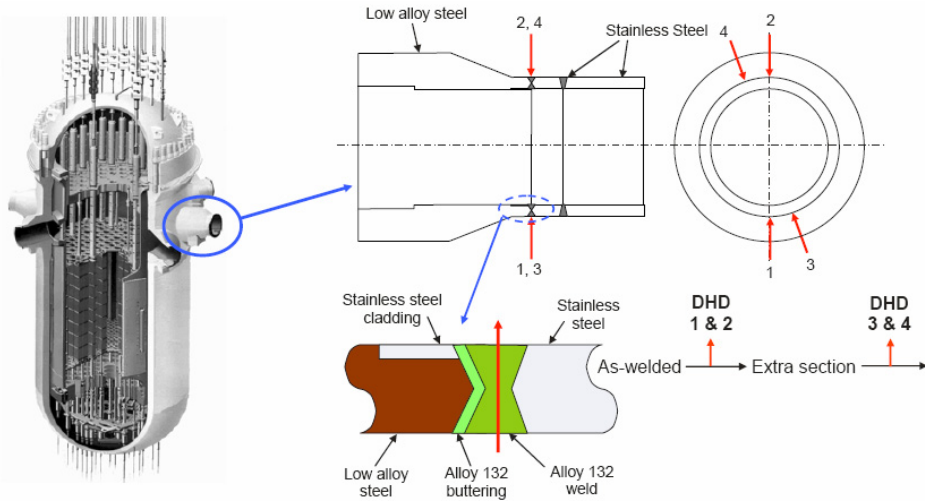


Figure 1. Drawing of a PWR, the safe-end nozzle, the measurement locations and timeline.

Results

Figure 2 shows the axial residual stresses measured at locations 1 and 2, i.e. in the as-welded state. It can be seen that there is excellent agreement between the DHD and inherent strain results, both showing peak tensile stresses at the inner and outer weld cap surfaces, reducing into compression in the centre at the meeting of the double-V grooves. Figure 3 shows the axial residual stresses measured at locations 3&4, i.e. after the stainless steel main coolant pipe was attached. It can be seen that after the attachment of the main coolant piping, the peak tensile axial residual stresses present at the inner surface have changed to compressive.

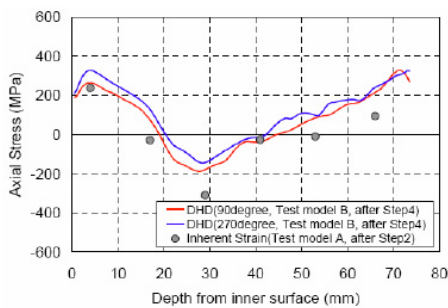


Figure 2. Axial residual stresses measured in the as-welded state.

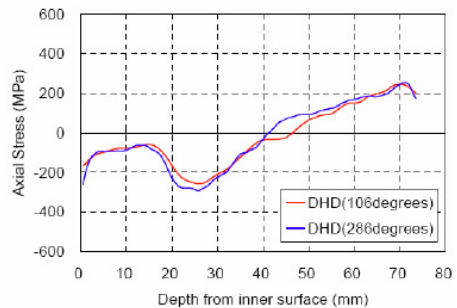


Figure 3. Axial residual stresses measured after main coolant pipe.

Conclusions

The semi-invasive, portable DHD technique allowed for the measurement of residual stresses within a single full-scale mock-up of a PWR safe-end component at different stages of manufacture. There is excellent agreement between the DHD measured residual stresses and those measured using other techniques. The peak tensile axial residual stresses present at the inner surface of the weld changed to become compressive following the attachment of the stainless steel main coolant pipe.

References

1. E.J. Kingston, D. Stefanescu, A.H. Mahmoudi, C.E. Truman, D.J. Smith. (2006). Novel applications of the deep-hole drilling technique for measuring through-thickness residual stress distributions. *Journal of ASTM International*, Vol. 3, No. 4, Paper ID JA112568.

Validation of Riera loading in LS-DYNA models of missile impact (4-1946)

John A. Vera, Ph.D.
U.S. Nuclear Regulatory Commission
11555 Rockville Pike, Rockville, MD 20852, USA
e-mail: John.Vera@nrc.gov

Interest in impact on concrete structures has sparked efforts to benchmark finite element codes to predict the effects of such loading. Recent work towards this end has included the efforts of the Technical Research Centre of Finland (VTT) [1] and Institut de Radioprotection et de Sûreté Nucléaire (IRSN) [2], who have used finite element codes such as ABAQUS/Explicit and LS-DYNA. A common thread of these efforts is the use of Riera loading to simulate actual missile impact. In the VTT tests modeled in [2] and [3], two types of missiles were used: “dry”, or hollow cylinder, and “wet”, a cylinder filled with water. While modeling results have shown good agreement with test data, there have been conflicting conclusions regarding the accuracy of Riera loading when representing “wet” missile conditions. Contrary to results presented in [3], the authors of [2] concluded that Riera loading was inadequate for a “wet” missile case.

The purpose of this paper is to benchmark the finite element code LS-DYNA and determine the adequacy of Riera loading for the impact cases reported in [2] and [3]. Riera loading from both references are used in LS-DYNA dynamic finite element models. Two different material models are used for the concrete. Analyses of models with missile impact instead of Riera loading are also investigated and results compared.

Results show the displacements and rebar strains obtained from finite element analyses agree very well with experimental results when using Riera loading. Models with missiles result in slightly more discrepant results, in part due to the assumptions in material models and mass distribution. The “wet” missile model also demonstrates a weakness of the Winfrith material model for certain impacts.

In conclusion, Riera loading is shown to produce very accurate results for the tests modeled, for both “dry” and “wet” missile cases.

References

1. Lastunen, A., Hakola, I., Järvinen, E., Hyvärinen, J., Calonius, K. Impact Test Facility. Transactions SMIRT 2007.
2. Tarallo, F., Ciree, B., Rambach, J.M. Interpretation of soft impact medium velocity tests on concrete slabs. Transactions SMIRT 2007.
3. Saarenheimo, A., Tuomala, M., Calonius, K., Lastunen, A., Hyvärinen, J., Myllymäkki, J. Numerical studies on impact loaded reinforced concrete walls. Transactions SMIRT 2007.

Evaluation of Indian nuclear coastal sites for tsunami hazard (4-1976)

R.K. Singh*, H.S. Kushwaha

Reactor Safety Division, Health Safety and Environment Group
Bhabha Atomic Research Centre, Trombay, Mumbai 400085, India
e-mails: rksingh@barc.gov.in, rksingh175@rediffmail.com

Recent tsunami generated on December 26, 2004 due to Sumatra earthquake of magnitude 9.3 resulted in inundation of the various coastal regions of India. BARC, Trombay initiated computational simulation for all the three phases of tsunami source generation, its propagation and finally run up evaluation for the protection of public life, property and various industrial infrastructures located on the coastal regions of India for the National Tsunami Warning System. Further, studies have also been carried out for the protection of the coastal nuclear facilities. The site selection and design of Indian nuclear power plants demand the evaluation of run up and the tsunami mitigation measures for the coastal plants. Besides it is also desirable to evaluate the early warning system for tsunamigenic earthquakes. The tsunamis originate from submarine faults, underwater volcanic activities, sub-aerial landslides impinging on the sea and submarine landslides. In case of a submarine earthquake-induced tsunami the wave is generated in the fluid domain due to displacement of the seabed. These studies have been effectively utilized for design and implementation of early warning system for coastal region of the country apart from catering to the needs of Indian nuclear installations. This paper presents results of tsunami wave modelling based on different analytical/numerical approaches with shallow water wave theory. The results of in-house finite element code Tsunami Solution (TSUSOL) is highlighted through numerical simulation of Sumatra-2004 and Makran-1945 tsunami events. The TSUSOL code is shown to have special capability of coupled tsunami and acoustic wave simulation, which is an important feature for the early warning system.

As an inter-code comparison and code benchmarking exercise, using a refined local bathymetry and land morphology, detail inundation modeling has been carried out for Kalpakkam nuclear site in South India with different codes through a systematic National Round Robin Exercise with participants from research, academic and industrial organizers. The paper describes the detail computational results of inundation reach and wave run up for Kalpakkam site, which are shown to have reasonable comparison with the post tsunami survey measurements. A sensitivity analysis of the results obtained from the different participants is carried out with regard to coupling of storm surges with tsunami waves, influence of bottom friction and Coriolis forces to evolve the design basis for the coastal nuclear facilities. The tsunami source modeling with regard to the

fault parameters, fault multiple segments and orientations are described to identify and characterize the tsunamigenic earthquakes in Indian Ocean. Coupled sea bed and water column dynamic models are presented for identifying the tsunamigenic earthquakes with help of tide gauge wave form time signal analysis and the associated tsunami periods and wave lengths. The evolved methodology has been further utilized for tsunami hazard evaluation of coastal nuclear plants in India.

On the site specific amplification functions for Center and Eastern United States (4-2029)

Julio Garcia¹, Antonio Fernandez², Juipin Wang³

¹Paul C. Rizzo Associates, Inc., Oakland, CA, USA
e-mail: julio.garcia@rizzoassoc.com

²Paul C. Rizzo Associates, Inc. Pittsburgh, PA, USA
e-mail: antonio.fernandez@rizzoassoc.com

³Paul C. Rizzo Associates, Inc. Pittsburgh, PA, USA
e-mail: juipin.wang@rizzoassoc.com

Introduction

The U.S. Regulatory Guide 1.208 provides criteria for satisfying the requirements of a performance-based approach to define the site-specific earthquake ground motion for Nuclear Power Plants, based on a Site-specific Probabilistic Seismic Hazard Analysis. As part of this process, Site-Specific Amplification Functions need to be computed to take into account the earthquake ground motion amplification from the hard rock through the rock and soil materials up to the foundation elevation and ground surface of the soil, considering the uncertainties in the spatial distribution of soils and rocks as well as those related to the ground motion parameters. The influence of all soil- and ground motion-related parameters on the Amplification Functions is not evident.

Aim of the work

To understand the behavior of the amplification functions, an analogy is established with the harmonic transfer functions. They are very well understood in the geotechnical and structural engineering community.

An investigation is developed starting from the harmonic transfer motion and dissects the influence of the different parameters: shear wave velocity profile and its variability, strain-dependent material parameters and their variability, Deaggregation-related parameters, response spectrum at the hard rock, and frequency content of the time histories associated with the ground motion at the hard rock.

Special attention is conferred to the definition of the hard-rock halfspace for sites located in the Center and Eastern United States (CEUS). For many sites, hard rock horizons cannot be reached with conventional geotechnical exploration

programs and a higher uncertainty is therefore associated with its depth as well as the mechanical parameters of the deep overlying materials.

Results and conclusions

The investigation shows the influence on the site specific amplification function of each parameter for an expected range of variability at a particular site. Besides, a comparison is established between the site amplification functions for two different rock sites: a shallow site and a deep site. The uncertainties associated with the characterization of the hard rock horizon influence mainly the high frequency range of the amplification function. This analysis illustrates the behavior of the amplification function for typical sites in CEUS.

Reference

U.S. Nuclear Regulatory Commission (2007). Regulatory Guide 1.208, A Performance-based Approach to define the Site-Specific Earthquake Ground Motion.

Sensitivity of PSHA in the region of Peninsular India (4-2041)

Roshan A.D¹, Prabir C. Basu²

¹Civil & Structural Engineering Division, AERB, Mumbai, India

²Director, Civil & Structural Engineering Division, AERB, Mumbai, India

Introduction

A rational assessment of the techniques used for estimation of input parameters as well as the approaches followed for calculation is a pre-requisite for conducting probabilistic seismic hazard analysis (PSHA). The outcome of PSHA depends on various data including the site specific information. Peninsular India poses unique challenges like sparse data on seismicity, lack of information on seismotectonic characteristics, and non-availability of regional specific attenuation relationships for application of PSHA. This paper elaborates some of the sensitivity studies that are carried out during the estimation of uniform hazard spectra for a site located in peninsular India.

Aim of work

The PSHA, as it is presently understood, was introduced by Cornell (1971). Based on the method presented in these publications, McGuire developed the computer program, EQRISK (Mc Guire, 1976). The corresponding approach is known as Cornell-McGuire method.

Sensitivity study of seismic hazard is carried out to identify the impact of different parameters on the hazard assessment. The sensitivity of the following parameters related to earthquake sources is conducted.

- a. Source models, SM1, SM2, SM3, SM4 (Figure-1)
- b. Increments in year and magnitude while conducting the completeness check of database using by Stepp's method.
- c. Apportionment of earthquake activity estimated for the whole region to individual source areas.

The assessment is done following Cornell-McGuire method. The software 'EQRISK', with some in-house augmentation, is used for this purpose. Peak ground acceleration (PGA) is taken as the reference parameter during the study.

Two approaches, based on energy apportionment and constant rate of activity, are adopted for apportionment of earthquake activity. Both approaches try to capture essentially the activity in individual sources based upon the total activity in the region.

From the outcome of the sensitivity analysis, the parameters that have significant influence on the seismic hazard are identified. De-aggregation of hazard estimated in each stage of sensitivity analysis is also carried out.

Essential results

- a. It is found that use of full database (without completeness check) results in higher hazard.
- b. With regard to bin sizes used for completeness check, it is noted that the estimated years of completeness did not vary significantly with respect to bin sizes unless very large sizes for year and magnitude bins are used.
- c. It is observed from the de-aggregated results that the maximum contribution to hazard results from the near earthquakes and relative contribution to hazard remains same irrespective of the shape of sources, provided their characteristics are reasonably represented
- d. Energy apportioning approach resulted in higher values of PGA (about 16%) for level of exceedance of $1e-4$, compared to calculation using equal activity rate. The model with uniform activity in all sources was found to produce lower values of accelerations.

Summary

Based sensitivity study of seismic hazard conducted for a site located in Peninsular India, it is observed that the among the parameters studied, methods followed for rate apportionment, play a major role in outcome of PSHA for the site where as source models have very low impact on the estimated hazard.

References

- Cornell, C.A. (1968). Engineering Seismic Risk Analysis. Bulletin of Seismological Society of America, 58(5), pp. 583-606.
- 'EQRISK', R.K. McGuire. U. S. Geological Survey, Denver, Colorado 1976.

4. Characterization of Loads

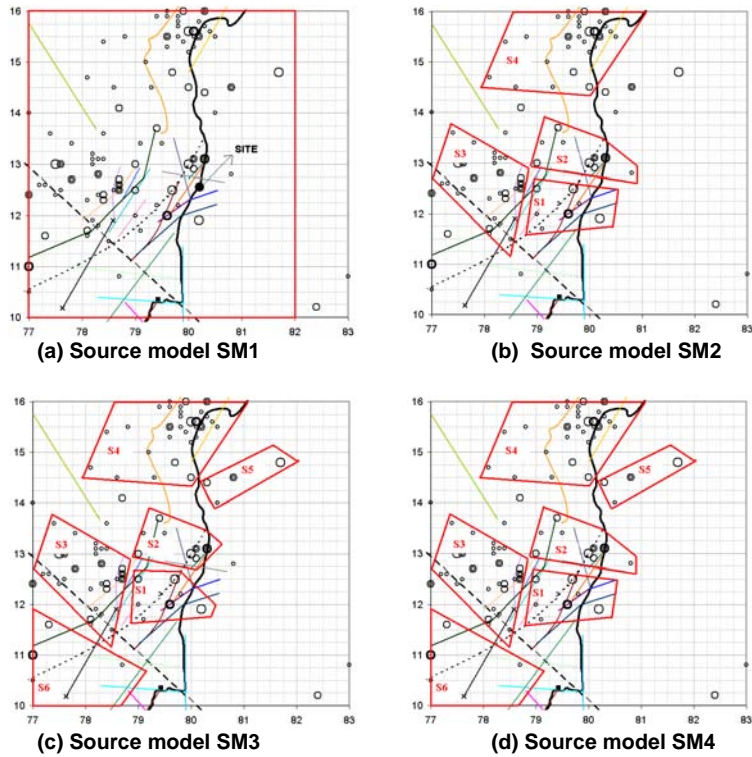


Figure 1. Possible source models of the region around the site.

- Note:
1. Distribution of earthquake epicenters and lineaments around site are taken from published literature.
 2. The magnitude of earthquake is indicated by proportional size of circle.
 3. The seismic events that are not falling inside any of the source are considered as the background seismicity in the corresponding source model.

Survey of tornado load research at Texas Tech: past, present and future (4-2506)

Kishor C. Mehta, Ph.D., P.E.

P.W. Horn Professor of Civil Engineering, Texas Tech University
Box 41023, Lubbock, TX, USA, e-mail: kishor.mehta@ttu.edu

Tornado research at Texas Tech started with the damage documentation of devastated areas in the city of Lubbock (hometown of the university) as a result of a severe tornado on May 11, 1970. The storm caused 26 fatalities, hundreds of injuries and huge amount of property loss. Since then, the personnel of the Wind Science and Engineering (WISE) Research Center have documented damages in more than 140 windstorm events around the country and overseas. The purpose of damage documentation and analysis was to assess modes of failures of buildings and structures, to ascertain type and distance traveled by debris, and to determine wind speed for correlation with F-scale. Some important results developed from the analysis of damages in the first decade including:

- Development of concept and design of above ground safe room in residences
- Best available safe place in a building is a small room in the center on the lowest floor. Damage and failures in almost all buildings are caused by wind, and not by atmospheric pressure change of the storm
- Maximum near ground wind speeds are less than 110 m/s (250 mph).

The results were presented and discussed at the 2nd Symposium on Tornadoes: *Assessment of knowledge and Implications for Man* held at Texas Tech University in Lubbock, Texas, in 1976.

Over the years, tornadic loads research has continued, though since 1980 at a slower rate because planning and construction of nuclear power plants came to a halt in the United States. Between 1980 and 2000 a tornado hazard model was developed that gave site specific wind speeds associated with the probability of occurrence. In addition, significant input was provided through the Chair of the Committee's capacity to update wind load standards for building and structures (ANSI A58.1 and ASCE 7). These standards convert wind speeds into loads for different shapes of buildings and structures. For nuclear facilities, the wind hazard loading was titled and published: "Natural Phenomena Hazards Design and Evaluation Criteria for Department of Energy Facilities," DOE-STD-1020-94, 1994.

In the recent past, since 2000, a major effort was made to update F-scale to rate tornadoes based on its ascertained wind speed. The damage documentation

4. Characterization of Loads

archive at Texas Tech and the data from other investigators were used to develop the enhanced Fujita scale, i.e. EF-scale. After review of the new scale by several committees in the engineering and meteorological communities, the EF-scale became operational by the U.S. National Weather Service beginning February 2007. A separate paper on EF-scale will be presented in this conference.

Two research pursuits are underway at Texas Tech which could have major impact on tornadic loads on nuclear facilities. The first one is the laboratory construction of a tornado simulator, VorTECH. This 10 m in diameter and 6 m in height research facility will be capable of producing a vortex in the range of one meter width. This size is large enough to obtain meaningful loads on 1:100 scale buildings and structures submerged in turbulent winds. The design of VorTECH is based on a small scale simulator that was constructed and tested in the mechanical engineering department. Results of the tests on this small scale simulator were published in the *Journal of Wind Engineering and Industrial Aerodynamics*.

The second effort is a mobile field project focused on assessing the thermodynamic and kinematic controls on the genesis and maintenance of tornadoes. Scientists have set out to map the pre-tornadic atmospheric state in four dimensions using a combination of remote (e.g., Doppler radar,) and in-situ (e.g., deployable meteorological instrumentation) technology. In 2009 and 2010, Texas Tech will be one of the universities and government agencies participating in the Verification of the Origin of Rotation in Tornadoes Experiment (VORTEX2), sponsored by the National Science Foundation. The mission of VORTEX2 is to improve our understanding of the genesis and structure of tornadoes. Texas Tech researchers will use 24 “Stick-Net” probes – instrumented, rapidly-deployable, engineering tripods – to document horizontal gradients in temperature, vapor pressure, and wind direction/magnitude at the Earth’s surface in the area immediately upwind of severe thunderstorm updrafts. In addition, emerging TTU Ka-band mobile Doppler radar will be deployed to capture the low-level horizontal and vertical structure of the tornado inflow layer and corner flow region. This data, in addition to input to numerical modeling, will provide inflow requirements for the VorTECH simulator.

The plenary session paper will present past, current and future research at Texas Tech University in context with research conducted at other institutions.

Smaller-size NPP for isolated area, and its net-work stability consideration (4-2624)

Heki Shibata, University of Tokyo
2-10 Shimouma 2, Setagaya, Tokyo 154-0002, Japan

There are many isolated power net-work from large net-work in an area like an island, or a large city far from main areas. For such a net-work a NPP, who has two or three units of rather smaller system might be better.

Some designers of NPP are planning a smaller power plant unit under 600 Mwe based on a developed ABWR. Such a smaller unit may be easy to be arranged for a safer plant against high seismic input compare to ordinary size ABWRs. If we try to introduce such a plant for an economical power supply source to isolated area or island in seismic countries, the author wants to discuss how to design their net works in this paper. However, if we use NPP for main power source, we should consider the stability of power supply to the area. In general, one unit failure is a usual situation; therefore, the net can keep its power supply without any condition. However, under a destructive earthquake condition, its seismic trigger system may shut down all NPP units simultaneously. In Japan, the automatic seismic trigger level has been designed as 0.8 ~ 1.0 S1 (SL1) in 1980s by the report to MITI. And such a trigger level has been kept upto now, and as a result they could be cool down without any difficulty. But it took more time than we planned, because unexpected reason in some case. The standard procedure to cool down immediately after the seismic event should be studied as well as its trigger level for this separate island network system.

The author examine that an adequate capacity of such a system and how to consist of the net work on four typical areas, Lassa, Tibet (PRC), and Martinique Isl.(F), Oahu Isl.(USA) and Okinawa Isl. (Japan). These latter three areas are almost 1,000 km² wide isolated islands, except Lassa, Tibet (PRC). The population of these three islands is quite different, and the condition of necessity of twin-units of smaller BWR is different. Okinawa Isl. is ordinary ABWRs are enough to make their net.

The author wants to discuss, how to decide the trigger level of each unit structurally, and how to organize their net under seismic condition.

Development, implementation and implications of the enhanced Fujita Scale (4-3136)

J.R. McDonald, Ph.D., P.E.¹, K.C. Mehta, Ph.D., P.E.²

¹Professor and Chairman of Civil Engineering, Texas Tech University Wind Science and Engineering, Lubbock, Texas, Retired

²Horn Professor of Civil Engineering, Texas Tech University Wind Science and Engineering, Lubbock, Texas

Texas Tech University, Box 41023, Lubbock, TX, USA

e-mails: Jim McDonald: mcdonald3182@sbcglobal.net,

Kishor C. Mehta: e-mail: kishor.mehta@ttu.edu

The Fujita Scale (F-Scale) was introduced in 1971, and quickly became the preferred method for estimating the intensity of tornadoes, based on appearance of damage. It had been in use until February 2007 when the US National Weather Service (NWS) implemented the Enhanced Fujita Scale (EF-Scale). The EF-Scale is designed to overcome the limitations and inconsistencies of the original scale.

Based on numerous calls for improvement of the F-Scale, the Wind Science and Engineering Research Center at Texas Tech University took on the job of enhancing the F-Scale, or developing a completely new one. A group of interested users concluded that the original form should be retained. Thus, the enhanced scale retains the same general form as the original scale. The damage categories are now EF0 to EF5, but the wind speeds and damage descriptions are different. Extensive efforts were made to keep the engineering and meteorological communities informed, so that a final consensus could be obtained.

One of the limitations was a lack of damage indicators for making wind speed estimates. In the new version, 28 different buildings, structures and trees are identified as damage indicators (DIs). With each DI from 3 to 12 degrees of progressive damage (DODs) defined, depending on the complexity of the structure. A method of expert elicitation was employed to estimate wind speeds associated with each degree of damage. Following a specific protocol, a panel of experts went through several iterations to arrive at an expected wind speed along with an upper and lower bound. The expected wind speeds for a DI are arranged in ascending order. If the observed damage corresponds to a specific DOD, the wind speed causing the damage is likely lower than the DODs above it, and higher than those below. This feature is not available with the F-Scale.

In order to preserve the usefulness of the historical tornado records, there was a need to establish a correlation between the wind speeds of the F-Scale and the EF-Scale. A second panel, consisting of NWS experts, assigned an F-Scale

category to each DOD. The F-Scale ratings were then converted to expected value wind speeds. Linear regression produced a remarkable correlation between the two scales. The F-Scale category wind speeds were then used to obtain the corresponding EF-Scale category wind speeds. All wind speeds have been converted to three-second gust speeds at 10 m height in open terrain.

After extensive review by both engineers and meteorologists and numerous presentations and workshops, a general consensus among various interested parties was achieved. The National Weather Service then adopted the EF-Scale, and began its implementation after considerable additional review. The EF-Scale has been used to assign ratings to all tornadoes in the USA since the tornado season of 2007. Adoption was preceded by extensive training of NWS personnel. The EF-Scale can be applied to a single building or structure that matches one of the DI's. To assess the intensity of a storm, it is recommended that the rating be based on several DI's. Although Fujita applied the F-Scale to both tornadoes and hurricanes, the EF-Scale should only be applied to the rating of tornadoes.

Comparisons of the two scales show that in categories 0–1 the wind speeds are slightly higher in the EF-Scale, but in categories 2–5 the wind speeds in the EF-Scale are lower than in the F-Scale. EF-Scale categories 4–5 are significantly lower. This observation has significant implications in the design and evaluation of critical facilities. For example, in the nuclear power industry the latest revision of Regulatory Guide 1.76 specifies design criteria based on the EF-Scale. The design wind speeds are significantly lower than in the previous edition. Implications of this change are preliminary, but they could mean significant reduction in construction costs of future facilities. Some existing facilities that fail to meet the old criteria might not require the same extent of retrofit under the new criteria.

Structural integrity evaluation of shielding blocks for HANARO's cold neutron guide (4-3137)

Jeong-Soo Ryu, Yeong-Garp Cho, Kang-Soo Kim
Korea Atomic Energy Research Institute
150, Dukjin-dong, Yuseong-gu, Daejeon 305-353, Korea
e-mail: jsryu@kaeri.re.kr

HANARO (Hi-flux Advanced Neutron Application Reactor) is a multi-purpose research reactor with a thermal power of 30 MW. KAERI has been developing a HANARO's cold neutron source (CNS) system since 2003. Cold neutron guide system consists of neutron guide, in-pile plug, primary shutter and shielding blocks. A total of 15 shielding blocks are placed surrounding the primary shutter and cold neutron guides between the outer wall of reactor pool and the CNS guide bunker in reactor hall. The shielding blocks are designed to do the biological shielding of neutrons and gamma from the CN port, the primary shutter and the neutron guides. These consist of block type walls and roofs that can be necessarily assembled or disassembled. Design criteria for them are classified as non-nuclear safety (NNS), seismic category II, and quality class T. These shielding blocks are designed with a sufficient strength not to collapse when a SSE (Safe Shutdown Earthquake) occurs.

The objective of this paper is to evaluate the structural integrity for shielding blocks according to the technical requirements. The shielding blocks must shield effectively the radiation emitted from facilities related to neutron guide and satisfy the requirements of the movable type facilities in the case of the necessity. Each shielding block shown in Fig. 1 and Fig. 2 is a steel casemate (steel housing), which are filled with the heavy concrete (3.5 g/cc) and polyethylene with 5% boron. The weights of shielding blocks are in the range of 1.3 ton ~ 21 ton. The modal analysis for 3 model types according to the shielding block configuration and the seismic analysis were performed. 3D finite element model is made in order to calculate the maximum displacement for the shielding block. The seismic analysis for the shield blocks was performed by using the response spectrum analysis method and the SAP 2000 code.

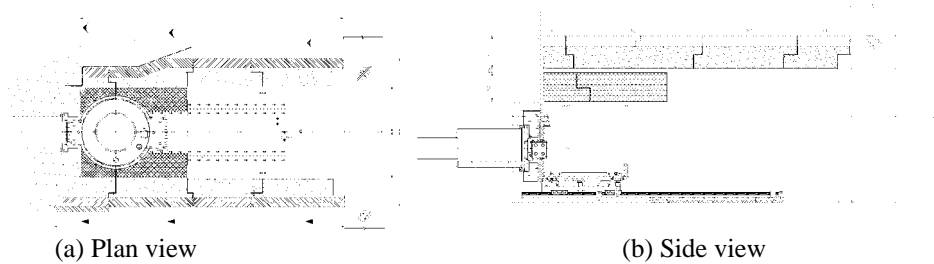


Figure 1. Configuration of shielding blocks.

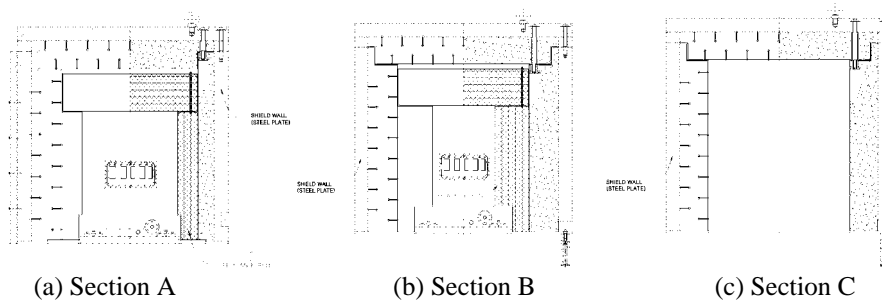


Figure 2. Cross section shape of shielding blocks.

Dead weight (D) is a total weight of all the elements calculated considering the specific weight. The design live load (L) of the 500 kgf/m² is only applied to the roof. The seismic live loads are defined as the mass corresponding to the 25% of the applied live load and considered as the node mass at the node of the analysis model. The floor response spectrum as a seismic load (E) at the reactor hall floor SSE was used. This spectrum had been made when the reactor building was designed. The structural damping values were applied to the 7% of the critical damping values used at the steel frame structure jointed by the bolts. The load combinations for the shielding block design were performed according to the AISC Specification 7-05, section 2.3.2 for steel structures and ACI Code 349 section 9.2 for concrete structure.

The analysis results show that the maximum stress and displacement are within the code limits. From the modal analysis for the 3 types, the basic natural frequencies were 20 Hz through 25 Hz. The maximum displacement for the shielding block is 0.363 mm. This value is below the 5 mm of the allowable displacement. The calculated stresses for the shielding block and the lifting eye bolts were below the allowable stresses. The diameter of the connection bolt was chosen with larger than that obtained from the structural calculation results. The member diameter and embed depth of the anchor bolt was determined in accordance with ACI 349. Tension and shear stresses applied to the polyethylene

4. Characterization of Loads

casemate were below the allowable stress. Also, the seismic analysis results for the foundation slab show that there is a sufficient margin at the cutting part of the reinforced bar for the installation of the support anchor bolts. Therefore, the structural integrity for the shielding blocks and related structures was evaluated. Finally the detailed design was performed for each structural element by using the data based on the seismic analysis for the shielding blocks.

References

- Ryu, J.-S. et al. Technical Requirements for Fabrication and Installation of Removable Shield for CNRF in HANARO, KAERI/TR-3573/2008, 2008.4.
- ACI 349, Building Code Requirements for Nuclear Safety Related Concrete Structures and Commentary.
- ACI 318, Building Code Requirements for Structural Concrete and Commentary.
- AISC Specification, Manual of Steel Construction – Allowable Stress Design.
- AISC Specification, Manual of Steel Construction – Allowable Stress Design.
- ASCE Standard 4-98, Standard for Seismic Analysis of Safety-Related Nuclear Structures and Commentary.
- ASCE Standard 7-05, Minimum Design Loads for Buildings and Other Structures.

Analysis of the strong motion records obtained from the 2007 Niigataken Chuetsu-oki earthquake and determination of the design basis ground motions at the Kashiwazaki Kariwa Nuclear Power Plant.

Part 1. Outline of the strong motion records and estimation of factors in large amplification (4-3189)

Ryoichi Tokumitsu¹, Masatomo Kikuchi², Isao Nishimura³, Yoshiaki Shiba⁴,
Shinya Tanaka⁵

¹Nuclear Asset Management Department, Tokyo Electric Power Company,
1-1-3, Uchisaiwai-cho, Chiyoda-ku, Tokyo 100-8560, Japan,
e-mail: tokumitsu.r@tepcoco.jp

²Nuclear Asset Management Department, Tokyo Electric Power Company,
1-1-3, Uchisaiwai-cho, Chiyoda-ku, Tokyo 100-8560, Japan,
e-mail: kikuchi.masatomo@tepcoco.jp

³Nuclear Asset Management Department, Tokyo Electric Power Company,
1-1-3, Uchisaiwai-cho, Chiyoda-ku, Tokyo 100-8560, Japan,
e-mail: nishimura.isao@tepcoco.jp

⁴Earthquake Engineering Sector, Civil Engineering Research Laboratory,
Central Research Institute of Electric Power Industry, Chiba, Japan,
e-mail: cbar@cripi.denken.or.jp

⁵Architectural Department, Tokyo Electric Power Services CO., LTD.,
Tokyo, Japan, e-mail: s.tanaka@tepscoco.jp

Introduction

The Niigataken Chuetsu-Oki Earthquake (Mj6.8) occurred on July 16, 2007. With this earthquake, a large ground motion was observed at the Kashiwazaki Kariwa Nuclear Power Plant, which was larger than the ground motion supposed as the design basis seismic ground motion. The ground motion observed at the power plant was larger than the ground motion of Mj6.8 that is supposed from the attenuation relationship of Noda et al. (2002) [1]. In addition, even in the Kashiwazaki Kariwa Nuclear Power Plant, there was large variation in recorded ground motion at different parts of the observation point

Aim of the work

In order to investigate the primary factor of the large ground motion observed at the Kashiwazaki Kariwa Nuclear Power Plant in the Niigataken Chuetsu-Oki Earthquake, we examined the source, propagation and site effect of the Niigataken Chuetsu-Oki Earthquake, with the analysis and ground motion simulation analysis of observation record [2].

Study on the source effect

In regard to the source effect, we estimated the moment density distribution on the fault through the inversion analysis using the empirical Green's function method, with the observation records of the Kashiwazaki Kariwa Nuclear Power Plant and other regional records. We also estimated a characterized source model that describes the observation records of the site. From the characterized source model, we concluded that the short-period source spectrum is about 1.5 times larger than the average short-period source spectrum evaluated from the seismic moment by the National Research Institute for Earth Science and Disaster Prevention (NIED), and the scaling rule between the seismic moment and short-period source spectrum [3].

Study on the propagation effect

In order to evaluate the propagation effect of the Niigataken Chuetsu-Oki Earthquake, we analyzed the characteristics of the ground motion records obtained in the Kashiwazaki Kariwa Nuclear Power Plant in the past. For the analysis, we used the ground motion records obtained in the borehole array of Unit 1 and Unit 5, as free field records. From these records, we calculated the ground motions on the free surface of the base stratum by 1-D wave propagation analysis with the soil model of each observation point. From the analysis, we concluded that the ground motion of the offshore event becomes larger than that of the inland event, and we supposed that the ground motion of the Niigataken Chuetsu-Oki Earthquake, which had the characteristic of the offshore event, was more 2 times as large as the average ground motion.

Study on the site effect

In regard to the site effect, we analyzed the spectral ratio between the recorded ground motion in the free field near Unit 1 and 5. We used the observation record obtained in the Kashiwazaki Kariwa Nuclear Power Plant in the past. From these spectral ratios, we concluded that seismic ground motion that comes from the offshore events are amplified larger at Unit1, the southern part of the

site, than at Unit5, the northern part of the site, and we assumed these characteristics of spectral amplitude to be the site effect.

Conclusions

We concluded that the short-period source spectra in the Niigataken Chuetsu-Oki Earthquake was higher than the average event of Mj6.8, and the ground motion became about 1.5 times higher. We also concluded that the ground motion became over 2 times larger due to the propagation effect for offshore events. In addition, the ground motion in the southern part of the site is amplified 2 times larger than that in the northern part due to the site effect.

References

1. Noda, S. , K.Yashiro, K.Takahashi, M.Takemura, S.Ohno, M.Tohdo and T.Watanabe, RESPONSE SPECTRA FOR DESIGN PURPOSE OF STIFF STRUCTURES ON ROCK SITES , OECD-NEA Workshop on the Relations between Seismological DATA and Seismic Engineering, Oct. 16–18, 2002, Istanbul, pp. 399–408
2. A Report on Analysis of Seismic Observation Data Obtained at the Time of the 2007 Niigata-Chuetsu-Oki Earthquake at the Kashiwazaki-Kariwa Nuclear Power Station, and the Formulation of the Design-basis Seismic Motion, Tokyo Electric Power Company, 2008.
3. Kazuo , D., M. Watanabe, T. Sato, T. Ihii, SHORT-PERIOD SOURCE SPECTRA INFERRED FROM VARIABLE-SLIP RUPTURE MODELS AND MODELING OF EARTHQUAKE FAULTS FOR STRONG PREDICTION BY SEMI-EMPERICAL METHOD , J. Struct., Eng., AIJ, No. 545, Jul., 2001, pp. 51–62.

**Analysis of the strong motion records
obtained from the 2007 Niigataken Chuetsu-
oki earthquake and determination of the
design basis ground motions at the
Kashiwazaki Kariwa Nuclear Power Plant.
Part 2. Difference of site amplification
based on the 2D FEM analysis of the folded
structure (4-3190)**

Tetsushi Watanabe¹, Takafumi Moroi², Masayuki Nagano³, Ryoichi Tokumitsu⁴,
Masatomo Kikuchi⁵, Isao Nishimura⁶

¹Kobori Research Complex, Kajima Corporation, 6-5-30, Akasaka, Minato-ku,
Tokyo 107-8502, Japan, e-mail: w-tetsushi@kajima.com

²Kobori Research Complex, Kajima Corporation, 6-5-30, Akasaka, Minato-ku,
Tokyo 107-8502, Japan, e-mail: moroi@kajima.com

³Faculty of Science and Technology, Tokyo University of Science, 2641,
Yamazaki, Noda-shi, Chiba 278-8510, Japan,
e-mail: nagano-m@rs.noda.tus.ac.jp

⁴Nuclear Asset Management Department, Tokyo Electric Power Company,
1-1-3, Uchisaiwai-cho, Chiyoda-ku, Tokyo 100-8560, Japan,
e-mail: tokumitsu.r@tepcoco.jp

⁵Nuclear Asset Management Department, Tokyo Electric Power Company,
1-1-3, Uchisaiwai-cho, Chiyoda-ku, Tokyo 100-8560, Japan,
e-mail: kikuchi.masatomo@tepcoco.jp

⁶Nuclear Asset Management Department, Tokyo Electric Power Company,
1-1-3, Uchisaiwai-cho, Chiyoda-ku, Tokyo 100-8560, Japan,
e-mail: nishimura.isao@tepcoco.jp

Introduction

The Niigataken Chuetsu-oki earthquake, with a moment magnitude (M_w) of 6.6, occurred on 16 July 2007 in the western offshore of Niigata Prefecture in Japan. The Kashiwazaki Kariwa Nuclear Power Plant site is located about 16 km south of its epicenter. The site has seven units, with four units (Units 1-4) at south side of the site and the other three units (Units 5-7) only about 1.5km away from Units 1-4. However, the strong motion records at Unit 1 side were significantly larger than those at Unit 5 side [1].

It is important to investigate the difference of site amplification in the local area. This paper describes modeling of the folded structure based on boring and seismic reflection survey and the 2D FEM analysis.

Modeling of the 2D folded structure

Past geological survey indicates that the folded structure exists in the site area and the Madonosaka syncline runs along the direction of north 55 degrees east. Soil structure probably has continuity of shape in this direction, and 2D models orthogonal to the syncline are made at Unit 1 side and Unit 5 side respectively.

Boundaries of strata are evaluated based on the latest seismic reflection and boring survey [2], and confirmed by balanced cross section. The model is about 7km wide and 5km deep, and consists of seven strata, Nishiyama stratum, Shiiya stratum, Upper Teradomari stratum, Lower Teradomari stratum, Nanatani stratum, Green tuff, and Seismic bed rock. S-wave velocities are 0.7, 1.0, 1.7, 2.0, 2.6, 2.6, and 3.1km/s. The model has irregular structure with the fold of upper three boundaries and the slope of lower three ones. Unit 1 is located above the syncline, while Unit 5 is located above the anticline.

Fundamental characteristics of site amplification

Numerical analysis is performed by finite element method (FEM) in frequency domain [3]. Finite elements are created for the target frequency of 5Hz.

In order to grasp fundamental characteristics of site amplification, parametric studies are conducted on vertically incident angles of S-wave inside the 2D model section. Their results show that site amplification of 2D model at Unit 1 is larger than that of 1D model directly under Unit 1 when the angle is closer to 0 degrees (vertical incidence). However, site amplification of 2D model at Unit 5 generally corresponds to that of 1D model. The irregularity of structure has a greater impact on Unit 1.

Simulation analysis

Three asperities are defined by the waveform source inversion in the 2007 Niigataken Chuetsu-oki earthquake [1]. The third asperity caused a pulse in the latter part of the waveform, and it determined the difference in the strong motion records between Unit 1 and Unit 5. The positions of asperities are located outside the 2D model section, and simulation analysis is performed considering horizontally incident angles in addition to vertically incident angles. Concerning the angle projected on the 2D model section, the third asperity has the smallest angle in the three asperities.

4. Characterization of Loads

For the first and second asperities, Unit 1 and Unit5 show similar transfer functions. For the third asperity, site amplification at Unit 1 is larger than that at Unit 5. This feature is similar to fundamental characteristics mentioned above. Waveform simulation is carried out using these three transfer functions and the Unit 5 records as control motion. The results show good agreement with the Unit 1 records, including the pulse from the third asperity. It is estimated that folded structure caused difference in strong motion records in the local area.

Sensitivity analysis of the folded structure

It is estimated which part of the folded structure affects site amplification. A soil property of a certain stratum is replaced with other one, and effect of an arbitrary boundary is extracted. As a result, both first and second boundaries (Nishiyama stratum - Shiiya stratum, Shiiya stratum - Upper Teradomari stratum) amplify the seismic motion at Unit 1. Even if the folded structure is some smoother, site amplification doesn't change so much.

Conclusions

The 2D FEM analysis is performed using the folded structure, and simulation results show good agreement with the observed strong motion records at Unit 1. It is suggested that the difference of site amplification in the local area is caused by the folded structure.

References

1. Tokyo Electric Power Company, Analysis of the seismic observation records obtained during the 2007 Niigataken-Chuetsu-Oki earthquake at the Kashiwazaki Kariwa Nuclear Power Plant, 2nd follow-up IAEA mission, 2008.
2. Iwao Kobayashi, Masaaki Tateishi, Naohisa Yoshimura, Tetsuro Ueda, and Hirokazu Kato, Geology of the Kashiwazaki region, Geological Survey of Japan, 1995.
3. Masayuki Nagano and Masato Nagano, Response analysis of 2D structure subjected to obliquely incident waves with arbitrary horizontal angles, Transactions of AIJ, Journal of structural and construction engineering, No. 474, pp. 67–76, 1995.

Analysis of the strong motion records obtained from the 2007 Niigataken Chuetsu-oki earthquake and determination of the design basis ground motions at the Kashiwazaki Kariwa Nuclear Power Plant. Part 3. Determination of the design basis ground motions considering findings from the earthquake (4-3191)

Masatomo Kikuchi¹, Ryoichi Tokumitsu², Isao Nishimura³

¹Nuclear Asset Management Department, Tokyo Electric Power Company,
1-1-3, Uchisaiwai-cho, Chiyoda-ku, Tokyo 100-8560, Japan,
e-mail: kikuchi.masatomo @tepco.co.jp

²Nuclear Asset Management Department, Tokyo Electric Power Company,
1-1-3, Uchisaiwai-cho, Chiyoda-ku, Tokyo 100-8560, Japan,
e-mail: tokumitsu.r @tepco.co.jp

³Nuclear Asset Management Department, Tokyo Electric Power Company,
1-1-3, Uchisaiwai-cho, Chiyoda-ku, Tokyo 100-8560, Japan,
e-mail: nishimura.isao@tepco.co.jp

Introduction

On 2006 September 19th, “the Guidelines for Seismic Design Evaluation of Nuclear Power Reactor Facilities” was revised by Nuclear Safety Committee(NSC), which relates to the seismic safety of the nuclear reactor installation in Japan. After the revision, re-evaluation on the seismic safety of the all operating nuclear power plants which includes the determination of the design basis ground motions based on the revised guidelines had been started.

At the Kashiwazaki Kariwa nuclear power plant, re-evaluation of the seismic safety was also being conducted , but the Niigataken Chuetsu-oki earthquake (Mj6.8) occurred on 2007 July 16th, and observation record at the Kashiwazaki Kariwa nuclear power plant exceeded the original design basis ground motion which was determined under the previous guidelines.

On the basis of the circumstance, determination of the design basis ground motion for Kashiwazaki Kariwa Nuclear Power Plants conducted considering the lessons learned from the Niigataken Chuetsu-oki earthquake.

Aim of the work

In this paper, we determined the new design basis ground motion on the basis of the factors that magnified the earthquake ground motion at the Kashiwazaki Kariwa nuclear power plant in the Niigataken Chuetsu-oki earthquake, which were examined in the part 1 and the part 2.

Essential results

On the basis of the examination result of the part 1 and the part 2, following items 1–3 were mainly considered as knowledge which is acquired from the Niigataken Chuetsu-oki earthquake, when the design basis ground motions of the Kashiwazaki Kariwa nuclear power plant were evaluated.

-1: The characteristics of the earthquake ground motion propagated from the offshore sources are different from those propagated from the inland sources. Therefore, we selected the active faults to be evaluated, classifying them into the offshore faults and the inland ones.

-2: The characteristics of the earthquake ground motion propagated from the offshore sources are different between Arahama area (where Unit 1-4 are installed) and Ominato area (where Unit 5-7 are installed). Therefore, we evaluated the design basis ground motions by offshore active faults for Arahama area and in Ominato area separately.

-3: The Niigataken Chuetsu-oki earthquake generated 1.5 times larger ground motion in the short period range in comparison with the average earthquakes of Mj6.8. Therefore, we applied 1.5 times larger short period ground motion level than that of average level to the earthquake ground motion evaluation using the source fault model.

As the active faults which is thought to have large impacts on the Kashiwazaki Kariwa nuclear power plant, we chose the F-B fault (Mj7.0) for the offshore area, which is thought to be the causative fault of the Niigataken Chuetsu-oki earthquake, and Katagai fault which is located on east side of the site for the inland area. Additionally, we considered the Nagaoka Plain Western Boundary fault Zone (Mj8.1) where simultaneous activity of the Katagai fault, the Kakuda/Yahiko fault and the Kihinomiya fault are taken into account adopting conservative assumption.

In order to evaluate the ground motion by the chosen sources, we adopted both the empirical method using response spectrum based on attenuation relation, and the numerical simulation method based on the source fault model.

Conclusions

As the new design basis ground motions for Kashiwazaki Kariwa nuclear power plant, we determined 5 earthquake ground motions on the basis of the evaluation of the chosen sources. Peak ground acceleration (PGA) value of the design basis ground motions for horizontal component is 1,209Gal at Arahama side, and is 2,300Gal at Ominato side.

References

1. A Report on Analysis of Seismic Observation Data Obtained at the Time of the 2007 Niigata-Chuetsu-Oki Earthquake at the Kashiwazaki-Kariwa Nuclear Power Station, and the Formulation of the Design-basis Seismic Motion, Tokyo Electric Power Company, 2008

5. Modeling, Testing and Response Analysis of Structures, Systems and Components

Modeling and response analysis of structures (including foundations), systems, lifelines and components subjected to extreme loads. Validation of analytical methods based on experimental results.

(Part 1. 1577–1840)

Part 2 of the abstracts of Division 5 is included in Volume 2 of the SMiRT20 abstracts

PBMR loop acoustics (5-1577)

Yerishca Mudaly¹, M.M. Cepkauskas²

¹Eskom PBMR Client Office, Cape Town South Africa
e-mail: MudalyY@Eskom.co.za

²Eskom PBMR Client Office, Cape Town South Africa
e-mail: CepkauM@Eskom.co.za

The present paper provides a method to determine the acoustic pressure waves due to compressor operations throughout the primary loop of the PBMR Helium cooled reactor. This is accomplished by combining simple one dimensional analytical pipe solutions with the output of the Flownex computer code for both steady state and transient conditions. Simple one dimensional pipe models consisting of an acoustic wave equation with non-homogeneous boundary conditions are modeled via a transformation technique. It is demonstrated that these models can be used to properly couple various individual pipes, while still maintaining the proper physical acoustic behavior. A subroutine is developed where by the geometry and temperature from Flownex is used as input for the acoustic loop model for steady state conditions. A series of unknown constants required at the pipe/pipe interface are solved for via matrix operations to obtain the required solution. This same procedure is followed via a time step for transient results. This results can be then imported to a finite element pipe model to determine pipe vibration response.

Frequency-dependent impedances in the time-domain SSI analysis: modification of seismic input (5-1592)

Alexander Tyapin
“Atomenergoproject”
7 Gasheka Str., Suite 750, Moscow, 123056, Russia
e-mail: atyapin@bvcp.ru

The time-domain SSI analysis is usually performed using “platform model”: the model of the structure is placed on the distributed springs and dashpots resting on a rigid platform. Seismic input corresponding to the “kinematical interaction” is put on the platform.

The problem, however, is that spring and dashpot in the frequency domain provide constant real part and linear imaginary part of the dynamic stiffness, so the integral “platform impedances” cannot follow the “actual impedances” in the frequency domain (rather sophisticated for the layered soil sites). The obvious way out – to use more sophisticated springs and dashpots, additional masses, etc. – proved to be inconvenient and is not used in practice.

The aim of the work is to implement the advanced approaches to the SSI analysis (currently available in the frequency domain only) into the common engineering practice (based on the time-domain calculations).

The author suggests the accounting for the frequency dependence of the “actual impedances” in the time domain by means of the modification of the seismic input on the platform. The criterion for this modification is to provide the same structural response with “platform” impedances as for the “actual” frequency-dependent impedances in the limit case of a rigid basement slab.

The first stage of the proposed approach is to get the “actual” response of the slab in the frequency domain. The upper structure on a rigid slab is represented by “dynamic inertia” matrix linking the integral forces (acting on the slab from the upper structure) to the displacements of this slab. This 6×6 frequency-dependent complex matrix is obtained using the information about the structural inertia and about the eigenfrequencies/eigenforms of the structure with fixed basement. “Actual impedances” and “kinematical interaction” transfer functions are obtained in the frequency domain (e.g., by SASSI). The rigidity of the basement slab enables to combine the “dynamic inertia” and “actual impedances” in the format of the 6×6 matrices.

The second stage is to get the “platform” transfer functions from the 6D movement of the platform to the rigid slab response. This time the “platform” impedances (derived from springs and dashpots) are used instead of “actual” ones. “Platform” impedances are combined with the same “dynamic inertia”

matrix of a structure, as previously used. The resulting transfer functions form the 6×6 complex frequency-dependent matrix.

The criterion of the similar slab response in the “actual” and “platform” cases enables to obtain the modification matrix from “actual” to the “platform” seismic input. The modification matrix in the frequency domain is complex and frequency-dependent. It has some special properties useful to understand the results better.

The initial three-component “actual” accelerogram after the modification turns into the six-component one. The modification in the time domain is performed using direct and inverse FFT.

The proposed approach enables to get “true” movement of the rigid basement slab in the time-domain analysis with platform model, considering the frequency dependence of the impedances. This approach may be called “combined” as it combines initial calculations in the frequency domain (“actual” impedances and the modification matrix) and calculations in the time domain (final dynamic analysis). The approach may be also called “asymptotic” as it is precise for the rigid basement slabs (excluding stresses in the slab itself). However, the main NPP buildings usually have comparatively stiff basements, so the error will be likely not so great.

The time-domain calculations are performed using the same structural model and the same software as now. The whole modification is done at the SSI specialists’ side using the information about the upper structure easily obtained in the general FEM codes.

Earthquake-induced sloshing effects on seismic qualification of liquid storage tanks (5-1594)

Xian-Xing (Lambert) Li

Chief Civil/Structural Engineer, SNC-Lavalin Nuclear Inc.
2275 Upper Middle Road East, Oakville, Ontario, Canada L6H 0C3
e-mail: lambert.li@snuclear.com

Introduction

Seismic analysis of liquid storage tanks differs from building structures because the liquid exerts hydrodynamic force on tank walls and base during seismic excitation. Sloshing response under seismic events is of particular importance for a reliable estimate of the total horizontal force and the corresponding overturning moment. Nevertheless, the applicable seismic codes for tanks of general shape are quite limited and not well developed as compared with the large number of codes applicable to vertical-cylindrical tanks.

There has been an upsurge of interest in developmental activities aimed at producing better seismic design methods for liquid storage tanks due to stringent requirements on the safety of liquid storage tanks in nuclear power plants. In many applications, hydrodynamic forces due to liquid sloshing needs to be understood and has to be considered.

Classical solutions are available for rectangular and vertical-cylindrical tanks. For heavy storage tanks in a nuclear power generation plant, horizontal-cylindrical tanks, spherical tanks, and other types of tanks are more frequently used. Exact analytical solutions for these types of tanks are unavailable, except for some special cases such as half-full of liquid. Approximate solution can be developed as an alternative toward a successful evaluation of sloshing effects.

Aim of the work

The purpose of this work is to develop a general approach for seismic analysis of storage tanks of general shape under sloshing hydrodynamic force. In review of the present development state of prediction for seismic response of liquid storage tanks, this paper is to present the following objectives:

- Review seismic codes on liquid storage tanks to establish the present state of the art

- Propose an efficient and unified methodology for earthquake-induced sloshing analysis with tanks of general shape or type
- Provide a response spectrum method for the seismic analysis of liquid storage tanks.

Essential results

Assuming ideal fluid conditions and small-amplitude elevation of the free surface of the liquid, classical modal analysis method can be used for the analysis of the sloshing in rectangular tanks. The modal analysis results are obtained including modal frequencies and modal shapes. The impulsive and convective masses and their height of centroids of liquid motions can be calculated. This seismic force and overturning moment can be obtained based on the modal analysis results.

The solution of the sloshing in the rectangular tank can be extended to a general tank of any shape or type. An important point to note is that the shape of a general tank does not fit into any standard coordinate system; therefore, it is difficult to develop an exact analytical methodology to evaluate the sloshing behavior. Although the velocity potential functions for sloshing in the rectangular and vertical-cylindrical tanks have been derived explicitly by the separation of variables, current sloshing theory has not yet developed an explicit velocity potential function for sloshing in horizontal-cylindrical tanks. Approximate analytical procedure for the sloshing evaluation is used.

A horizontal-cylindrical tank can be converted to an “Equivalent Rectangular Tank” [1] without considering overturning moment. This paper extends the methodology to a general tank of any shape by considering all required seismic analysis factors including sloshing frequencies, the corresponding impulsive and convective masses, and the corresponding height of centroids of masses. Modal analysis results for general tanks are obtained based on the corresponding results of the equivalent rectangular tank.

Sloshing response spectrum is developed based on seismic codes. The liquid response, total seismic horizontal force and overturning moment are then readily calculated using the response spectrum analysis method.

The proposed method is validated by comparing with some available experiment results [2] for horizontal-cylindrical and spherical tanks. The proposed predictions are in well agreement with the corresponding experiment results.

Summary

This paper presents a methodology to evaluate earthquake-induced sloshing effects for seismic qualification of liquid storage tanks. The modal sloshing properties are derived based on an “Equivalent Rectangular Tank” method.

Response spectrum analysis is used to be calculated the sloshing response. The total tank base shear and overturning moment are obtained which can be used for seismic qualification analysis of tanks and tank supports/foundations. This general approach is applicable to general tanks such as vertical-cylindrical, horizontal-cylindrical, spherical, elliptical, and other irregular practical tanks.

References

1. Eurocode 8 (2006). Design of Structures for Earthquake Resistance – Part 4: Silos, Tanks, and Pipelines. European Committee for Standardization, Brussels.
2. Dodge, F.T. (2000). The New “Dynamic Behavior of Liquids” in Moving Containers. Southwest Research Institute, San Antonio, Texas.

Nonlinear impact analysis of pipe whipping onto restraints (5-1595)

Xian-Xing Li

Chief Civil/Structural Engineer, SNC-Lavalin Nuclear Inc.
2275 Upper Middle Road East, Oakville, Ontario, Canada L6H 0C3
e-mail: lambert.li@slnuclear.com

Introduction

Nuclear power plant regulations concern the effects of high energy pipe break. Generally, design codes provides requirements on structures, systems, and components (SSCs) important to safety, being designed to accommodate the effects of postulated accidents, including appropriate protection against the dynamic effects of postulated pipe ruptures such as main steam line break (MSLB).

The USNRC Standard Review Plan [1] requires that information concerning break and crack location criteria and methods of analysis of evaluating the dynamic effects associated with postulated breaks and cracks in high- and moderate-energy fluid system piping should be provided in the applicant's safety analysis report (SAR). This review is to confirm that there is appropriate protection of SSCs to mitigate the consequences of a postulated pipe rupture.

The review criteria [1] also requires that dynamic analysis methods be used to verify the integrity and operability of mechanical components, component supports, and piping systems, including restraints and other protective devices, under postulated pipe rupture loads. It also requires that the design adequacy of systems, components, and component supports ensure that the intended design functions are not impaired as a result of pipe-whip or jet impingement loadings.

Pipe restraint systems are generally design to arrest high energy pipe whipping. Actual dynamic jet loading on the high energy pipe and restraint during the course of impact is not well investigated. The extreme jet load can be calculated based on standards such as ANSI/ANS [2]. However, the impact loading effects on the ruptured pipe and restraint structures are not well understood, especially the post-yield behavior of the pipe-restraint system and the validation of the dynamic jet loading application. This paper provides an insight into the catastrophic failure modes of pipe-restraint system, so that efficiency of the restraints can be investigated.

Aim of the work

The objective of this work is to assess the structural behavior of the restraint system and high energy pipe in the course of a pipe whipping event caused by a

high energy pipe break. By doing so, the capability and performance of the restraint structures to arrest pipe whipping can be evaluated.

This analysis is concerned with potential failures of the restraint structures as well as the pipe under the pipe whipping impact and the performance of the restraint structure and steam pipe under a postulated MSLB event. The Main purpose of the work is to gain better understanding how a postulated high energy pipe break event may interact and affect the existing concerned restraints.

Another purpose of this analysis work is to show how can a structure-pipe interaction system under the dynamic and impact loads be simulated in order to understand potential failure modes which have to considered in the restraint design.

Essential results

The impact analysis is carried out using the nonlinear dynamic finite element methodology. Shell elements are used for modeling pipe and restraint structures. Shell element is able to reveal realistic structural failure modes in the course of the impact event. Both material and geometrical nonlinearities are considered in the simulation. The dynamic analysis with time integration and contact configuration is used to solve the transient impact problem.

Stress states of the restraint-pipe interaction system resulting from the transient thrust loading are obtained at instants in time. The deformation and displacement time history of the restraint-pipe system is presented. Both the impact stress and deformation responses can be used for the evaluation of the post-yield structural behavior. Impact failure modes can be investigated.

From the numerical simulation results, the pipe impact sequence can be realized. Pipe impact forces at the contact interfaces between the pipe and the restraint structure can be obtained. The impact force is of time-history nature which is dynamic effects of the applied thrust load. This transient impact force can be compared to the applied transient thrust load to get into understand the real design impact force.

The catastrophic failure mode investigation can guide us to optimize the restraint structure design so that the high energy pipe whipping can be effectively restrained.

Summary

Nonlinear impact analysis of high energy pipe whipping onto the restraint structure is performed. The potential catastrophic failure modes of the pipe and restraints are investigated to understand the potential consequence of pipe whipping. Dynamic impact force is obtained and can be used for the restraint design. The transient dynamic impact force is compared to the applied transient jet loading so the dynamic effects can be understood.

The post-yield behavior of the high energy pipe and restraint structure is presented. Recommendations are made to the restraint structure design, so that the restraint system is able to arrest the pipe whipping effectively.

References

1. USNRC, NUREG-0800, Standard Review Plan, Section 3.6.
2. ANSI/ANS-58.2-1988, Design Basis for Protection of Light Water Nuclear Power Plants against Effects of Postulated Pipe Rupture.

Seismic response evaluation of safety related nuclear structure with yielding dampers using linearization techniques (5-1597)

Y.M. Parulekar¹, G.R. Reddy¹, K.K. Vaze¹, A.K. Ghosh¹,
H.S. Kushwaha¹, R. Ramesh babu²

¹Bhabha Atomic Research Centre, Mumbai-400085, India

²Central Power Research Institute, Bangalore, India

Aim

Old safety related structures of nuclear facilities were designed for seismic criteria less rigorous than the present. To meet the current seismic safety requirements, detailed re-evaluation of structures need to be performed. Some of the structures may need retrofitting to meet the present demand. There are various methods of retrofitting such as, steel jacketing, concrete jacketing, fiber wrapping, using dampers etc. In the present paper use of dampers for retrofitting RCC structures is discussed.

Scope

Elasto-plastic dampers are known to dissipate earthquake input energy by yielding thus reducing the demand on the structure. Shake table testing has been carried out on RCC model of a structure (Fig. 1) with and without yielding dampers under design response spectrum compatible time history.

Nonlinear Time History (TH) analysis has also been carried out and the results of the response are compared with test results (Fig. 2). Linearization techniques can be used to evaluate the response of structure with yielding damper to avoid time-consuming TH analysis method. In the present paper two such linearization techniques are discussed and using these techniques the response is compared with TH analysis and test results. In one method linearization is carried out using equivalent Cauchy's stiffness and damping. In another method equivalent secant stiffness and equivalent damping obtained from hysteresis energy dissipated is used. Iterative response spectrum analysis is then carried out using these linearization techniques to cater the non-linearity of yielding dampers.

Conclusions

Significant reduction in response of RCC structure is obtained when yielding damper plates were attached in the frames of the structure. Plates with two dampers at each location with plates having lesser yield displacement gives optimum reduction in the response without much change in the fundamental frequency of the structure. Time history analysis and iterative response spectrum analysis results of the structure with and without dampers are in good agreement with the test results.



Figure 1. Shake table test setup.

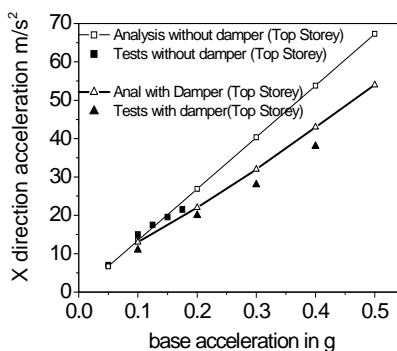


Figure 2. Comparison of test and analysis results.

Seismic stability of glove boxes – experiments and analysis (5-1598)

Y.M. Parulekar¹, G.R. Reddy¹, K.K. Vaze¹, A.K. Ghosh¹, C. UmaShankar¹,
H.S. Kushwaha¹, R. Ramesh babu², K.N. Mahule¹
¹Bhabha Atomic Research Centre, Mumbai-400085, India
²Central Power Research Institute, Bangalore, India

Aim

In a nuclear facility radiotoxic materials are being handled in leak tight enclosures called glove boxes. These glove boxes serve as primary confinement for these radiotoxic materials. Hence there is a need to check stability of glove boxes under earthquake loading such that their functional requirements and structural integrity are maintained. The pressure boundary of the glove boxes also should not be jeopardized in case of seismic excitation. For this requirement, extensive shake table experiments were carried out on a single glove box and two glove boxes connected by transfer tunnel. Detailed nonlinear sliding analysis of the glove boxes is also carried out in order to obtain the stresses in supporting framework and bolt connections.

Scope

Seismic evaluation of glove boxes is carried out using experiments and nonlinear dynamic analysis. General guidelines stated by Department of Energy (DOE) were used for evaluating and upgrading the seismic adequacy of glove boxes. The glove box system is a series of physical barriers provided with glove ports and gauntlets, through which process and maintenance operations may be performed, together with an operating ventilation system. The glove boxes are anchored to a steel framework through bolts and the framework is placed on the ground without anchoring. The present paper deals with sliding analysis of a single glove box and two glove boxes connected by transfer tunnel subjected to design spectrum compatible time history considering friction coefficient of 0.15. Shake table tests were carried out on the glove boxes (Fig. 1) for the series of the spectrum compatible time histories with peak ground acceleration from 0.05 g to 0.4 g. The integrity of pressure boundary is checked during tests by actually measuring the outside and inside pressure of glove boxes during shake table testing.

The displacement of the glove boxes at the end of each earthquake time history loading is also compared with that obtained by analysis.

Conclusion

During the tests the pressure boundary integrity is maintained as the leak tightness of the glove box was checked after each test. The glove boxes slid without over toppling for 0.2 g to 0.4 g base acceleration. Friction at the structural supports is known to reduce the seismic response of the structures by its energy dissipation. Thus the stresses in the structural supports of the glove boxes were within allowable limits and the glove boxes were safe for the earthquake time history of 0.2 g to 0.4 g. The analysis and experimentally obtained displacements of the glove boxes were also found to be in good agreement.



Figure 1. Shake table test setup of Glove box.

Pipe behaviour under radiolysis gas detonations (5-1601)

E. Roos, W. Stadtmüller, S. Offermanns
Materialprüfungsanstalt Universität Stuttgart
Pfaffenwaldring 32, D-70569 Stuttgart, Germany
e-mail: werner.stadtmueller@mpa.uni-stuttgart.de

General aim

Within the scope of the reactor safety research of the German Federal Ministry of Economics and Technology (BMWi) the basis for the assessment of the danger potential of detonations of radiolysis gas (oxyhydrogen generated by radiolysis) in nuclear power plant piping should be provided.

Particular objectives and programme of work

The pipe detonation tests and numerical investigations should simulate situations in which conglomerations of hydrogen and oxygen will ignite inside a pressurised pipe. In the test the steam was simulated by gaseous nitrogen, the hydrogen and oxygen was taken in its stoichiometrical relation of about 66.6 volume percent hydrogen and 33.4 percent oxygen. The volume proportion in percent of oxyhydrogen / nitrogen was varied between 100/0 and 40/60. The filling pressure was given by 7 MPa and simulates a defined operational piping pressure. As test material practice orientated seamless stainless steel pipes (material: X10CrNiTi18-9) of the dimensions O.D. x t = 114.3 × 6.02 mm were used. Straight pipes up to lengths of 6 m as well as pipes including an elbow and flange were tested.

Due to the very high danger potential of the detonations the tests were carried out in the 32 m deep underground test pit of the MPA Universität Stuttgart. In addition to the tests the pipe behaviour was assessed with numerical FE-calculations. For these purposes stress-strain-curves of the material were developed under high strain rates up to 50000/s.

Some results

The tests verified that the oxyhydrogen detonation is preceded in all cases by a so-called deflagration. Deflagration means a subsonic combustion that usually propagates through thermal conductivity only. Contrary to that the detonation propagates through shock compression with supersonic speed. The ideal detonation

is described by the Chapman-Jouguet theory and called Chapman-Jouguet (CJ) detonation. Under technical aspects this ideal detonation is characterised by the constant pressure peak PCJ at its front and the following Taylor wave. The Taylor wave is time dependant and describes the pressure decrease from the PCJ-value to the pressure of the burned gas. Regarding volume proportions of oxyhydrogen between 60 and 100% under a filling pressure of 7 MPa the PCJ-value was experimentally determined between 130 MPa and 155 MPa and the detonation velocity (DCJ) between 2300 m/s and 3000 m/s.

Concerning the pipe behaviour under oxyhydrogen detonations some significant results are summarised in the following:

50% volume proportion of oxyhydrogen, pipe length about 6 m:

- No detonation occurred, the deflagration propagated over the whole pipe length.

60% volume proportion of oxyhydrogen, pipe length about 5 m, two tested pipes:

- The run up distance of the deflagration from the ignition up to the deflagration to detonation transition (DDT) was determined by about 3500 mm. The pipe bursting occurred with the starting detonation at the DDT-point and propagated catastrophically up to the pipe end.

80% volume proportion of oxyhydrogen, pipe length about 3.7 m, two tested pipes:

- The deflagration to detonation transition (DDT) occurred at a distance from ignition of about 500 mm. After the DDT-point the detonation propagated over a pipe length of 1900 mm without pipe bursting in one of the two tests. Adding the propagation length of the deflagration (500 mm) and of the detonation (1900 mm) the pipe bursting started at a distance of 2400 mm from the ignition point. In the second test with the same test parameters the detonation propagated up to the pipe end without the pipe bursting. The different pipe behaviour may be due to the scattering of the wall-thickness and pipe diameter. Along the detonation propagation the diameter widening in percent amounted to about 35% and 33%.

Within this scope it should be noted that the quasi static burst pressure of the pipes was determined by 52 MPa and the maximum diameter widening by 30%.

Summary

The oxyhydrogen detonation tests with seamless stainless steel pipes showed that not in all cases the ignition of the oxyhydrogen resulted in a pipe bursting. The gas reaction dividable into the phase of the deflagration and that of the detonation needs a run up distance until the pipe bursting occurs at a specific distance from the ignition point. Among other things this run up distance depends first on the volume proportion of oxyhydrogen inside the pipe but also on the pipe dimensions and the pipe material.

Missile impact on structural members (5-1603)

Xian-Xing (Lambert) Li

Chief Civil/Structural Engineer, SNC-Lavalin Nuclear Inc.
2275 Upper Middle Road East, Oakville, Ontario, Canada L6H 0C3
e-mail: lambert.li@slnuclear.com

Introduction

A variety of impact loads caused by tornado-generated or turbine-generated missiles must be considered in nuclear power plant design. A major portion of the plant structures must be designed against these loads. Although the loads are localized, the structural response of target members may be substantial.

Currently, most design work related to impact load is based on the methodologies as described in the ASCE Manual No. 58 [1]. This manual provides general guidance on the structural design and analysis for impact loads. The formulae for the penetration and perforation calculations of concrete plates are based on an assumption of rigid targets, which is not the case for this project.

For flexible targets, the maximum response is calculated based on impact forces determined from the rigid target assumption or projectile failure. For example, impact force was calculated based on the concrete local penetration, crushing strength of the projectile, or the compressive stress wave propagation. This approximation violates the Conservation Theorems of Energy and Momentum for flexible members, because the impact force directly relates to the plastic deformation of targets and can not be predicted in advance without knowing the plastic displacement, and vice-versa.

Li, et al. [2] summarizes recent research works for the concrete target penetration and perforation due to missile impact. These works are based on rigid target assumptions that energy adsorbed by the overall structural members can be neglected and the overall collapse is not an issue.

The penetration calculation for rigid steel plates has been provided in ASCE manual [1]. However, flexible steel members subjected to missile loads were not addressed, which requires new development of rational methodologies, so that steel target can be designed without concern of perforation and overall collapse.

In this paper, a unified methodology will be developed to evaluate impact effects of hard missiles on reinforced concrete and steel members including plates/walls and beams. The solution will be investigated based on two ultimate limit states: local perforation and structural collapse of flexible plates and beams.

Aim of the work

The purpose of this work is to develop a unified approach for structural analysis of concrete or steel plate/beam subjected to hard missile impact. Following objectives are presented:

- Propose an efficient and unified methodology for evaluation of missile impact effects on reinforced concrete and steel members: plates/walls and beams.
- Investigate potential failure modes of structural members, so that structural performances under impact loads can be understood and structural capacities can be determined to ensure structural safety.
- Develop criteria to identify perforation limit state due to local shear failure and collapse limit state due to excessive plastic deformation.
- Develop an analytical procedure to determine structural capacity based on code-specified structural ductility limits. Evaluate the collapse limit state of the structural members due to full yielding of a plastically affected zone and excessive plastic deformation.

Essential results

Structural assessment can be done according to the structural ductility demand based on the impact energy absorption mechanisms. Based on the theorems of energy and momentum conservation, yield-line theory of plates, and theory of engineering mechanics, a relationship between the plastic deformation and the initial impact energy that is known parameter is established.

The unified analytical methodology for plastic analysis is, then, developed for the structural members subjected to localized missile impacts. The failure modes of local perforation and structural collapse are investigated and identified using proposed criteria.

Plastically affected zone bounded by circumferential plastic hinge locations are determined using the developed formulae. The maximum plastic deformation in terms of maximum plastic displacement and maximum hinge rotation is then calculated based on the velocity profile of the plastically affected zone. The overall capacity of the members is determined when the plastic deformation exceeds the ductility limits. Analytical formulae for the structural ductility are provided to investigate yielding failure of the members.

Summary

A unified methodology is presented for structural analysis of concrete and steel plates/beams subjected to hard missile impact. Two ultimate limit states including overall collapse due to excessive plastic deformation and perforation due to local shear penetration are addressed. Analytical equations are proposed for the overall collapse mechanism due to yielding of a portion of the member. The proposed method yields reasonable and conservative results as comparing with available experimental results.

References

1. ASCE – Manuals and Reports on Engineering Practice – No. 58 (1980). Structural Analysis and Design of Nuclear Plant Facilities. New York, N.Y.
2. Li, Q.M. et al. (2005). Local impact effects of hard missile on concrete target. International Journal of Impact Engineering, Vol. 32, No. 1–4, pp. 224–284.

A model for the hysteresis of concrete to describe the cyclic fatigue of reinforced concrete structures during an earthquake (5-1632)

Attinger, Richard, Kluegel, Jens-Uwe
NPP Goesgen-Daeniken, Daeniken, Switzerland, e-mail: rattinger@kkg.ch

Keywords: earthquake, damage, cyclic fatigue, hysteresis, reinforced concrete, simulation

The damage measure of an earthquake is indicated by the intensity. A certain intensity can be due to earthquakes of different characteristics. Earthquakes of short duration with large acceleration amplitudes can have the same intensity as earthquakes of long duration with lower acceleration amplitudes. This behaviour is explained in this paper by cyclic fatigue of concrete for reinforced concrete structures.

A model for the hysteresis for concrete is introduced with a stiffness reduction built-in at re-loading if a predefined strength limit is exceeded. This strength limit is set to the transition from the stable crack growth to the unstable crack growth and coincides with the fatigue strength.

In a first step, the hysteresis model for concrete is checked on the basis of a micromechanical model, where a section through a reinforced concrete wall is simulated by concrete elements with the hysteresis model included and of steel elements. In a second step, the hysteresis model for concrete is implemented into a finite element code where the consequences of earthquakes of different magnitudes to a reinforced concrete building are demonstrated.

Both implementations of the hysteresis model for concrete show the need of a increased acceleration amplitude to get the same damage when the duration of an earthquake is shortened, i.e. when the magnitude is lowered. One concludes from this statement that the peak ground acceleration (PGA) can not be the measure for the damage state of buildings.

Introduction

Damage potential of an earthquake to structures

Parameters related solely to the amplitude of the ground motion, such as the peak ground acceleration (PGA), are often poor indicators of structural damage. For example, a large recorded PGA associated with a short-duration impulse usually causes less damage than a more moderate PGA associated with a long duration impulse. In the first case, most of the seismic energy is absorbed by the

inertia of the structure with little deformation, whereas in the second case, the more moderate acceleration can result in a significant deformation of the structure due to cyclic loading.

Because structure damage is measured by its inelastic deformation, the earthquake-damage potential depends on the time duration of motion, the energy absorption capacity of the structure, the number of strain cycles, and the energy content of the earthquake. Electric Power Research institute (EPRI, 1988) found that the best correlation between the onset of damage and ground motion occurred when the cumulative absolute velocity (*CAV*) and the Arias intensity (I_{Arias}) are used. *CAV* and I_{Arias} are defined by eqn (1) and eqn (2), respectively:

$$CAV = \int_0^t |a(t)| dt \quad (1)$$

$$I_{Arias} = \pi/2g * \int_0^t a(t)^2 dt \quad (2)$$

where t is the total duration of the record, $a(t)$ is the acceleration time history and g is the acceleration of gravity. In both equations, one observes that the time t is reciprocal to the acceleration $a(t)$ for a constant value of *CAV* and I_{Arias} , respectively.

The current seismic-design practice for structures has different shortcomings: The design is mainly based on strength principles by using the acceleration spectra, and does not directly account for the influence of the duration of the strong motion or for the hysteretic behaviour of the structure. The aim of this paper is to present a hysteresis model for concrete to overcome these shortcomings.

Behaviour of concrete

When a concrete specimen is monotonically loaded, micro cracks are formed for loads above about 30% of the compression strength. The stable crack growth leads to a disaggregation of the structure of the concrete for loads above about 65% of the compression strength. A critical stress is reached between 75% and 85% of the compression strength when axial cracks are formed, the lateral strain rapidly increases and the volume grows. This critical load describes approximately the fatigue strength (Hohberg, 2004).

Cyclic mechanical loads above the fatigue strength tire the concrete over time. Three phases of permanent deformation, i.e. the damage degree, can be recognized, if one looks at the progress of deformation as function of the number of load cycles. The first phase indicates a large deformation release when crack growth is initiated, the rate of deformation will than lower due to stress rearrangement. The second phase is characterized by a constant, low rate of deformation increase where the damage constantly but little rises due to the formation of micro cracks. The instable crack growth results in the third phase in an excessive increase of the deformation and ultimately to the collapse of the concrete.

It is observed during cyclic loading that the slope of the hysteresis loops is reduced with increasing deformation and that the secants through the hysteresis

loops may cut in a common point, the so called pivot point (Hohberg, 2004). One can conclude from the existence of such a pivot point that the cyclic fatigue effects – decrease of stiffness and increase of permanent deformation – are in a linear relation.

Material law for reinforced concrete

Hysteresis model for concrete

It is assumed that the damaging effect of an earthquake on reinforced concrete buildings can be explained by the cyclic fatigue of concrete. Therefore, the material behaviour of concrete is extended by a hysteresis model. Based on the findings in the literature, the hysteresis model for concrete consists of the following elements (Fig. 1):

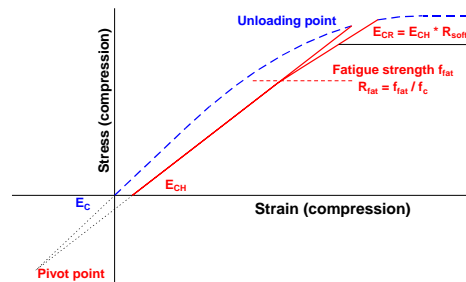


Figure 1. Hysteresis model for concrete.

- The stiffness E_{CH} is newly evaluated at each unloading from the unloading point and the pivot point.
- When the load exceeds the fatigue strength f_{fat} during re-loading, the stiffness E_{CH} is reduced with the factor R_{soft} to the re-load stiffness E_{CR} .
- In the post failure region, the ratio R_{fat} of the current fatigue strength f_{fat}^* to the current strength f_c^* is constant and equal to the ratio of the fatigue strength f_{fat} to the compression strength f_c .

Material parameters for reinforced concrete

The material law for concrete is defined as it is the rule by a standard, in this case by the Swiss standard SIA 262 (2003), and is extended to describe also the post failure behaviour (Fig. 2). The material parameters for the used concrete C20/25 are according to SIA 262 (2003): Tensile strength $f_{ct} = 2.2 \text{ N/mm}^2$, compression strength $f_c = -28 \text{ N/mm}^2$, ultimate compression strain $\varepsilon_{cu} = -0.003$, modulus of elasticity $E_c = 30'365 \text{ N/mm}^2$. The following parameters are assumed for the hysteresis model for concrete: Tensile strength f_{pivot} at the pivot

point = 100 N/mm², fatigue strength ratio $R_{fat} = 0.7$, and softening factor $R_{soft} = 0.8$ for the re-load stiffness E_{CR} .

The behaviour of the used reinforcement B500B is described by a bilinear material law with kinematic hardening and the parameters according to the Swiss standard SIA 262 (2003): Yield limit $f_{sk} = 500$ N/mm², ultimate strength $f_{tk} = 540$ N/mm², ultimate strain $\varepsilon_{uk} = 0.050$, modulus of elasticity $E_k = 205'000$ N/mm².

Micromechanical model

Model assumptions

The effect of the hysteresis model for concrete is shown on a section through a reinforced concrete wall using a micromechanical model, where the structure is subdivided into small elements. It is assumed that these elements are loaded only uniaxial and do not have any impact on the other elements. The calculations are performed for a wall element of a thickness of 300 mm and a unity depth of 1 mm. The overall wall thickness is divided into 1 mm thick concrete elements. The orthogonal reinforcement is placed on both sides of the wall in a distance of 40 mm from the surface. Three cases are studied: Without reinforcement, reinforcement of 336 mm²/m (diameter 8 mm each 150 mm), and reinforcement of 1334 mm²/m (diameter 16 mm each 150 mm).

Behaviour of concrete under pure compressive loading

The strain controlled stress-strain diagram for concrete (without reinforcement) is shown in Fig. 2. In re-loading, the two curves for complete and partial unloading require a larger deformation to join again the virgin loading due to the softened stiffness. The filleting between the hysteresis loops and the abscissae as well as the virgin loading is a result of the strain increments, which were chosen too large for these calculations. As a result of the implemented pivot point, the unloading stiffness E_{CH} is reduced in this example from its initial value to about one third in the final stage.

The behaviour of the hysteresis model for concrete during cyclic fatigue is examined for a stress driven cyclic loading between the stress levels σ_{upper} and σ_{lower} . The upper stress level σ_{upper} was increased in the different runs from 0.71 to 0.99 times the maximal stress σ_{max} of monotonic loading. The lower stress level σ_{lower} was kept constant at 0.60 times the compression strength f_c since only stresses above the fatigue strength f_{fat} account for fatigue and σ_{lower} is less than the fatigue strength f_{fat} . Fig. 3 shows the number of cycles needed for collapse. Based on the stress levels 75% and 95%, an approximately constant value for the collapse index I_{coll} (eqn (3)) is achieved with a rather high exponent m : the exponent m takes a value of 8 for concrete and a value of 4 for reinforced concrete. The collapse index I_{coll} for reinforced concrete is similar to the characteristic index I_c (eqn (4)) proposed by Park and Ang (1985). The characteristic index I_c is a

parameter that has a reasonable representation of the destructiveness of ground motions because it correlates well with structural damage.

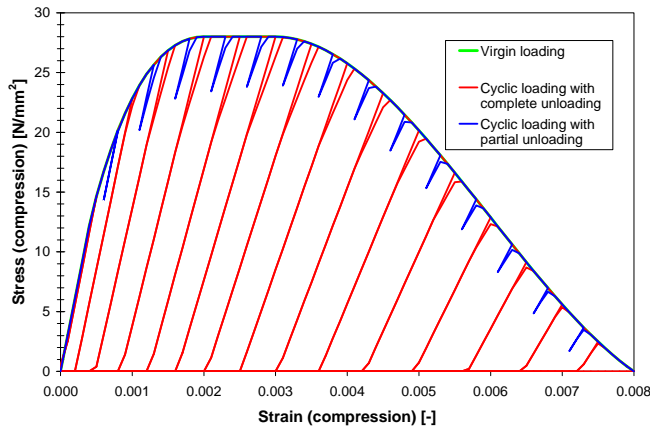


Figure 2. Stress-strain diagram for concrete (without reinforcement) under strain controlled loading.

$$I_{coll} = \sigma_{upper}^m * \text{number of load cycles} \quad (3)$$

$$I_c = a_{rms}^{1.5} * t_s^{0.5} \quad \text{with} \quad a_{rms}^2 = 1/t * \int_0^t a(t)^2 dt \quad \text{and} \quad t = t_s \quad (4)$$

where σ_{upper} is the upper stress level of the cyclic loading, the exponent m , $a(t)$ is the acceleration time history and t_s is the significant duration of the ground motion. Significant duration t_s is defined as the interval between the times at which 5% and 95% of the Arias intensity I_{Arias} is attained.

Fig. 3 proves that concrete can fail either by a few strong load cycles or by a lot of weak load cycles. However, the large weight of the stress level given by the exponent m indicates that the benefit for higher stress levels may be quite small due to a too small reduction of the number of load cycles.

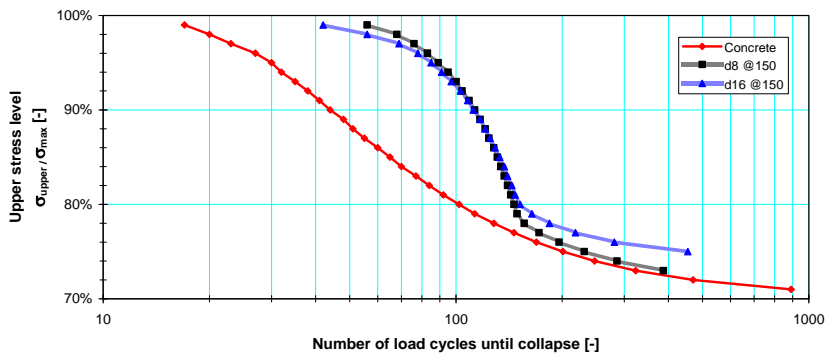


Figure 3. Number of load cycles until collapse.

The first phase with decreasing deformation against the number of load cycles is missed in the fatigue lines of concrete (Fig. 4), since the hysteresis model for concrete neglects the large release of deformation during the initiation of crack growth. The stabilizing effect of a reinforcement helps to form also the first phase: It is well pronounced for a reinforcement with diameter 16 mm each 150 mm which demonstrates the effect of reinforcement to inhibit the structure from collapse as long as concrete is not loaded far beyond the fatigue strength. The second phase with a constant deformation rate is roughly reached: The small increase of the rate of deformation with load cycles is a result of the assumed weakening by the applied pivot point.

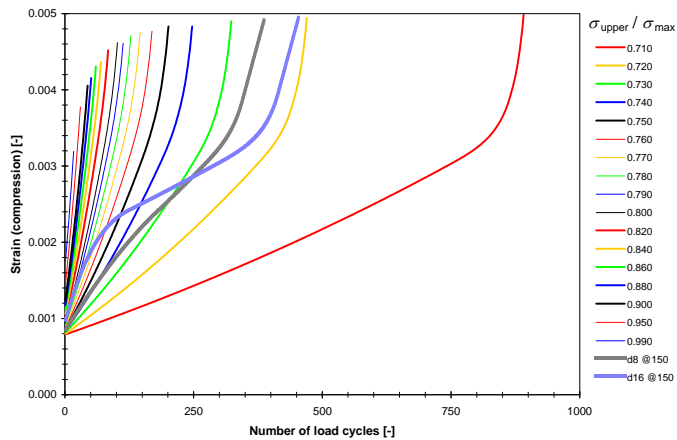


Figure 4. Fatigue lines for different upper stress levels σ_{upper} .

The beginning of the third phase with the excessive increase of deformation leading to collapse is only recognized for lower stress levels σ_{upper} .

Behaviour of concrete under pure shear loading

Basis for the assessment under shear loading are inclined compression fields with uniaxial compression and constant stress intensity. The compression fields are taken by the concrete, whereas the compensating tensile forces are taken by the reinforcement. Since the pressure field acts like concrete under pure compression loading, shear loading of reinforced concrete will not be looked at separately.

Behaviour of reinforced concrete under pure bending loading

The form of the load cycles is mainly driven by the reinforcement through its elastic and its plastic material behaviour. During the first cycle, one observes a very stiff loading and unloading (Fig. 5) until the bending moment drops due to the cracked concrete. The further cycles exhibit a bend in the elastic deformation phase of the reinforcement when the compressed concrete is unloaded and the

cracks start to open. Beginning with cycle 5, a jump in the bending moment is observed, when the cracks close in the plastic deformation phase of the reinforcement. Collapse is reached in the eighth cycle when concrete starts to crush.

The number of load cycles could not be determined in bending loading when the bending moment is varied between an upper value M_{upper} and a lower value M_{lower} of about half the maximum bending moment M_{max} in monotonically loading. This behaviour is well-founded in that the reinforcement is cyclic loaded in a range with practical constant strain limits. Because of this strain limitation, the concrete can degrade only by reducing the loading in each cycle as long as the fatigue strength is reached well before the concrete collapses.

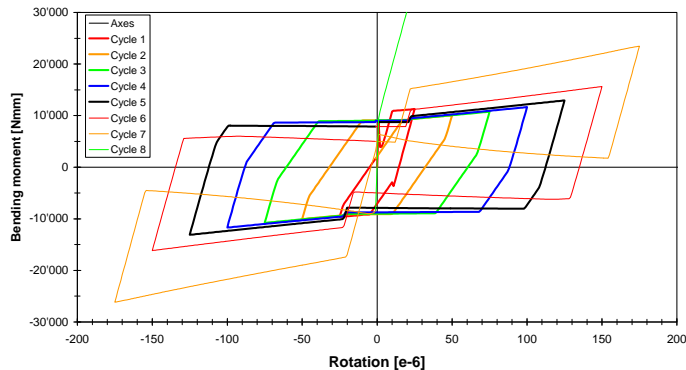


Figure 5. Bending moment-rotation diagram for reinforced concrete (d8 each 150 mm) under rotation moment controlled loading.

Finite element analyses

Implementation of the hysteresis model for concrete into a finite element code

The hysteresis model for concrete was implemented as a user supplied material model into the finite element code ADINA (1984). The user supplied material model is based on the three dimensional concrete model of ADINA. An equivalent isotropic material law is assumed based on the deviatoric stress-strain relationship. Since this paper is focused on the effect of the hysteresis behaviour, tension cut-off is neglected for the concrete.

Effects of earthquakes to a reinforced concrete building

A cubical structure with outer dimensions 3.5 m*3.5 m*3.5 m was chosen as an example. The thickness of the concrete walls is 0.25 m, and the orthogonal reinforcement on both sides of the wall is taken to be 1334 mm²/m (diameter 16 mm each 150 mm). The base of the building is completely fixed. The density of the concrete in the roof plate is increased from 2500 kg/m³ to 420'000 kg/m³

to lower the resonance frequency. Thus, the additional mass of $1.28 \cdot 10^6$ kg brings the resonance frequency down to 9 Hz. In the finite element code, the concrete is simulated by 8-noded three-dimensional solid elements with side length 0.25 m, and the reinforcement by 4 noded two-dimensional solid elements with side length 0.25 m and appropriate thickness.

Basis for the earthquake loading is the design response spectrum according to the Regulatory Guide 1.60 (1973) for a damping of 5%, and anchored to a PGA of 0.375 g. With the same seed, two artificial time histories are generated for magnitude M5.5 and M7.0. The time histories are multiplied by a tripartite function to result in a parabolic rise to unity at a rise time T_r , a plateau of value unity for the strong motion duration T_s , and a linear ramp down to zero for a decay time T_d . These time parameters as functions relating to a specified earthquake magnitude estimate (M) are determined by fitting empirical data obtained from Salmon et al (1992) and are given in Table 1. The time histories are base line corrected to result in zero velocity and zero displacement after the earthquake. During the calculations, a tremendous effect of small changes in the time histories has been observed. Therefore, the time history of magnitude M7.0 has been merged from the time history of magnitude M5.5 till the end of the strong motion (i.e. till 6.065 s) and from the tail (after 6.065 s) of the original time history for magnitude M7.0 (Fig. 6).

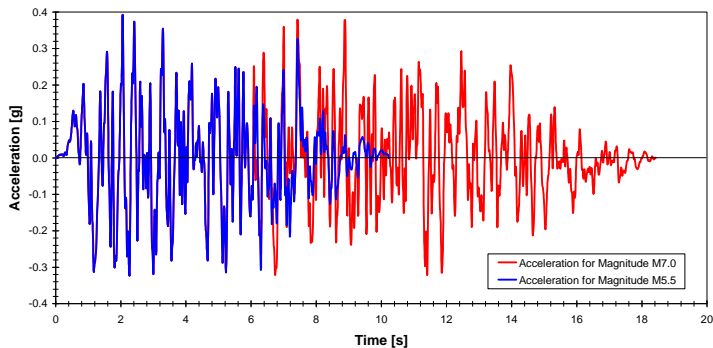


Figure 6. Artificial time histories for Magnitude M5.5 and Magnitude M7.0 used for comparison.

Table 1. Time parameters used for the artificial time histories.

Magnitude M	Rise time T_r	Strong motion duration T_s	Decay time T_d	Total duration
5.5	1.260 s	4.805 s	4.165 s	10.230 s
7.0	2.240 s	9.735 s	6.705 s	18.680 s

It was found in a parametric study that the same damage state of the building is reached when the acceleration amplitudes are increased in the case of magnitude M5.5 by a factor of 1.25, and when they are kept constant in the case of magnitude M7.0. The evolution of the maximal deviatoric strain is depicted in Fig. 7 for both earthquakes. The maximal value of Fig. 7 indicates that the maximal strength of the concrete is just reached. Since the heavily damaged material is concentrated in some small regions, the hysteresis behaviour is of minor importance for the overall behaviour of the structure.

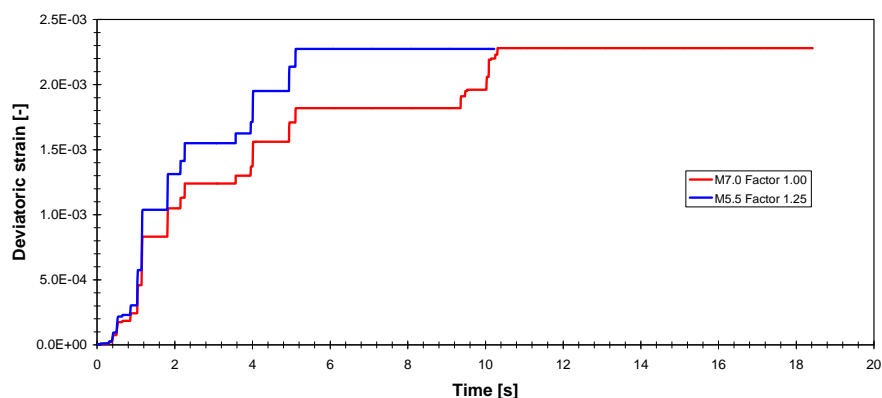


Figure 7. Deviatoric strain as measure for the damage state.

Table 2 shows the CAV value, the Arias intensity I_{Arias} , the acceleration during strong motion a_{rms} , and the characteristic index I_c of Park and Ang for the same damage state, when the strength of the concrete is reached. None of these parameters give identical values for both magnitudes. Hence, this study shows no favoured parameter as a predictor for collapse.

Table 2. Ground motion parameters for the same damage state of the building, when the strength of concrete is reached.

magnitude M	PGA	CAV eqn (1)	I_{Arias} eqn (2)	a_{rms} in eqn (4)	I_c eqn (4)
5.5	0.469 g	1.230 gs	0.409 gs	0.196 g	0.0418
7.0	0.375 g	1.791 gs	0.475 gs	0.148 g	0.0153

Conclusion

- A hysteresis model for concrete was presented, which accounts for the degradation of concrete.
- It was demonstrated by means of the hysteresis model for concrete in a micromechanical model for a reinforced concrete wall under cyclic loading:
 - Under compression and shear loading, strong earthquakes need less load cycles than weak ones until the concrete collapses.
 - The hysteresis model accounts for the three phases of fatigue with decreasing, constant and excessively increasing rate of deformation with the number of cycles.
 - At pure bending, the reinforcement dominates the behaviour whereas the influence of concrete is marginalized.
- A simplified reinforced concrete building was studied for two earthquakes of magnitude M5.5 and M7.0, respectively:
 - Damage is reached for the earthquake of magnitude M5.5 at a higher PGA than for the earthquake of magnitude M7.0.
 - This study shows no favoured parameter as a predictor for collapse.
 - It is obvious, that the level of the PGA is not a measure for the damage of buildings.

References

- EPRI 1988. A criterion for determining exceedance of the operating basis earthquake. EPRI NP-5930. Electrical Power Research Institute, Palo Alto, California.
- Hohberg, R. 2004. Ermüdungsverhalten von Beton. Technische Universität Berlin, Thesis.
- Park, Y.J., Ang, A.H.-S. 1985. Mechanistic seismic damage model for reinforced concrete. J. Struct. Eng., ASCE, 111, No. ST4. P. 722–739.
- Regulatory Guide 1.60 1973. Design Response Spectra for Seismic Design of Nuclear Power Plants. U.S. Nuclear Regulatory Commission, Rev. 1.
- SIA 262 2003. SIA Norm 262 – Betonbau. Schweizerischer Ingenieur- und Architektenverein, Zürich (CH).
- Salmon, M.W., Short, S.A., Kennedy, R.P. 1992. Strong Motion Duration and Earthquake Magnitude Relationships. USDOE, UCRL-CR-117769.
- ADINA 1984. Automatic Dynamic Incremental Nonlinear Analysis – Users manual. ADINA Engineering, Watertown (MA/USA).

Systematic errors in the numeric analyses of computer programs used for the determination of the flexible structure seismic response (5-1635)

Viorel Serban, Marian Androne

Subsidiary of Technology and Engineering for Nuclear Projects – SITON

At present, the determination of the building seismic response is done by finite element computer models, by in-time or frequency dynamic response analyses of the building.

For the in-time analyses, the computation is just the solving of a differential equation system of 2nd degree in the relative displacement variables, x , for which the initial conditions (displacement x and velocity \dot{x} at $t = 0$) need to be specified.

All the current computer programs known by the authors, are considering $x=0$ and $\dot{x} = 0$ as initial conditions. The initial relative velocity cannot be zero when the initial displacement is zero and considering it null together with the initial displacement, is introducing errors in the determination of the seismic response. These errors are important when speaking about flexible buildings such as tall buildings, seismically isolated buildings or buildings where plastic hinges are accepted.

Some recorded or generated accelerograms, also include harmonic components of long and very long period (which may be due to the measurement instrument or its location or due to the generated time-history generation process) which alter the calculated seismic response of the structures, especially in respect of seismic isolation issues. The response in displacements, especially for flexible structure, could be overestimated due to its dependence on the square of long vibration period, while the response in accelerations does not show this type of dependence. The presence of long periods in the accelerograms, even very low in amplitude, leads to high resonance amplifications in the displacements around that period, proportionally with its square.

The paper is an evaluation of the calculation errors resulted from the computer programs employed today (the examples are based on the results obtained with a well known computer program) in the calculations for structures and it also includes solutions to eliminate such errors. Also, the errors occurring in the determination of the relative displacement response spectra for earthquakes with time-history acceleration records are performed.

On scale effects and mesh independence in dynamic fracture analysis by means of the discrete element method (5-1640)

Jorge D. Riera¹, Ignacio Iturrioz², Letícia F.F. Miguel²

¹Department of Civil Engineering

²Department of Mechanical Engineering, Universidade Federal do Rio Grande do Sul, Porto Alegre, RS, Brazil

Keywords: fracture, brittle materials, size effect, numerical analysis, inhomogeneous materials, mesh objectivity

The authors determined numerically the response of geometrically similar reinforced concrete beams built in four different sizes, tested to rupture by Leonhart & Walter (1965) and later reproduced by Ramallo *et al.* (1993), to quantify size effects in reinforced concrete beams. For such purpose the so-called Discrete Element Method (DEM) was employed, modeling the inhomogeneous character of concrete and steel by assuming that their stiffness and specific fracture energies are random fields in 3D-space. The constitutive criterion, based on Hillerborg's model (1971), presents advances in the consideration of the spatial correlation of the random fields. The discrete numerical model was also used to reproduce experimental results due to Vliet *et al.* (2000) on the influence of sample size on the tensile strength of concrete and to theoretically predict the strength of large rock dowels subjected to shear (Miguel *et al.*, 2008). In all cases, in order to represent the stress-strain relation for concrete in tension, a bi-linear diagram was resorted to, which proved adequate when the size of the elements is sufficiently small and the inhomogeneous properties of the material are properly accounted for. These conditions require large DEM or FEM models, which cannot be usually employed in engineering practice due to cost-effectiveness considerations. In a previous paper Riera & Iturrioz (2006) contend that predictions of the failure load of concrete structures, accounting for size effects, can be made using larger elements and therefore reduced computational costs, if the appropriate stress-strain relations were adopted. These relations depend both on the size of the element and on the correlation lengths of the random fields that describe the relevant material properties. The proposed equations were determined by Monte Carlo simulation but it was later verified that they did not satisfy conditions of mesh objectivity.

In response determinations of structures with initial cracks or high stress gradients, which result in the localization of fracture, well established procedures lead to results that are mesh independent. However, in elements subjected to approximately uniform stress fields a hitherto unknown problem arises in the

analysis of non-homogeneous materials: the need to know *a priori* the degree of damage (fracturing) of the element. This should also affect finite element analysis in cases in which there is no clear fracture localization, requiring a careful evaluation of the energy dissipated by fracture in the course of the loading process. In the paper, a new approach is proposed to account for the effect in non-linear dynamic fracture analysis of large structural systems employing the discrete element method.

References

- Riera, J.D., Iturrioz, I. Size effects in the analysis of concrete or rock structures. 19th. International Conference on Structural Mechanics in Reactor Technology (SMiRT 19), Div. H, Toronto, Canada, CD, 2006.
- Miguel, L.F.F., Riera, J.D., Iturrioz, I. Influence of Size on the Constitutive Equations of Concrete or Rock Dowels. (Accepted for publication). International Journal for Numerical and Analytical Methods in Geomechanics, 2008.
- Rios, R.D., Riera, J.D. Size effects in the analysis of reinforced concrete structures. Engineering Structures, Vol. 26, pp. 1115–1125, 2004.
- Riera, J.D., Iturrioz; Miguel, L.F.F. On Mesh Independence in Dynamic Fracture Analysis by Means of the Discrete Element Method. ENIEF 08, San Luis, Argentina, Oct. 2008.

Steam generator tube plugging FEM analysis (5-1641)

Jukka Kähkönen

Fortum Nuclear Services Ltd, P.O. Box 100, 00048 FORTUM, Finland
e-mail: jukka.kahkonen@fortum.com

A mechanical steam generator tube plugging system was introduced to Loviisa nuclear power plant in 2005. Interest was raised concerning the loads imposed by the new plugging system to the steam generator tubes and the collector. The effect of operational conditions to the plug contact behavior and the tube inner diameter deviation effect were also issues that had to be addressed. The decision to use finite element (FE) modeling as part of plugging system validation process was made.

The constructed FE model was a one quarter model using symmetry boundary conditions which included mechanical plug, steam generator tube and part of the collector. The choice to use explicit time integration to solve problem was evident due to the fact that mechanical plugging event involves highly plastic deformations and drastically changing contact conditions. The quasi static assumption enabled the use of mass scaling to increase the explicit time integration method stable time increment so that the problem was solvable within decent CPU time.

In order to validate FE model the associated training block was used for strain gauge measurements in the plugging concept validation process. Strain gauge measurements provided information of the collector deformation in the vicinity of the plugged tube.

The effect of the tube inner diameter deviation was assessed using three versions of the FE model with different tube inner diameters. All the FE model versions were subjected to same loading scenario which was: 1) installation of the plug, 2) operational pressure and 3) operational pressure + temperature.

The validation analysis of the FE model resulted quite good correspondence with the measurements and it motivated to proceed with the analyses. Subsequent analyses showed that operation pressure itself doesn't have much effect on plug contact forces but when operational temperature is introduced contact forces drop drastically. Analyses with different tube inner diameters pointed that tube inner diameter have only slight effect on contact forces.

Examinations of contact force results allowed estimating the pressure difference that is needed to move installed plug in operational conditions. The estimation in Loviisa nuclear power plant case is ≥ 230 bar.

References

1. ABAQUS version 6-6. 2007. Users documentation, Simulia Inc., Dassault Systèmes.
2. Shah, V.N., MacDonald, P.E. 1993. Aging and Life extension of Major Light Water Reactor Components. Elsevier, USA, pp. 317–321.
3. Wang, M., Yang, H., Sun, Z., Guo, L., Ou, X. 2006. Dynamic explicit FE modeling of hot ring rolling process. Transactions of Nonferrous Metals Society of China 16, pp. 1274–1280.

An optimal solution search under design for a pipeline support system to withstand a seismic excitation (5-1653)

Andrey V. Petrenko

AtomEnergoproject, 2nd Sovetskaya str, 9/2A, St-Petersburg, 191036, Russia
e-mail: dr_petrenko@mail.ru

Pipelines are an essential part of the equipment in any nuclear power plant (NPP). They transport nuclear media as well as the ordinary water and steam. Pipelines of basic NPP circuits are required to carry over heat and mechanical energy. So the safety of a NPP depends on the safe and appropriate operation of pipelines within the circuits and safety systems. The safety of pipelines depends on their capacity to withstand operational and accidental loads and on the maintenance of their operational function. There are a few basic items primarily responsible for this – parameters of materials, geometric characteristics of cross sections, and the routing of the whole pipeline. Also a design of the pipeline support system (PSS) is a very important point, and relates directly to the strength capacity and the durability of any pipeline. Today there are a number of companies providing NPPs with various types of reliable supports (sliding, guide, fixed, dynamic etc.), and so the questions surrounding the detailed design of supports of any type are assumed to be well known. This paper considers only the places of supports installation and mechanical function of supports under the ‘PSS’ term. It corresponds to the consideration of a pipeline as a beam structure where pipeline supports are treated as constraints of degrees of freedom of a pipeline.

Usually it is not a problem to design a support system of a pipeline that is connected at two points in free space. But a general design of a NPP becomes more compact along with a desire to increase total effective power. It leads to the increasing of internal loads on the pipelines such as pressure and temperature. Moreover, the safety guides of national authorities and the IAEA require taking into account accidental external events with extremely high energy such earthquakes, accidental aircraft crashes, tornados, and so on. An earthquake usually has the highest energy among these events. It is the most dangerous event for a NPP because induced seismic inertial loads act on each point and each system of the NPP. Thus, NPPs are ideally built in areas with potentially low seismic activity. But often, the selection of an NPP site is more an economical problem than a technical one. For example, in Russia it is now popular to consider a uniform design for a NPP for erection in various seismic and soil conditions. On practice, it leads to artificially increased seismic response spectra. Under those circumstances it is extremely important to design the NPP’s PSS assuring strength capacity and durability. At the same time, it can be difficult to do so due to all of the reasons mentioned above. Only experience

and skill can help an engineer to solve these issues and the designer must often solve these issues alone. Although the common practice is to follow basic design rules, most of these rules were developed about thirty years ago. In Russia, for example, a real seismic design of the NPP pipelines arose only in the end of 70's after a strong earthquake occurred in Romania.

However, it is important to note that the power of computers increases significantly every year. As a result, the regular analysis of whether pipelines to meet specific technical guidelines takes only seconds. It also means that variant calculations with a number of iterations are possible now and take reasonable time. A main idea of this paper is to use a theory of optimization and its approaches to find an optimal design of a PSS. It is most urgent that the seismic design takes as much time to satisfy all of the necessary conditions of strength due to the complexity of dynamic behavior of pipeline systems and the artificial methods for taking into account seismic loads. On one hand, a response spectra method is the most accepted way to compute seismic stresses and forces. On other hand, this method uses different combination rules for seismic modal responses. But, each rule leads to either different numbers of support units or different places of their installations.

This paper uses the method of Nelder-and-Mead to search for the local optimal solution. The paper also discusses the possible common application in computational software and the advantages and shortcomings of such an approach. An application of optimization theory in design of PSS to withstand a seismic excitation allows to minimize manual design and to significantly reduce work time. Moreover, solving for the optimum solution reduces number of support units and doesn't lead to possible excessive supports decreasing sometimes a safety factor of fatigue.

Seismic qualification of class II buildings of nuclear power plants on the basis of non-nuclear seismic codes (5-1656)

Dietrich Klein¹, Fritz-Otto Henkel¹, Ruediger Meiswinkel²

¹Woelfel Beratende Ingenieure GmbH + Co. KG

Max Planck Strasse 15, 97204 Hoechberg, Germany, e-mail: klein@woelfel.de

²E.ON Kernkraft GmbH

Tresckowstrasse 5, 30457 Hannover, Germany

e-mail: ruediger.meiswinkel@eon-energie.com

The currently valid code for the seismic qualification of class I buildings of nuclear power plants in Germany is the KTA 2201, part 3, from June 1990. The required methods for the dynamic analysis of the buildings are the response spectrum modal analysis (RSMA) or time history methods. The design is based on force controlled approaches with linear response of the buildings. It is not allowed to take advantage of the inelastic energy absorption capacity of the building. The strength of the building and its parts is verified by use of the allowable stress concept with one global safety factor. For class II buildings which may effect class I buildings in case of failure, the nuclear code KTA 2201 allows the use of the national German seismic code DIN 4149 for seismic qualification of buildings other than nuclear buildings.

In the context of the harmonization of the European technical codes, the national German codes were revised. The main focus of the revision is on the introduction of the load and resistance factor concept with partial safety factors and combination factors for actions and resistance. The German seismic code DIN 4149 as national application document of the European seismic code EC 8 was completely revised on this behalf with regard to the actual state of art.

At the time, the German nuclear codes are adjusted to the revised building codes. The seismic nuclear code KTA 2201, part 3, needs a basic revision with respect to the actual state of art. Especially the application of the seismic code DIN 4149 for the qualification of class II buildings must be redefined. The proposed paper gives supports for the application of the revised seismic code DIN 4149 in the context of the qualification of nuclear class II buildings. This is shown at the main turbine building of a pressure water reactor plant. The main turbine building is rated as class II building. In this building, however, are highly energized vessels, the failure of which during earthquake may endanger class I buildings.

Experiments on gamma-ray shielding performance of cracked reinforced concrete (5-1660)

Katsuki Takiguchi¹, Koshiro Nishimura², Isao Yoda², Kazuteru Kojima³,
Yoshinari Munakata⁴, Keiji Sekine⁴

¹Department of Mechanical and Environmental Informatics,
Graduate School of Information Science and Engineering,
Tokyo Institute of Technology, Tokyo, Japan
e-mail: ktakiguc@tm.mei.titech.ac.jp

²Tokyo Institute of Technology, Tokyo, Japan

³Shimizu Corporation, Tokyo, Japan

⁴Japan Nuclear Fuel Limited, Aomori, Japan

In nuclear related facilities, some reinforced concrete (R/C) walls are expected to have two performances, i.e. structural and shielding. Concrete of structural R/C walls are permitted to crack. Therefore, shielding performance of a cracked R/C wall has to be clarified.

In order to improve the precision to predict the shielding performance of a cracked R/C wall, an experimental study has been planned. At this moment, September, 2008, three R/C wall specimens are under concrete curing and just before tests. Additional three specimens will be made, and will be tested in January and February, 2009.

Test parameters are (1) thickness of R/C wall, (2) width of crack, and (3) crack (natural crack and artificial straight slit crack).

Crack width will be stepwise controlled from small to large. Shielding performance against gamma-ray will be measured at every crack width step. After gamma-ray irradiation tests of all crack width steps, the specimen will be broken up and irregularities of the crack surface will be inspected.

Experimental procedures and results will be reported in this paper. The data reported should be available to evaluate the gamma-ray shielding performance of a cracked R/C wall. Simulation using Monte Carlo method will generalize the best result.

K. Takiguchi, the first author, has experience in the experimental studies of gas leakage through cracks in a R/C wall, and he has written many papers about the studies. The experiment will be carried out successfully.

SSI Analysis of PBMR module building to South African high frequency input motions (5-1665)

Aleksandar Paskalov¹, Dan M. Ghiocel², Gary Styger¹

¹Murray & Roberts SNC-Lavalin Nuclear (Pty) Ltd. (EPCM contractor to Pebble Bed Modular Reactor (Pty) Ltd on the PBMR DPP Project), Pebble House, 1279 Mike Crawford Avenue, Centurion 0046, South Africa, e-mail: aleksandar.paskalov@slnuclear.com

²Ghiocel Predictive Technologies Inc., 38 Harper Drive, Pittsford, New York 14534, USA, e-mail: dan.ghiocel@ghiocel-tech.com

The Pebble Bed Modular Reactor (PBMR) is developed by Pebble Bed Modular Reactor (Pty) Limited located in Centurion, South Africa with the intention to build a demonstration power plant (DPP) reactor at Koeberg site near Cape Town. Increased energy demands, escalating and increasingly volatile natural gas and oil costs, and a desire for energy security and environmental sustainability are stimulating investments in technologies that will contribute to reliable, affordable and clean energy on a global scale. South Africa's PBMR technology fits each of these requirements. It is a high-temperature helium-cooled, graphite-moderated high temperature reactor using fuel spheres (pebbles) that circulate through the reactor core.

The Koeberg site is comprised of three horizontal layers of sand approximately 23 m deep resting on siltstones and sandstones of the Tygerberg formation. The upper regions of the rock are fractured and in places highly weathered and hence, the dynamic properties are varied from a soft to hard rock.

The PBMR module building consists of reactor building, generator house and auxiliary building sharing a common baseslab. It is deeply embedded and founded on the rock. The structural dynamic behaviour of the module building under design earthquakes is determined using the ACS SASSI finite element (FE) code specialized for soil-structure interaction (SSI) analysis. The SSI model includes the structural FE model with a surrounding layers of near-field soil elements and the far-field soil layering model. The near-field soil element layer is required to capture nonlinear soil behavior near foundation walls and mat, and potential soil separation from side walls and mat.

The analysis is carried out for Koeberg site-specific ground spectra, characterized with high frequency content. The seismic analysis results include calculation of floor response spectra (FRS) at representative locations inside the module building.

The SSI methodology incorporates the effects of motion incoherency, nonlinear soil behavior and separation from foundation walls, that could affect

significantly the SSI response of such large-size, deeply embedded structures as DPP. If negative wall pressures are identified at some locations, after including the static soil bearing pressures and gravity effects, this indicates that soil separation occurs. For a site-specific seismic input that is much richer in higher frequency components, the motion incoherency effects on computed FRS are anticipated to be significant. The effect of the high frequency excitation content for Koeberg site is investigated.

A unique set of tools is used for performing accurate incoherent SSI analyses that includes a rigorous stochastic approach (accurate for 3D SSI models with flexible foundations). Sensitivity studies with respect to interpolation of incoherent transfer functions is done for different smoothing parameters, phase adjustment options and interaction nodes spatial distribution.

Aircraft crash analysis of PBMR module building (5-1666)

Aleksandar Paskalov¹, Norbert Krutzik²

¹Murray & Roberts SNC-Lavalin Nuclear (Pty) Ltd. (EPCM contractor to Pebble Bed Modular Reactor (Pty) Ltd on the PBMR DPP Project), Pebble House, 1279 Mike Crawford Avenue, Centurion 0046, South Africa

e-mail: aleksandar.paskalov@slnuclear.com

²NJK-Consulting, Balduinstrasse 72, 60599 Frankfurt/Main, Germany

e-mail: norbert@krutzik.com

The Pebble Bed Modular Reactor (PBMR) is developed by Pebble Bed Modular Reactor (Pty) Limited with the intention to build a demonstration power plant (DPP) reactor at Koeberg site near Cape Town, South Africa. It is a high-temperature, helium-cooled, graphite-moderated reactor using fuel spheres (pebbles) that circulate through the reactor core.

This paper describes the methodology followed in the PBMR project for the dynamic analyses and evaluation of the design of the PBMR module building when subjected to aircraft crash impact.

As increasingly heavier and faster aircrafts will probably be designed and put into service, it should be anticipated that the aircraft loading spectra will change and possibly increase in future.

The prevention of penetration of the affected outer shells and walls against the applied aircraft crash impact represents the first goal in the design of the PBMR module building. The indication for the possibility of penetration is the local overstressing of the impacted structure as a consequence of high load per unit area. The danger of penetration should be therefore checked not only for the maximum load of the whole airplane, but also for its parts (engines, landing gear) impacting with the same velocity but acting, after separation, on much smaller area. Of significant importance are also the induced excitation vibrations (dynamic response) on the structures and the global stability (overturning) of the structure.

Since the detail structural data are limited at this stage a complex airplane-building structure, analyses can not be performed. Using help of some of the airplane manufactures and authorized institutions “rigid” load functions can be obtained, specified for the assumption of infinitively rigid targets. This load functions are in fact inadequate in this form for impact regions on real structures which could be generally characterized as “thin shell design”. Very severe nonlinear processes are expected in the impacted region of the reinforced concrete structure especially: cracking of concrete, confinement effects, overstressing

of concrete and steel, large deformations, damping, filtering effects, hardening and softening effect of concrete, increase of steel strength due to high strain velocity, yielding and sliding of reinforcement, scabbing/penetration. Rapid increase of stresses and utilization of the bearing capacity of the concrete and the reinforcing steel over the stress limits is expected. This process is resulting also in high energy dissipation and reduction of the forces transferred to the part of the global structure which still remains in the linear-elastic range. The global forces acting on the boundary of the partially plastified zones of the structure are accordingly reduced when comparing with the loads originally applied by the aircraft. In order to model the structure for the local impact analyses, refined FE models considering in detail the geometry of the impacted area, arrangement and percentage of reinforcement, as well as, the material properties of the concrete and reinforcing steel are used. The size of the refined local model at impact region is conditioned by the expected extent of the nonlinear effects and by the displacement shape around the perimeter under the linear elastic load.

The main results derived by nonlinear analysis are deformations and stresses and subsequently forces and moments acting in the characteristic area of the target section i.e. on the border between the plasticized and remaining linear part of the model. Transferring the time histories of the forces and moments obtained for the characteristic section of the local non-linear model (LS-DYNA) to the compatible global FE-model (ANSYS) the execution of a linear-elastic dynamic response analysis can be performed. For the case that compatibility of the local and global model can not be achieved, a procedure for derivation of verified (modified) load function will be established. The procedure of developing modified load functions is based on two steps:

- (a) Nonlinear dynamic calculations using refined local FE models for the impacted area to derive the internal forces at significant sections, adjacent to the plastified zone in which the reinforcing steel remains linear elastic, and
- (b) Request for a (verified) load function which, when applied to a linear elastic model of the structure, induces internal forces in the significant section which are in good agreement with those determined for this region by means of nonlinear analyses. The verified load function will have, in comparison to the specified rigid load function, a longer duration and lower load level.

The analyses will be done considering the local soil conditions and embedment effects. The concrete is assumed to have linear elastic material properties and the corresponding damping values for the soil and the structure are used for dynamic analysis of the global response. Special attention will be paid to the FE idealization of the structure and especially the discretization ratio of the model in order to achieve realistic dynamic response results.

The dynamic response of the structure due to the impact loading will be finally calculated by means of an appropriate compatible linear/nonlinear FE model or an individual local (non-linear) and global (linear) FE model using a corresponding rigid or modified loading function obtained for the local conditions in the corresponding impact locations. Following either approach, the dynamic response i.e. response time histories of acceleration and displacements and corresponding floor response spectra will be derived.

Finally, the absolute accelerations at equipment anchoring points derived for various impact locations will be used to derive the corresponding enveloping floor response spectra. Characteristic results obtained following this approach will be derived and comparisons with floor spectral accelerations due to seismic and blast excitation performed.

The obtained global forces by dynamic analysis will be used as a basis for the final assessment of the global stability (overturning), as well as, evaluation of the local deformation of the impacted wall/shell in the vicinity of the loaded area.

More precise definition of Rayleigh damping matrix in dynamic analysis of NPP civil structures on ABAQUS (5-1667)

Korotkov Vladimir, Kapustin Dmitry

OAO “Atomenergoproekt”, Moscow, Bakuninskaya str, 7, building 1, Russia
e-mail: iliine@mail.ru

Introduction

At the dynamic analysis of civil structures of NPP the most acceptable appeared a direct integration method of the equations of movement of soil – structure system. This method considers geometrically nonlinear effects and dashpots with high damping level. However, the analysis of resultant response spectra showed very high level of spectral accelerations at the elevations of equipment arrangement. One of the main reasons of this is in high conservatism degree, which provides for application of Rayleigh damping in material as compared to modal damping.

An approach, which allows obtaining the specified damping matrix in the form of Caughey series is described in this work. It results in conservatism removal when determining the dynamic reaction in the system and floor response spectra. The results of the analysis are also given.

Aim of the work

Work purpose is in development of the generalized damping matrix in the form of Caughey series and approbation of the approach by means of a particular task.

Essential results

The work represents comparative analysis of dependence schedules Rayleigh damping and damping in the form of Caughey series subject to the frequency. Under standard value of damping ratio in concrete 0.04 Rayleigh damping on operating oscillation frequencies of the structure goes down to 0.01. It leads in very conservative results when obtaining floor response spectra. When using Caughey series for damping function in dynamic analysis, damping ratio on operating oscillation frequencies of the system has no so radical distinction from the standard value. It allowed reducing spectral accelerations in places of installation of the equipment by 35% in NPP spent fuel store building with VVER –1500, taking into account four members of Caughey series already.

Conclusion

For conclusion we'd like to mention, that the developed technology allows significantly reduce conservatism under development of floor response spectra. However, it requires computing time increase since damping matrix in the form of Caughey series is more closely filled, than Rayleigh damping matrix.

We'd like to mention also, that approbation of the method was carried out by roundabout way using a modal method and program – ABAQUS. Access to the stiffness matrixes and masses in the program ABAQUS is required for using the suggested procedures in the method of direct integration.

The approach can be used in other program codes.

References

1. K. Bate, E. Vilson. Numerical methods of analyses and finite elements method. Moscow, Stroyizdat, 1982.

Reducing of spectral accelerations in NPP civil structures at the expense of optimization of their geometry (5-1668)

Ilin Kirill, Korotkov Vladimir

OAO "Atomenergoproekt", Moscow, Bakuninskaya str, 7, building 1, Russia
e-mail: iliine@mail.ru

Introduction

Problem of determination the floor response spectra has significant value when NPP designing. When solving this task it often happens that the calculated spectral accelerations reach unacceptably high values. Therefore the problem of spectral accelerations reducing is actual. This work suggests an approach, which allows reducing spectral accelerations in NPP civil structures at the expense of optimization of their geometry. Calculating researches are made based on the program ABAQUS in combination with optimization program IOSO NM. The results of calculations of standby diesel building (UBN3) and transport portal for reactor building of NV NPP2 are also given.

Aim of the work

Work purpose is in development of the method for analysis and obtaining corresponding results by means of concrete task.

Essential results

The work represents the method of analysis based on optimization of the functional using the random figures method by Monte-Carlo. Dynamic calculation method description and variations of initial geometric parameters are given. In resultant calculations with optimal geometric parameters the values of geometric parameters have been reduced by 30%.

It is significant, that the considered method requires using quick-operating computers, since for to obtain optimal results, about 60 deterministic calculations shall be carried out beforehand.

Conclusion

For conclusion we'd like to mention, that the developed technology allows significantly reduce floor response spectra at the expense of use of structure optimal geometrical parameters. However, it requires use of high-performance personal computers for large as per dimension tasks.

References

1. Korotkov, V., Kapustin, D., Ilin, K. Application of optimization technology and ABAQUS at designing of NPP civil structures. 2007 ABAQUS Users' Conference, Paris.
2. Egorov, I.N. Indirect Optimization Method on the Basis of Self-Organization. Curtin University of Technology, Optimization Techniques and Applications (ICOTA'98), Vol. 2, pp. 683–691, Perth, Australia, 1998.
3. Egorov, I.N., Kretinin, G.V., Leshchenko, I.A. Two Approaches to Multidisciplinary Optimization Problems. Presented at European Congress on Computational Methods in Applied Sciences and Engineering – ECCOMAS-2000, Barselona, Spain, 2000.

Seismic analysis of reactor building of a NPP including soil structure interaction effects and comparison with two additional sites (5-1669)

Khawaja Ahsan Qadeer¹, Muhammad Sadiq², Rong Pan³, Hou Chunlin⁴

¹School for Nuclear and Radiation Safety SNRS, Pakistan Nuclear Regulatory Authority, P.O. Box 1912, Islamabad, Pakistan, e-mail: khajason@gmail.com

²Directorate of Nuclear Safety NSD, Pakistan Nuclear Regulatory Authority P.O. Box 1912, Islamabad, Pakistan, e-mail: sadiqcivil@gmail.com

³Siting and Structure Division, Nuclear and Radiation Safety Centre, SEPA P.O. Box 8088, Beijing, P. R. China, e-mail: rong-pan@263.net

⁴Siting and Structure Division, Nuclear and Radiation Safety Centre, SEPA P.O. Box 8088, Beijing, P. R. China, e-mail: hou.chunlin@gmail.com

This paper is a part of the outcomes of joint research program between Nuclear and Radiation Safety Centre (NSC), SEPA, and Pakistan Nuclear Regulatory Authority (PNRA) in the dynamic seismic analysis of a NPP including the soil structure interaction (SSI) effects and comparison of two additional sites in P. R. China where the same design NPPs with some minor modifications are being built. These sites have their own soil conditions and seismicity with significant differences in terms of SSE and soil stiffness parameters. Simplified lumped mass stick model for time history analysis of reactor containment building along with internal structures is made in SAP2000 advanced V 11.0.2. The load-dependent Ritz vectors are used in modal analysis in stead of eigen vectors for more accurate results in seismic analysis. In SSI analysis, the elastic half space theory is used for calculating translational and rotational springs from both RCC-G and ASCE 4-98 Standard with also taking the layering effects of soil. Floor response spectra are generated and enveloped for their lower and upper stiffness values of soil at various floors of each site and compared with the design FRS. These FRS are developed for the two standards and also with and without taking the layering effects of soil using RCC-G and comparison is made. This analysis not only gives a better understanding of the differences between RCC-G and ASCE 4-98 in terms of SSI which found to be insignificant, but also the evaluation of new SRP section 3.7.2 rev 3 in considering layering effects of soil media for half space modeling. It is suggested that the layering effects of soil should not be mandatory for the seismic evaluation of existing nuclear facilities especially for shallow foundation. This research enhances the capabilities of PNRA in the areas of seismic safety review and dynamic seismic analysis of nuclear power plants.

The effect of cover unit drop on Loviisa NPP primary circuit during maintenance outage (5-1670)

Jukka Kähkönen, Pentti Varpasuo
Fortum Nuclear Services Ltd, P.O. Box 100, 00048 FORTUM, Finland
e-mail: jukka.kahkonen@fortum.com, pentti.varpasuo@fortum.com

The Loviisa Nuclear Power Plant (NPP) in Finland obtained an extended operation license for the period of 2007–2027 in July 2007. One of the conditions set in the safety assessment document that accompanied the license extension approval was the requirement to update the probabilistic risk assessment (PRA) of the plant. For the PRA update, knowledge of damage caused by a very unlikely accident of cover unit dropping during the maintenance outage was needed.

For this purpose a large finite element (FE) model of the primary circuit was prepared. The model included all the major primary circuit components and the supporting foundation for the reactor pressure vessel (RPV). The model had ca. 200 000 elements and about 900 000 degrees of freedom. The cover unit dropping accident was considered in FE analysis as an event where 180 ton rigid object impacts directly on the RPV main flange at velocity of 17 m/s. This impact velocity corresponds roughly situation where object is dropped from the height of 15 meters.

The FE analysis was carried using Abaqus/Explicit -software with nonlinear material properties and contact formulations. The simulated time frame of the impact event was 75 ms.

Based on the FE analysis the following conclusions could be made: 1) the primary piping doesn't exhibit much plastic deformations, 2) the RPV damages locally at the supporting area, 3) the supporting foundation damages severely but 4) the integrity of the primary circuit in not jeopardized.

Reference

ABAQUS version 6.7-EF1, 2007. Users documentation, Simulia Inc., Dassault Systèmes.

Study on the MOX fuel manufacture glovebox containment for earthquakes – deformation and leakage tests for window panels (5-1680)

Akihiro Matsuda¹, Yuichi Uchiyama², Masakatsu Inagaki², Susumu Tsuchino³,
Hiroyuki Umetsu⁴, Koji Shirai⁵

¹Graduate School of Systems and Information Engineering
University of Tsukuba, Ibaraki, Japan
e-mail: a_matsuda@kz.tsukuba.ac.jp

²Seismic Safety Division, Japan Nuclear Energy Safety Organization
Tokyo, Japan

³Nuclear Energy System Safety Division, Japan Nuclear Energy Safety Organization
Tokyo, Japan

⁴Fuji Electric Systems Co., Ltd., Power Plant Business Headquarters Kanagawa, Japan

⁵Civil Engineering Research Laboratory, Central Research Institute of Electric
Power Industry, Chiba, Japan

This paper shows the results of the leakage tests and the large deformation analysis of a full-scale glovebox window to establish the capacity of the containment of the MOX fuel manufacturing glovebox during an earthquake.

In leakage tests, the stainless steel container installed on the reverse of the glovebox window was pressurized with a halogen-air mixture after deformation was applied to the upper part of window frame using micro handy jacks, and to the four glove-ports using electrical actuators. The acrylic and polycarbonate resin panels were applied to the test specimens.

The atmospheric pressure, the pressure differential between atmosphere and the sealed container, temperature of air and the container were measured to evaluate the leakage rate.

In numerical simulation, the finite element analysis was applied to evaluate sealing mechanism of glovebox window. The numerical model of rubber seal was obtained by biaxial loading tests of chloroprene sheet specimens. Tensile loading tests of acrylic resin specimens were conducted to measure the material modulus. The FEM code ABAQUS was applied to the numerical simulation and the user-subroutine function for the hyperelastic model was used to duplicate the deformation of rubber seal.

Furthermore, the contact boundary condition was applied to simulate the deformation of rubber seal and resin panels under the deformation of glove-port.

In deformation and leakage tests, 3-modes of deformations were applied to the frame and glove-ports. Neither damage to the resin panel nor leakage greater than the standard was observed in all examination cases.

From the numerical simulations, it is observed that the rubber seal follow the resin panel flexibly and the double lip accomplished the key role to the confinement capability.

References

- Test Method for Leakage of Gloveboxes, Japan Standard Association, Japan Industrial Standard, JIS Z 4820, 2002.
- Miura, S. et al. Earthquake resistant test of new type glovebox, Transaction of SMiRT17, Prague, Czech Republic, 2003.
- Miura, S. et al. Confirmation test on confinement performance of improved glovebox, Transaction of SMiRT13, Vol. 3, pp. 405–410, Alegre, Brazil, 1995.
- Hargett, S.T., Kennedy, W.N. Evaluation of Seismic Capacity of Glovebox Windows Using Deformation Tests, Fifth Department of Energy Natural Phenomena Hazard Mitigations Symposium, Denver, 1995.
- ABAQUS Theory manual Version 6.6, Simulia corp., 2007.
- Seki, W., Fukahori, Y., Iseda, Y., Matsunaga, T. A Large Deformation Finite Element Analysis for Multilayer Elastomeric Bearings, Rubber division, 133rd American Chemical Society, Montreal, Canada, 1987
- Fukahori, Y., Seki, W. Stress analysis of elastomeric materials at large extensions using the finite element method. Journal of material science, Vol. 28, pp. 4143–4152, 1993.

Safety significance of a type of seismic input motions and consequences on nuclear industry practice – results of the IAEA coordinated research project on the “Safety significance of near-field earthquakes” (5-1683)

Pierre Labbé

EDF-Nuclear Engineering Division

IAEA when the hereunder reported coordinated research project was conducted

Context and scientific background

The facts usual practices of earthquake engineering result in a poor estimate of the damaging effects of near field input motions generated by low-medium magnitude earthquakes (LMME) was identified in 1997 by the OECD/NEA/CSNI as “the most significant issue” in the field of engineering characterization of seismic input motion. In 2002 the IAEA launched a 3 year Coordinated Research Project (CRP) “Safety significance of near-field earthquakes” (also funded by the European Union) to address this issue. 22 institutions from 18 countries joined the CRP that consisted of:

- Carrying out a benchmark on Near Field Earthquake (NFE) effects
- Making proposals for evolution of engineering practice.

Substance of the benchmark

The benchmark consisted of:

- Step 1: Interpreting existing experimental data, provided by France, relating to a concrete wall, the CAMUS specimen, clamped on a shaking table.
- Step 2: Numerical simulations of the specimen response with two natural input motions provided by Japan.
- Step 3: Sensitivity studies about the impact of non-linearity on floor response spectra.

The CAMUS specimen consists of two similar parallel shear walls, strongly clamped on a shaking table and subjected in their plane to 1-D horizontal seismic input motions. It is a mock-up at 1/3 scale of typical shear walls of a six

level conventional structure. Its total mass is 36 t. The R-bar system was designed in compliance with the French regulation for conventional buildings against a conventional (referred to below as ‘Nice type’) 0.2 g input motion.

The shaking table was activated by input motions representative of far-field (Nice type) and near-field (San Francisco type) cases, scaled to different peak ground acceleration (PGA) values according to the series presented in the table below. Recorded top displacements substantiated the fact that a near-field type motion is less damaging than a far-field type at the same PGA value. A key point for the CRP is that design criteria were not exceeded during these tests and that consequently only relatively small nonlinearity occurred.

Input motions (g)	Top displacements (mm)
Nice 0.24g	7.0
San Francisco 0.13g	1.5
San Francisco 1.11g	13.2
Nice 0.41g	13.4

Major conclusions

Major conclusions are as follows:

There is a consensus that the damaging capacity of LMME input motions is very low in spite of their possible high PGAs. The poor capability of nuclear practice to predict this result is linked to the fact that seismic input motions are conventionally regarded as force controlled loads, while high frequency input motions act principally as displacement controlled loads [Newmark 1978]. Consequently the favourable combination of:

- High frequency content of this type of input motion and
- Ductile capacity of structures is ignored. The NFE origin of the input does not pertain in the analysis. What pertains is the frequency content, irrespective of the so called far field or near field origin.

It is therefore recommended by the IAEA that nuclear industry goes towards a more systematic and codified use of simple non-linear structural analysis techniques (such as linearization techniques) that realistically account for the behaviour of structures subjected to strong motions.

Conclusions of the IAEA-JRC CRP as well as recommendations made by the IAEA will be presented in an IAEA technical document (TECDOC) to be published very soon.

Analysis of behaviour of raft foundations under seismic and impulsive loading (5-1689)

Suchibrata Dalal¹, Dr. Mahua Chakrabarti²

¹Post-Graduate Student, Department of Structural Engineering, Veermata Jijabai Technological Institute, Dr. H.R. Mahajani Marg, Matunga, Mumbai 400 019, India
e-mail: suchibrata.jucon@gmail.com

²Professor, Department of Structural Engineering, Veermata Jijabai Technological Institute, Dr. H.R. Mahajani Marg, Matunga, Mumbai 400 019, India
e-mail: mchakrabarti@vjti.org.in

Moderately thick plates are frequently encountered in civil engineering. Typical plate structures on elastic foundations are machine foundations and raft foundations, concrete pavements of highways and airfields etc subjected to impulsive and harmonic type of loadings. These structures are predominantly subjected to dynamic loadings and can be modeled mathematically by assuming a thick to moderately thick plate resting on an elastic foundation.

Some of the most important types of dynamic loadings, nuclear reactors' raft foundations are subjected to are seismic loading due to earthquake ground motion and impact loading such as due to explosion etc. These raft foundations have been modeled as thick plates on elastic foundations and the plates are analyzed using Reissner-Mindlin plate theory which considers first order shear deformation effects thus leading to better representation of actual behaviour of thick plates. The present study aims at analyzing behaviour of reactors' raft foundations during earth quake ground motion considering plate-foundation interaction. The foundation parameters characterize the compressive strain and shearing strain in the foundation.

In this paper two formulations have been investigated for studying dynamic behaviour of moderately thick plates. The first formulation is based on the Reissner-Mindlin plate theory, considering the first order shear deformation effect and including the plate-foundation interaction and thermal effects. The formulations have been extended to the case of large deflections of Reissner-Mindlin plates. The second formulation assumes Mindlin plate theory; the governing equations of dynamic equilibrium have been derived using Hamilton's principle and Euler – Lagrange equation of calculus of variation. Using these two formulations, programs have been prepared and validated.

For determination of dynamic responses viz. deflection and bending moment the governing equations of dynamic equilibrium have been derived based on First order Shear Deformation Plate theory (FSDPT). The analysis assumed appropriate Fourier expansion of seismic loading. Impulsive loading have also

been considered, using suitable form of Fourier expansion not simultaneously with seismic loading. The equations are solved by assuming admissible functions and using Modal Superposition Approach (MSA). Programs have been developed for prediction of dynamic behaviour of plate foundation system subjected to earth quake ground motion and various kinds of pulse loadings.

The numerical illustrations concern moderately thick plates with all four edges simply supported and resting on Pasternak-type elastic foundations. Effects of foundation stiffness, transverse shear deformation, plate aspect ratio, shape and duration of impulsive load, loaded area, and initial membrane stress etc, on the dynamic response of Reissner-Mindlin plates have been studied in terms of displacements and stress resultants and results are presented in the form of graphs. Based on the parametric studies time histories of deflection can be obtained for any point on the raft. The plate-foundation interaction has been considered in the analysis and the plate is assumed to vibrate and deform along with the foundation simultaneously. The study assumes flexibility of the raft as opposed to conventional engineering practice which assumes the raft foundation as fixed leading to larger stress resultants under dynamic loading conditions. Appropriate dynamic analysis will lead to economical structures and the present study has tried to develop formulations for appropriate dynamic analysis. Similarly design charts can be prepared based on different kinds of impulsive loads, different foundation properties, and different condition of temperature stresses if considered etc. which would provide plate thickness for permissible dynamic deflection. These types of charts would be very handy for regular analysis and design of moderately thick plates on elastic foundations.

Generation of dynamic mechanical model of inertial soil foundation in consideration of NPP structures basement finite stiffness (5-1692)

Akop Sargsian¹, Andrey Grishin², Elena Gukova³

¹Doctor of Science, Professor, Head of Dynamics and Seismic Safety Dept.
Atomenergoproject, Moscow, Russia, e-mail: ilk@aep.ru

²PhD, Leading Research Assistant, Atomenergoproject, Moscow, Russia
e-mail: ilk@aep.ru

³Leading Research Assistant, Atomenergoproject, Moscow, Russia
e-mail: ilk@aep.ru

Modern methods and approaches used for dynamic analyses of system “soil-structure” were based on assumption that structure basement was considered as a rigid body with 6 DOF. It is obvious that this assumption leads to distortion of kinematical parameters of structure basement motion, stress-strain state on the contact surface and also excludes evaluation of internal forces for foundation slab.

Evaluation of internal forces for foundation slab sections is required for validation of the design. So, the mentioned-above hypothesis is not acceptable in this case.

In order to model structure spatial motion in consideration of its basement finite stiffness three pairs of spring and dashpot at every nodal point on the contact soil-structure surface of FEM were placed along global Cartesian coordinate system axes. Top ends of every spring-dashpot pair were fixed on nodal point of bottom of foundation and bottom ends were clamped.

It is necessary to determine the distribution law for static and viscous stiffness for the bottom of foundation slab accounting with the soil inertial properties and finite basement stiffness of structure FEM.

In order to define the distribution law for the stiffness of soil foundation the following assumption was accepted. The foundation stiffness at an arbitrary nodal point of FEM is in proportional to stress arisen on soil on the contact surface. Thus, the distribution of stiffness is identical to distribution of stress developed on structure-soil contact surface on their interaction.

For rigid foundation slabs the following assumption was accepted. Viscous stiffness was distributed uniformly throughout bottom of foundation. Static stiffness was distributed by saddle-shaped law on bay zones and tended to finite extreme values on edge zones of bottom of foundation.

The validity criterion of accepted distribution law of integral stiffness and FEM mesh requirements were provided.

References

ASCE, 1998. Seismic Analysis of Safety-Related Nuclear Structures and Commentary. ASCE4-98. Reston, Virginia, USA.

Sargsian, A.E. 2008. Structural Mechanics (in Russian). High School, Moscow, Russia.

FORTUM Participation in BARCOM Round Robin pre-test simulation: mid-term analysis (5-1696)

Pentti Varpasuo, Jukka Kähkönen

Fortum Nuclear Services Ltd, P.O. Box 100, 00048 FORTUM, Finland

e-mails: jukka.kahkonen@fortum.com, pentti.varpasuo@fortum.com

Key words: containment experimental tests, large FEM models, pre-stressed reinforced concrete

In this report a preliminary mid-term analysis of the BARCOM test model is presented. The BARCOM test model is a 1:4 scale of an existing pressurized heavy water reactor (PHWR) pre-stressed concrete inner containment of 540 MW Tarapur Atomic Power Station 3&4 units in India. The goal of this mid-term analysis is to illustrate the modeling approach and achieve a prediction of the failure mode. The analysis was carried out using ABAQUS/CAE and ABAQUS/EXPLICIT version 6.7-EF1 software. In the analysis explicit time integration was used such way that the solution was quasi static. For the concrete material presentation the brittle cracking model available in ABAQUS/EXPLICIT was adopted. In the brittle cracking model the value used for the ultimate tensile stress was 3.6 MPa which is slightly higher than the value specified in the BARCOM documentation. The Young's modulus and Poisson's ratio used for concrete were 30 GPa and 0.2, respectively. The tendons were assigned ideal plastic von Mises material model with 1.683 GPa yield stress. The Young's modulus and Poisson's ratio used for tendons were 190 GPa and 0.3, respectively. The mesh of the containment consists of 4 -node quadrilateral and 3 -node triangle general purpose elements. In the analysis the bottom edge of the containment is fixed.

The results of the simulation analysis are presented in Fig. 1 and 2, where dome top node vertical displacement and von Mises stress at concrete outer surface in the internal over pressure is of 0.7 bar are presented.

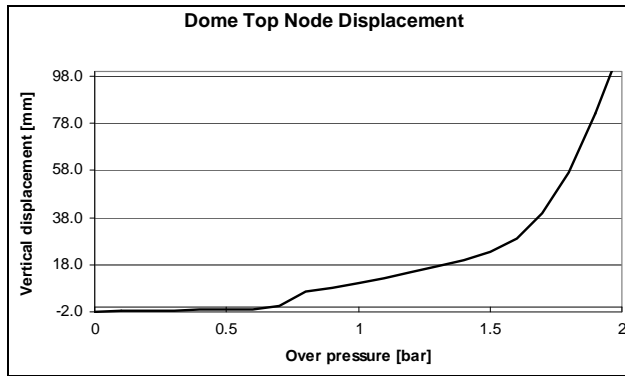


Figure 1. Dome top node vertical displacement.

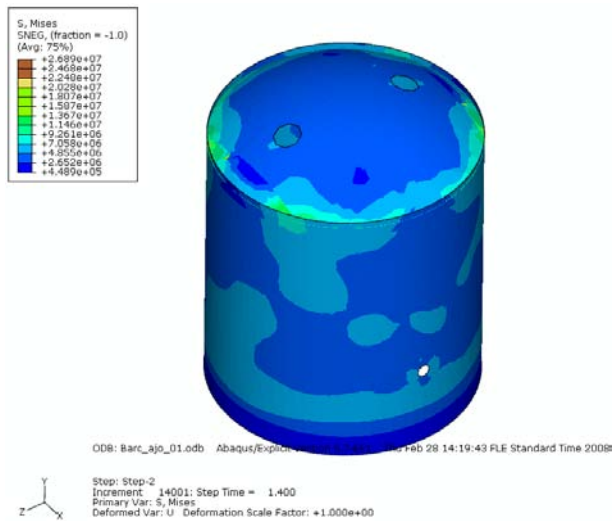


Figure 2. Von Mises stress at concrete outer surface. Over pressure is 0.7 bar.

References

BARC Containment Model Round Robin Analysis. Model Documents. Mumbai India, 2007.

ABAQUS version 6.7-EF1, Users Documentation, Simulia Inc. Dassault Systems, 2007.

Damping values for seismic design of nuclear power plant SC structures (5-1697)

Wonki Kim¹, Seung Joon Lee², Rae Young Jung³ and Moonsoo Kim⁴

¹ Professor, Architectural Engineering Dept., Hoseo University, Korea
e-mail: wonkikim@hoseo.edu

² Professor, Architectural Engineering Dept., Ajou University, Korea

³ Senior Researcher, Structural Systems & Site Evaluation Dept., Korea Institute of Nuclear Safety

⁴ Senior Researcher, Structural Systems & Site Evaluation Dept., Korea Institute of Nuclear Safety

Background

Structural damping values for seismic design of nuclear power plant structures are specified in Regulatory guide 1.61 for reinforced concrete structures of 4%(OBE) and 7%(SSE), and for steel structures of 3%(OBE) and 4%(SSE), but not for steel-plate concrete(SC, hereinafter) structures. SC structures have been being developed in the worlds for long time, but no research investigates the damping values except that Akiyama et al. concludes the identical damping value of 5% for both RC and SC structures for nuclear power plants. However, the experimental tests conducted by Akiyama are static cyclic loading tests and hydraulic-shaker vibration tests without any mass in the test specimens of both test types.

Objectives and investigations

This paper describes the research work of experimental testing method, analysis of test results and proposed damping values for seismic design of nuclear power plant SC structures. The concept of this research is to investigate the relative difference in damping values between RC and SC structures rather than to find out the absolute values of SC structures, so that tested are 4 specimens of RC-S, RC-M, SC-S and SC-M where S stands for shear-govern and M for moment-govern. As described in Table 1, the moment-govern specimens are higher than the shear-govern ones, but all the specimens are 1,700mm wide and 1,700mm long with wall thickness of 240mm.

Table 1. Descriptions of 4 specimens.

RC Specimens				SC Specimens			
Symbol	Height (mm)	Re-bars		Symbol	Height (mm)	Surface Plate	Stud Diam. (mm)
		Vertical	Horizontal				
RC-S	1,650	2D22@129	2D16@133	SC-S	1,650	3mm thk.	Ø6
RC-M	2,850			SC-M	2,850		

Conducted method is free vibration testing by rupturing a brittle steel plate which links an actuator and the center of 50 ton mass as shown in Figure 1. Rupturing load levels on each specimen are controlled by pre-designed tensile strength of the linking steel plate.

Results

Natural frequencies of 4 specimens are determined from the experimental test results with respect to the load level as illustrated in Figure 2. It is noticed that those frequencies are similar to the values in design practice.

Figure 3 shows an example of time vs. acceleration curve measured for specimen SC-S at rupturing load of 420kN, together with fitted curves of exponential function representing free vibration. Consequently, damping value is determined from the exponential function and its natural frequency. Similar analyses are performed to determine damping values of 4 specimens at the different rupturing load.



Figure 1. Test Setup of SC-M Specimen.

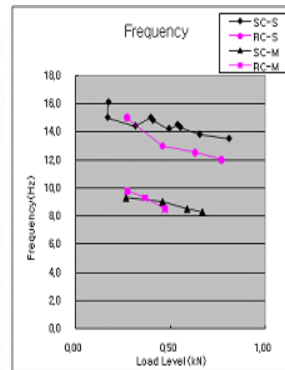


Figure 2. Natural Frequency of 4 specimens.

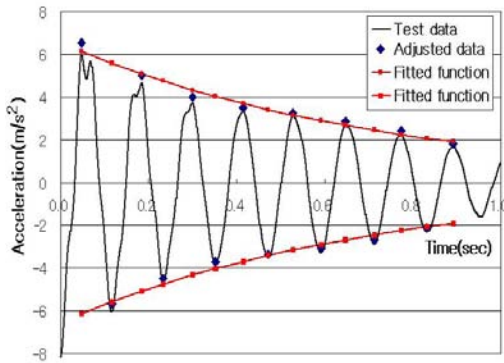


Figure 3. Example of Time vs. Acceleration.

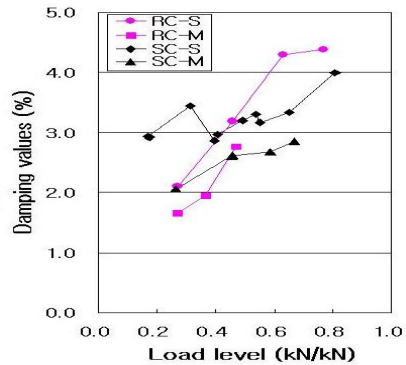


Figure 4. Damping values of 4 specimens.

Figure 4 shows comparison of damping values of 4 specimens with respect to load level, where the load level is the rupturing load divided by designed load which corresponds to specimen design strength.

Conclusions

By examining the relative differences in damping values of 4 specimens, it is proposed for SC structure to use the same damping values of 4% as RC at OBE, but 1% less value than RC resulting in 6% at SSE.

References

1. U.S. Nuclear Regulatory Commission, "Regulatory Guide 1.61, Damping Values for Seismic Design of Nuclear Power Plants", March 2007.
2. Hiroshi Akiyama et al, "1/10th Scale Model test of Inner Concrete Structure Composed of Concrete Filled Steel Bearing Wall". SMiRT 10, 1989.
3. Japan Electric Association, 2005. Technical Guidelines for Aseismic Design of Steel Plate Reinforced Concrete Structures, JEAG 4618-2005.
4. Korea Electric Power Industry Code, "Specification for Safety-Related Steel Plate Concrete Structures for Nuclear Facilities(Draft), KEPIC-SNG-09, 2009.

SMART 2008 project. Experimental tests of a reinforced concrete building subjected to torsion. Part 2: presentation of the tests results (5-1700)

Sandrine Lermite¹, Thierry Chaudat¹, Alexis Courtois²

¹CEA DEN/Saclay, Laboratoire d'Etudes de Mécanique Sismique,
91191 Gif-sur-Yvette Cedex, France

e-mail: sandrine.lermite@cea.fr, thierry.chaudat@cea.fr

²EDF – SEPTEN, Groupe Dynamique et Séisme 12-14 avenue Dutrievoz –
69628 Villeurbanne Cedex, France
e-mail: alexis.courtois@edf.fr

Introduction

Reinforced concrete (RC) buildings exhibiting tri-dimensional effects and non-linear response are a main concern in the field of earthquake research and regulation. In the last decade, several experimental tests have been performed on reinforced concrete structures under seismic excitations (i.e. “CAMUS” program), in order to study the seismic behaviour of shear walls, but without significant 3D effects. The recent evolution of the different codes and the new French zoning map had emphasized the importance to better understand the capacity of irregular structure under seismic loadings.

Commissariat à l’Energie Atomique (CEA) and Electricité de France (EDF) launched in 2007 a project named SMART-2008 project” (Seismic design and best-estimate Methods Assessment for Reinforced concrete buildings subjected to Torsion and non-linear effects). A reduced scaled model (scale of 1/4th) was designed and built to be tested between June and October 2008 on AZALEE shaking table at Commissariat à l’Energie Atomique (CEA Saclay, France) as part as this project. The aim is (1) to compare and validate approaches used for the dynamic responses evaluation of RC structures subjected to earthquakes and exhibiting both 3D and non-linear behaviours, (2) to evaluate loads induced to internal equipments, (3) to quantify margins in design methodologies and (4) to carry out realistic methods to quantify variability in order to produce fragility curves.

The part 2 of this paper presents the main results of the seismic tests (Phase 2 of the SMART -2008 project), and exhibits the effect of structural irregularities on the structure behaviour.

Aim of the work

The 1/4th scaled model to be tested is a trapezoidal, three-story reinforced concrete structure. It is representative of a typical, simplified half part of an electrical nuclear building. It is composed of three walls forming a U shape. Two of those walls have openings.

The specimen has been designed according to the French nuclear methods, with a peak ground acceleration for the response spectrum anchored at 0.2 g. This seismic loading corresponds to a Safe Shutdown Earthquake (SSE) in a low to medium seismic area (equivalent to a magnitude of 5.5 with a distance of about 10 km).

The experimental test started in June 2008. The tests sequence was realised as follows:

- 2 seismic tests with 2 different set of real accelerograms, at 0.05 g pga level
- 10 seismic tests with the set of synthetic accelerograms scaled from 0.1 g up to 1 g pga level.

Because an extensive set of instrumentation has been set up on the specimen, only partial results will be presented at the time. This paper will focus on the global behaviour of the structure at under-design level, design level and over-design level. Special attentions will be given to the frequency evolution, the cracks evolution in the different elements and the absolute acceleration recorded. The main results will be compared to the one expected according to the design regulation used.

FORTUM participation in IAEA EBP benchmark for Kashivazaki-Kariwa NPP unit 7 response in July 2007 event (5-1701)

Pentti Varpasuo

Fortum Nuclear Services Ltd, P.O. Box 100, 00048 FORTUM, Finland

e-mail: pentti.varpasuo@fortum.com

Keywords: seismic safety of nuclear power plants, seismic response, plant structures and equipment

In this report Fortum participation in a benchmark related to the structural behavior of structures including the soil and equipment response of the Kashivazaki-Kariwa Nuclear Power Plant (K-K NPP) of Tokyo Electric Power Company (TEPCO) in Japan, during the 16 July 2007 Niigataken-Chuetsu-Oki earthquake (Niigataken-Chuetsu-Oki earthquake) is described. The goal of this benchmark is to conduct a comparison between different analytical techniques, as used in the usual engineering practice and the recorded response of a structure. Detailed goals can be summarized as follows:

- 1) Understanding of soil and structures response during the Niigataken-Chuetsu-Oki earthquake
- 2) Understanding of margins
- 3) Calibration of different simulation methodologies
- 4) Identification of main parameters influencing the soil-structure response
- 5) Simulation of equipment response for some selected equipment.

In order to carry out this simulation task a detailed model of the reactor building of unit 7 of K-K NPP will be developed. The most important piping system to be simulated is the residual heat removal-system which will be modeled explicitly in the structural model. Also the pools sloshing of fuel pools will be simulated directly in the structural model. The third important equipment response to be simulated is the buckling of yard tanks.

The main results will be the transfer of response spectra from base raft to main operating floor in reactor and the peak values of the stresses in the most critical equipment items.

References

MSC/NASTRAN, User's Manual, Los Angeles, 2003.

ABAQUS version 6.7-EF1, Users Documentation, Simulia Inc., Dassault Systems, 2007.

Identification of modal parameters of a containment building using ambient vibration measurements (5-1702)

Sooyong Park¹, Yung-Moo Shin¹, Ha-Yeon Kim¹,
Sanghyun Choi², Dae-Hyuk Kim²

Chang-Hun Hyun³, Moon-Soo Kim³, Sang-Yun Kim³

¹Div. of Architecture & Ocean Space, Korea Maritime University
Dongsam-dong, Pusan 606-791, Korea

²Korea National Railroad College, Dept. of Railroad Facility Engineering
Uiwang, Kyunggi-do 437-763, Korea

³Korea Institute of Nuclear Safety, Structural Systems & Site Evaluation Dept.
Yuseong-gu, Daejeon 305-600, Korea
e-mail: schoi86@nate.com

Introduction

The importance of maintaining the structural integrity of a containment building (CB), which preserves the nuclear reactor and the other safety related systems from man-made as well as natural disasters, and protects publics from hazardous radioactive materials can never be exaggerated. So far, the structural integrity of the CB has been evaluated periodically via visual inspections, chemical tests, nondestructive strength tests, etc. However, these methods can only provide the local information on the structural condition and require considerable time and cost to estimate overall structural integrity [1].

During the past few decades, research on monitoring the structural integrity of civil structures using dynamic response measurements has actively conducted [2], and successful applications have been reported [3]. In this paper, the possibility of monitoring the structural integrity of a CB utilizing ambient vibration (AV) measurements is explored. The AV testing has gained attention which can avoid the interruption of normal operation of civil structures [4]. To fulfill the objective, the ambient vibration of the CB of the Ulchin 5th unit, located in Ulchin, Korea, was measured, and the modal parameters, i.e., resonant frequencies and corresponding modeshapes, were extracted.

Aim of the work

The aim of this research is to find the modal parameters which may represent the overall structural integrity of the CB. In order to achieve the aim of this research, the following sub-tasks were performed:

- AV responses of a CB were measured using sensors
- A finite element (FE) model for the CB was built and modal parameters were computed
- Modal parameters were extracted from the measured responses and
- The correspondence between the computed and the measured modal parameters was established.

Experiment

The AV of the CB of the Ulchin 5th unit was measured to explore the feasibility of identifying modal parameters from AV measurements. The accelerometers were mounted on the outer surface of the CB at 9 locations of the same level. The fixed reference data were measured at 3 m above the other sensors. The measurement duration was about 170 min. Instrumentation used to conduct the AV testing consisted of 6 strain-gage-type accelerometers, a digital dynamic strain meter, an amplifier, and a portable computer. Data acquisition software was the Visual Log DRA-7630.

The autopower spectrum (AS) was obtained using the power spectral density (PSD) function of the MATLAB. The final PSD was calculated via averaging PSDs for every 2,048 data. To reduce leakage error, the Hanning window and data overlapping of 1,024 data were applied. The cross spectrum (CS) between the reference measurements and the other measurements were obtained using the CSD function of the MATLAB. From the frequency response functions, obtained using the AS of the reference location and the CSs, modal parameters were extracted.

Numerical model

The numerical analysis was performed using the FE model developed by Jeon et al. [5]. The concrete part of the CB including the wall, the dome, and the buttresses were modeled using the 3-D solid elements. Main reinforcing bars were idealized as distributed stiffness in the wall, and tendons were modeled using the truss elements. The free vibration analysis was conducted using the ABAQUS.

Results

From the AV response measurements, three distinct resonant frequencies and corresponding modeshapes were identified. The correspondence between the computed and the measured modal parameters was established using the modal assurance criteria (MAC) [6].

Conclusions

AV of the CB of the Ulchin 5th unit was measured to explore the feasibility of identifying modal parameters from AV measurements. Using the measured acceleration data, three distinct resonant frequencies and corresponding modeshapes were identified. The MAC values show good agreements between computed and the measured modal parameters.

References

1. S. Park, S. Choi. Development of methodology for estimating the effective properties of containment buildings, Midterm Report, Korea Institute of Nuclear Safety, KINS/HR-836, 2008.
2. S.W. Doebling, C. Farrar, M.B. Prime, D.W. Shevitz. Damage identification and health monitoring of structural and mechanical systems from changes in their vibrational characteristics: a literature review, Technical Report LA-13070-MS, Los Alamos National Laboratory, 1996.
3. S. Choi, S. Park, R. Bolton, N. Stubbs, C. Sikorsky. Periodic monitoring of physical changes in a concrete box-girder bridge. *Journal of Sound and Vibration*, Vol. 278, pp. 365–381.
4. C. Gentile, G. Bernardini. Output-only modal identification of a reinforced concrete bridge from radar-based measurements. *NDT&E International*, Vol. 41, pp. 544–553, 2008.
5. S.J. Jeon, Y.S. Lee, C.H. Chung, Y.S. Chung. Dynamic nonlinear response of domestic nuclear containment buildings subjected to large aircraft impact load. *Journal of Korea Society of Civil Engineers*, Vol. 25, No. 1A, pp. 1–10.
6. D.J. Ewing. *Modal Testing: Theory and Practice*, Research Studies Press, Letchworth, U.K., 1984.

Expansion of the Riera approach for predicting aircraft impact damage to steel and concrete buildings – Part 2 – simplified analysis methodology (5-1711)

Steven W. Kirkpatrick, Robert T. Bocchieri
Applied Research Associates, Inc.
2672 Bayshore Parkway, Suite 1035, Mountain View, CA 94043, USA
e-mail: skirkpatrick@ara.com. rbocchieri@ara.com

The Riera [1] approach for applying aircraft impact loads is typically used to evaluate the response of a relatively rigid, non-responding uniform structure, such as strongly reinforced nuclear reactor containment buildings. More recently, for more complex geometrical structures that sequentially fail during impact, modern finite element codes have been used to model both the aircraft and building, such as was done for the World Trade Center Towers as part of the Federal Building and Fire Safety Investigation of the World Trade Center Disaster [2]. The former approach provides the ability to analyze these complex events, but at a high computational cost. In order to conduct studies with a broad scope, considering a range of building types and aircraft impact scenarios, a fast-running computational tool is needed.

Here the Riera approach is expanded to consider impacts on weaker and more detailed building designs, such as those of typical steel and concrete frame construction. With this approach, loads from multiple segments of an aircraft are applied to a complex geometrical structure through use of ray tracing algorithms. Penetration of the aircraft segments through a failing structure and through non-structural mass inside of these structures are included.

An aircraft impact module (AIM) was developed to apply aircraft impact loads to the computer code BAM (Building Analysis Module). BAM is an accredited engineering tool developed to evaluate conventional weapon effects on above ground buildings due to internal and external detonations. The resulting computational tool (AIM/BAM) provides a means for performing rapid assessments of impact damage for a wide variety of impact scenarios and standard building types. A methodology was also developed to quickly generate the input parameters for a wide array of aircraft based on geometrical simplification of the aircraft structure and knowledge of similar aircraft weight distributions.

Several modifications were also made to BAM to account for different building component failure modes unique to aircraft impacts. The changes were aimed at adding specific component failure modes anticipated under aircraft

impact loads that have not been considered in blast response. Neglecting these failure modes might underestimate the damage inflicted by the aircraft impacts and would lead to damage estimates that are not conservative. The additional failure modes added to BAM were: (1) shear failure modes for localized loading on structural columns and beams of framed structures; and (2) breach of columns, beams, walls and floors of framed structures. In addition, a feature was added to track the effects of the non-structural building components (e.g. office furnishings). The non-structural mass has been shown to have a significant effect on the distance that an aircraft can penetrate into a building and produce impact damage.

Finally, validation studies were performed. The first compares the aircraft loading of a Boeing 707 predicted with AIM against that traditionally used for assessing the safety of nuclear power plant structures. The second validation is for the impacts of the two Boeing 767-200ER aircraft with the World Trade Center Towers on September, 11 2001. All validation studies yielded good agreement with these events.

References

1. Riera, J.D. A Critical Reappraisal of Nuclear Power Plant Safety Against Accidental Aircraft Impact. *Nuclear Engineering and Design*, Vol. 57, pp. 193–206, 1980.
2. Kirkpatrick, S.W., R.T. Bocchieri, F. Sadek, R.A. MacNeill, S. Holmes, B.D. Peterson, R.W. Cilke, C. Navarro. Federal Building and Fire Safety Investigation of the World Trade Center Disaster: Analysis of Aircraft Impacts into the World Trade Center Towers, NIST NCSTAR 1-2B. National Institute of Standards and Technology, Gaithersburg, MD, September, 2005.

Experimental study on seismic reduction effectiveness of main control room in N.P.P using 3-directional isolation system (5-1713)

Kyung-Won Hahm¹, Kyung-Jin Lee², Yong-Pyo Suh³

¹Researcher, Korea Electric Power Research Institute, KEPCO, Korea
e-mail: hkw@kepri.re.kr

²Principal Researcher, KEPRI, KEPCO, Korea, e-mail: Leekj@kepri.re.kr

³Principal Researcher, KEPRI, KEPCO, Korea, e-mail: ypsuh@kepri.re.kr

Introduction

The main control room of a nuclear power plant operates many important N.P.P facilities such as N.S.S.S (Nuclear Steam Supply System), so it is highly recommended to secure seismic safety of main control room during and after earthquakes. A number of isolation systems installed between equipment and foundation have been widely studied [1]. We used 3-Directional isolation systems which consist of a FPS (Friction Pendulum System), an air spring and a viscous damper. A FPS is resistant to horizontal motion and an air spring is resistant to vertical motion and a viscous damper is resistant to rocking motion and excessive displacement.

In this study, we designed two types of main control floor systems. A number of shaking table tests with or without isolation system were conducted to evaluate isolation effectiveness.

Shaking table test

The test specimen used in this study is a PCS cabinet installed in 1st and 2nd main control room at 144 ft elevation of ULJIN N.P.P. The specimen is placed on top of two types of access floor as shown in figure 1. During shaking table tests, electric parts of the cabinet were removed, so the weight of the PCS cabinet was 400 kgf. Four identical 3-D isolation systems were mounted beneath the bare frame model under OBE, SSE horizontal and vertical input motions. Properties of 3-D isolation systems are summarized in Table 1.

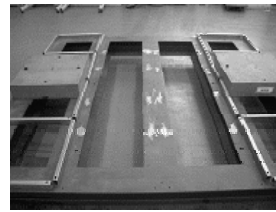
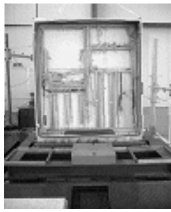


Figure 1. PCS cabinet.

Access floor Type I.

Access floor Type II.

Table 1. Specification of 3-D isolation system.

FPS (Friction Pendulum System)	Natural Frequency	0.5 Hz
Air Spring	Natural Frequency	2.0 Hz
Viscous Damper	Damping Coefficient	15,000N·sec/m

Figure 2. shows acceleration response spectrum of S.S.E. In vertical direction, there were significant frequency drift as well as large spectral acceleration reduction. In horizontal one, it also showed large spectral acceleration reduction, but there was no obvious frequency drift.

Conclusions

To evaluate the floor isolation effectiveness of the 3-D isolation system, several shaking table tests with or without the isolation system were conducted. From the test, it is observed that both types have showed large acceleration reduction effect depending on input earthquake signals. Especially, both types have showed larger seismic reduction effect when subjected to long periodic earthquake motions than short ones. In vertical direction, significant frequency drift was observed due to the vertical isolation device whereas there was no obvious frequency drift in horizontal one.

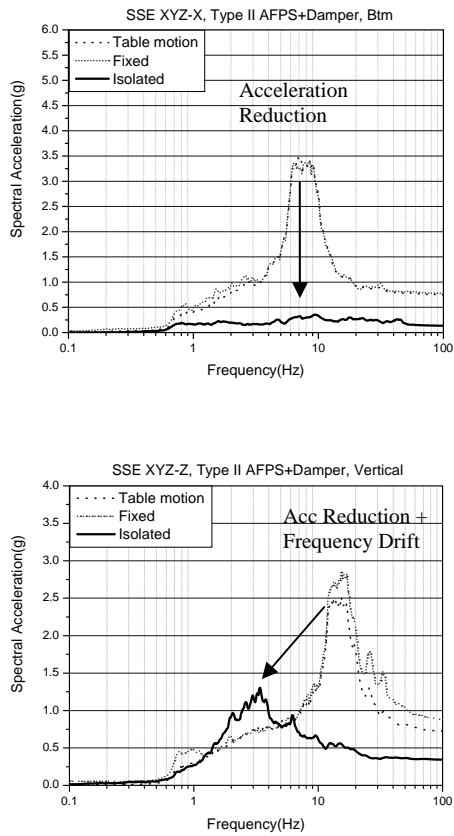


Figure 2. Acceleration Response Spectrum (Horizontal, Vertical).

Reference

- K. Ebisawa, K. Ando, K. Shibata. (2000). Progress of a research program on seismic base isolation of nuclear components. Nuclear Engineering and Design, 198, pp. 61–74.

Activities of OECD/NEA in the fields of seismic hazard assessment & earthquake engineering (5-1721)

Andrew J. Murphy¹, Andrei Blahoianu², Alejandro Huerta³

¹U.S. Nuclear Regulatory Commission, Washington, DC, USA
e-mail: ajm1@nrc.gov

²Canadian Nuclear Safety Commission, Ottawa, ON, Canada
e-mail: andrei.blahoianu@cnsccsn.gc.ca

³Organization for Economic Cooperation and Development Nuclear Energy Agency
Nuclear Safety Division, Paris, France
e-mail: alejandro.huerta@oecd.org

The Organization for Economic Cooperation and Development (OECD)/Nuclear Energy Agency (NEA) established the seismic group to address high-level seismic safety issues from an international perspective to provide information to member countries and to help them in assessing their facilities. The seismic group supports the Working Group on the Integrity and Aging of Components and Structures established under the Committee on the Safety of Nuclear Installations (CSNI) dealing with safety-related research and development aspects. The seismic group makes recommendations with the objective to exchange information, to overcome discrepancies and to reach international consensus on technical issues. The group operates through annual plenary meetings and technical workshops and by issuing state-of-the-art reports and topical opinion papers. Among other items, the recent and planned activities of the group include the following:

- updating a strategic plan for seismic group activities for the next 5 years
- conducting a meeting of specialists on seismic hazard assessment in April, 2008 in Lyon, France, with planned publication of the proceedings
- publishing a report summarising the main findings and conclusions of a series of OECD/NEA workshops and extracting the seismic information most relevant to current nuclear practices
- discussing the worldwide implications on nuclear facilities of the July 16, 2007 Niigata-ken Chuetsu-oki earthquake and its effects at the Kashiwazaki-Kariwa Nuclear power Station
- supporting a benchmark, SMART 2008, being conducted in Saclay, France, on seismic design and assessment analysis for multi-story reinforced concrete buildings subjected to torsion and nonlinear effects

- supporting the IAEA extra-budgetary programme on seismic safety of existing NPP's.

In April, 2008, the group held a workshop on seismic hazards assessments. The objective of this workshop was to address recent findings and issues in Probabilistic Seismic Hazard Analysis raised during the Specialists Meeting on Seismic Probabilistic Safety Assessment of Nuclear Facilities, held in Jeju, Korea on 6–8 November 2006. The Lyon workshop addressed the issues of: a. management of epistemic and random uncertainties. b. the issues associated with PSHA results for areas of low-to-moderate seismicity and of the difficulties with conducting a PSHA in such an area, and c. comparison of PSHA results to available observations, especially for return periods where records are available. The workshop was attended by over 60 participants from 15 countries, and 30 papers were presented, including five invited lectures and six panel discussions

About 25 high-level experts and specialists from 15 countries, representing safety authorities, research organizations, electric utilities, and other international organizations (e.g., the International Atomic Energy Agency and the European Union) regularly participate in seismic group activities. During a yearly plenary session, the group defines its program of work and presents it to the CSNI for approval. As conditions warrant, the CSNI provides top-down direction. The seismic group is recognized as a forum to exchange technical information. It has no budget of its own, and activities are completed solely on a voluntary basis.

As its first task, the seismic group developed strategic recommendations to describe its activities and identified the following topics or issues for the group to address:

- seismic analysis and design of piping
- engineering characterization of seismic input
- aging effects, particularly as it affects seismic design
- validation of analysis methods
- re-evaluation of existing facilities and assessment of margins beyond the design basis.

The seismic group has refined these topics for specific actions: to promote greater synergy between engineers and seismologists in the areas of probabilistic, performance-based approaches and reliability-based approaches to the above strategies, development of a proposal on better understanding of soil-structure interactions, and improvement of knowledge management .

This paper will detail some of the recent activities and products of the seismic group.

Experimental studies of confinement integrity of metal cask subjected to impulsive loads due to aircraft engine crash (Part 1) (5-1730)

Koji Shirai, Kosuke Namba, Toshiari Saegusa
Central Research Institute of Electric Power Industry (CRIEPI)
1646, Abiko, Abiko-shi, Chiba-ken, 270-1194, Japan
e-mail: shirai@criepi.denken.or.jp

In Japan, the first Interim Storage Facility of spent nuclear fuel away from reactor site is being planned to start its commercial operation around 2010, in use of dual-purpose metal cask in the northern part of Main Japan Island. Business License Examination for safety design approval has started since March, 2007. To demonstrate the more scientific and rational performance of safety regulation activities on each phase for the first license procedure, CRIEPI has executed demonstration tests with full scale casks, such as drop tests onto real targets without impact limiters and seismic tests subjected to strong earthquake motions. Moreover, it is important to develop the knowledge for the inherent security of metal cask under extreme mechanical-impact conditions, especially for increasing interest since the terrorist attacks from 11th September 2001. To evaluate damage of cask in aircraft crash event at a storage facility, the simulated crash test has been started since 2007. To investigate the integrity of the lid structure of the metal cask without impact limiters during the extreme impact loads due to aircraft crash, the numerical evaluation was performed for two impact scenarios, a vertical impact onto the lid structure and a horizontal impact hitting the cask¹⁾. Moreover, according to these scenarios, the horizontal impact test using scale model engine of aircraft has been executed and leak rate from the metal gasket in the cask also measured at the impact in the test. This paper presents dynamic mechanical behavior and confinement integrity of the metal cask lid closure system (especially, leak tightness based on relative dynamic displacements between metallic seals) obtained in the horizontal impact test.

As a relevant aircraft engine, turbo-fan engine, which was used for big passenger planes, such as Boeing 747 and Air-Bus 300, was chosen. Its length, outer diameter and weight are 2.7 m, 4.3 m and 4.4 ton, respectively. The local penetration damage of the interim storage facility building against a relevant aircraft engine crash has been examined. The impact velocity was set to 90 m/s considering the taking-off, landing speed of the passenger aircraft, and the Type C package test conditions in the IAEA Transport Regulation. The penetration depth can be calculated by the local damage formula, such as Degen formula for

concrete structure. According to the design concept of the storage building (wall thickness 80 cm), the reduced velocity of the engine missile was estimated as about 60 m/s.

In the horizontal impact test, the similarity law was employed for the test model. As important parameters, the velocity and the material were assumed to be the same for both model and prototype. The geometry scale factor for the test was set at 1/2.5, based on the limited condition of the testing facility. The lid gasket of the scale-model cask is double type metal gasket made of aluminum coating material. To simulate the aging effect, the lid part was heated over 30 hours under 175°C. As a missile, a simplified deformable missile was used considering the rigidity of the actual aircraft engine. For safety reasons, the test apparatus of aircraft crash test for horizontal impact was constructed in the open air. The missile was accelerated to the specified impact velocity by the driving force caused by the explosion of gunpowder inserted in the tail of the missile. The velocity was controlled by the amount of powder and the traveling distance of the missile. To measure the impact velocity of the missile, fine carbon pins were installed at four points near the front face of the cask. Its velocity was calculated from the time differences when the missile cut the pins as it passed. The scale cask was mounted on a supporting frame structure by the specific panel. The reaction forces were measured by six load cells installed between the panel and the supporting frame.

The peak value of the reaction force measured with the load cells was 485 kN and the impact duration time was 10 msec. Although the outer shell of the metal cask, which enclosed the neutron absorber (resin), was ruptured in the vicinity of the impacted area, there was not so considerable damage of the cask body and the lid structure according to the visual inspection after the impact test. Although the leak rate value from the lid increased by 5 orders of magnitude during the impact immediately, the leak rate shows the goodness of the leak-tightness at the lid, as the value is under 1.0×10^{-5} Pa·m³/s. From this test result, it seems that the loss of the inner pressure of the cask cavity may be avoided in the impact event with the horizontal orientation even if the severe impact load was applied on to the metal cask due to aircraft engine crash.

Reference

1. Shirai, K. et al. Safety Analysis of Dual Purpose Metal Cask Subjected to Impulsive Loads due to Aircraft Engine Crash, Proc. of ICONE16, 2008.

Amplification of seismic motion at deep soil sites (5-1740)

Farhang Ostadan¹, Tarek Elkhoraibi²

¹Bechtel Fellow and Chief Soils Engineer, Bechtel National
50 Beale St, San Francisco, CA, USA, e-mail: fostadan@bechtel.com

²Senior Engineer, Bechtel National
50 Beale St, San Francisco, CA, USA, e-mail: telkhora@bechtel.com

Recently, numerous utilities in the United States have submitted license applications for construction of new power plants mostly at the existing plant sites. As part of the preparation of the safety analysis report for each application, an extensive study is performed to collect geological, geotechnical and seismological data for the site in order to develop the seismic design motion for design and qualification of the plant structures and components. Computation of the design motion follows the requirements of the performance-based design stipulated in the Regulatory Guide 1.208 [1] and ASCE 43-05 [2]. Once the probabilistic seismic hazard analysis is performed and the uniform hazard motion for rock is obtained, soil amplification analysis is performed and the results are processed to obtain the design motion at the horizon(s) of interest in the soil column. To provide the necessary input data for soil amplification analysis, extensive field and laboratory investigations are performed to characterize the soil profile and dynamic soil properties including the nonlinear soil properties of the soil layers at the site. In the case of nonlinear properties, the preferred approach is the use of the resonant column-torsional shear test device to develop the strain-dependent soil shear modulus and damping for a wide range of soil shear strains. To account for the uncertainties and variation in soil profile and soil data, careful randomization of the data is performed to develop a suite of soil column velocity profiles and associated soil nonlinear data for use in the amplification analysis. In this paper, a summary of the method used for soil amplification modeling and analysis is described. Specifically, for very deep soil sites where the location of the base rock is not known, the techniques for modification of soil models are discussed. The results of the soil amplification studies for four deep soil sites are presented and discussed. The effect of soil nonlinearity and the extent of amplification of motion are presented. The resulting amplified motions are used to obtain the performance-based motion for design.

References

1. Nuclear Regulatory Commission. A Performance-Based Approach to Define the Site-Specific Earthquake Ground Motion. Regulatory Guide 1.208, March 2007.
2. American Society of Civil Engineers. Seismic Design Criteria for Structures, Systems, and Components in Nuclear Facilities. ASCE 43-05, 2005.

VTT IMPACT program – First phase: Lessons gained by IRSN (5-1746)

François Tarallo¹, Jean Mathieu Rambach¹, Nicolas Bourasseau¹,
Nguyễn-Ngoc-Loan Phatthanasinh²

¹Institut de Radioprotection et de Sûreté Nucléaire (IRSN)
Fontenay-aux-Roses, France

e-mail: francois.tarallo@irsn.fr

²Université Joseph Fourier, Grenoble, France

Introduction

This paper presents some results of impact tests performed in VTT premises within the framework of the first phase of the Finnish IMPACT program, described in [3] and [4]. The tests discussed here relate either to rigid targets able to record the impact forces or to one-way slabs made in reinforced concrete and simply supported along 2 opposite edges. The targets and slabs are impacted by crushable missiles whose mass is around 50 kg and velocity between 100 and 150 m/s. The set of tests includes variations on missiles (with or without water) and concrete slabs (with or without stirrups).

The authors have analyzed and simulated numerically a few sets of tests, in an attempt to improve the calculation models and to give useful recommendations for the second phase of the program. The results are interpreted by using analytical models. Lessons to be learnt from the first phase of the program are developed in order to improve the testing set-up, the quality of recordings and the knowledge of the useful and relevant mechanical properties of reinforced concrete to be introduced in the models.

Analysis of tests on rigid targets

The analysis of force plate tests indicates some difficulty to understand a few tests, while others provide consistent force time functions that quantify the loading of a rigid target by a deformable missile. Cylindrical missiles filled with water seem more “severe” than the empty ones; however more tests are necessary to confirm that result. Recommendations for the second phase of the program are proposed: metallic pipes must be selected in order to achieve reliable and constant buckling of the cylindrical missiles during the impact, and the instrumentation of the force plate (strain gauges) can be improved in order to provide consistent force time functions.

Use of empirical formulae to predict the perforation of reinforced concrete slabs by deformable missiles

As a general rule, the empirical formulae presented in the technical literature ([1] and [2]) deal with hard missiles and do not allow a perforation prediction by a deformable missile, with the exception of the “reduction factors” proposed [6] after the tests performed in Sandia National laboratories in the 1980s, that seem pessimistic when applied to the “soft” VTT tests on concrete slabs. The authors think this conservatism can be explained by differences between Sandia and VTT tests. The 2 way slabs to be tested in the second phase of the VTT program should bring useful information concerning the reduction factors to be applied to “hard” missile formulae, when the missile is deformable.

Analysis of the scattering of the results of concrete slabs tests

The repetition of a number of tests gives some information concerning the possible scattering of the behavior of “real” structure: the experimental scattering of reinforced concrete slabs tests appears to be significant. Therefore, it should be taken into account when the tests data are used to fit a calculation code, or when some predictions of displacements of concrete structures under impacts are made in the actual projects.

Simplified numerical simulations of concrete slabs tests

The numerical simulations of three tests were performed using a simplified analytical code proposed in [4], in order to quantify the parameters governing the dynamic flexural behavior of reinforced concrete slabs submitted to an impulsive load. The purpose of this work is to improve the prediction of deflections of structural elements that exhibit plastic bending caused by large but “soft” impacts. The decrease in rigidity and the increase in structural damping are clearly pointed out as witnesses of the damage in the structure, when the calculations are fitted to the experimental displacements of the slabs during and after the impact. It seems that transversal reinforcement in a slab does not reduce the damage level caused by plastic bending. Tests to be performed in the next phase of the program may add some insight on that issue.

References

1. Buzaud, E. et al. Assessment of empirical formulae for local response of concrete structures to hard projectile impact, in CONSEC'2007 Tours, France.
2. Chang, W.S. Impact of solid missiles on concrete structures. ASCE J Struct Div 1984, 110(5), 948–60.
3. Lastunen, A. et al. Impact Test Facility in Transaction SMiRT-19 August 2007, Toronto, Canada.
4. Rambach, J.M. Behavior of a reinforced concrete beam under impact loading: a simplified approach, in Transaction SMiRT-19 August 2007, Toronto, Canada.
5. Saarenheimo, A. et al. Numerical and experimental studies on impact loaded concrete structures, in Icone-14 2006 Miami (Florida, USA).
6. Sugano, T. et al. Local damage to reinforced concrete structures caused by impact of aircraft engine missiles. Part 2. Evaluation of test results, in Nuclear Engineering and Design 140 (1993) 407–423.
7. Tarallo, F. et al. Interpretation of Soft Impact Medium Velocity Tests on Concrete Slabs, in Transaction SMiRT-19 August 2007, Toronto, Canada.

Conservatism in the use of stick models in dynamic SSI analysis (5-1749)

Ragunath Sankaranarayanan¹, Oliver Schneider²

¹AREVA NP Inc, NEEC-A, 7207 IBM Drive, Charlotte, NC, USA

e-mail: ragu.sankara@areva.com

²AREVA NP GmbH, NEEC-G

Kaiserleistrasse 29, 63067 Offenbach am Main, Germany

e-mail: oliver.schneider@areva.com

Dynamic Soil-Structure-Interaction (SSI) analysis models for nuclear islands or other buildings that support safety-related equipment should be capable of adequately representing the input motions and structural responses. Historically, simplified, lumped-mass-equivalent stick models were used in the SSI analysis of large nuclear island (NI) structures. In a simplified model, the buildings are idealized as shear-wall structures in which the sticks represent the composite effects of the building walls and slabs. While the simplified models are limited to accurately capturing only the global response of the NI, detailed Finite Element Models (FEM) can capture both the global and local responses. This study compares the SSI response of the structures of a hypothetical but typical nuclear island using two different models, namely, a detailed finite element model and a simplified stick model. The NI basemat is considered to be rigid. The SSI analysis is performed for three hypothetical site conditions namely soft soil, medium soil and hard rock. The soft and medium soil sites are considered as layered sites with varying shear wave velocities along the depth of the soil profile. The hard rock site is represented by a uniform half-space. Synthetic acceleration time-histories that were modified to match the spectral shapes defined in European Utility Requirements (EUR) document for soft-to-hard sites are used as input motions. The input control motions are anchored to 0.3 g spectral acceleration in both the horizontal and vertical directions. The NI is assumed to be surface founded, and the input control motions are applied at grade. SSI analysis is performed using SASSI code. The results of this study shows that the Zero Period Accelerations (ZPAs) obtained from the stick model match those from the FEM model, closely but with some conservatism. The In-Structure Response Spectra (ISRS) from the two models are comparable, in general, for lower frequencies. However, the study shows that the ISRS for flexible floors obtained from the stick-model using decoupled single-degree-of-freedom (SDOF) accelerators are very conservative when compared to those obtained from the detailed FEM model.

Earthquake fatigue analysis for CANDU® nuclear power plants (5-1772)

Tarek S. Aziz

Principal Engineer, Engineering and Technology Delivery
Atomic Energy of Canada Limited, Mississauga, ON, Canada
e-mail: azizt@aecl.ca

This paper presents the results of an investigation into the number of cycles for seismic fatigue analysis for equipment located in CANDU®¹ nuclear power plants. Seismic fatigue analysis has been identified as a governing factor for different equipment analysis and fitness for service. The primary objective of the paper is to review the earthquake fatigue analysis requirement in Canadian, USA codes and other regulatory requirements. Following this the paper derives the number of seismic full stress cycles to be used for seismic fatigue analysis for nuclear power plants equipment, piping and their supports.

By subjecting the overall system to different earthquake records and using the material fatigue life curve, a method is developed to calculate the number of fatigue cycles equivalent to the total seismic response. This method is applied to the response results of key points of the dynamic model of the system in order to determine the maximum number of equivalent seismic fatigue cycles for various conditions. The results are used to make recommendations for fatigue evaluations in the design of nuclear power plant equipment. From the investigation, convenient rules were established for estimating the fatigue usage factors to apply to the design of nuclear power plant equipment.

The supporting structure (Reactor Building) and the equipment (Reactor) are modelled as a three-dimensional dynamic system. The building and reactor responses are calculated for realistic structural and equipment frequencies, subjecting the overall system to different design ground motions as well as real earthquakes records. Analyses were performed for a suite of earthquakes that represent the ground motions used in seismic design. For comparison with real earthquakes another suite of historical earthquakes was added. The earthquake ground motions were applied to a Reactor Building three-dimensional model. The equivalent numbers of cycles for the input ground motions are calculated. The response time histories for the reactor building are calculated as well as the equivalent number of cycles. By subjecting the three-dimensional model of the reactor to the building motions, the equivalent numbers of cycles for reactor components are obtained.

¹ CANDU® is a registered trademark of Atomic Energy of Canada Limited.

The paper reviews codes and standards related to seismic fatigue analysis being practiced in the nuclear industry, with a focus on the number of the equivalent full stress seismic cycles. Particular attention is given to the application of the ASME design fatigue curves. Based on the results of the new time-history analyses performed for CANDU reactor systems, recommendations related to the number of seismic stress cycles are given for seismic qualification of CANDU equipment, piping and their supports. The paper concludes that 25 cycles for seismic fatigue analysis is adequate for all applications. The current practice of using 200 cycles for fatigue analysis (e.g. piping is excessive).

The results of the current work should help the justification for additional life for existing plants and cost effective design for new plants and systems by the use of realistic number of cycles in seismic fatigue analysis.

Case study: seismic Soil-Structure-Interaction analysis for a site with varying soil thickness (5-1776)

Alidad Hashemi¹, Stephen Kadysiewski²

¹Senior Engineer, PhD, PE, Bechtel National, 50 Beale St
San Francisco, CA, USA, e-mail: sahashem@bechtel.com

²Senior Engineer, SE, Bechtel National, 50 Beale St, San Francisco, CA, USA
e-mail: sjkadysi@bechtel.com

Seismic responses of structures are significantly influenced by Soil-Structure-Interaction (SSI) effects. These effects are more pronounced for stiff structures typical of the nuclear industry on relatively soft soil sites and must be included in any viable structural analysis. Generally, SSI analyses are computationally costly and detailed modeling of the structure and site conditions are often not practical. Therefore, a number of modeling simplifications are needed prior to proceeding with any SSI analysis. This paper addresses the viability of one such simplification for the case of a structure located on a soil profile with varying depth of soil and rock formations in the vicinity of the structure, i.e. ignoring the effects of slopped soil and rock formations. Implicit in this assumption is that a bounding analysis with hypothetical soil layer depths bounding the variation of the actual soil profile under the subject structure would envelop the seismic response of the structure.

The case study structure is a 58 ft high concrete shear wall structure with footprint of 71 ft × 136.5 ft located at surface on a layered alluvium and tuff (welded volcanic ash) soil site. The structural walls and slabs are 4 ft thick and are supported by a 6 ft thick mat foundation (locally increased to 13 ft thick). The alluvium depth under the structure varies from 30 ft to 60 ft along the longer dimension (with an azimuth of about 77.5 degrees) as shown by the contour lines in Figure 1.

The case study structure is modeled using 3-D finite element program SASSI 2000. The structural members (concrete mat, walls and slabs) are modeled using shell elements with approximately 5 ft × 5 ft mesh size. The variation of the alluvium depth under the structure is modeled by including a wedge of tuff modeled as FE solid elements protruding in the alluvium layers modeled as layered infinite horizons. The wedge is extended in plan in each direction by the corresponding dimension of the structure as shown in the plan view of Figure 1. The acceleration time-histories of the input ground motion (X, Y, and Z) corresponding to a 2000 year return period seismic event and consistent with strain-compatible soil properties for the site are applied at the foundation level of the structure, i.e. ground surface.

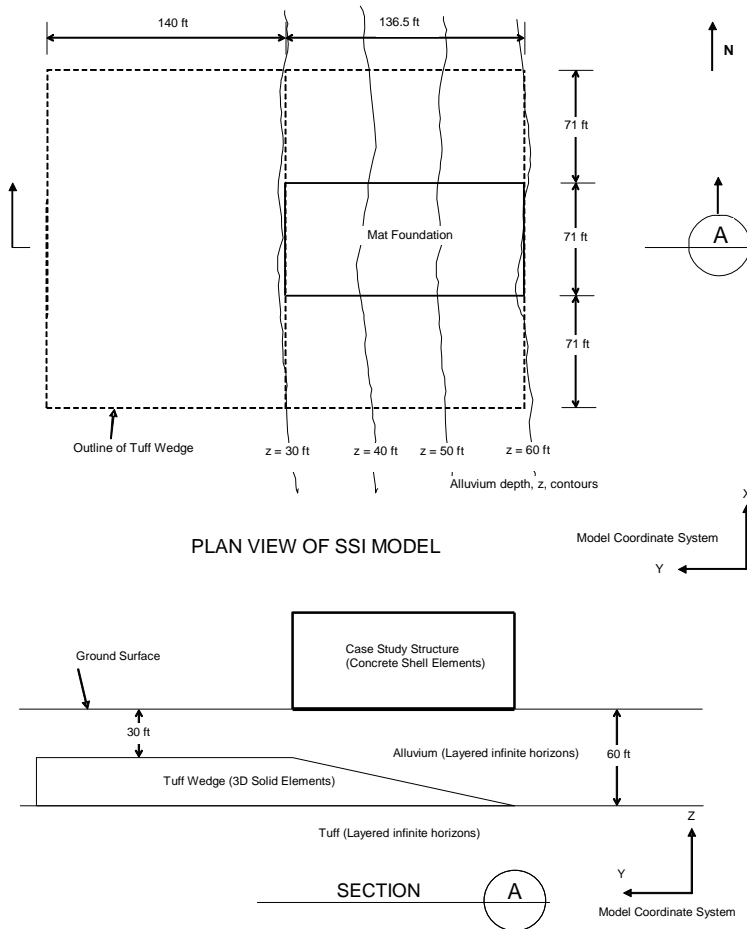


Figure 1. SSI model of the Case Study Structure.

In order to provide a valid basis for comparison between the sloping tuff model and results from horizontal alluvium and tuff models bounding the sloped site profile, it is necessary to create reference SASSI models for the case study structure. The structural portions of these models are identical to the structural portion of the sloping tuff model discussed above. One model assumes horizontal alluvium and tuff, with an alluvium depth of 30 ft, i.e. minimum depth of the tuff under the case study structure. The soil material property profile for this model is identical to the profile used in the free field sloping tuff model described above except that tuff properties are used from 30 ft to 60 ft depth. The other reference model also assumes flat alluvium and tuff, with an alluvium depth of 60 ft, which is the maximum depth of alluvium under the case study structure. The soil material property profile for this model is identical to the free field profile used in the sloping tuff model described above.

The results of the study are obtained in terms of 1) Transfer functions at different locations in the structure, 2) maximum roof and mat accelerations in three directions (X, Y, and Z) due to the input motion in three directions (X, Y, and Z) with special attention given to the horizontal torsional motion around a vertical axis and rocking motion around an axis in the sloping plane of the interface between alluvium and tuff layers, and 3) In-Structure Response Spectra (ISRS) obtained at different locations throughout the structure. These results are compared to the results obtained for the reference horizontal alluvium and tuff cases and the differences and limitations of the underlying assumption for typical bounding analyses are discussed.

Verification test for integrity of equipment foundations affected by dynamic load (5-1777)

Shuichi Orita¹, Nobuaki Oshima², Norihide Tohyama², Yoshihiro Orito³

¹Nuclear Asset Management Department, Tokyo Electric Power Company

1-3 Uchisaiwai-cho 1-chome Chiyoda-ku Tokyo, Japan

e-mail: orita.shuichi@tepcoco.jp

²Plant Design Department, Hitachi-GE Nuclear Energy, Ltd.

1-1, Saiwai-cho, 3-chome, Hitachi, Ibaraki, Japan

e-mail: nobuaki.oshima.sj@hitachi.com

³Nuclear Projects Division, Shimizu Corporation

No. 2-3, Shibaura 1-chome, Minato-ku, Tokyo, Japan

e-mail: orito@shimz.co.jp

In the design of equipment and pipe supporting systems for nuclear power plants of Japan, anchor bolts embedded in concrete structures are designed to conform with Japan Electric Association's guideline, which were established on the basis of experimental study. However, the tests were performed under static loads. The capacities of anchor bolts for dynamic loads, therefore, have not been confirmed experimentally. Because the seismic load is one of the dominant loads in the anchor bolt design, it is essential and important to verify the behavior and integrity of concrete anchoring portion for dynamic loads.

In this study, seismic tests of concrete anchoring portion installed in concrete slab of 1 m thickness were conducted, and these tests consisted of pull-out loading test, shear force loading test and actual equipment model test. Various models were installed on the same concrete slab on a shake table for the tests, and excited on it at a time. These models were planned to have various bearing capacities including relatively smaller capacity to investigate damage condition at anchoring portion, and shaking force was settled much larger than design acceleration level of nuclear power plants.

After seismic tests, concrete internal damages and residual pull-out strength were evaluated to confirm the influences on anchorage by dynamic loads.

The above seismic tests were performed in Hyogo Earthquake Engineering Research Center, E-Defense, of National Research Institute for Earth Science and Disaster Prevent.

From the result of pull-out loading test, internal cracks were found in a few models after the seismic test, however, no surface cracks appeared in any models. Test result showed that a lot of ratios of bolt pull-out forces to short term design allowable values ($III_{AS}: 0.45A_c\sqrt{F_c}$, A_c : Effective shear cone area, F_c : Specified compressive strength of concrete) were experimented. Even

though the pull-out forces loaded to many models beyond the design allowable values, no model collapsed by dynamic loads.

From the result of shear loading test, cut off of the anchor bolt was occurred in a model which the twice of design allowable shear force was loaded. Models affected by the load equal or under allowable value, slight pull-out of anchor bolts and flaking of concrete were occurred, no significant damage which affects the capacities of anchorage could be observed in tests for shear loading.

In actual equipment model test, representative foundation types were selected among those installed in Kashiwazaki-Kariwa nuclear power plant unit 7 (ABWR, 1356 MWe) operated by Tokyo Electric Power Company. Test models were fabricated so as to have the same structure with the representatives and set on the reinforced concrete slab. One of the test models are RHR (Residual Heat Removal System) heat exchanger model, which is one of most important systems. The model was of the same weight (about 330 KN) and of the same length with the representatives, and three times of shaking tests in total were conducted to the RHR test model, using different target waves each time including the Niigataken Chuetsu-oki Earthquake in 2007, and larger wave. Shaking waves were three dimensional wave, and maximum horizontal acceleration on the reinforced concrete floorboard was 18 m/s^2 which is 2.6 times of the actually observed strong motion at Kashiwazaki-Kariwa nuclear power plant unit 1 (KK-1) in the Niigataken Chuetsu-oki Earthquake in 2007. However, no visual damage could be found on the surfaces of concrete bases and anchor bolts.

As a result, it is confirmed that anchor bolts, which are designed in accordance with the existing Japanese design guidelines, have sufficient capacities even after application of dynamic loads.

References

- Japan Electric Association. Technical Guidelines for Aseismic Design of Nuclear Power Plants. Supplement, 1991.
- Ichihashi et al. Strength of Embedded Plates with Anchor Bolts in Nuclear Power Plants. Architectural Institute of Japan, Summaries of Technical Papers of Annual Meeting. Pp. 157–166, 1987. (In Japanese)

Fuel assembly two-beam dynamic model response to faulted condition loads (5-1780)

Sudhir J. Shah, Berenger d'Uston, Gary T. Williams
AREVA NP Inc., Fuel America
P.O. Box 10935, Lynchburg, VA-24506-0935, USA
(434) 832-2306 phone, (434) 832-2629 fax
e-mail: sudhir.shah@areva.com

Keywords: core structural seismic model

Current analytical faulted core models used to analyze seismic or Loss-of-Coolant Accident (LOCA) are built by means of one equivalent beam per assembly. In this paper the fuel assembly is modeled with two beams, utilizing the rudimentary finite element technique of grouping items with common properties as they would exhibit common behaviors. Hence, the two-beam fuel assembly model provides more realistic internal forces for the subsequent stress analysis of the fuel assembly components. With the "two-beam" linear model it is possible to benchmark more closely to both the first natural frequency and lateral stiffness, since it represents the more realistic internal connections and boundary conditions. Also the two beam model allows analysts to predict the fuel assembly analytical lateral impact test results closer to the test results and eliminates the need for the representation of the internal stiffness of the grid. Lastly the two-beam model is a good base for any further development, particularly for introducing the non linear rod to grid mechanical behavior.

In the paper, the two-beam-per-assembly model is briefly discussed first and then results of a seismic study for a row of assemblies are addressed. The model is excited by input acceleration at its boundaries. Specifically these boundaries are the lower and upper core plates at the time-history of the core supporting plates. These input data come from the reactor system analysis.

Analytical study on seismic energy balance of NPP buildings. Part 1. Formulation and validity of lattice model (5-1781)

Shigeru Furukawa¹, Michiya Kuno¹, Ryu Shimamoto¹
Minoru Kanechika², Haruhiko Kurin², Yoshinori Mihara²

¹Chubu Electric Power Co., Inc., Nagoya, Japan

²Kajima Corporation, Tokyo, Japan

Introduction and aim of the work

Recently in Japan, there have been many earthquake records with large amounts of acceleration data. It is important to evaluate the nonlinear behavior of buildings under these large earthquake ground motions. To understand the non-linearity of the seismic response model, it is necessary to quantitatively evaluate the seismic energy flow by the effect of damping, plasticity and soil-structure interaction in addition to the conventional approach focusing on maximum response values.

However, there have been few studies, e.g., Yang et al. (2000) and Mizutani et al. (2006), on seismic energy balances with soil-structure interaction for massive structures such as nuclear reactor buildings of NPP, compared to those on high-rise buildings with vibration control systems.

Thus, the objective of this study is to develop and verify a method for evaluating the seismic energy balance for nuclear reactor buildings of NPPs using the so-called advanced lattice model with soil-structure interaction proposed by Hiraki et al. (2007). Furthermore, it is aimed to provide clear data for aseismic design.

Essential results

In this paper, Part 1, seismic energy balances is formulated for a lattice model. In particular, methods for evaluating soil dissipation energy and building damping energy are studied and compared with other soil-structure seismic response models such as the sway and rocking model (SR model). It is thus shown that the seismic energy balances for the lattice model correspond closely to those of the SR model which has been already studied by Yang et al. (2000) and Mizutani et al. (2006).

Next, the proposed methods are theoretically validated in both soil parts and building parts, which are the components of the lattice model.

In conclusion, a new method for evaluating the seismic energy balance for the lattice model is proposed and theoretically validated by comparison with results obtained from the SR model.

Conclusion

Based on previous research, a new method for evaluating seismic energy balance for a lattice model is proposed and theoretically validated by comparison with the SR model.

References

- Yang, Z., Akiyama, H. 2000. Evaluation of soil-structure interaction in terms of energy input. Journal of structural and construction engineering. Transactions of AIJ, No. 536. Pp. 39–45.
- Mizutani, M., Akiyama, H. et al. 2006. Evaluation of effective energy input to a structure considering soil-structure interaction. Journal of structural and construction engineering. Transactions of AIJ, No. 601. Pp. 43–51.
- Hiraki, T., Onouchi, A. 2007. Study on a Seismic Response Analysis Model of Nuclear Reactor Buildings – Study on an Advanced Lattice Model. 19th International Conference on Structural Mechanics in Reactor Technology (SMiRT19), Toronto, Canada, K03-4.

Dynamic interaction between the shaking table and the specimen during earthquake tests (5-1783)

Le Maout Alain¹, Bairrao Rogerio², Queval Jean-Claude³

¹CEA/DEN/SEMT/EMSI, 91191Gif Sur Yvette Cedex, France

e-mail: alain.lemaout@cea.fr

²LNEC/DE/NESDE, Av. do Brasil 101, 1700-066 Lisboa, Portugal

e-mail: bairrao@lnc.pt

³CEA/DEN/SEMT/EMSI, 91191Gif Sur Yvette Cedex, France

e-mail: jean-claude.queval@cea.fr

The improvement of shaking table technologies is clearly of paramount importance to reduce the seismic vulnerability of the building stock and also to mitigate the consequences of future, and inevitable, seismic events by contributing significantly to the amelioration of new construction techniques.

Much advancement is on progress among the members of the European consortia of earthquake engineering laboratories (Bairrao et al., 2006) and the more important needs of the experimental facilities were already identified in detail (Taucer et al., 2005). Concerning specifically the shaking tables facilities, the improvement of two technologies has priority: Real-time Control and Sub-structuring. The current advantages of a real-time control are well known, but that technology will be absolutely necessary to follow the sub-structuring technique developments.

The global capacities of the biggest European shaking tables are very moderate when compared with the ones of the more recent Japanese laboratories. Therefore the shaking table test of real and very large structures is not foreseen in Europe for the near future. Consequently, the use of sub-structuring techniques must be developed in order to fix to the simulator platform just a part of the structure while all the remainder will be tested on computer, like in the pseudo-dynamic testing procedure (Bairrao, 2008).

To use this technique in shaking table tests it will be need a real-time control and an indeed very high speed of the data transfer between the control system of the shaking table and the computer system modelling the numerical part of the experiment.

Another very important need in shaking table testing is a comprehensive study about the interaction between the dynamic characteristics of the facilities (the platforms and all the hydraulics systems) and the specimens during the experiments. In fact, since quite a long time (Blondet and Esparza, 1988), that interaction has been clearly observed whenever the mass of the specimen

becomes too big when compared with the one of the shaking table platform (Combesure and Ragueneau, 2002).

In this paper the specimen/structure interactions observed in the platforms and all the hydraulic systems of the shaking table facilities of CEA (France) and of LNEC (Portugal) will be discussed. Moreover, the developments under progress will be presented.

References

- Bairrao, R. Shaking Table Testing. Chapter of the book "Modern Testing Techniques for Structural Systems". (2008). Editors O.S Bursi, D.J. Wagg. Publisher Springer Verlag. pp. 165/196. (ISBN-978-3-211-09444-0).
- Bairrao, R., Falcao, M.J., Carydis, P., Mouzakis, H., Karapitta, L., Queval, J.C. Performance Benchmark of Three Major European Shaking Tables. 13th European Conference on Earthquake Engineering, paper 110, Geneva, Switzerland (September/2006).
- Blondet, M., Esparza, C. Analysis of Shaking Table-Structure Interaction Effects during Seismic Simulation Tests. Earthquake Engineering and Structural Dynamics, Vol. 16, pp. 473/490 (1988).
- Combesure, D., Ragueneau, F. CAMUS2000 Benchmark. Experimental Results and Specifications to the Participants. (2002). Report CEA/SEMT/EMSI/RT/02-067/A.
- Taucer, F. (Editor). Severn, R., Bairrao, R. (General Editors). Recent Advances and Future Needs in Experimental Earthquake Engineering. CASCADE – Cooperative Advancements in Seismic and Dynamic Experiments, report No. 7 (2005). Publisher LNEC (ISBN-972-49-1971-4).

Comparison of approximate methods for sliding and rocking evaluation of unanchored platforms (5-1784)

Sohrab Esfandiari¹, Christopher Wandell²

¹ENOVA Engineering Services, Walnut Creek, California, USA

²Arizona Public Service Company, Tonopah, Arizona, USA

There are many unanchored structures in use in commercial nuclear power plants. Most widely used are scaffolding frames which are erected and dismantled in support of various projects mostly during plant outages. In general, unanchored structures are not safety related and are of no safety concern unless Seismic Category 1 SSCs (Structures, Systems, or Components) are present in their zone of influence. For such situations, the stability of the unanchored bodies under a seismic event must be checked to ensure that adverse interaction between the source (the unanchored structure) and safety related targets, does not occur. This phenomenon is commonly referred to as “II over I” interaction, “Seismic separation” or “Zone of influence” interaction. The issues of concern for seismic stability of an unanchored body, are typically the extent that it could slide, as well as maximum angle of rotation associated with rocking of the body and eventual potential for tip-over (thus, instability).

At the Palo Verde Nuclear Generating Station (PVNGS), the Spent Fuel Dry Cask loading operation in the Fuel Handling building utilizes 3 separate platforms which are essentially designed to provide support for personnel and equipment. These platforms are portable and are moved by the building crane into position during the campaign. When not in use, these platforms are stored in an area, which is within the zone of influence of safety related systems. As such, their stability under the plant SSE seismic event must be ensured. Therefore as a prudent part of the design process, the sliding and rocking of these platforms is checked to ensure that adverse interactions are avoided and that sufficient clearance is provided in their permanent storage configuration.

Since the stability evaluation of unanchored bodies is a non-linear phenomenon, this problem can only be accurately solved by performing non-linear time history analysis of the platform allowing for proper geometric non-linearity at the contact interface. However, this solution requires the development of multiple time histories which typically do not exist for in-structure elevations of nuclear plant structures. As such, most engineers use the approximate sliding method developed by Newmark for sliding of structures, as well as approximate energy balance method for evaluation of rocking and instability of unanchored bodies. Recently a newer more accurate method which utilizes in-structure spectra as the source of seismic demand was published in

ASCE/SEI 43-05. Since this approach utilizes plant spectra, it presents a good alternative to time history analysis for performing such stability evaluations.

This paper summarizes the methodology and the results of performing such stability analyses for the 3 unanchored platforms which are used in support of Dry Cask loading operations at PVNGS. The methodology is based on the procedure outlined in ASCE/SEI 43-05 for sliding and rocking of unanchored bodies. For comparison purposes, the results of seismic stability analysis of one of the platforms is also presented using the more traditional Newmark method for sliding, as well as the conventional energy balance method for rocking.

Effects of liner degradation on the severe accident consequences at a PWR plant with a reinforced concrete containment (5-1786)

Jason P. Petti¹, Donald A. Kalinich¹, Joonyub Jun¹, Herman L. Graves III²

¹Sandia National Laboratories

P.O. Box 5800, MS 0744, Albuquerque, New Mexico, USA

e-mails: jppetti@sandia.gov, dakalin@sandia.gov, jjoonyu@sandia.gov

²U.S. Nuclear Regulatory Commission, Washington, DC, USA

e-mail: Herman.Graves@nrc.gov

Various forms of degradation have been observed in the containment vessels of a number of operating nuclear power plants in the United States. Examples of degradation include corrosion of the steel shell or liner, corrosion of reinforcing bars and prestressing tendons, loss of prestressing, and corrosion of bellows. The containment serves as the ultimate barrier against the release of radioactive material into the environment. Because of this role, compromising the containment could increase the risk of a large release in the unlikely event of an accident. Previous work in this area has assessed the effects that degradation has on the pressure retaining capacity of the containment vessel through structural analysis that account for degradation. These analyses have provided useful information about the effects of the degradation on the structural capacity of the containment in both a deterministic and probabilistic fashions. However, the appropriate metric to use in assessing containment degradation effects during a severe accident was determined to require additional study. The previous work with probabilistic descriptions of the containment capacity were obtained from the results of the structural analysis models, and used as input for the risk models (PRA analyses). The risk was formulated in terms of the large early release frequency (LERF). The relative LERF values were computed for various postulated cases of degradation. In that study, an instance on degradation was treated as a change in the plants license basis and assessed with U.S. NRC Regulatory Guide 1.174. The Reg. Guide provides the limits of the acceptable increases in LERF due to changes in the plant. Many cases of postulated degradation were those consisting of local corrosion in the liner or shell that produce leaks that do not contribute significantly to LERF, and in come cases, cause no change in LERF. Early releases due to small leaks were found to contribute to the small early release frequency (SERF). Since Reg. Guide 1.174 does not provide guidance on the limits SERF, additional deterministic analyses were performed in this study to assess the effects of degradation on the

consequences beyond LERF. These analyses were performed using the Sandia codes MELCOR and WinMACCS. These codes were used to simulate two different accident scenarios (long- and short-term station black-outs) and compute the resulting consequences for a PWR plant with a reinforced concrete containment. The structural analyses used in the previous probabilistic study were used to develop the containment behavior models for the accident simulations. Several different postulated cases of liner corrosion were considered to enable a comparison of the consequence.

High energy pipe rupture effects elimination – experience from projects dealing with WWER 440 V2 NPP piping assessment (5-1787)

Miloslav Hrázský¹, Ivan Lopoš², Milan Mikuš³

¹VUJE, Inc., Okružná 5, 91864 Trnava, Slovak Republic, hrazsky@vuje.sk

²VUJE, Inc., Okružná 5, 91864 Trnava, Slovak Republic, lopos@vuje.sk

³VUJE, Inc., Okružná 5, 91864 Trnava, Slovak Republic, mikusM@vuje.sk

Introduction

The general construction criterion requiring the separation of high energy pipings was not fully respected during the design of WWER 440 NPP type units. Arising problem of the elimination of effects of potential high energy pipe rupture was not thoroughly covered by the original design.

Accelerated development of knowledge and the growth of operational experience facilitated general innovation of procedures applied in this area originally. New sophisticated procedures and methods occurred and were applied on Slovak WWER 440 NPP high energy pipings including V2 NPP ones gradually.

The aim of work

The main aim of our paper is to demonstrate basic results and problems connected with the application of high energy pipe rupture effects elimination methods on the example of recent V2 NPP analyses.

In principle there are two solutions available for the purpose of of high energy piping rupture effects elimination. The first one is based on the verification of extremely low probability of piping rupture. This procedure is well known as LBB status validity assessment too. LBB status validity evaluation procedure for given piping systems is based on extensive analyses containing piping static and seismic calculations, fracture mechanics calculations and leak calculation from postulated cracks. Moreover granting LBB status to assessed piping is possible only under the condition three independent systems for the detection of leaks from piping are operating in NPP.

The second possibility for high energy pipe rupture effects elimination is based on the design and the realization of technical construction measures, which prevent effectively from negative effects of postulated rupture in given piping locations. In the first step stress analyses in normal operation conditions and at operating base earthquake (OBE) are performed and locations of rupture

postulation are determined on the basis of conservative criteria. The second step is the determination of consequences, which result from the pipe rupture. Effects of a fluid jet impingement from the postulated pipe rupture location, pipe whip effects on nearby structures, components and safety equipment, which can be affected, shall be assessed. Corresponding specific construction modifications have to be developed in the third step in each case taking into account main factors like mass inertia and stiffness properties of the system, impact and rebound, elastic and inelastic deformation of piping and restraints, carrying capacity of supports and acceptable reaction forces on building structure.

Essential results

Both of above mentioned methods for high energy piping rupture effects elimination have been utilized for Slovak WWER 440 NPPs pipings, including V2 NPP pipings, in the past. LBB procedure was applied in case of MCP (including pressurizer surge lines) based on repeated positive “home” experience and considering necessary technical conditions to carry out such assessment. The second alternative method for high energy piping rupture effects elimination was utilized for other high energy pipings located inside confinement.

Conclusions

Application of methods for high energy piping rupture effects elimination has been necessary with a view to ensure basic safety of Slovak WWER 440 NPPs. Two applied methods differ both in the range and content of assessment means and in the resulting technical measures too. Regardless of great advantages arising from their application, several partial steps or detail procedures of both methods were found not sufficiently defined in available guideline documents. Improper application of such steps would be able to result not only in negligible effects on outputs in some cases.

References

NUREG 0800 Standard Review Plan (SRP), Chapter SRP 3.6.3, US NRC

Requirements for arrangement and content of safety reports and their appendixes. Procedure for evidence of leak before break status. Detection systems of the leakage from the pressure cooling circuit of nuclear reactor. CSKAE, 1/1991, UJI Praha-Zbraslav.

M. Hrázský, P. Hermanský, I. Lopoš. Application of the LBB method applied to MCP and pressurizer surge lines of NPP V2 in the status after reconstruction, MODV2/M04.02/PS/0098/V0350/MI, 2003.

5. Modeling, Testing and Response Analysis of Structures, Systems and Components

NUREG 0800 Standard Review Plan (SRP), Chapter 3.6.2. Determination of Rupture Locations and Dynamic Effects Associated with the Postulated Rupture of Piping. US NRC.

NRC Generic Letter 87-11 including revised MEB 3-1 of SRP 3.6.2 from June 1987.

BTP MEB 3-1, Postulated rupture locations in fluid system piping inside and outside containment, revision 2, June 1987.

ASME Boiler and Pressure Vessel Code, Section III.

ANSI/ANS 58.2-1988, Design Basis for Protection of Light Water NPPs against Effects of Postulated Pipe Rupture.

I. Činčura, I. Lopoš.: Determination of postulated pipe rupture locations for selected high energy pipelines inside confinement of NPP V2 unit 3 and unit 4, VUJE, MODV2/V04.02/PS/0142/V0350/ČI, 2004.

I. Činčura, I. Lopoš. Minimization of postulated pipe rupture locations for selected high energy pipelines inside confinement of NPP V2 unit 3 and unit 4, VUJE, MODV2/V04.02/PS/0207/V0350/ČI, 2006.

I. Činčura, I. Lopoš, M. Krajčovič. Functional pipe whip restraints design for selected high energy pipelines inside confinement of NPP V2 unit 3, VUJE, MODV2/M04.02/TDVZ/5217/V0350/ČI, 2006.

I. Činčura, I. Lopoš, M. Krajčovič. Functional pipe whip restraints design for selected high energy pipelines inside confinement of NPP V2 unit 4, VUJE, MODV2/M04.02/TDVZ/5117/V0350/ČI, 2006.

Stress analysis criteria for piping. RCC-M 2002 rules and validation (5-1790)

Le Breton Francis, Petesch Cécile
AREVA, Paris La Defense, France
e-mail: Francis.LeBreton@Areva.com

Introduction/background

In situ or laboratory tests have shown the very good behavior of piping systems under seismic loads. Seismic movements do not significantly damage piping systems unless large differential anchor motions are applied. Nevertheless, severe piping design criteria lead to require a large number of supports which overly rigidify the piping systems and reduce overall safety.

During the eighties and nineties, many R&D programs have been devoted to seismic design of piping systems. Common objective of these programs was to reduce the current conservatism, using different means: higher damping values (PVRC, from 2% to 5%), higher design stress limits (ASME, from $3 S_m$ to $4.5 S_m$), lower stress indices (RCC-MR). All these different approaches were not totally accepted: 5% damping is a mean value of an experimental data base with very scattered results, ASME equations enhanced limits were not accepted by NRC, RCC-MR stress indices are not used by other Design Codes.

So some R&D programs are still going on, in order to reach sounder and more justified conclusions. The aim is to reduce the difference between real behaviors and codified design methods. Criteria are applied on elastically calculated behaviors that are significantly different from real ones: the effect of plasticity is considerable, even with low incursion in the plastic domain.

New RCC-M rule

A new rule was included in the 2002 addendum of the RCC-M code for stress classification of seismic loads in piping systems stress analysis. It allows the application of a reduction factor on the elastically calculated seismic moment in order to quantify its primary part which shall be introduced in the stress limitation equations.

In linear response spectrum analysis using widely broadened spectra, with an usual low damping ratio ξ (between 2% and 5%), the primary part M_E of elastic resultant moment M_{Dyn} can be determined by :

$$M_E = \tau M_{Dyn} \text{ with } \tau = \sqrt{\xi / 10} .$$

This reduction factor is a behavior coefficient, similar to those used in structural design codes. It is equivalent to the use of elastic spectra with an additional damping value or to the use of inelastic spectra. For a damping ratio from 4% to 5%, the reduction factor applied to the seismic loads is close to the reduction factor on stress indices included in the current ASME code.

The main piping frequencies shall be located below or in the high amplification zone of the seismic spectra, in no case higher than twice the main frequency of the seismic excitation, otherwise the response is rather quasi-static and the acceleration loading becomes close to a primary loading.

R&D validation

The R&D actions have quantified available margins under seismic loadings and evaluated alternative criteria, in particular the behavior under mechanical fatigue-ratchet mechanism, based on seismic tests (ELSA and ASG). Equations in piping design codes for faulted loading conditions are compared and applied to these piping test results.

Available R&D results validate the new RCC-M 2002 criteria for seismic design of piping, where elastic moment limitation was only slightly reduced, as in the ASME code 1995/2004 editions. The application of the new rule with level D criteria gives allowable loads two times lower than allowable loads in piping tests. The new criteria have also been validated by non linear calculations on more industrial cases. Some consequences of the criteria modification have been studied: design modification, in particular the number of supports, global displacements, loads on supports.

Conclusions

Stresses resulting from dynamic loads have only partly a primary character and RCC-M 2002 addendum has introduced a formula defining the primary part of dynamic earthquake loads. This new rule provides margins in piping analysis still larger than two. The industrial practice as codified in the 2002 addendum remains consequently severe.

Further code evolution should include more detailed guidance for stress classification of loads resulting from applied controlled displacements, for seismic loadings or restraint of thermal expansion. Additional limitations may appear appropriate in view of facilitating the justification of potential defects. Enhanced and simplified calculation methods should be developed in order to take into account the beneficial plasticity effect on actual piping loads, for crack assessment, or on global displacements, for functional verification.

References

RCC-M Code, B-C 3600. Design and Construction Rules for Mechanical Components of PWR Nuclear Islands. 2000 Edition plus 2002 Addendum.

ASME Code, Section III Division 1, NB-NC 3600. Rules for Design and Construction of Nuclear Facility Components. 2004 Edition.

F. Touboul et al. French Program on the Seismic Behavior of Piping Systems. PVP Conf. 1999.

Vibration tests on nuclear power station stacks equipped with structural control oil dampers (5-1792)

Haruhiko Kurino¹, Ryu Shimamoto², Fukashi Mori³, Tomonori Kitaori³,
Satoru Aizawa⁴, Yukio Naito¹

¹Kajima Corporation, Tokyo, Japan

²Civil & Architectural Engineering Dept., Chubu Electric Power Co., Inc.
Nagoya, Japan

³Hamaoka Nuclear Power Station, Chubu Electric Power Co., Inc.
Shizuoka, Japan

⁴JFE Engineering Corporation, Tokyo, Japan
e-mail: kurino@kajima.com

Introduction and aim of the work

This paper presents forced vibration tests conducted on 100 m-high steel stacks at Hamaoka Nuclear Power Station, whose seismic margin has been widely enhanced through an upgrading project using structural control techniques. Three stacks are considered in this project. A new target earthquake load, which is much stronger than the original design loads, was set up for this project. The original stacks were designed as self-standing without any supporting frames, and we first examined the possibility of conventional reinforcement by building up a new supporting truss-tower around the existing stack. However, it became apparent that several difficult problems would remain unsolved with such a simple technique. Thus, we planned to link each stack with a supporting tower via oil dampers to improve the structural damping as well as the strength. The estimated damping ratios come up to about 10%, and remarkable response reduction effects were displayed by numerical analyses. This project has become the first full-scale application of structural control to an actual nuclear power station facility in Japan. The details of the project were discussed in the paper submitted to the last conference. [1]

Essential results

In order to examine the dynamic characteristics of the stacks with the oil dampers, forced vibration tests were carried out just before project completion. Since large structural damping is expected (about 10%), and at least a few millimeters of stroke should be generated in the damper portion to avoid an undesirable effect of a friction force of the oil damper between the piston and the cylinder, a large

excitation force was required in this test. We set three slide-mass-type exciters on the top level of the supporting tower (maximum force about 50 kN when the three exciters work together). Although the observed displacement at the top of the stack was about 10 mm, which is much smaller than the response to the target earthquake, damping ratios of 8 to 9% were recognized from the test results. In addition, it was confirmed that the test results could be well simulated by the numerical model used for seismic design.

Conclusion

This paper first describes the specification of the stack with oil dampers, and presents the results of the vibration test. Next, it presents simulation results and discusses the control effect of the oil dampers.

References

1. R. Shimamoto et al. Seismic-upgrading of Existing Stacks by Structural Control using Oil Dampers. Transactions, SMiRT 19, Toronto, August 2007, Paper # K17/1.

Performance based capacity assessment of WWER-1000 containment structure for internal accidents (5-1807)

Anton Andonov¹, Dimitar Stefanov², Marin Kostov³

¹Risk Engineering LTD., 10, Vihren Street, 1618 Sofia, Bulgaria
e-mail: Anton.Andonov@riskeng.bg

²Risk Engineering LTD., 10, Vihren Street, 1618 Sofia, Bulgaria
e-mail: dstefanov@geophys.bas.bg

¹Risk Engineering LTD., 10, Vihren Street, 1618 Sofia, Bulgaria
e-mail: Marin.Kostov@riskeng.bg

Introduction

An essential component of the nuclear power plant safety is the capacity of the containment shell structure. The containment has to prevent the reactor installation from external impacts as well as to provide a tide physical barrier against release of radioactive materials during and after severe internal accidents. The standard procedure for containment capacity assessment is connected with derivation of its ultimate capability, failure mode and ultimate leak tightness by using finite element analyses. In the recent years sufficient progress was made in this direction including verification of the numerical techniques with experimental results. The work is summarized in [3, 4] and in many papers in SMiRT 18 and SMiRT 19.

Aim of the work

It is recognized that the containment ultimate conditions as structural integrity and leak tightness are preceded by increasing intensity of cracking (at the concrete) and plastic strains (at the liner). Furthermore, the recent regulatory provisions [1, 2] recommend the design or the assessment of the containment structures should be based on different limit states or performance levels, correlating the structural response with the loading intensity. Therefore different performance criteria are required for the different loading conditions. Also the performance criteria differ for existing structures and new design.

The standard capacity assessment procedure is based on finite element simulation of the structural response due to particular set of internal pressure and temperature loadings derived from the thermo-hydraulic analyses and assessment of the structural integrity and leak-tightness. The computed in such way structural response is loading dependent and therefore if some modifications

of the loading histories occur in the future (change of the mechanical layout, improvements in the thermo-hydraulic models and codes and etc.) the calculations should be repeated. Furthermore, if the structure does not lose integrity under these particular accident loading sets, its ultimate capacity will remain unknown. Instead of this, at the presented approach, a direct procedure for capacity assessment, in terms of structural integrity and leak tightness is proposed and corresponding to different limit states or performance levels and without referring to particular loading history. In such way the computed capacity is function only of the structural strength and ductility. The assessment of the structural response to particular accident loading is based on graphical comparison between the structural capacity and the loading intensity by plotting both parameters at the same “temperature gradient – overpressure” coordinate system and is further development of the work presented in [6].

Essential results

The capacity in terms of structural integrity and leak tightness, corresponding to different limit states or performance levels is evaluated. For the purpose, the ultimate pressure capacity and the pressure response corresponding to different performance levels is calculated using finite element approach. The influence of the temperature loading on the structural response and capacity is also studied and the main failure mode and the critical zones of the structure are derived. A new damage index is proposed in order to correlate the intensity of damages at the shell structure with the intensity of the loading. The criteria for leak tightness and structural integrity are adopted for WWER-1000 structure.

Conclusions

Integrated multi level capacity assessment depending on both the internal overpressure and the temperature gradient is performed. The capacity is represented as envelopes in “temperature gradient – overpressure” coordinate system. The structural response to particular internal accident loading is assessed by graphical comparison between the loading intensities and the capacity envelopes, plotted at the same format. The obtained results from the performed assessment are compared with the results obtained by direct simulation of particular overpressure – temperature loading sets and good comparison is found.

Conclusions for the WWER-1000 overpressure capacity and its response to different design basis and severe accidents are drawn. The effect of the temperature loading, the main failure mode and the critical zones of the structure are also commented.

References

1. European Utility Requirements for LWR Nuclear Power Plants, 2002.
2. Design of Reactor Containment Systems for Nuclear Power Plants, Safety Guide, No. NS-G-1.10, IAEA, Viena, 2004.
3. Hessheimer, M.F, Klamerus, E.W., Lambert, L.D., Rightley, G.S., Dameron, R.A. Overpressurization Test of a 1:4-Scale Prestressed Concrete Containment Vessel Model, NUREG/CR-6810, SAND2003-0840P, Project Report No. R-SN-P-010, March 2003.
4. Hessheimer, M.F. (ed.). International Standard Problem No. 48 Containment Capacity, Phase 2 Report, Results of Pressure Loading Analysis. NEA/CSNI/R(2004)11, OECD Nuclear Energy Agency, Committee on the Safety of Nuclear Installations, Issy-les Moulineaux, France, July, 2004.
5. SOLVIA Finite Element System, Version 03, Uuser Manual, SOLVIA Engineering AB, Vasteras, 2003.
6. Kostov, M., Todorova, Ts., Andonov, A. Ultimate Capacity Assessment Of VVER 1000 Containment Structure, Proc. Of the 19th International Conference on Structural Mechanics in Reactor Technology (SMiRT 19), Toronto, Canada, August 2007.
7. Analysis of the Engineering Reliability and Assessment of the Maximum Strength of the Containments of the 5th and 6th Blocks of "Kozloduy" Nuclear Power Plant, Project Report, Risk Engineering Ltd., Sofia, Bulgaria, 2007.
8. Probabilistic Safety Analysis level 2 of Unit 5 of "Zaporozie" Nuclear Power Plant, Project Report, Risk Engineering Ltd, Sofia, Bulgaria 2007.

Seismic analysis of WWER–1000 control rod drive system (5-1810)

Leonid Lakishev¹, Alexander Schukin², Maxim Vayndrakh²

¹FSUE OKB “GIDROPRESS”

142103, Moscow district, Ordzhonikidze str., 21, Podolsk, Russia

e-mail: lla@grpress.podolsk.ru

²“CKTI-VIBROSEISM” Co. Ltd.

195220, Gzhatskaya str., 9, St.-Petersburg, Russia

e-mail: sasha@cvs.spb.su

This paper presents a seismic analysis of control rod drive (CRD) system of NPP with WWER-1000 type reactor.

One of the most important requirements to CRD is reliable control of its response in case of emergency signal in all operational conditions including seismic dynamic impact.

It is assumed that during seismic impact reactor operates in the normal mode. If intensity of earthquake is equal or greater than OBE a shutdown of reactor is needed. Therefore, the most important requirement in respect to the nuclear safety of NPP during strong earthquakes is reliable control of the rod insertion in the reactor core. As result of seismic impact an insertion time of the control rods in reactor core could be delayed due to non-linear effects between falling rods and channel's clearances and the bending of channel.

Hence, the basic parameter that determines seismic capacity of WWER-1000 CRD System is rod's insertion time in AZ mode.

Seismic loads in the form of accelerograms corresponding to the top of reactor have been applied to CRD for analysis of its seismic resistance. Nine sets (X, Y, Z-components in each set) of time histories were used for CRD insertion time estimations:

- SSE-1 – with dominant frequencies in the range of 2–4 Hz;
- SSE-2 – with dominant frequencies in the range of 4–6 Hz;
- SSE-3 – with dominant frequencies in the range of 5–8 Hz.

For all above mentioned seismic inputs a variation of soil conditions was considered for “soft”, “medium” and “hard” soil.

Off-axis underground soil pressures from surface impact loads (5-1811)

W. Johnson, N. Akinci

Bechtel Power Corporation, Frederick, Maryland, USA

The heavy rigging operations necessary at nuclear plant sites during construction, routine maintenance, and special activities such as steam generator replacement require assessment of safety related buried utilities for the effects of postulated accidental impact loads in the form of dropped loads, crane boom drops, etc. The conventional system response methodology is to estimate the free-field wave motion resulting from the surface impact loading, to apply these free-field soil motions to the buried pipeline or duct bank and to determine the structural response using methods such as those available in [1, 2]. Published solutions for this response emphasize the special and more mathematically tractable cases of either the soil surface response at distance from the impact or the on-axis soil response at depth directly below the location of impact. This investigation considers the analysis for the general off-axis, below surface response.

In principle, the free field, off-axis, sub-surface soil response can be approximated by solving the linear problem for the dynamic response of an elastic half-space to a time dependent impact loading $p(r)F(t)$, either by analytical solution of the partial differential equation formulation or by an axisymmetric finite element solution. These approaches, for application to design, compound a number of difficulties. Firstly, development of the impact loading function requires address of the soil local material nonlinearity. Given the loading function, general analytical solutions must numerically invert the Laplace-Hankel transform, a formidable task, requiring either numerical complex integration with extremely refined localized meshes at singularities or the numerical evaluation of numerous real integrals. Such solutions have been published in the literature [3, 4], but only for special and limiting loadings (step functions) and for specific response locations (surface or on-axis). In some cases, the simplifying assumptions required to achieve a solution, render the results (such as infinite velocities for finite loadings) unsuitable for design application.

This investigation provides parametric results for estimation of the off-axis free-field response at arbitrary locations below the ground surface based on non-dimensionalized elastic half-space dynamic transient finite element solutions. The results, developed using the LSDYNA finite element software, are benchmarked with known analytical results for the limiting cases at the surface and on-axis (beneath the loading). Triangular and rectangular temporal pulses of constant amplitude over a small circular impact area are considered. The non-

dimensionalized responses are presented as a set of design charts which relate missile energies and geometries to soil stresses. Guidelines, based on empirical penetration formulae are provided for development of the applied surface impact loads. Application of the results are demonstrated through evaluation of the stresses in a buried pipeline.

References

1. McClellan, R.E. Ground Shock Effect of Soil Field Inclusions. *The Shock and Vibration Bulletin*, June 1984, pp. 203–208.
2. Yeh, G.K. Seismic Analysis of Slender Buried Beams. *Bulletin of Seismological Society of America*, Vol. 64, No. 5, October, 1974, pp. 1551–1562.
3. Eason, G. The Displacements Produced in an Elastic Half-Space by a Suddenly Applied Surface Force, *J. Inst. Math. Applics.*, 1966, Vol. 2, pp. 299–326.
4. Laturelle, F.G. The Stresses Produced in an Elastic Half-Space by a Normal Step Loading Over a Circular Area – Analytical and Numerical Results, *Wave Motion*, Vol. 12, 1990, pp. 107–127.

On the floor response spectra due to aircraft impact (5-1816)

Anton Andonov¹, Kiril Apostolov², Dimitar Stefanov³, Marin Kostov⁴

¹Risk Engineering LTD., 10, Vihren Street, 1618 Sofia, Bulgaria
e-mail: Anton.Andonov@riskeng.bg

²Risk Engineering LTD., 10, Vihren Street, 1618 Sofia, Bulgaria
e-mail: Kiril.Apostolov@riskeng.bg

³Risk Engineering LTD., 10, Vihren Street, 1618 Sofia, Bulgaria
e-mail: dstefanov@geophys.bas.bg

⁴Risk Engineering LTD., 10, Vihren Street, 1618 Sofia, Bulgaria
e-mail: Marin.Kostov@riskeng.bg

Background

The load case – aircraft crash, is not new in the nuclear power plant design. In Germany, it was introduced as design basis in the early 1970's concentrated on impact of military jet [3]. More recently, after the event of September 11 new activities were prompted in this direction but this time concentrated on the effects from large commercial aircraft impact.

Traditionally, the effects of an aircraft impact on a NPP reactor building are categorized into local and global. The local effects are related to the region of the impact and include spalling, penetration, perforation, scabbing and punching. The global effects are related with the complex structural response and include, overall axial, bending and shear effects in the structural elements, global stability and the induced vibration over the structure.

Depending of the type of impact one effects can prevail over the others. It is accepted that impacts of military jets are more demanding for the local response and are governing the local failure modes, while the impacts of commercial aircrafts control the global response and govern the floor response spectra.

According to the today state-of-the-art, the aircraft impact loading can be presented as load function [1] with corresponding impact area or by direct numerical simulation of two bodies with limited stiffness.

Aim of the work

The presented work is concentrated on the assessment of the floor response spectra due to impact of large scale commercial aircraft. The aircraft is presented by load function according to the Riera method [1]. The reactor building is represented by detailed spatial model taking into account the non-linear material behavior and soil-structure interaction. The basic goals are to perform parametric

study of the factors influencing the floor response spectra and to propose alternative approach for assessment of the damage potential of the induced vibrations. For the purpose series of non-linear time history analyses of complex spatial model are performed varying all significant parameters – mass and velocity of the aircraft, impact location, strength parameters of the concrete, soil stiffness, soil damping, material damping of the internal structure, thickness of the impact resistant wall. Afterwards, the influence of these parameters over the response spectra shape is investigated. Furthermore, a review of selected motion parameters, widely used in earthquake engineering is performed. The applicability of using parameters as Housner spectrum intensity (SI), Aires intensity (I_a), the root-mean-square acceleration (RMS accel.), the cumulative absolute velocity (CAV) and specific energy density (SED) in the vibration damage potential assessment is also done.

Essential results

As an initial step, envelope floor response spectra at representative levels obtained from different impact scenarios are compared. In such way, the influence of the impact location over the structural response is investigated. It was found, that the shape of the floor response spectra depends mainly from the frequency content of the input loading, the dynamic characteristics (mode shapes) of the sub-structure facing the impact (changing during the response due to accumulated damages) and the dynamic characteristics of the transmission path. Based on these results, a parametric study was performed for selected aircraft scenarios. The influence of the aircraft impulse (mass and velocity), the thickness (stiffness) and the reinforcement ratio (ductility and failure mode) of the impact resistant wall over the response is analyzed. The effect of the soil-structure interaction is also studied, varying the spring stiffness and damping. Also, sensitivity analysis for the chosen concrete strength parameters is performed. Finally, for chosen representative impact scenarios assessment of the damage potential of the induced vibrations is performed. The acceleration, velocity and displacement floor response spectra, together with representative node acceleration histories are used for calculation of specific “ground” motion parameters. Also, applicability of using response spectra in ADRS format (Acceleration – Displacement Response Spectrum) and the Capacity Spectrum Method [7] for indirect assessment of the equipment response is investigated.

Conclusions

Integrated assessment of the response of NPP reactor building under large aircraft impact is performed. Conclusions for the factors influencing the floor response spectra at the equipment locations are drawn. The applicability of alternative “ground” motion parameters for assessment of the vibration damage

potential is studied and subsequent conclusions are made. Procedure for indirect equipment capacity assessment is discussed.

References

1. Riera, J.D. On the stress analysis of structures subjected to aircraft impact forces. Nuclear engineering and design, Vol. 8, 1968, pp. 415–426.
2. Eibl, J. Airplane impact on nuclear power plants. Transactions of the 17th SMiRT, Paper J03-6, Prague, Aug. 2003
3. Henkel, F., Klein, D. Variants of Analysis of the Load Case Airplane Crash. Transactions of the 19th SMiRT, Paper J03-2, Toronto, Aug. 2007.
4. Mukesh Kukreja, R.K., Singh, K.K, Vaze, H.S. Kushwaha, Damage Evaluation of 500 MWe Indian Pressurized Heavy Water Reactor Nuclear Containment for Air Craft Impact, Structural Mechanics in Reactor Technology (SMiRT 17) Prague, Czech Republic, August 17 –22, 2003.
5. Riera, J.D., Rios, R., Iturrioz, I. Determination of the Load-carrying Capacity of a Reinforced Concrete Shell Subjected to Impact Loading, Structural Mechanics in Reactor Technology (SMiRT 17), Prague, Czech Republic, August 17–22, 2003, Paper # J04-4.
6. Jovall, O. Airplane Crash Simulations: Comparison of Analyses Results with Test Data, Paper WJ2/2, SMiRT 19, Toronto, 2007.
7. ATC-40, Seismic Evaluation and Retrofit of Concrete Buildings, Applied Technology Consul, Redwood City, California, USA, 1996.

Structural responses of conventional and base-isolated nuclear power plants for blast loadings (5-1819)

Yin-Nan Huang¹, Andrew Whittaker²

¹Postdoctoral Research Associate, State University of New York at Buffalo
221 Ketter Hall, Buffalo, NY 14260, USA

e-mail: yh28@buffalo.edu

²Professor, State University of New York at Buffalo, USA

e-mail: awhittak@ascu.buffalo.edu

Blast loading due to malevolent attack became a design consideration for nuclear power plants (NPPs) and spent nuclear fuel (SNF) after the terrorist attacks of September 11, 2001. The study presented in this paper assesses the performance of sample conventional and base isolated NPP reactor buildings subjected to blast loading, including air blast and blast-induced ground shock (Huang et al. 2008).

The sample NPP reactor building studied is composed of containment and internal structures with a total weight of approximately 75,000 tons. Two configurations of the reactor building are studied, including a conventional fixed-base reactor building and a base-isolated reactor building using lead rubber bearings.

A blast assessment of the sample reactor building is performed for an assumed threat of 2000 kg of TNT explosive detonated on the surface with a closest distance to the reactor building of 10 m. The air and ground shock waves produced by the design threat are generated and used for performance assessment. The air blast loading to the sample reactor building is computed using a Computational Fluid Dynamics code Air3D (Rose 2006) and the ground shock time series is generated using an attenuation model for soil/rock response. Response-history analysis of the sample conventional and base isolated reactor buildings to external blast loadings is performed using the hydrocode LS-DYNA (LSTC 2003). The structural responses, including acceleration, drift and floor spectral demands on the secondary systems attached to the internal structure are identified for both the conventional and base-isolated sample NPP. The isolators are extremely effective at filtering out high acceleration, high frequency ground shock loading.

References

- Huang, Y.-N., Whittaker, A.S., Luco, N. (2008). Performance assessment of conventional and base-isolated nuclear power plants for earthquake and blast loadings. MCEER-08-0029, Multidisciplinary Center for Earthquake Engineering Research, State University of New York, Buffalo, NY.
- Livermore Software Technology Corporation, Livermore (LSTC). (2003). LS-DYNA keyword user's manual, Livermore Software Technology Corporation, Livermore, California.
- Rose, T.A. (2006). A computational tool for airblast calculations – Air3d version 9 users' guide, Engineering Systems Department, Cranfield University, Shrivenham, United Kingdom.

Seismic margin assessment of Demineralized Water Reserve Tank (5-1829)

Alexander V. Kultsep¹, Alexey M. Berkovsky²

¹CKTI-Vibroiseism Ltd., Gzhatskaya str. 9, 195220, Russia
e-mail: akultsep@cvs.spb.su

²CKTI-Vibroiseism Ltd., Gzhatskaya str. 9, 195220, Russia
e-mail: bam@cvs.spb.su

A Demineralized Water Reserve Tank (DWRT) used for the reactor shut-down cooling of an existing Nuclear Power Plant has been examined for its seismic capacity. The performed analysis has demonstrated, that the full filled tank cannot withstand to the prescribed Review Level Earthquake. At the same time it was found that reducing of water level in the Tank up to allowable limits provides some additional seismic resistance and could be recommended as one of measures for Tank's seismic upgrading.

Seismic Capacity of the Tank was assessed on the basis of FE calculations for the combination of loads including Normal Operation Conditions (NOL) and Review Level Earthquake (RLE). To define RLE loads non-linear Time History Analysis of DWRT has been performed taking into account non-linearity of bitumen lining between tank's bottom and concrete pedestal, bottom uplift and sloshing effects as well. It was found that the governed failure mode of DWRT is a buckling of the tank's shell due to bottom uplift during earthquake. In order to establish seismic capacity of the partially filled tank an investigation of the tank with different water levels and with different supporting was performed as well. The main results of performed analyses were also verified using simple engineering approach.

The calculation series have demonstrated very different tank response depending on water level. Based on these results, recommendations to the allowable water level and to the possible tank reinforcement were developed.

Study on non-stationarity of frequency by synthesis method of earthquake motions (5-1830)

Masahiko Nakamura¹, Fumio Sasaki², Mitsuru Mine³, Kazuki Yokoyama³,
Tetsuo Tamaoki⁴, Akira Tanabe⁵, Wataru Mizumachi⁶, Michio Yamada⁷

¹General Production Center, Tokyo Building Dept., Shimizu Corporation, Japan
e-mail: masahiko.nakamura@shimz.co.jp

²Prof., Dept. of Architecture, Tokyo University of Science, Ph. D.
e-mail: fsasaki@rs.kagu.tus.ac.jp

³Graduate Student, Dept. of Architecture, Tokyo University of Science
e-mail: minemitsuru@yahoo.co.jp

⁴Nuclear Technology Development Division, Aitel Corporation
e-mail: tetsuo1a.tamaoki@glb.toshiba.co.jp

⁵Social & Environmental Division of Atomic Energy Society of Japan
e-mail: tanabeaki@aol.com

⁶Japan Nuclear Energy Safety Organization (JNES)
e-mail: mizumachi-wataru@jnes.go.jp

⁷Prof., Research Institute for Mathematical Sciences, Kyoto University, Dr. Sci.
e-mail: yamada@kurims.kyoto-u.ac.jp

Artificial earthquake motion is employed seismic proof structural design and seismic hazard analysis on structure and machinery. In this case, the fundamental and important task is that the settling of the seismic hazard. Although there are various methods of constructing artificial earthquake motions, the method which conforms to a target response spectrum by superimposing sine waves is widely used (Say, Synthesis Method of Trigonometric Function). In Synthesis Method of Trigonometric Function, the artificial earthquake motion is composed to multiply stationary motions which are calculated with phase given steady random numbers and envelope function which is given in advance. It is also possible that instead of the use of the phase as mentioned above, the phase of specific observed earthquake motion is used as well. However, those methods which provide a phase at random or use a specific phase characteristics make it difficult to consider the change of phase characteristics. Therefore those methods do not reflect a large portion of phase characteristics of observed earthquake motion.

In this paper, artificial earthquake motion is constructed by using Synthesis Method of Earthquake Motions from the classification earthquake mechanism. Synthesis Method of Earthquake Motions is the non-parametric method that satisfies target response spectrum using a number of observed earthquake motions. Firstly, wavelet coefficients of observed earthquake motion by using

orthonormal wavelet transform is generated and then earthquake motions are constructed by using inverse wavelet transform in each frequency band. Secondly, weights are multiplied to them in each frequency band to obtain initial artificial earthquake motion. Thirdly, response spectrum is calculated from obtained artificial earthquake motion. The weights for observed earthquake motions are adjusted to reduce the difference between the response spectrum of the artificial earthquake motion and the target response spectrum, until a tolerance level given in the input is satisfied.

For the comparison of constructed artificial earthquake motion, we make artificial earthquake motion by those Synthesis Method of Trigonometric Function which are given phase from steady random numbers and from specific observed earthquake motion. Several artificial earthquake motions are constructed by above three methods and analyzed which method is more considered non-stationarity of frequency. The way of comparison is how much the portion of quantity about standard deviation of group delay time occupies in the total quantity about standard deviation of group delay time and gradient of Fourier amplitude. Moreover, In order to examine the non-stationarity of frequency of artificial earthquake motion, Synthesis Method of Earthquake Motions and Observed Earthquake Motion are compared by using average and standard deviation of group delay time of the wave which is obtained inverse wavelet transform in each frequency band.

To conclude, as for the average of non-stationarity of observed earthquake motions, artificial earthquake motion constructed by Synthesis Method of Earthquake Motion is obtained good result than those of Synthesis Method of Trigonometric Function given phase at steady random numbers and from specific observed earthquake motions. At the same time, we show artificial earthquake motion by Synthesis Method of Earthquake Motions has average characteristics of time-frequency shown from observed earthquake motions. The artificial earthquake motion constructed by Synthesis Method of Earthquake Motions is supposed to be available for seismic proof structural design.

Generation of an artificial time history matching multiple-damping floor design response spectra (5-1832)

P. Vasilyev

CKTI-Vibroseism, Gzhatskaya str. 9, Saint Petersburg, Russia

e-mail: peter@cvs.spb.su

An acceleration time history in the seismic design is required for nonlinear analytical models, for structures that have different damping at their parts and for structures with a local damping such as piping protected by viscous dampers. When an equipment or pipeline is anchored at some floor than we have to apply the seismic input from this part of the building. There are two ways to get required acceleration time history. You can use records from time history analysis of the building or you can generate time history from floor design response spectra.

First way has a following weak point. According to regulatory design requirements usual floor design spectrum is a combination of spectra corresponding several input time histories, variation of the soil properties, etc. Finally floor design spectrum has broadened peaks. Therefore a big number of time history records have to be used to achieve the same conservatism as in classical response spectrum method.

Second way allows carrying analysis using only one spatial set of artificial time history.

Artificial time history should match multiple damping floor response spectra and meet other requirements of the regulatory design guides.

An algorithm to generate acceleration time history from floor design response spectra is proposed. Software program based on this algorithm is verified through numerical examples.

Seismic analysis of the pipeline protected by viscous dampers is carried out to estimate probable response deviations due to improper input time history.

References

1. U.S. Nuclear Regulatory Commission Regulatory Guide 1.122 – Development of Floor Design Response Spectra for Seismic Design of Floor-Supported Equipment or Components. Revision 1, February 1978.
2. U.S. Nuclear Regulatory Commission NUREG-0800. Standard Review Plan. Revision 2, August 1989.

5. Modeling, Testing and Response Analysis of Structures, Systems and Components

3. US Nuclear Regulatory Commission Regulatory Guide 1.60. Design Response Spectra for Seismic Design of Nuclear Power Plants. Revision 1, 1973.
4. ASCE-4-98, Seismic Analysis of Safety-Related Nuclear Structures and Commentary, 2000.
5. ASCE/SEI 43-05, Seismic Design Criteria for Structures, Systems, and Components in Nuclear Facilities, 2005.
6. NP-031-01, Standard for Seismic Design of Nuclear Power Plants, GOSATOMNADZOR, Russia, 2001.
7. ASME Boiler and Pressure Vessel Code, 1995, Appendix N.
8. European Utility Requirements for LWR Nuclear Power Plants, 2002.

Modeling of high viscous dampers in piping dynamic analysis. Different approaches and acceptable limits for simplifications (5-1833)

Alexey Berkovsky, Peter Vasilyev, Oleg Kireev
“CKTI-VIBROSEISM” Co. Ltd.
195220, Gzhatskaya str., 9, St.-Petersburg, Russia
e-mail: bam@cvs.spb.su

During recent decades High Viscous Dampers (HVD) were intensively implemented in Nuclear and Conventional Industry for protection of piping systems and equipment from the wide range of dynamic loads: earthquake, water/steam hammer, operational vibration, etc.

Application of these devices requires from the Designer/Analyst to implement a proper procedure covering all stages of design: selection of damper's location along pipeline, choosing damper's type, and finally modeling of damper in the frame of piping dynamic analysis.

Presented paper addresses namely the last issue: modeling of viscous dampers in piping analysis. It's well-known that High Viscous Damper exhibits essential frequency-dependent characteristic of dynamic stiffness that hardly could be described by the conventional approach available in the most commercial piping software programs: representing of damper's action by the spring element active for dynamic loads only. From the other hand more sophisticated 4-parametrical Maxwell model [1] that allows accurately reproduce damper's characteristics over frequency range of interest is not widely used in the specialized piping software. Besides, application of Maxwell model requires performing of Time History Analysis while the conventional design procedure for seismic calculations is Response Spectrum Method that uses Floor Response Spectra as seismic input.

Paper presents several numerical examples of piping calculations with different models of dampers for different kinds of dynamic loads and discusses acceptability and limits for implementation of simplified approach when damper is modeled by means of spring elements.

Reference

1. V. Kostarev, A. Berkovsky, O. Kireev, P. Vasilyev, Application of Mathematical Model of High Viscoelastic Damper in Dynamic Analysis of NPP Piping and Equipment. SMIRT-12, 1993, Paper K20/6.

Vibration analysis and fatigue assessment of the RBMK-1000 primary piping considering actual operational conditions (5-1836)

Sergey L. Butorin¹, Victor V. Kostarev², Alexander Yu. Shchukin²

¹International Nuclear Safety Center

P.O. Box 788, 101000, Moscow, Russia

e-mail: butorin@insc.ru

²“CKTI-VIBROSEISM” Co. Ltd.

195220, Gzhatskaya str., 9, St.-Petersburg, Russia

e-mail: sasha@cvs.spb.su

In view of the fact that the service life of some nuclear units comes to its design end, considerable recent attention has been focused on primary components and piping safety margin analysis as well as on developing of a special program for operational time limit extension. It is apparent that the vibration and dynamic loading in various operational modes and conditions should be considered as one of most essential factors of equipment safe operation. The given paper presents a procedure description and results of fatigue calculations made for the Repeated Forced Circulation Piping (RFCP) of RBMK-1000, based on the Russian nuclear standards requirements.

At the first stage piping stress calculations were carried out within the general program and bounds of works for piping safe operation and residual life assessment. They have shown that low cycle fatigue and life extension criteria for RFCP of RBMK-1000 are met. But as usual for many existing and old NPP no account has been taken in such calculations for the essential operational vibration loading effects in spite of these effects are covered by the Russian Nuclear Codes and Standards.

Comprehensive vibration measurements in situ in high radiation zone have been carried out by CKTI-VIBROSEISM for the set of piping systems essential for a safety: repeated forced circulation, feed water, steam and down flow primary piping of RBMK-1000. Together with the design low cycle fatigue parameters these new data allow to give the refined basis necessary for the piping systems life time extension assessment.

The results of vibration analysis and special fatigue calculations' techniques made for RBMK-1000 piping systems with due regard for vibration effect in various operational conditions are presented in this paper.

Analytical study on seismic energy balance of NPP buildings. Part 2. Verification, application and ultimate state with energy index (5-1838)

Shigeru Furukawa¹, Michiya Kuno¹, Ryu Shimamoto¹
Minoru Kanechika², Kazuhiro Kusama², Yoshinori Mihara²

¹Chubu Electric Power Co., Inc., Nagoya, Japan

²Kajima Corporation, Tokyo, Japan

Introduction and aim of the work

In this paper, Part 2, the energy balance estimation methods proposed in Part 1 are theoretically and experimentally verified for both soil parts and building parts, which are the components of the lattice model. Energy balance in the soil parts of the lattice model is similar to that calculated from wave propagation theory. Energy dissipation in the building parts of the lattice model correspond to input energy evaluated from the observed earthquake records.

Using the evaluation method verified above, a quantitative parametric study is carried out on the energy balance of nuclear reactor buildings. As a result, correlation between building damping energy and soil dissipation energy in strong earthquake motions is demonstrated. Also, normalized plastic strain energy is highly correlated to conventional building damage index such as maximum response values.

Essential results

The energy balance estimation methods proposed in Part 1 are theoretically and experimentally verified for both soil parts and building parts, which are the components of the lattice model. Energy balance in the soil parts is similar to that calculated from wave propagation theory. Energy dissipation in the building parts corresponds to the input energy evaluated from the observed earthquake records.

Next, as the results of the parametric study on building damping constant and also the amplitude of earthquake motions, the energies related to building damping and soil sway dissipation have the opposite relationship. Thus, if the building damping energy decreases, the soil sway dissipation energy increases. In addition, the summation of soil dissipation energy for building rocking mode and building plastic stain energy, which influences the maximum response value, is almost the same irrespective of building damping constant. Also, Soil dissipation energy by building sway and rocking mode and dissipation energy by

building damping increase in proportion to the amplitude of earthquake motions. However, the building plastic strain energy increases exponentially. As shown, the soil dissipation energy does not increase but rather slightly decreases, although building plastic strain energy increases if the amplitude of earthquake motions increases.

Moreover, as the results of the parametric study on various random phases of strong artificial earthquake motions, not a plastic strain energy but normalized plastic strain energy that is pointed out in the previous study by Nakamura et al. (1995) is highly correlated to the conventional building damage index such as the maximum response shear strain for earthquake-resisting walls.

Conclusion

The correlation between building damping energy and soil dissipation energy in strong earthquake motions is shown in this parametric study using the verified evaluation method. Also, normalized plastic strain energy is highly correlated to conventional building damage index such as maximum response values.

Further study regarding the configuration of an acceptable value of normalized plastic strain energy should be performed in the future, considering the real phase by observed earthquake records, experimental data on accumulated energy and also detailed elasto-plastic analyses.

References

- Nakamura, N., Sugawara, Y. et al. 1995. Evaluation on consume energy of R/C shear walls. Part 1. Investigation of static tests. Summaries of technical papers of Annual Meeting Architectural Institute of Japan. No. 23106. Pp. 211–212.

Heat-mechanics interaction behavior of lead rubber bearings for seismic base isolation under large and cyclic lateral deformation.

Part 1. Dynamic loading test of LRB and development of analytical method (5-1839)

Akihiro Kondo¹, Yasuo Takenaka², Eiji Takaoka³,
Makiko Hikita⁴, Yo Hyodo⁵, Haruyuki Kitamura⁶

¹Kajima Corporation, Tokyo, Japan, e-mail:kondo-akihiro@kajima.com

²Kajima Corporation, Tokyo, Japan, e-mail:takenaka-yasuo@kajima.com

³Kajima Corporation, Tokyo, Japan, e-mail:takaoka-ei@kajima.com

⁴Kajima Corporation, Tokyo, Japan, e-mail:oim@kajima.com

⁵Kajima Corporation, Tokyo, Japan, e-mail:hyodo-y@kajima.com

⁶Tokyo University of Science, Chiba, Japan, kita-h@rs.noda.tus.ac.jp

When base-isolated buildings are subjected to long-period strong earthquakes emanating from oceanic trenches, base-isolation devices such as Lead Rubber Bearings (LRB) can be subjected to larger and more cyclic deformations than anticipated in structural design.

In an LRB, seismic input energy is absorbed as hysteresis energy of a lead plug, and finally transformed into thermal energy. The resulting large and multiple cyclic deformations of the LRB generate a large amount of heat, causing high temperatures of the lead plug. The resulting deterioration of damping characteristics which encompasses a complex thermal and mechanical phenomenon provides a serious concern for the base-isolated building responses.

However, there is insufficient experimental data on this phenomenon, and no analytical method for evaluation of heat-mechanics interaction behavior has been derived.

This paper describes experimental results and derivation of analytical methods for determining the heat-mechanics interaction of the LRB under a large and cyclic lateral deformation.

In the experimental stage, dynamic loading tests were conducted applying sinusoidal waves and earthquake response waves using full-size devices 1,000 mm in diameter, and 1/2 and 1/4 scale models to clarify the scale effect of the thermal and heat transfer behavior.

Sinusoidal loading tests were carried out to confirm the effect of rises in temperature caused by larger and more cyclic deformation on their mechanical properties. The parameters of these tests were period T and shear strain of rubber γ .

Earthquake response time-history loading tests based on the preliminary response analysis of a base-isolated building under various long-period ground motions were also conducted.

During the experiments, the horizontal force, horizontal deformation and temperature in the specimens were measured.

In the loading tests, increase in temperature and decrease in yield stress of the lead plug were clearly observed. However, the stiffness of the rubber was almost stable during the tests.

Figure 1 shows the relationship between horizontal force Q and displacement δ of the rubber bearing of the full-scale LRB device under a sinusoidal and earthquake response time-history loading test.

In the analytical stage, an analytical method was developed to simulate the changes in the mechanical properties of the LRB under a cyclic loading test. The analysis consists of two phases: a heat transfer analysis based on the finite difference equation and an analysis to determine the relationship between the temperature and the yield stress of the lead plug.

Analytical results obtained by the developed method show good agreements with experimental ones.

To evaluate the effects of the deterioration of damping characteristics of LRB for the base-isolated building responses, an earthquake response analysis method was also developed. In the analysis method, the heat transfer equation and the vibration equation were solved step by step in parallel. Examples of the earthquake response analysis showed that the changes in mechanical properties of the lead rubber bearings led to an increase in the horizontal displacement of the base-isolated building. Those investigations suggest the importance of considering the heat-mechanics interaction behavior of lead rubber bearings.

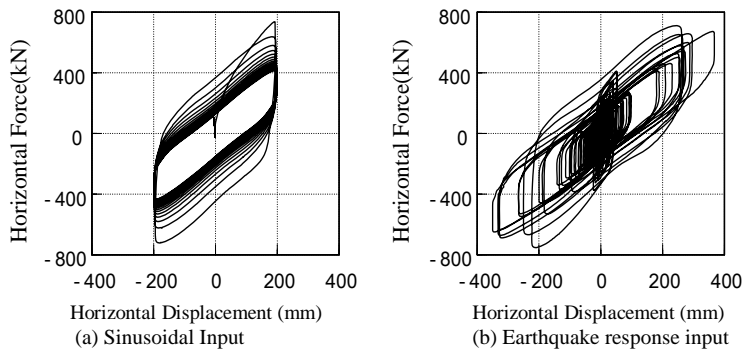


Figure 1. Example of Q - δ relationships obtained in LRB loading test.

Reference

- E. Takaoka, Y. Takenaka, A. Kondo, M. Hikita, H. Kitamura. (2008). Heat-Mechanics Interaction Behavior of Laminated Rubber Bearings under Large and Cyclic Lateral Deformation. The 14th World Conference on Earthquake Engineering, Oct. 12–17, 2008, Beijing, China.



SMiRT 20 Secretariat

VTT Technical Research Centre of Finland

P.O. Box 1000, FI-02044 VTT, Finland

Tel +358 20 722 111

Fax +358 20 722 7053

www.vtt.fi/smirt20, www.iasmirt.org



**INTERNATIONAL ASSOCIATION FOR STRUCTURAL MECHANICS in
REACTOR TECHNOLOGY**

Heat-mechanics interaction behavior of lead rubber bearings for seismic base isolation under large and cyclic lateral deformation. Part 2. Seismic response analysis of base isolated reactor building subjected to horizontal bi-directional earthquake motions (5-1840)

Nobuhisa Sato¹, Shigeru Furukawa², Michiya Kuno², Ryu Shimamoto²,
Yasuo Takenaka³, Takashi Nakayama⁴, Akihiro Kondo⁵

¹Kajima Corporation, Tokyo, Japan, e-mail:satohno@kajima.co.jp

²Chubu Electric Power Co. Inc, Nagoya, Japan
e-mail:Shimamoto.Ryuu@chuden.co.jp

³Kajima Corporation, Tokyo, Japan, e-mail: takenaka-yasuo@kajima.com

⁴Kajima Corporation, Tokyo, Japan, e-mail: nakayama-takashi@kajima.com

⁵Kajima Corporation, Tokyo, Japan, e-mail: kondo-akihiro@kajima.com

Introduction

According to the Regulatory Guide for Aseismic Design of Nuclear Reactor Facilities in Power Plants, reactor buildings constructed in Japan before 2006 were required to be built on bed rock as rigid structures. However, the Regulatory Guide was revised in 2006, and allowed reactor buildings using base isolation systems. Thus, the application of isolated structures to reactor buildings is increasingly expected because of their enhanced seismic safety.

The Lead Rubber Bearing (LRB) was selected as a suitable isolation device for reactor buildings following parametrical studies of many types. The yield stress of lead has thermal dependency, as discussed in Part 1. As a result, the restoring force characteristics of the LRB are altered by heat rise of lead due to cyclic loading during an earthquake. The alteration of the restoring force characteristics of the LRB affects the seismic response of an isolated building.

However, the heat-mechanics interaction behavior of the LRB has never been taken into account in seismic response analysis of isolated reactor buildings.

We conducted a seismic response analysis for an isolated ABWR reactor building for one directional and bi-directional input, using the seismic analysis method of the isolated building taking into account the influence on the response due to the thermal dependency of the LRB as discussed in Part 1, which coupled the seismic response analysis with the thermal conduction analysis.

Seismic response analysis

(1) Analytical model

a. Building model

The analytical model consists of an ABWR reactor building model and an LRB isolation system. Its cross sectional area of the lead plug is double that of a conventional LRB in Japan, so that the maximum response displacement of the isolation layer would be within the allowance level. For the upper structure we used the one-axis elastic lumped mass model. For the isolation layer we used the Multiple Shear Spring model (MSS) for the horizontal direction, which can express non-linear interaction behavior under bi-directional input. Elastic rocking springs were also considered. The horizontal restoring force characteristics of the isolation layer were modeled by the bi-linear model.

b. Earthquake motion

The artificial earthquake motions were used referred to the regulatory guide, which regulates the shape of the amplitude spectra characteristics. The input level was determined to study the safety margin for the response of the isolator. The phase characteristics of the artificial earthquake motions were determined by the fault model, which simulates the motion caused by the fault.

(2) Summary

As the first step the seismic response analysis was conducted for a one-directional input. We compared the building responses taking into account the LRB heat-mechanics interaction behavior with those not taking into account the LRB heat-mechanics interaction behavior. We confirmed the influence on the building response of the alteration of the LRB restoring force characteristics caused by heat rise of the lead for the cyclic loading during an earthquake.

Next a seismic response parametric analysis was conducted for bi-directional input taking into account the LRB heat-mechanics interaction behavior. The parameter for the bi-directional input was the orthogonal input level. At first we compared the rate of heat rise of the lead for the one-directional input with that for the bi-directional input. We confirmed the influence on the building response of the orthogonal input level compared with the one-directional input.

Reference

Kondo et al. Heat-Mechanics Interaction Behavior of Lead Rubber Bearings for Seismic Base Isolation under Large and Cyclic Lateral Deformation. Part 1. Dynamic Loading Test of LRB and Development of Analytical Method.

The rest of the abstracts of Division 5 can be found in Volume 2 of the SMiRT20 abstracts



Series title, number and report
code of publication

VTT Symposium 256
VTT-SYMP-256

Author(s) Seppo Vuori & Rauno Rintamaa (eds.)		
Title 20th International Conference on Structural Mechanics in Reactor Technology SMiRT 20. Book of abstracts. Vol. 1		
Abstract <p>The international conferences on Structural Mechanics in Reactor Technology (SMiRT) have traditionally provided innovative and practical mechanics-based solutions to the planning, design, construction, operation, and regulation of NPPs and related facilities. SMiRT 20 will continue this tradition, bringing together experts and practitioners from around the world to share their knowledge of technology that is most relevant at this time in the nuclear energy industry for both current operations and future development like Generation IV design.</p>		
ISBN 978-951-38-6335-7 (soft back ed.) 978-951-38-6336-4 (URL: http://www.vtt.fi/publications/index.jsp)		
Series title and ISSN VTT Symposium 0357-9387 (soft back ed.) 1455-0873 (URL: http://www.vtt.fi/publications/index.jsp)		Project number 27180
Date July 2009	Language English	Pages 450 p.
Name of project		Commissioned by
Keywords Nuclear power plants, Nuclear facilities, Nuclear safety, Structural safety, Advanced reactors, Mechanics of materials, Aging, Plant life management, Inspection, Maintenance, Design and qualification, Fracture Mechanics, Structural evaluation, Structural reliability, Probabilistic safety assessment, Extreme loads, Earthquakes, Fuel and core structures, Severe accident management, Computational mechanics, Metal materials, Concrete materials, Containment structures, Seismic loads, Seismic analysis, Design methods		Publisher VTT Technical Research Centre of Finland P.O. Box 1000, FI-02044 VTT, Finland Phone internat. +358 20 722 4520 Fax +358 20 722 4374

20th International Conference on
STRUCTURAL MECHANICS IN REACTOR TECHNOLOGY
Dipoli Congress Centre, Espoo (Helsinki), Finland
August 9–14, 2009

The international conferences on Structural Mechanics in Reactor Technology (SMiRT) have traditionally provided innovative and practical mechanics-based solutions to the planning, design, construction, operation, and regulation of NPPs and related facilities. SMiRT 20 will continue this tradition, bringing together experts and practitioners from around the world to share their knowledge of technology that is most relevant at this time in the nuclear energy industry for both current operations and future development like Generation IV design.